MONITORING SHALLOW CONTROLLED GRAVES CONTAINING SMALL CADAVERS USING GROUND PENETRATING RADAR

by

JOANNA MAE FLETCHER
B.A. University of Florida, 2005

A thesis submitted in partial fulfillment of the requirements
for the degree of Master of Arts
in the Department of Anthropology
in the College of Sciences
at the University of Central Florida
Orlando, Florida

Spring Term
2011

ABSTRACT

Ground-penetrating radar (GPR) can be a useful geophysical instrument in the search and detection of clandestine graves in a forensic context. Controlled research in the field of forensic archaeology has demonstrated the applicability of this technology and is vital for improving GPR search methods. The objectives of this research was to evaluate the applicability of GPR, using 250 MHz and 500 MHz antennae, to locate shallow graves containing small pig cadavers in various burial scenarios over a 12 month period. Data was collected on a controlled grid containing six graves at 0.5 m in depth: five graves containing pig carcasses and one control grave. The five graves containing the pig carcasses were devised to test a number of common forensic burial scenarios. The reflection profile data was processed using the computer program REFLEXW. The results demonstrate that the additional grave items did not always increase the detection of the grave for this monitoring period. Further, the low demarcation of the grave containing disturbed backfill illustrated that the hyperbolic reflection features were the result of the pig carcasses and not the disturbed soil. In terms of antenna performance, the 250 MHz data initially provided a higher resolution within the first few months. However, over time the higher detail provided by the 500 MHz data consistently resulted in easily discernable reflections.

This work is dedicated to my sister, Jennifer. Your guidance and love has helped me to achieve my goals in both my education and my life. I am eternally grateful to have you as a sister and I am excited for both of us to start the next chapter in our lives.

ACKNOWLEDGMENTS

This research would not have been possible without the support of numerous individuals. I am extremely grateful for the assistance from my committee throughout this long process. Thank you to my advisor, Dr. John Schultz, for his continual guidance throughout my time at UCF and for the numerous opportunities he has provided me with during my Masters program. I would also like to thank Dr. Tosha Dupras and Dr. Stacy Barber for their support and guidance in making my thesis as sound as possible.

I also want to express my overwhelming thanks to the numerous students at UCF who have assisted me in the field throughout the long 12 months of data collection. Without their help I may not have completed this research. I especially want to thank William Hawkins for being with me every step of this process and helping me keep my sanity. I also want to thank Michael Martin for taking the time to train me with the GPR and computer processing software. Lastly, I would like to thank Brittany Walter and Carrie Healy for their help in data collection week after week without objection.

Finally I would like to thank my family, friends, and my boyfriend. Without their support and guidance throughout my life this education would not be possible and I would not be the person I am today.

TABLE OF CONTENTS

LIST OF FIGURES

LIST OF TABLES

CHAPTER ONE: INTRODUCTION

Law enforcement agencies, medical examiners, and coroners continually request the assistance of forensic archaeologists in forensic investigations to aid in searches forbodies or skeletal remains (France et al. 1992; Schultz 2007; Schultz 2008; Schultz et al. 2006; Strongman 1992). Training in archaeological methods such a line searches, probing, excavation methods, and geophysical prospecting methods make anthropologists valuable personnel in these types of forensic investigations. Geophysical tools are often a part of a multidisciplinary search protocol used by anthropologists, and more recently CSIs. Geophysical tools help pinpoint anomalies and narrow down the search area, which is especially helpful in large search sites. Geophysical tools assist in locating clandestine graves and physical evidence in forensic investigations and have gained recognition by criminal investigators (Davenport 2001; France et al. 1992; Schultz 2007). This equipment often times cannot locate the exact object that is being searched for, but can locate target areas that then can be investigated more closely with more invasive techniques (Schultz 2007). In addition, geophysical tools canbe used to clear suspected areas allowing law enforcement agencies to direct investigation resources elsewhere (Dupras et al. 2006). According to Dupras et al. (2006), one of the main advantages of using geophysical tools is the ability to use them in areas where traditional search methods cannot be used, such as over a foundation of a house.

There are two different categories of search techniques; invasive and noninvasive. Invasive techniques include probe searches, shovel testing/shining, and the use of a backhoe or other heavy equipment. Anthropologists must use invasive techniques with extreme caution due to the destruction the method may cause to the site or evidence. In contrast, noninvasive

techniques do not result in any destruction to the site or evidence . These techniques include the use of cadaver dogs, line searches, and geophysical tools (Schultz and Dupras 2008). In forensic investigations, non-invasive techniques should be exhausted before the use of invasive techniques in order to preserve any evidence that may be recovered. Invasive techniques can be used as a follow up to inspect areas of interest marked by the non-invasive technique.

Geophysical tools can be divided into two types: passive and active. Passive geophysical tools measure contrasts using naturally existent fields, such as magnetism and therefore do not introduce a signal into the earth (Dupras et al. 2006).Passive geophysical tools only have a receiver and lack a transmitter. Magnetometers, magnetic locators, and thermal imaging are examples of passive geophysical tools. In contrast, active geophysical tools send a signal into the earth using a transmitter and then read the returning signal that is detected by a receiver(Kearey et al. 2002; Killam 2004). The signal is altered when the waves penetrate into contrasting subsurface materials, these alterations in the signal result in an anomaly in the data(Davenport 2001). Active geophysical tools include electromagnetic profiling (conductivity meters), resistivity meters, and ground penetrating radar (GPR).

Ground penetrating radar is one type of geophysical tool utilized by forensic archaeologists to assist in locating clandestine graves and physical evidence during investigations (Davenport 2001; France et al. 1992; Schultz 2007). This tool is generally used at archaeological sites to locate buried structures (Bevan 1983; Conyers 1995; Conyers and Cameron 1998; Imai et al. 1987; Sternberg and McGill 1995; Vaughan 1986; Vickers et al. 1977) and archaeological graves (Bevan 1991; Conyers 2006b; Dionne et al. 2010; King et al. 1993; Vaughan 1986).

In forensic investigations GPR has been used successfully to locate bodies, clandestine graves, and/or evidence (Calkin et al. 1995; Davenport 2001; Instanes et al. 2004; Mellett 1992; Nobes 2000; Parker et al. 2009; Schultz 2007). This technique has also been used to locate avalanche victims (Instanes et al. 2004; Modroo and Olhoeft 2004), and locate bodies or evidence in fresh water (Parker et al. 2009; Ruffell 2006). This equipment is able to detect graves due to multiple grave components such as the buried remains, the disturbed soil, and items placed in the grave with the body. Also, ground penetrating radar can accurately detect human remain through various stages of decomposition and skeletonization(Schultz 2003; Schultz 2008; Schultz et al. 2006; Schultz and Martin 2011).

Controlled Research

Due to the success of GPR in forensic investigations, numerous controlled studies have been conducted that simulate buried bodies without any other grave items(Freeland et al. 2003; Hammon et al. 2000; Koppenjan et al. 2003; Schultz 2007; Schultz 2008; Schultz et al. 2006). Thisresearch most often employs burying pig carcasses (*Susscrofa*) as proxies for human remains. These carcasses are then buried in known soils and monitored for a period of time. Pig carcasses are used in numerous controlled studies because they are easier to acquire than human cadavers and pigs are similar to humans in weight, fat to muscle ratio, and are not heavily haired (France et al, 1992). Pigs also have similar rates of decay as humans due to biochemical and physiological similarities (France et al. 1992). Controlled research is beneficial to GPR surveys because it provides experience in performing geophysical surveys in a forensic context, helps to understand the abilities and limitations of GPR in the detection of graves, and helps to understand changes in GPR imagery as a body goes through various stages of decomposition (France et al. 1992; Freeland et al. 2003; Schultz 2008; Schultz et al. 2006).

Although various controlled studies have been performed using GPR in forensic contexts, to date there have been limited studies that have tested GPR in different burial scenarios.Martin (2010) tested the applicability of GPR to locate carcasses in different burial scenarios;however this research used large bodies in deeper graves and did not test applicability of GPR to detect small body size at shallow depths. Ground penetrating radar studies need to incorporate real-life burial scenarios, such as buried remains wrapped in blankets or tarps or bodies covered in various materials or debris, such as rocks or lime, in order to expand the knowledge of GPR usefulness in forensic investigations (Dupras et al. 2006).

Research Objectives

The primary objective of this study is to advance GPR methods used in the detection of small pig carcasses buried at shallow depths in a forensic context. The research design will involve constructing various burial scenarios, representing common forensic examples, with each grave containing a small pig carcass used as proxy for a small adult or child sized-body. This research will, (1) incorporate multiple real-life burial scenarios, (2) document GPR's ability to locate small carcasses in shallow graves for 12 months, and (3) compare GPR data and imagery between 250 MHz and 500 MHz antennae.

Thesis Outline

This thesis will be separated into four chapters: Chapter 1 will provide an introduction for this research; Chapter 2 will discuss the GPR results using thestandard 500 MHz antenna, Chapter 3 will present the GPR results using the lower frequency250 MHz antenna, and Chapter 4 will compare the results of both antennae and summarize the results of the research project.

CHAPTER TWO: DETECTING VARIOUS BURIAL SCENERIOS IN A CONTROLLED SETTING USING A GROUND PENETRATING RADAR WITH A 500 MHz ANTENNA

Introduction

Increased credibility and knowledge of geophysical search methods has led to ground penetrating radar (GPR) being broadly accepted in forensics as a useful tool in locating clandestine graves. One reason for this acceptance is that GPR is noninvasive and allows for an investigation of the search area without resulting in destruction to any evidence or the scene. The forensic applicability of GPR has been demonstrated in various case studies bylocating grave or clearing suspected areas(Calkin et al. 1995; Hammon et al. 2000; Instanes et al. 2004; Mellett 1992; Parker et al. 2009; Schultz 2007). If the GPR detects areas of interest during a survey, invasive techniques can be applied to locate the forensic target in question.While the ability of GPR to locate clandestine graves is important, the ability to clear suspected areas is equally important during forensic investigations because it allows law enforcement to save valuable time and resources (Dupras et al. 2006).

Controlled research utilizing GPR has been shown to be the most useful method for gaining experience and information on performing geophysical surveys in forensic investigations (France et al. 1992; Freeland et al. 2003; Hammon et al. 2000; Koppenjan et al. 2003; Schultz 2007; Schultz 2008; Schultz et al. 2006). Controlled GPR studies have also shown how soil conditions and environment affect the ability of GPR to locate clandestine burials(Conyers and Goodman 1997; Martin 2010; Schultz 2007; Schultz 2008; Schultz et al. 2006). Controlled research is useful for developingguidelines that can be applied to forensic GPR searches. In addition to guidelines, controlled research provides experience for operators in the field. Although various controlled studies have been performed using GPR in forensic contexts, to date

there has been few studies testing the applicability of GPR in different burial scenarios (Martin 2010). Ground penetrating radar studies need to incorporate real-life burial scenarios in order to expand the knowledge of the use of GPR in forensic investigations(Dupras et al. 2006). Scenarios where the body is placed in the ground with additional objects are important to study because these different materials will likely affect the detection of the grave due to changes in the signal and resolution of the anomaly. Martin (2010) tested the applicability of GPR to locate pig carcasses in common real-life burial scenarios over a 12 month period. However, this research only tested the applicability of GPR to locate large bodies buried in deep (1m) graves, leaving a gap in current literature regarding the detection of small bodies in shallow graves.

Purpose

The research presented here will expand upon Martin (2010) by testing the applicability of GPR to detect common real-life burial scenarios using small bodies at shallower (0.5m) depths. This portion of the research will (1) investigate the applicability of using GPR with a 500 MHz antenna to detect shallow burials that mimic real-life forensic scenarios, (2) identify which of the burial scenarios produces the best and poorestresolution throughout the 12 month monitoring period, (3) compare the results throughout the 12 month monitoring period using reflection profiles and horizontal slices.

Materials and Methods

Ground penetrating radar

Ground penetrating radar systems used in archaeology and forensic investigations typically use a monostatic antenna, where the transmitter and receiver are in the same unit (Dupras et al. 2006). A variety of monostatic antennae, differing in frequencies from 10 to 1000 megahertz, can be interchanged on the GPR unit (Conyers and Cameron 1998). The proper

antenna frequency should be chosen depending primarily on the soil and size of the forensic target in question. Under ideal conditions, low frequency antennas produce long wavelengths that are capable of penetrating up to 50 m in ideal conditions. Due to the ability to penetrate deeper, low frequency antennas are only capable of resolving larger buried objects (Conyers and Cameron 1998). Conversely, high frequency antennae, such as 800MHz, have a higher resolution allowing smaller objects, as small as a couple of centimeters in dimension, to be detected. However, high frequency antennae are not capable of penetrating as deep, typically limited to penetration of 1 m in depth (Conyers and Cameron 1998). The higher resolution in high frequency antennas may result in noise which can cause difficulties differentiating between true subsurface anomalies and clutter in the data (Schultz 2003). Schultz et al. (2006) suggests using the 500 MHz antenna due to the balance between depth of penetration and vertical resolution.

A standard GPR has three basic parts: a monostatic antenna, with a transmitter and receiver, the control unit, and a display monitor. Some models have a laptop with software to control the GPR which is used in place of the monitor. The display unit allows for the data collected to be observed in real time and allows the investigator to determine the depth at which the anomaly was detected in the field. The GPR also has an internal hard drive to store the data and allow it to be transferred to an external computer to be analyzed, processed, and printed (Schultz 2007).

When in the field there are multiple configurations for the GPR equipment. One option is to have an operator hand pull the antenna while the monitor is strapped with a harness to their body. This option can be performed with one or two people. The most common operation method is to use a cart that houses all the equipment and only requires one person. The antenna is suspended from the middle of the cart, allowing it to skim over the ground. The monitor is

mounted by the handle so the operator can easily read the output. The cart also has a survey wheel built into one of the cart's wheels to allow for easy calculation of distance. Another option is to have the monitor in a stationary location operated by one individual while another individual hand pulls the antenna. Schultz (2007) states that this method is useful in areas where a cart cannot be utilized due to limited space, such as inside a home.

Ground penetrating radar uses electromagnetic pulses which are sent into the ground to read the composition of the subsurface. These pulses are transmitted by the antenna and are reflected and refracted off subsurface features, soil horizons, and buried items, and then received by the antenna. Reflections occur when the velocity of the radar waves are altered due to differences in the physical and chemical properties of the subsurface material (Conyers 2006c; Conyers and Goodman 1997). The greater the electrical and magnetic properties of subsurface materials differ from surrounding material, that greater the strength and amplitude of the reflection waves (Conyers and Goodman 1997). Reflections occur when the antenna pulse encounters changes in relative dielectric permittivity, electrical conductivity, or magnetic permeability (Powers 1995). Soil, sediment, or rocks that are considered dielectric allow the passage of large amounts of electromagnetic energy with no dissipation. Material that is more electrically conductive is less dielectric therefore will have more dissipation at shallower depths which causes attenuation. High conductive material causes the whole wave to quickly dissipate (Conyers 2004). These radar reflections allow the GPR to detect anomalies that are in the ground, such as a changes in soil horizons or soil density, or a weapon or body (Schultz 2007).

The reflections are then detected by a receiver in the antenna and outputted on a screen to show the ground composition. These reflections are put together and processed in the control unit which produces an accurate two-dimensional image of the ground's stratigraphy and buried

features, referred to as a reflection profile (Conyers 2006c). The x-axis of the two dimensional profile represents depth and the y-axis represents the distance of the transect. One major advantage of GPR is that the raw data can be analyzed and anomalies can be identified in real time in the field (Table 1). On the screen, the anomaly will show up as hyperbolic shape in the two dimensional reflection profile. These hyperbolic shapes are what the GPR operator must be trained to recognize (Schultz 2007). A hyperbolic shape is formed because the pulse beam emitted penetrates into the ground in a conical pattern, as the signal goes deeper, the cone gets larger (Conyers and Goodman 1997). Due to the conical shape of the antenna penetration, objects in the ground are detected before the GPR is directly over them and after the GPR has passed over the area. The apex of the hyperbola represents the true location of the anomaly detected. The radiating sides, or tails, of the hyperbola are the result of reflected energy traveling to and away from the subsurface anomaly when the GPR is not directly over the object (Conyers 2006b; Schultz 2007). Tails are an artifact that can be removed with processing; however recognition of anomalies in the reflection profile is easier with the tails present. The depth of the anomaly should be measured from the apex of the hyperbola because that is when the GPR is immediately over the subsurface feature. Depth of anomalies represented in the reflection profiles are determined within the control unit by measuring the travel times of energy pulses (Conyers and Lucius 1996).

Table 1-Advantages and disadvantages of using GPR for forensic applications.Adapted from Schultz (2007).

Advantages	Disadvantages
Results displayed in real time in the field	Equipment is expensive
Can be used over blacktop or concrete	Operator must have specialized training
Can be used in snow or over fresh water	Site and soil conditions can affect GPR results
Data can be saved on hard drive for computer processing	Additional training necessary for computer processing
Depth and dimension of anomalies can be calculated	Data collection can be time consuming
Non-invasive	

Research Site and Controlled Graves

The research site is located in the Geotechnical Engineering Test Site on the main campus of the University of Central Florida in Orlando (UCF)(Figure 1). The site is secured by a locked chain link fence. A grid measuring 15 m on the north-south axis by 9 m on the east-west axis was set up containing six graves, arranged in two rows with three graves in each row (Figure 2). Five pig carcasses weighing between 25-26.7 kg (55-59 lbs.) were used as proxies for human bodies (Table 2 and Figure 1). The pigs were euthanized on March 5, 2010 and brought back to UCF the same day and placed in graves that were dug on March 3, 2010. Each grave was 1m x 0.75m and 0.5m deep. Grave 1A contained only the pig carcass. Grave 1B contained a pig carcass with 45 kg (100 lbs.) of calcitic and dolomite lime over the carcass. Once the pig carcass was placed in grave 1B, soil was added around the pig to level the depth of the grave to the shallowest part of the pigcarcass. The lime was then evenly dispersed on top of the carcass and the remaining soil was added to fill in the grave. Grave 1C contained a pig carcass wrapped in a fleece blanket. Grave 2B contained a pig carcass under .05m^3(2 ft^3) of river rocks. Similar to the lime scenario, soil was used around the carcass to level the depth of the grave to the shallowest

part of the pig carcass. The rock was then evenly dispersed over the carcass and the grave was filled with the remaining soil. Grave 2C contained a pig carcass wrapped in tarpaulin. Grave 2A was used as a control hole and therefore only contained disturbed backfill. The control hole was used to compare data of a grave with just disturbed soil to the graves containing a body. Grave 1A was used as a control pig carcass and was used in order to compare data of a grave containing only a body with the graves containing additional material. These control holes were used to distinguish which component(s)of the grave, the disturbed backfill, the body, or the additional material added to the grave, produced the geophysical response during GPR detection.The burial scenarios used in this research were modeled after the common forensic burial scenarios used in Martin (2010). Thus comparisons a can be made with Martin (2010) to study the effect of the controlled variables in grave detection.

Table 2- Detailed information for each burial

Grid location	Burial Date	Pig Weight (kg/lbs)	Depth of Unit	Scenario
1A	3/5/2010	26.76/59	0.5 m	Control pig carcass
1B	3/5/2010	25.4/56	0.5 m	Layer of 45 kg (100 lbs.) of calcitic and dolomite lime over pig carcass
1C	3/5/2010	25.4/56	0.5 m	Pig carcasses wrapped in fleece blanket
2A	3/5/2010	N/A	0.5 m	Control hole- no pig carcass
2B	3/5/2010	26.3/58	0.5 m	Layer of .05 cubic meters (2 cubic feet) of stone river rocks over pig carcass
2C	3/5/2010	24.9/55	0.5 m	Pig carcass wrapped in 1.8 m x 1.8 m (6’ x 6’) tarpaulin
Calibration unit (outside grid)	1/9/2009	N/A	1.0 m	Rebar hole

Figure 1- Various burial scenarios

Each pig carcass was placed in the grave on their left side with their back along the north wall and their head facing the east wall and each pigwas placed relatively the same distance from each wall. Five measurements were collected from the surface of the grave to the hind quarter, abdomen, shoulder, cheek, and snout of each carcass. Grave 1B, containing a layer of lime over the carcass, had an additional measurement collected from the surface to the center of the grave after the lime layer was added. Grave 2B, containing a layer of rocks over the carcass, had an additional measurement collected from the surface to the center of the grave after the layer of rocks was added (Table 3).

Table 3-Depths, in meters,from the ground surface to designated areas of the pig carcass

Grave	Hind quarter	Abdomen	Shoulder	Cheek	Snout
1A	0.35	0.33	0.33	0.41	0.46
1B*	0.33	0.30	0.32	0.38	0.38
2B**	0.34	0.29	0.32	0.38	0.46
1C	0.36	0.35	0.35	0.39	0.43
2C	0.33	0.31	0.31	0.39	0.41

*Measurement to center of grave with lime layer: 0.30 m
**Measurement to center of grave with rock layer: 0.26m

Permanent non-metal markers were placed at the corners of the grid for the exact position of survey lines could be replicated during each data collection. The marker at the NW corner of the grid was the 0 m, 0 m marker. Each grave also had a permanent non-metal marker in the NW corner to document the exact position of each grave.

Figure 2-Research area at the Geotechnical Engineering Test Site (designated within square) on UCF main campus in Orlando, Florida. Site is located within the arboretum off Gemini Blvd. (seen on left)

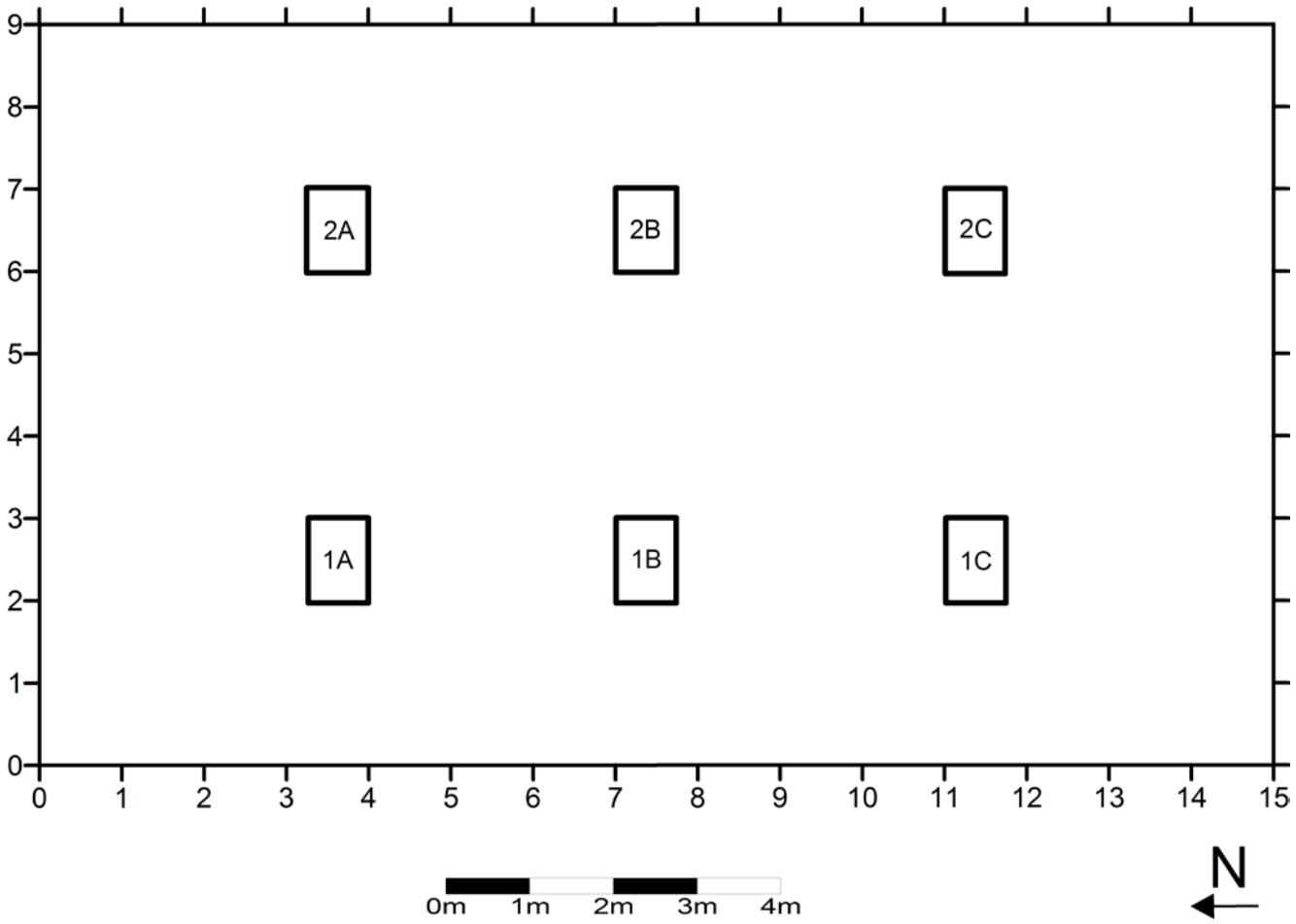

Figure 3- Geophysical Research Site Grid and Location of Burials

Data Collection

A Mala RAMAC X3M GPR unit was used in the research project(Figure 3). The GPR unit was used with a 500 MHz antenna integrated into a cart, that was hand pushed over the research grid. The 500 MHz antenna typically provides an excellent compromise between depth of viewing and vertical resolution and is a common antenna used in shallow archaeological and forensic GPR surveys (Schultz 2007; Schultz et al. 2006).On February 23, 2010, pre-burial data was collected before the graves were dug to have an undisturbed comparison of the subsurface of

the grid. Data was collected approximately every two weeks, during the middle and end of each month, for the duration of 12 months. Data was collected at 0.25 m transects in a north-south and east-west direction (Figures 4 and 5). By taking collections over a 12 month period it allowed data to be collected through all phases of decomposition.

Prior to each data collection event, the GPR unit was calibrated for fluctuations in the soil moisture of the research site. By using an object buried at the known depth, such as a metal pole, to calibrate the equipment, it can help determine the sensitivity of the GPR in the soil (Conyers 2004). This research employed a metal bar placed into an excavation wall at the depth of 1m. The calibration ensures an accurate estimation of depth of the reflection features located within the grid. The calibration pit is located approximately 3 m away from the west end of the research grid. To calibrate the GPR, data was collected over the calibration pitto calibrate the buried rebar at the depth of 1 m.

The soil moisture was also collected prior to each data collection event. The soil moisture was tested using a moisture meter manufactured by Lincoln Irrigation Incorporation. The meter measures the moisture in the soil on a scale from 1 to 10, with 10 being the wettest. The moisture meter was calibrated to 10 occasionally by placing the tip of the probe into tap water. It is important to collect moisture measurements prior to data collection to determine how the soil moisture levels will affect the GPR imagery. The moisture was measured at the rebar hole and the 0 m, 0 m corner of each grave before each data collection.

Figure 4- Mala RAMAC X3M GPR unit integrated into a cart

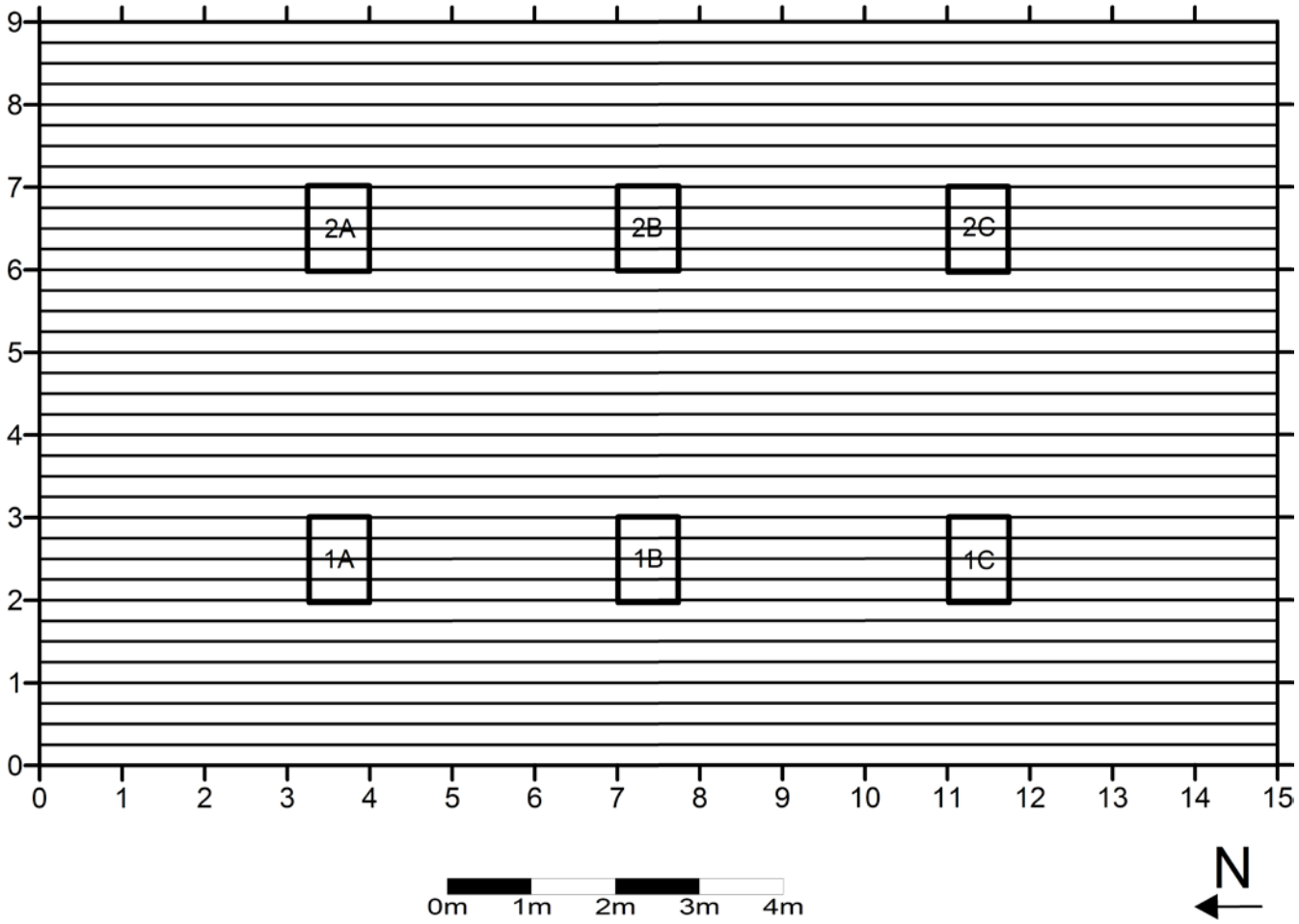

Figure 5- Geophysical Research Site Grid and Location of Burials with 0.25 m transects in North to South direction on X-axis.

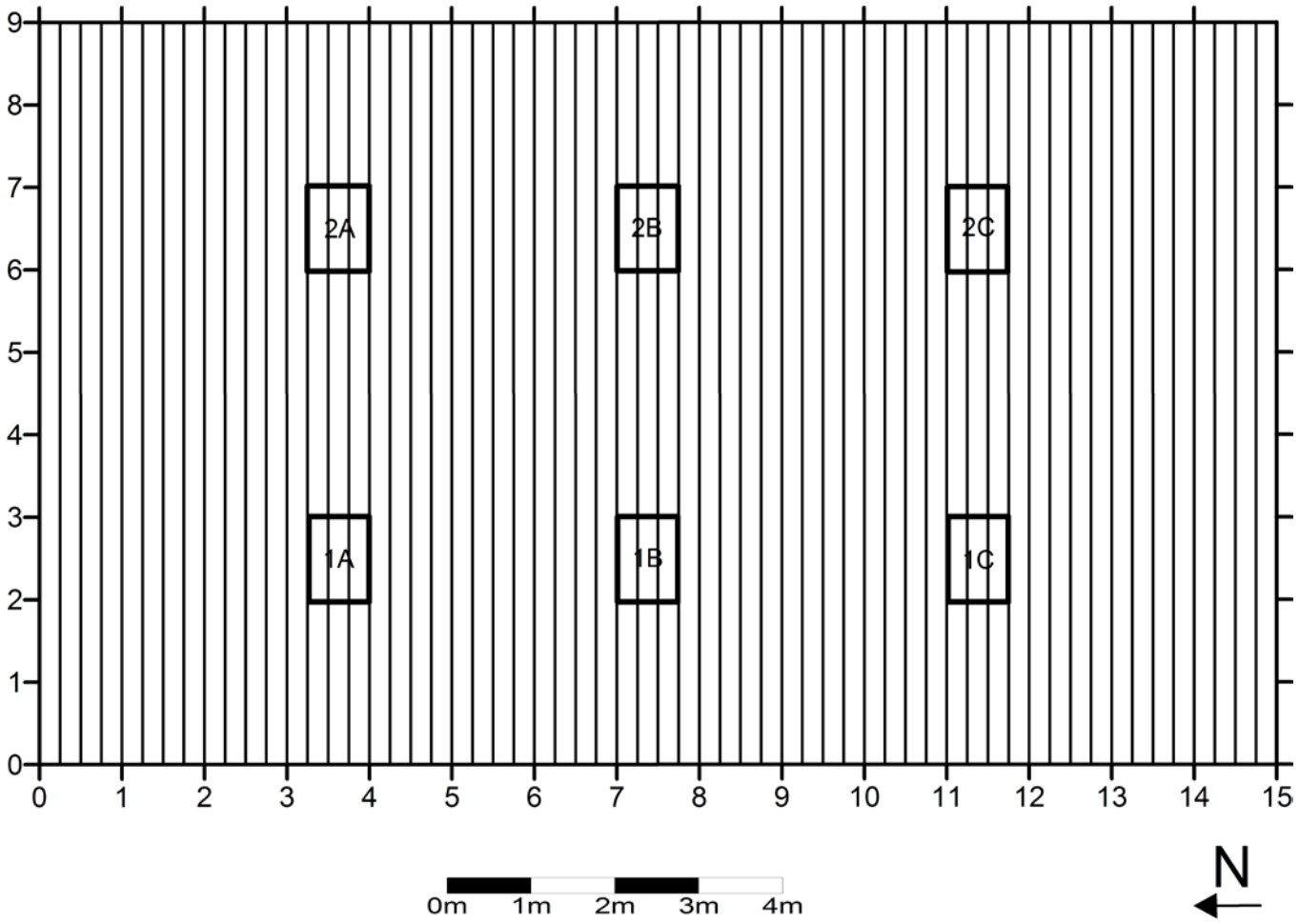

Figure 6- Geophysical Research Site Grid and Location of Burials with 0.25 m transects in East to West direction on Y-axis.

Data Processing

The last component of this research was processing and evaluating the data. All data collected was processed using REFLEXW, version 4.5. Processing provides an increased resolution of hyperbolic features and more advanced analysis of data. Using REFLEXW the data was processed into two different imagery options: reflection profiles and horizontal slices. Reflection profiles consists of a single transect over the grid and represented length (left to right) and depth (top to bottom). The processing procedures for theof reflection profiles completed in REFLEXW included scale correction, removal of horizontal banding, removal of high-frequency

noise, and increasing the gain. Scale correction allows inconsistencies in antenna towing speed to be corrected by removing noise located at the top of the reflection profiles. Various filters, such as background removal and band pass frequency, were used to clean up the reflection profile image. Gain was added to each reflection profile to increase the visibility of subtle reflections (Conyers 2004).

Using REFLEXW 3-D analysisof all reflection profiles collected over the grid in the X or Ydirection were welded together to create a 3-D cube. REFLEXW was used for 3-D data analysis due to the program's increased detection and resolution of smaller subsurface features, such as the grave scenarios with small cadavers utilized in this study, represented in a horizontal slice. The same processing steps and filters used on reflection profiles were used on the 3-d analysis slice files to remove noise and clean up the data. In addition, a migration filter was applied to the data to remove the hyperbola tails so the anomalies view on the horizontal slices represented the actual size and depth of the detected grave features. Slice maps are created horizontally by comparing amplitude variations in traces recorded in a certain time window, or depth. Each slice within the map shows the spatial distribution of amplitudes at a certain depth. Slice maps are important when surveying a site because, by displaying the distribution of reflected wave amplitudes, the map illustrates important subsurface changes in lithology or physical properties in the ground (Conyers 2006a). Areas exhibiting low amplitude waves in a slice map represent uniform soil matrixes. Areas exhibiting high amplitude waves represent areas with high subsurface contrast that could be indicative of buried features, voids, or a grave. These changes in amplitude are represented by a gray or color scale (Conyers 2006a). Horizontal slices are especially important to understanding the data because this imagery option provides a plan view representation of the data within the grid and at varying depths. Computer processing of

GPR data can be beneficial in forensic searches because byincreasing the accuracy of the representation of subsurface anomalies, it allows for increased detection and comparison of anomalies.

Results

Reflection Profiles

The use of 0.25m transects resulted in a total of five profiles collected over each grave in the NS direction. Each of the profiles collected over a grave exhibited noticeable differences in imagery characteristics after the data was processed. In the NS direction, reflection profile 1 represented the East wall of the grave, reflection profile 3 represented the middle of the grave, and reflection profile 5 represented the West wall of the grave. Figures 6-10show the processed reflection profiles for the 5 profiles over row 1 in the NS direction.

Profile 1 poorly demarcated the graves present in row 1(Figure 7). While profile 2 demarcated graves 1A and 1C, the resolution was reduced compared to other profiles (Figure 8). Profile 3, exhibited four distinct reflection features (Figure 9). All graves were represented by strong hyperbolic features. The feature produced by the burial containing only a pig carcass (1A) had the highest resolution. The burial containing a pig carcass covered by a layer of lime (1B) had the weakest resolution out of all the graves. The fourth feature present in the reflection profiles was not created by a grave and likely represents a natural subsurface anomaly, such as a tree root or stump. Profile 4 demarcated graves 1A and 1C with a decreased resolution in comparison to other profiles (Figure 10). Profile 5 only displayed grave 1A as discernable reflection (Figure 11). Overall, profiles 1 and 5 exhibited little to no discernable responses for the graves in row 1, and profiles 2 and 4 exhibited reduced resolution for all three grave

scenarios. Profile 3 produced the reflection profile with the strongest resolution and all 3 graves were easily demarcated.

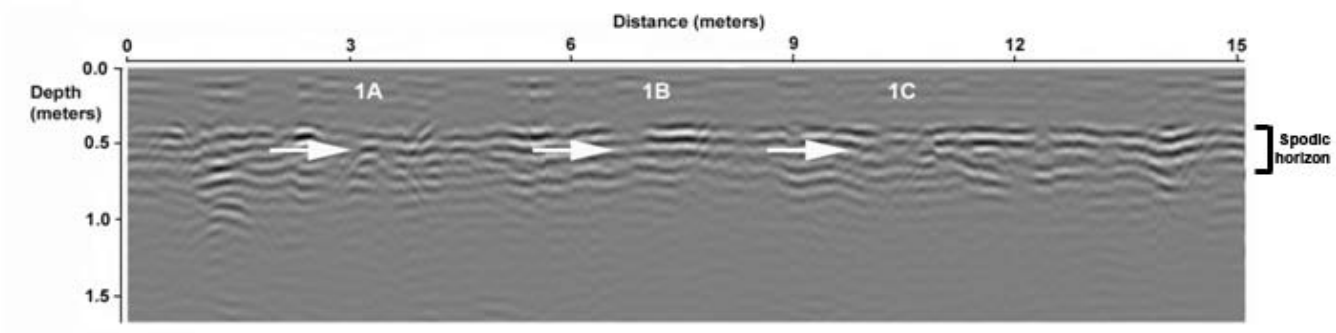

Figure 7- Processed GPR reflection profile using the 500 MHz antenna of row 1, NS, profile 1for month 1

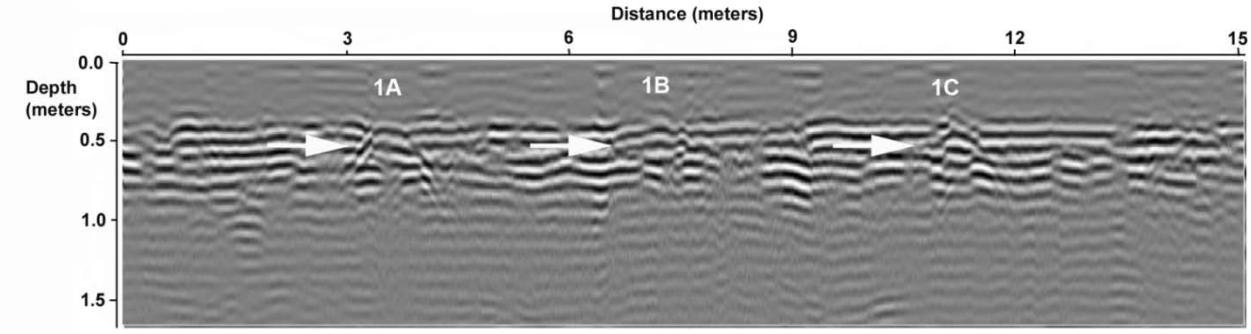

Figure 8- Processed GPR reflection profile using the 500 MHz antenna of row 1, NS, profile 2 for month 1

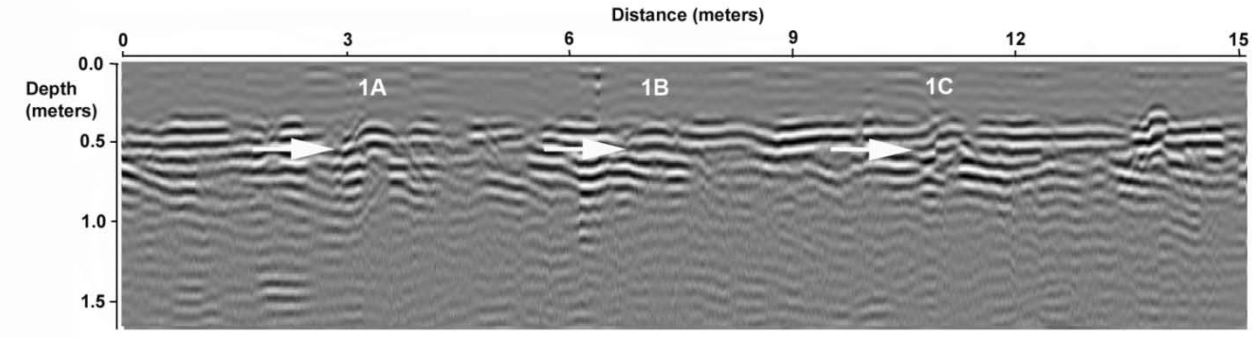

Figure 9- Processed GPR reflection profile using the 500 MHz antenna of row 1, NS, profile 3 for month 1

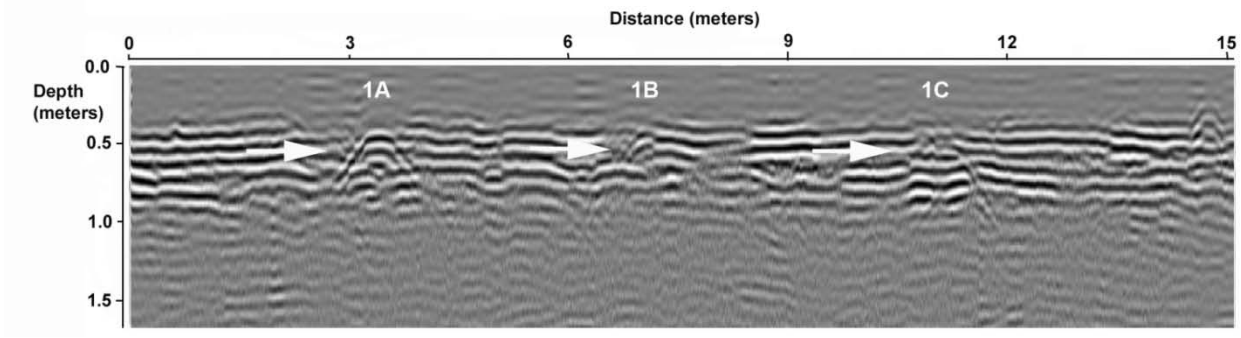

Figure 10- Processed GPR reflection profile using the 500 MHz antenna of row 1, NS, profile 4 for month 1

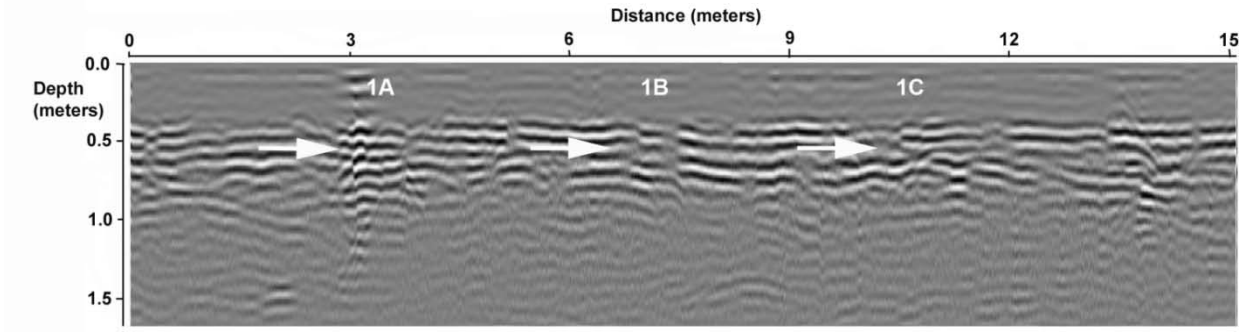

Figure 11- Processed GPR reflection profile using the 500 MHz antenna of row 1, NS, profile 5 for month 1

In grave row 2, profile 1 only demarcated graves 2A and 2B. Grave 2C was not delineated (Figure 12). While profile 2 exhibited a minimal response from grave 2B, the profiledoes not clearly demarcate any of the graves present in row 2 (Figure 13). Similar to row 1, the third profile, collected directly over the middle of the graves, produced a high resolution, clearly demarcating the three grave scenarios after one month of burial (Figure 14). The grave containing the pig carcass covered by a layer of rock (2B) had the strongest resolution. While the control grave, containing only disturbed backfill, had the weakest resolution, the grave was still clearly demarcated. Profile 4 displayed a reduced resolution compared to profile three. However, graves 2B and 2Cwere clearly demarcated. Profile 4exhibited no response from grave 2A (Figure

15). Profile 5 displayed minimal response from graves 2B and 2C and exhibited no response from grave 2A (Figure 16). Overall, profiles 1 and 5 displayed minimal discernable responses for the graves in row 2, and profiles 2 and 4 displayed reduced resolution for all three grave scenarios. Profile 3 was the reflection profile with the strongest resolution and all three burial scenarios were delineated.

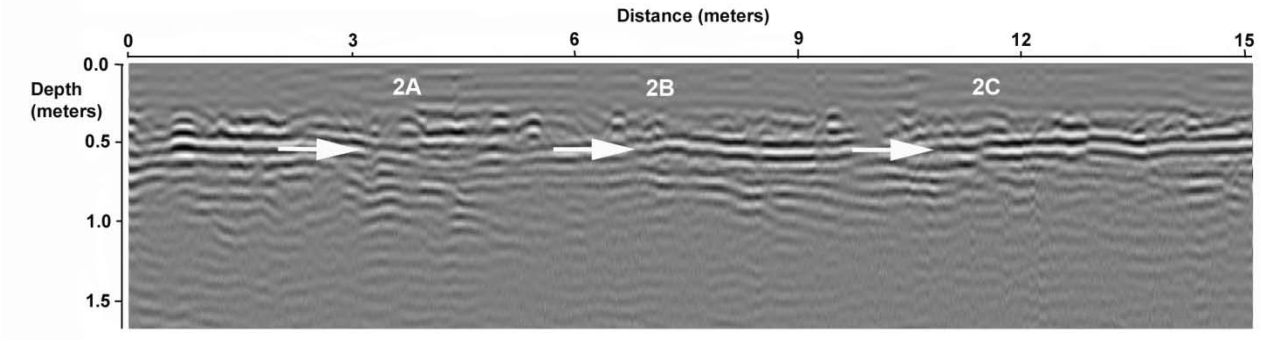

Figure 12- Processed GPR reflection profile using the 500 MHz antenna of row 2, NS, profile 1 for month 1

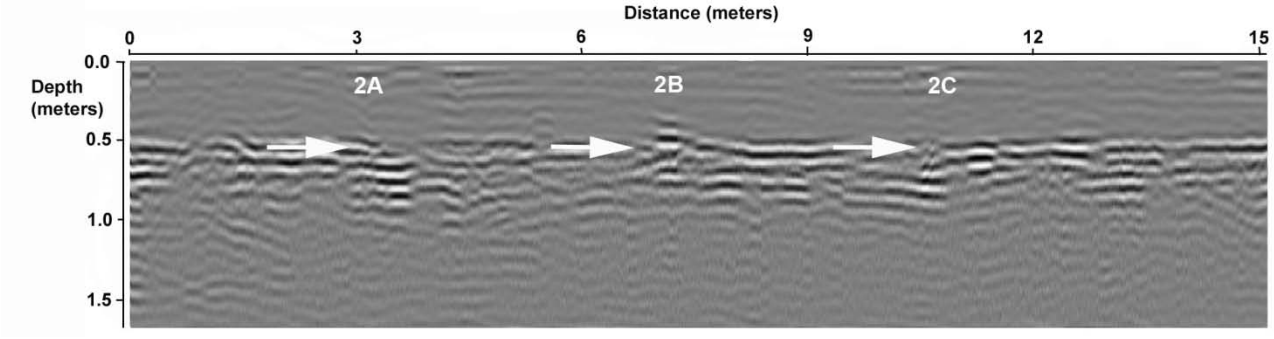

Figure 13- Processed GPR reflection profile using the 500 MHz antenna of row 2, NS, profile 2 for month 1

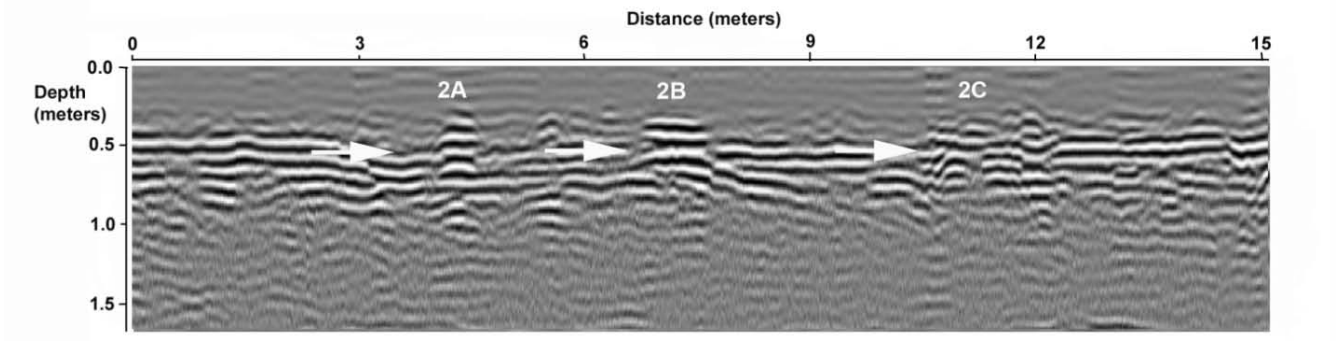

Figure 14- Processed GPR reflection profile using the 500 MHz antenna of row 2, NS, profile 3 for month 1

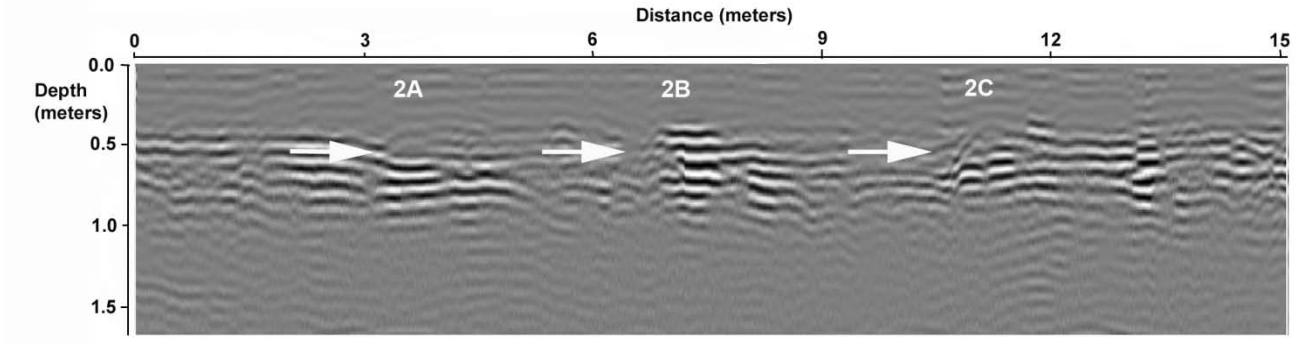

Figure 15- Processed GPR reflection profile using the 500 MHz antenna of row 2, NS, profile 4 for month 1

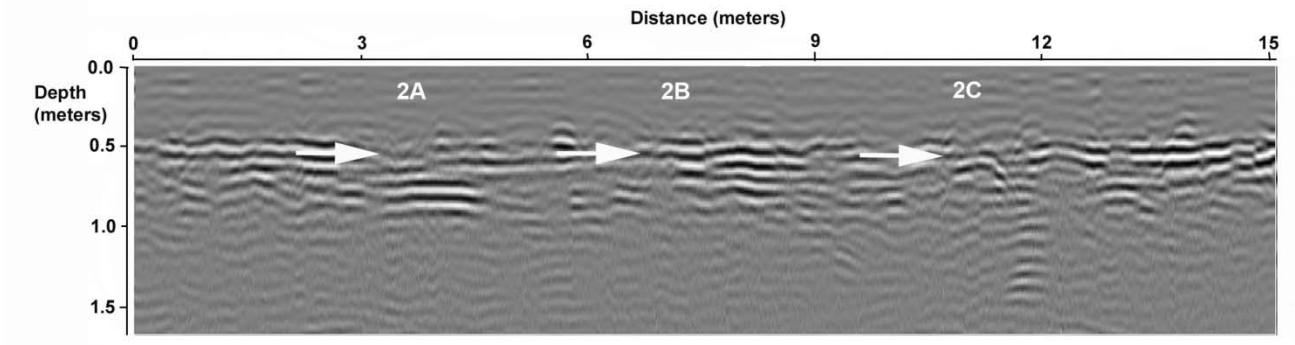

Figure 16- Processed GPR reflection profile using the 500 MHz antenna of row 2, NS, profile 5 for month 1

Processed reflection profiles collected over the middle of the graves were also analyzed each month. The results of this research only address profile 3 in row 1 and row 2 in the NS

direction (Tables 4 and 5). Reflection profiles for the remainder of data collection, months 2-12, are located in Appendix A.

After month 1 of the data collection, noticeable changes occurred with the reflection profile for the control grave containing only disturbed backfill (2A). The reflection profile became less discernable with month 2 data collection not producing any response for this grave. For the remainder of the data collection, months 3-12, no discernable anomaly was produced by the control grave (2A).

From month 1 to month 3, all graves containing a pig carcass were clearly discernable in the reflection profiles. During this time, the grave containing a pig carcass wrapped in tarpaulin (2C) produced the strongest reflection. Out of the graves containing a pig carcass, the grave containing a pig carcass covered by a layer of lime (1B) produced the weakest response, but was still discernable.

After 4 months of burial, the resolution for the grave containing the pig carcass covered by a layer of rock (2B) decreased in resolution and was not clearly discernable in month 4 or 5. During this time the grave containing only a pig carcass(1A) and the grave containing a pig carcass wrapped in tarpaulin(2C) had the strongest resolution and were more discernable than the other graves.

After months 6 and 7, the grave containing the pig carcass under rock (2B) was still less discernable than the other graves. However, overall the data had an increased resolution from the previous months. While in month 6 the grave containing a pig carcass covered by a layer of lime (1B) was poorly discernable, during month 7 this grave had a stronger resolution and was more discernable than the other graves. During months 6 and 7, graves 1A and 2C were still clearly

discernable and had a high resolution. In month 7, the grave containing a pig carcass wrapped in a blanket (1C) had poor resolution andwas not discernable.

During month 8, the data collected in the field was not able to discern hyperbolic features for any grave except the grave containing a pig carcass wrapped in the tarpaulin (2C). However, after processing in the laboratory, the graves were able to be delineated in the reflection profiles.Moisture levels during month 8 within the grid were noticeably lower than previous months due to a decrease in rainfall (see Appendix F). Reduced soil moisture resulted in poor reflection features for all grave scenarios except the grave containing a pig carcass wrapped in tarpaulin (2C) which had an excellent response and was easily discernable during this month.

After 9 and 10 months of burial, the graves containing a pig carcass wrapped in a blanket (1C) and the pig carcass covered by a layer of rocks (2B) produced the weakest resolutions; however both were still discernable. Graves 1A and 2C were more discernable from the other grave scenarios during these months. Grave 2C produced the strongest resolution.

After 11 months of burial, the graves containing a pig carcass wrapped in tarpaulin (2C) and the pig carcass under a layer of lime (1B) produced the strongest resolutions. Grave 2C produced more distinct hyperbolic tail than grave 1B. The grave containing a pig wrapped in a blanket (1C) produced the weakest response out of the graves containing pig carcasses. While the grave containing only a pig carcass produced a weaker resolution than the previous month, the grave was still delineated.

After 12 months of burial, the grave containing a pig carcass wrapped in a tarpaulin (2C) produced the strongest resolution. The grave containing only a pig carcass produced a reduced response from previous months. The graves containing a pig wrapped in a blanket (1C) and only disturbed soil (2A) did not produce responses.

Table 4- Monthly imagery results for each burial scenario based on reflection profiles (500-MHz antenna)

Month	Burial Scenarios					
	1A	**1B**	**1C**	**2A**	**2B**	**2C**
1	Excellent	Excellent	Excellent	Poor	Good	Good
2	Excellent	Good	Excellent	None	Good	Excellent
3	Good	Poor	Poor	None	Good	Good
4	Good	Excellent	Poor	None	Good	Good
5	Good	Good	Good	None	Poor	Good
6	Good	Good	Good	None	Poor	Good
7	Good	Good	Good	None	Poor	Excellent
8	Good	Poor	None	None	Poor	Excellent
9	Good	Poor	Poor	None	Poor	Good
10	Good	Poor	None	None	Poor	Excellent
11	Good	Poor	None	None	Poor	Excellent
12	Poor	Poor	None	None	Good	Excellent

Table 5- Summary information describing the GPR reflection profiles with a 500-MHz antenna for each month of data collection

Month #	Overview of GPR Imagery Results
1	Grave 2B and grave1A produced the strongest response whileGrave 1C produced the weakest response.
2	Grave 1A and grave 2C produced the strongest responses. The control grave produced the weakest response with responses from 1B and 2C remaining weak.
3	Grave 1A and 1B produced the strongest responses. The control grave continued to have a minimal response. All graves produced reduced responses during this month.
4	Excellent detection of all Graves in Row 1 and grave 2C. Grave 1A and grave 2C produced the strongest responses while grave 2B produced the weakest response. There is no detection of the control grave.
5	Strong detection of all Graves in Row 1 and grave 2C. Grave 2C had the strongest response while grave 2B had the weakest response. The control grave continued to not be detected.
6	Good detection of all Graves in Row 1 and Grave 2C. Grave 2C produced the strongest response while graves 1B and 2B produced the weakest response. The control grave was not detected.
7	Poor detection of graves 1A, 1C, and 2B. Graves 1B and 2C produced the strongest responses. The control grave was not detected.
8	Good detection of all Graves in Row 1 and Grave 2C. Grave 2C produced the strongest response while grave 2B produced the weakest response. The control grave was not detected.
9	Good detection of graves 1A, 1B, and 2C. Grave 2C produced the strongest response while graves 1C and 2B produced the weakest responses. The control grave was not detected.
10	Excellent detection of graves 1A and 2C. Poor detection of graves 1C and 2B. The control grave was not detected.
11	Excellent detection of grave 1B and 2C while grave 1C produced the weakest response. The control grave was not detected.
12	Excellent detection of grave 2C while grave 1C did not produce any response. The control grave was not detected.

Horizontal Slices

Using the software program REFLEXW, the transect data (reflection profiles) collected from the grid was processed using 3D data interpretation. The reflection profiles in either the X (NS) or Y (WE) directionwere then appended together creating a 3D cube. Data between the transectswas interpolated within REFLEXW to create a solid cube.The cube can be cut in three different planes to view the grid data. The most common cut and the one used for this research is the horizontal slice, akin to a map viewat different depths.These processed images provided plainview representations of the grid in either the X or Y direction. Grid data was collected prior to the construction of the graves to serve as a comparison with the data collected after burial.While there are a number of subsurface features present in the pre-burial horizontal slices (Figure 17 and 18), when the location of the graves is superimposed on the imageit is evident the features do not correspond with the locations of the six burials. The subsurface features present in the pre-burial data likely represent roots, stumps, or subsurface soil disturbances unrelated to the research.

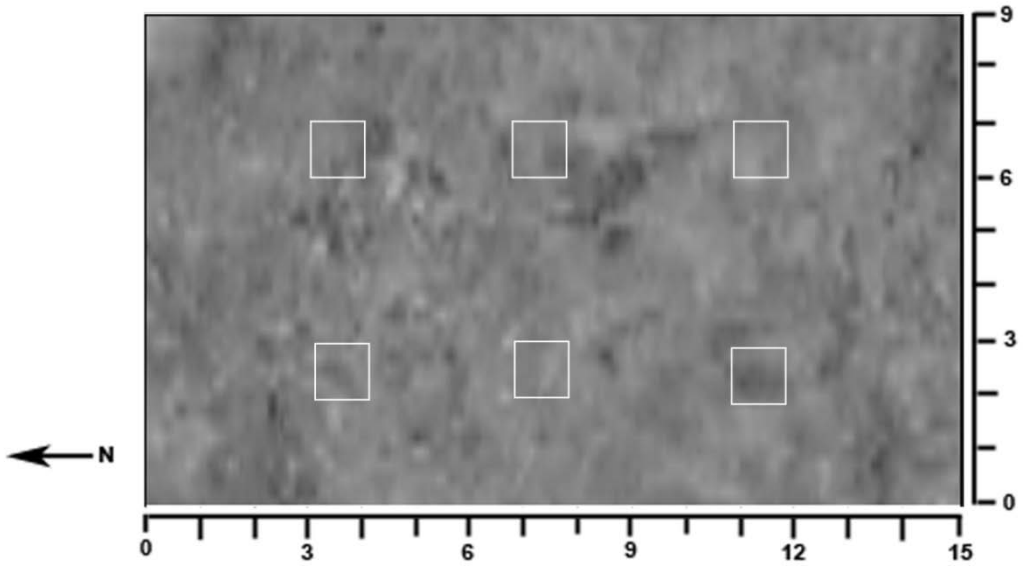

Figure 17- GPR pre-burial horizontal slice in the X direction using the 500 MHz antenna. The horizontal slice is approximately 0.4 m in depth (8.13 ns)

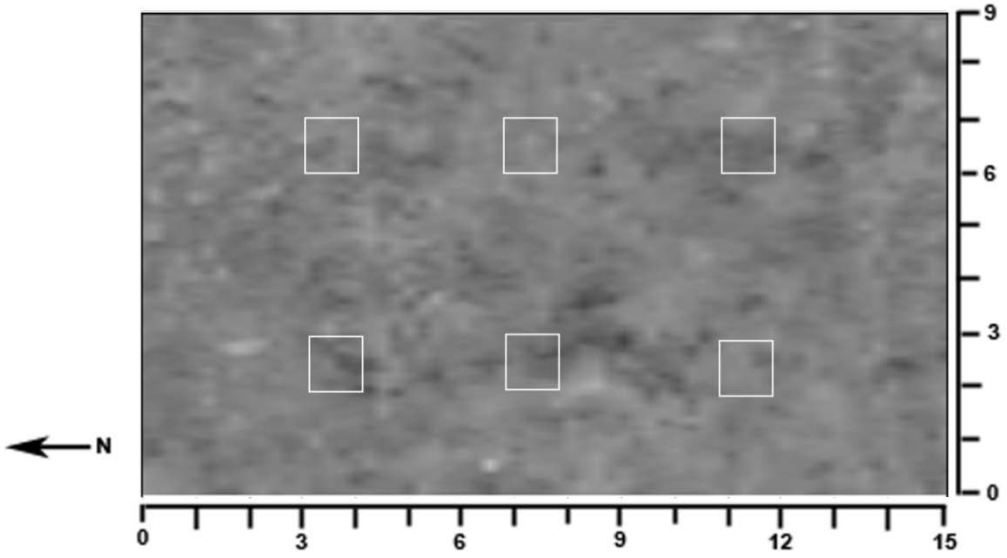

Figure 18-GPR pre-burial horizontal slice in the Y direction using the 500 MHz antenna. The horizontal slice is approximately 0.4 m in depth (8.13 ns)

When the location of the graves was superimposed on the horizontal slices displaying 1 month data, it is obvious that the GPR is detecting the graves within the grid (Figures 19 and 20). The horizontal slices presented here and in appendix B represent varying depths, ranging from 0.32m to 0.46 m.Each month is represented by X and Y direction horizontal slices. Both X and Y directions were considered when analyzing the data to determine the detection of the graves (Tables 6 and 7).

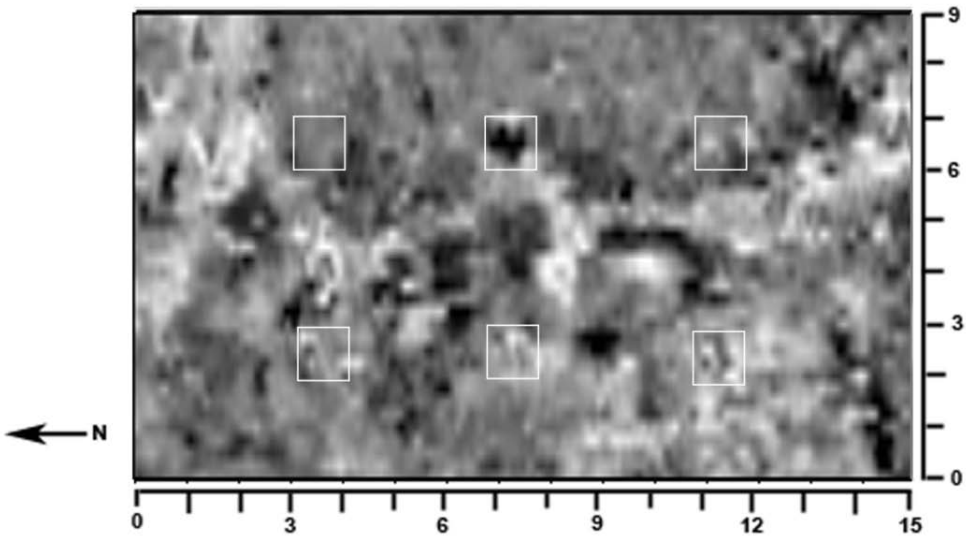

Figure 19- GPR horizontal slice in the X direction using the 500 MHz antenna at 1 month. The horizontal slice is approximately 0.43 m in depth (15.66 ns)

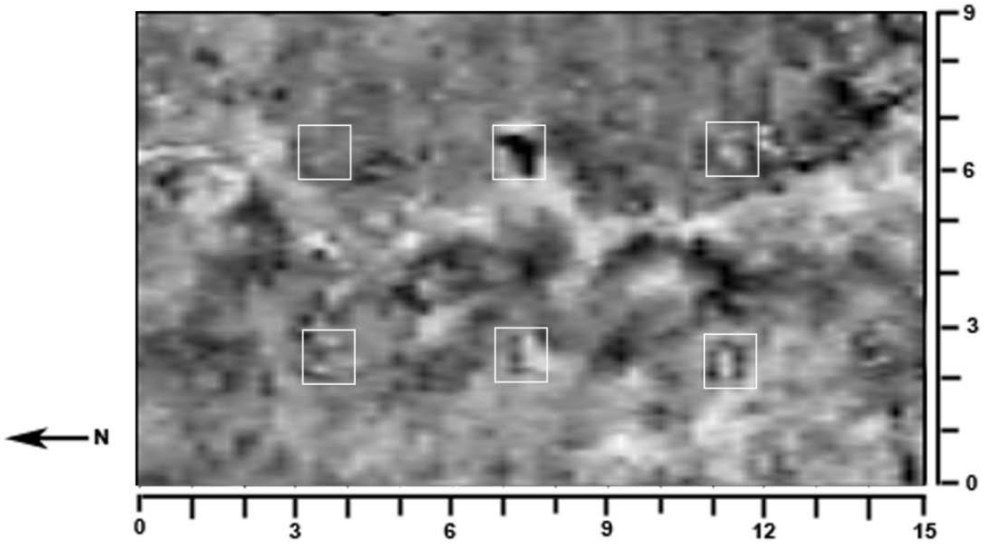

Figure 20- GPR horizontal slice in the Y direction using the 500 MHz antenna at 1 month. The horizontal slice is approximately 0.4 m in depth (14.62 ns)

After one month, all five of the burials containing a pig carcass were represented in the horizontal slice. The grave containing a pig carcass covered by a layer of rocks(2B) had a stronger resolution than the other graves containing pig carcasses. The grave containing only the

disturbed backfill (2A) was not represented in the horizontal slice. For the remaining months of data collection, the control grave is poorly represented and not discernable in the horizontal slices. As with the reflection profiles, the highly demarcated reflection of the graves containing a pig carcass when compared to the lack of representation of the control grave, demonstrates that the reflection features were created by the pig carcass and not the disturbed soil.

Months 2 and 3 show similar results with all five grave scenarios being detected in the horizontal slice. Similar to month 1, grave 2B was the most prominent in both months 2 and 3. While month 3 had a decrease in resolution for all the graves, similar to the decrease seen in this month in reflection profiles, the graves containing pig carcasses were still easily discernable. While this decrease in resolution continues into month 4 horizontal slices,all graves are still clearly discernable. During month 4, the grave containing a pig carcass covered by a layer of lime (1B) is the most easily detected out of the graves containing burial scenarios. During month 5 the resolution of the whole grid increased substantially and grave 1B was still the most discernable. The prominence of graves 1B and 2B in horizontal slices should be noted because these graves were the hardest, of the grave scenarios, to detect in reflection profiles.

Month 6 produced astrong resolution of all the graves containing pig carcasses and the graves were easily discernable. During this month the grave containing only the pig carcass (1A) and grave 2B were the most easily discernable. Also during this month, the grave containing a pig carcass wrapped in tarpaulin (2C) had a strong resolution which was a noticeable increase from previous months.

Months 7 and 8exhibited a substantial decrease in resolution of the graves containing pig carcasses. While all graves were present, the location of the graves was hard to determine due to the decrease in resolution. In month 7, grave 1B is most easily discerned.However, the resolution

is noticeably less than in previous months. In month 8, grave 2B had the highest resolution. However, the delineating feature was less visible than in previous months. This decrease in response from the graves coincides with the decrease in response seen in the reflection profiles. This decrease is most likely attributed to a decrease in moisture in the graves due to a lack of significant rainfall during these months.

During months 9 and 10 there is anincrease in delineation of all the graves containing a pig carcass in the horizontal slices. During this month, graves 1A and 1B are the most discernable. The increase in delineation is likely attributed to the significant rainfall which occurred between months 8 and 9.

After 11 months of burial, the grave containing a pig carcass under a layer of lime (1B) produced the strongest resolution followed by the grave containing a pig carcass wrapped in a tarpaulin (2C). The grave containing a pig carcass wrapped in a blanket (1C) and a pig carcass under a layer of rock (2B) produced poor responses. However, these graves were still detected. The grave containing only a pig carcass (1A) produced a weaker response compared to the previous month.

After 12 months of burial, the grave containing a pig carcass under a layer of lime (1B) continued to produce the strongest response in the horizontal slices. The graves containing only a pig carcass (1A), a pig carcass wrapped in a blanket (1C), and a pig carcass wrapped in a tarpaulin (2C) produced good responses. The pig carcass under a layer of rock produced the weakest response out of the graves containing pig carcasses.

Table 6- Monthly imagery results for each burial scenario based on horizontal slices (500-MHz antenna)

Month	Burial Scenarios					
	1A	**1B**	**1C**	**2A**	**2B**	**2C**
1	Poor	Good	Good	None	Excellent	Good
2	Good	Excellent	Excellent	None	Excellent	Good
3	Good	Excellent	Good	None	Excellent	Excellent
4	Good	Excellent	Good	None	Poor	Good
5	Poor	Excellent	Good	None	Poor	Good
6	Excellent	Good	Excellent	None	Excellent	Excellent
7	Poor	Good	Poor	None	Poor	Good
8	Poor	Good	Poor	None	Good	Good
9	Good	Excellent	Good	None	Poor	Poor
10	Excellent	Excellent	None	None	Poor	Good
11	Poor	Excellent	Poor	None	Poor	Good
12	Good	Excellent	Good	None	Poor	Good

Table 7- Summary information describing the GPR horizontal slices with a 500-MHz antenna for each month of data collection

Month #	Overview of GPR Imagery Results
1	Graves 1C and 2B produced the strongest response while graves 1A and 2A produced the weakest responses.
2	All graves containing a pig carcass produced responses. Graves 1C, 2B, and 2C produced the strongest responses. The control grave was not detected.
3	All graves containing a pig carcass produced good responses. Grave 2B and 2C produced the strongest responses. The control grave was not detected.
4	All graves containing a pig carcass produced good responses. Grave 1B produced the strongest response. The control grave was not detected.
5	All graves containing a pig carcass produced good responses. Grave 1B produced the strongest response. The control grave was not detected.
6	All graves containing a pig carcass produced excellent responses. Graves 1A, 1B, and 2C produced the strongest response. The control grave was not detected.
7	All graves containing a pig carcass produced reduced responses. Grave 1B produced the strongest response. The control grave was not detected.
8	All graves containing a pig carcass produced responses. Grave 2B produced the strongest response while grave 1A produced a reduced response. The control grave was not detected.
9	All graves containing a pig carcass produced excellent responses. Graves 1A, 1B, and 2C produced the strongest response. The control grave was not detected.
10	All graves containing a pig carcass were discernable. Graves 1A, 1B, and 2C produced the strongest response. The control grave was not detected.
11	All graves containing a pig carcass were discernable. Graves 1B and 2C produced the strongest response. Grave 1A produced a weaker response compared to the previous month. The control grave was not detected.
12	All graves containing a pig carcass were discernable. Grave 1B produced the strongest response while graves 1A, 1C, and 2C produced good responses. The control grave was not detected.

Discussion

Controlled research utilizing GPR tests the applicability of the technology in the detection of clandestine graves and provides guidelines on performing GPR surveys in a forensic context (France et al. 1992; Freeland et al. 2003; Hammon et al. 2000; Koppenjan et al. 2003; Schultz 2007; Schultz 2008; Schultz et al. 2006). In addition, controlled GPR studies have demonstrated how soil conditions and environment affect the ability of GPR to locate clandestine burials (Schultz 2007). Multiple burial characteristics affected the detection of the burials in this study:the various burial scenarios in which the bodies were placed, the moisture present in the soil, the properties of the soil, and the imagery options utilized to process the data.These factors will be discussed in detail.

Burial scenarios

Real life burial scenarios were used in this research in order to determine which component of the grave most effectively produced a geophysical response. Through an evaluation of the reflection profiles throughout the 12 months of data collection, it is evident that the pig wrapped in tarpaulin (2C) consistently produced the highest resolution and the clearest delineation. The increased resolution was due to the tarpaulin retaining moisture around the pig carcass, and moisture from rain water that likely pooled on the top of the tarpaulin. The additional moisture present, even after 12 months of burial, created a stronger geophysical response (Figure 94). It is unlikely that the increase in resolution was solely due to the additional goods in the grave because the grave containing only a pig carcass (1A) produced the second strongest response for the collection period. Contrary to results of Martin (2010)which tested the same burial scenarios with large pig carcass in deep graves, the high resolution produced

bygrave 1A suggests that grave items did not necessarily increase the detection of shallow graves. Grave 1C, which contained a pig carcass wrapped in a blanket,had overall reduced delineation throughout the 12 months. While the graves containing a pig carcass covered by a layer of lime (1B) and a pig carcass covered by a layer of rocks (2B) were both detected throughout the 12 months of monitoring, these graves produced lowerresolutions than graves 1A and 2C. Previous research found that the pig carcass covered in a layer of rock produced the best resolution through the 12 months of research (Martin 2010). The pig carcass covered by a layer of limetypically produced a stronger resolution than the pig carcass covered by a layer of rocks; this is especially true in the horizontal slices(Figure 106). Again, this is likely due to the increase in moisture in grave 1B due to the lime retaining moisture (Table 12). The grave containing only disturbed backfill was only detected during the first month of data collection (Figure 39)and after 1 month of burial itwas no longer detected. This lack of detection is likely due to the eventual soil compaction within the grave shaft.

The horizontal slice data is consistent with the assessment that additional grave items did not necessarily increase the ability to detect the graves. While the grave containing a pig carcass covered by a layer of lime had the highest resolution throughout the 12 months, all the graves containing a pig carcass were easily delineated. The grave containing only disturbed backfill was never delineated within the horizontal slice images.

Imagery options

Processing data in a laboratory using computer software andimagery options helps to maximize the delineation of subsurface features (Martin 2010). Multiple imagery options provided a more detailed and accurate analysis of the geophysical response produced by the burial features. The reflection profiles represent a single transect over the center of the graves,

displaying three graves in the NS direction. Reflection profiles were utilized to analyze the grave as a whole throughout the 12 months and were advantageous because they provided an accurate representation of the depth of each anomaly. The reflection profiles also illustrated changes in the detection of the graves from month to month. A tight transectspacingof only 0.25 m was utilized for the collection of the reflection profiles. When incorporating all the reflection profiles into a grid survey, the computer program will create a 3D cube that includes interpolating the space between the transects. The tighter transects results in an increased resolution of small features within the grid (Conyers 2006B). The cube can be cut in three different planes to view the grid data. The most common cut and the one used for this research is the horizontal slice, akin to a map view at different depths. The horizontal slices represent the grid as a whole and allow for delineation of all of the graves in either the X or Y direction at a given depth. These horizontal slices provided an easy comparison between all the graves and allowed all subsurface features within the grid to be analyzed at a single depth.

Multiple imagery options were imperative to this research because certain graves exhibited an increased resolution in reflection profiles while other graves exhibited an increased resolution through horizontal slices. Previous research also found that multiple imagery options were necessary to delineate all the graves present (Martin 2010). The grave containing only a pig carcass (1A) was easily delineated throughout the 12 months in the reflection profiles. However, this grave had poor demarcation during five of the months in the horizontal slices.In comparison, the grave containing a pig carcass covered by a layer of lime (1B) had good or excellent delineation for the entire 12 months in the horizontal slices. However, grave 1B had poor delineation during four of the months in the reflection profiles. The grave containing a pig carcass covered by a layer of rocks had similar results to grave 1B and was more easily

demarcated in horizontal slices. Through the use of data processing software, reflection profiles, and horizontal slices, this research was able to maximize the delineation of the hyperbolic features representing the graves.

Moisture

The soil moisture present within a search area has been proven to have a large effect on the delineation of graves when using GPR (Doolittle and Bellantoni 2009; Martin 2010). Doolittle and Bellantoni (2009) found that soil moisture can improve the detection of cemetery graves; however heavily saturated soils can restrict penetration and reduce the detection of subsurface anomalies. This research confirms the effect of moisture on the applicability of GPR. Table 12 in Appendix E gives the moisture levels for the graves during each month of data collection. Month 8 resulted in the poorest resolution for all the graves and the data required significant processing in order to delineate features(Figures 64-68), this coincides with a decreasein soil moisture due to a decrease in rainfall.During months 6(Figures 74-78)and 9 (Figures 79-83), which had increases in rainfall and in moisture present in the soil, the data had a higher resolution for the graves and graves were able to be delineated in the field before processing.When imagery results for the graves each month is compared to the moisture data in Appendix E, there is an apparent correlation between moisture in the grid and the strength of delineation for the graves.

When comparing moisture levels, graves 1A and 1B consistently had higher water levels within the grave shaft (Table 12). The higher moisture levels likely increased the detection of these graves. This is supported by grave 1A having one of the strongest resolutions in the reflection profiles and grave 1B having the strongest resolution in the horizontal slices throughout the 12 months. While grave 2C, which produced the strongest response throughout

the research, had moderate moisture levels within the grave shaft, it was concluded that significant moisture was held within the tarpaulin which would have resulted in the higher resolution. The moisture present within the tarpaulin was unknown because moisture in the grave was only tested at the side of the grave shaft to ensure the burial scenarios were not disturbed.

The grave containing the pig carcass wrapped in a blanket (1C) and the grave containing a pig carcass covered by a layer of rocks (2B) had moderate moisture present within the grave shaft over the research period. However, these levels were lower than the other graves. The grave containing only the disturbed backfill also had lower moisture levels throughout the 12 months. This is likely due to the grave not containing a pig carcass and therefore not having decomposition fluids present. The lower levels of moisture in these graves corresponds with the lower resolution produced by the graves.

Soil

Soil is an important factor to consider when testing the applicability of GPR to detect clandestine graves (Martin 2010; Schultz et al. 2006; and Schultz 2008). Schultz et al. (2006) and Schultz (2008) conclude that graves in soil which was predominately sandy were detected up to 21.5 months without difficulty due to a strong contrast between the body and the sandy soils. Schultz et al. (2006) also found that soil horizons comprised of clay or other denser soils can decrease the penetration of radar waves and limit the detection of subsurface features present. The dominantsoil present in this research grid was classified as Pomello series, which is moderately-well drained soil which is sandy throughout (Doolittle and Schellentrager 1989; Leighty 1989). Due to the sandy consistency, the soil likely had a minimal effect on the ability to discern the features present. A spodic horizon, a subsurface horizon characterized by an accumulation of amorphous materials(Brady and Weil 1999), was present below the floor of the

graves.However, due to the shallow depth of the graves the soil horizon had no affect on the results of this research. Previous research has shown that this type of soil had little effect on the GPR signal or the detection of burial features(Martin 2010).

Conclusion

This controlled research illustrated that the use of GPR with a 500 MHz antenna is a valuable option in the detection of gravescontaining small pig carcasses in common burial scenarios. In addition, this research has also shown that data processing software and multiple imagery options, reflection profiles and horizontal slices, provide maximum delineation of subsurface features. For the duration of the 12 months, the pig carcass wrapped in tarpaulin (2C) produced the best resolution out of all the graves. The graves containing a pig carcass covered by a layer of rocks (2B) and a pig carcass wrapped in a blanket (1C) produced the poorest responses. The grave containing only a pig carcass (1A) produced the second greatest resolution out of all the graves. This data suggests that the additional items in the burial scenarios did not always increase the delineation, which is evident by the high resolution and strong detection of the burial scenario only containing a pig carcass. Further, the low demarcation of blank control grave(2A), only containing disturbed backfill, illustrated that the hyperbolic reflection features were primarily the result of the pig carcass and grave items, not the disturbed soil. Lastly, moisture played a large role in delineation of the graves. Low soil moisture levels resulted in decreased resolution of the hyperbolic features and additional processing was required in order to demarcate the graves. Months with moderate to high levels of moisture resulted in an increased resolution and delineation of the graves.

Overall, this research has shown the strong applicability of GPR in the detection of small pig carcasses in shallow graves representing various burial scenarios using a 500 MHz antenna.

While there are some limiting factors when utilizing this technology, such as soil moisture and length of internment, the controlled research presented here has demonstrated the broad applicability of GPR in the detection of subsurface features.

CHAPTER THREE: DETECTING VARIOUS BURIAL SCENERIOS IN A CONTROLLED SETTING USING A GROUND PENETRATING RADAR WITH A 250 MHz ANTENNA

Introduction

Increased credibility and knowledge of geophysical search methods has led toground penetrating radar (GPR) being broadly accepted in the field of forensics as a useful tool in locating buried bodies or evidence. Forensic cases which have used GPR demonstrate the ability of this tool to either locate buried bodies or clear suspected areas where a body or evidence was thought to be located (Calkin et al. 1995; Hammon et al. 2000; Instanes et al. 2004; Mellett 1992; Parker et al. 2009; Schultz and Dupras 2008). In proper conditions, GPR offers law enforcement investigators an accurate means to search for burials through the detection of subsurface anomalies present within the site. Due to GPR being a noninvasive geophysical tool, searches of a site can be conducted with little to no damage to the site or associated evidence. In addition, GPR can save time and resources by clearing areas suspected of containing a body or evidence (Dupras et al. 2006).

Controlled research utilizing GPR has been conducted in order to demonstrate the ability this tool to locate bodies (France et al. 1992; Freeland et al. 2003; Hammon et al. 2000; Koppenjan et al. 2003; Schultz 2007; Schultz 2008; Schultz et al. 2006). Controlled research using GPR in a forensic context typically employs burying pig carcasses as proxies for human remains. These cadavers are buried in known soils and monitored through GPR surveys for a period of time. Controlled research provides guidelines and experience for GPR operators which can be applied in actual forensic investigations. Although various controlled studies have been performed using GPR in forensic contexts, to date there has been few studies testing the applicability of GPR in different burial scenarios (Martin 2010). Ground penetrating radar

studies should incorporate real- life burial scenarios in order understand the applicability of GPR in forensic investigations (Dupras et al. 2006). Scenarios where the body is placed in the ground with additional grave items are important to study because these different materials will likely affect the detection due to changes in the signal and the resolution of anomalies. Martin (2010) tested the applicability of GPR to locate pig carcasses in common forensic burial scenarios over a 12 month period. However,this research used large carcasses buried in deep (1m) graves, which leaves a gap in current published literature regarding the detection of small bodies in shallow graves.

Purpose

The research presented will increase the knowledge gained through Martin (2010) by testing the applicability of ground penetrating radar to detect burial scenarios using small body size at shallower (0.5 m) depths. The goals will be (1) investigate the applicability of using GPR with a 250 MHz antenna to detect shallow burials that represent real-life scenarios, (2) identify which of the burial scenarios produces the greatestand poorest resolution for the 12 month monitoring period, (3) compare the results throughout the 12 month monitoring period using reflection profiles and horizontal slices.

Materials and Methods

Ground penetrating radar

Ground penetrating radar systems used in archaeology and forensic investigations typically use a monostatic antenna, where the transmitter and receiver are in the same unit (Dupras et al. 2006). A variety of monostatic antennae, differing in frequencies from 10 to 1000 megahertz (MHz), can be interchanged on the GPR unit (Conyers and Cameron 1998). The proper antenna frequency should be chosen depending primarily on the soil andsize of

theforensic target in question.Under ideal condition, low frequency antennas produce long wavelengths that are capable of penetrating up to 50 m. Due to the ability to penetrate deeper, low frequency antennas are only capable of resolving larger buried objects (Conyers and Cameron 1998). Conversely, high frequency antennae, such as an 800 MHz, provide a higher resolution allowing smaller objects, as small as a couple of centimeters in dimension, to be detected. However, high frequency antennae are not capable of penetrating as deep, typically limited to penetration of 1 m in depth (Conyers and Cameron 1998). The increased resolution in high frequency antennas may result in noise which can cause difficulties differentiating between true subsurface anomalies and clutter in the data (Schultz 2003). Schultz et al. (2006) suggests using the 500 MHz antenna due to the balance between depth of penetration and vertical resolution.

A standard GPR has three basic parts: a monostatic antenna, with a transmitter and receiver, the control unit, and a display monitor. Some models have a laptop with software to control the GPR which is used in place of the monitor. The display unit allows for the data collected to be observed in real time and for the investigator to determine the depth at which the anomaly was detected in the field. A GPR has an internal hard drive to store the data and allow it to be transferred to an external computer to be analyzed, processed, and printed (Schultz 2007).

When in the field there are multiple configurations for the GPR equipment. One option is to have an operator hand pull the antenna while the monitor is strapped with a harness to their body. This option can be performed with one or two people. The most common operation method is to use a cart that houses all the equipment and only requires one person to operate. The antenna is suspended from the middle of the cart, allowing it to skim over the ground. The monitor is mounted by the handle so the operator can easily read the output. The cart also has a

survey wheel built into one of the cart's wheels to allow for easy calculation of distance. Another option is to have the monitor in a stationary location operated by one individual while another individual hand pulls the antenna. Schultz (2007) states that this method is useful in areas where a cart cannot be utilized due to limited space, such as inside a home.

Ground penetrating radar uses electromagnetic pulses which are sent into the ground to read the composition of the subsurface. These pulses are transmitted by the antenna and arereflected and refracted off surface features, soil horizons, and buried items, and are then received by the antenna's receiver. Reflections occur when the velocity of the radar waves are altered due to differences in the physical and chemical properties of the subsurface material (Conyers 2006c; Conyers and Goodman 1997). The greater the electrical and magnetic properties of subsurface materials differ from surrounding material, that greater the strength and amplitude of the reflection waves (Conyers and Goodman 1997). Reflections occur when the antenna pulse encounters changes in relative dielectric permittivity, electrical conductivity, or magnetic permeability (Powers 1995). Soil, sediment, or rocks that are considered dielectric allow the passage of large amounts of electromagnetic energy with no dissipation. Material that is more electrically conductive is less dielectric therefore will have more dissipation at shallower depths, causing attenuation. High conductive material causes the wave to quickly dissipate (Conyers 2004). These radar reflections allow the GPR to detect anomalies that are in the ground, such as a changes in soil horizons or soil density, or a weapon or body (Schultz 2007).

The reflections are then detected by a receiver in the antenna and outputted on a screen to show the ground composition. These reflections are put together and processed in the control unit which produces an accurate two-dimensional image of the ground's stratigraphy and buried features, referred to as a reflection profile (Conyers 2006c). The x-axis of the two dimensional

profile represents the depth and the y-axis presents the distance of the transect. One advantage of this technology for forensic application is that theraw data, or imagery, can be interpreted in the field for reflections that may represent the forensic target in question (Table 8). On the screen, the anomaly will show up as hyperbolic shape in the two dimensional reflection profile. These hyperbolic shapes are what the GPR operator must be trained to recognize (Schultz 2007). A hyperbolic shape is formed because the pulse beam emitted penetrates into the ground in a conical pattern, as the signal goes deeper, the cone gets larger (Conyers and Goodman 1997). Due to the conical shape of the antenna penetration, objects in the ground are detected before the GPR is directly over them and after the GPR has passed over the area. The apex of the hyperbola represents the true location of the anomaly detected. The radiating sides, or tails, of the hyperbola are the result of reflected energy traveling to and away from the subsurface anomaly when the GPR is not directly over the object (Conyers 2006b; Schultz 2007). Tails are an artifact that can be removed with processing; however recognition of anomalies in the reflection profile is easier with the tails present. The depth of the anomaly is measured from the apex of the hyperbola because that is the moment when GPR is immediately over the subsurface object. Depth of anomalies represented in the reflection profiles are determined within the control unit by measuring the travel times of energy pulses (Conyers and Lucius 1996).

Table 8- Table displaying advantages and disadvantages of using GPR for forensic applications. Adapted from Schultz (2007).

Advantages	Disadvantages
Results displayed in real time in the field	Equipment is expensive
Can be used over blacktop or concrete	Operator must have specialized training
Can be used in snow or over fresh water	Site and soil conditions can affect GPR results
Data can be saved on hard drive for computer processing	Additional training necessary for computer processing
Depth and dimension of anomalies can be calculated	Data collection can be time consuming
Non-invasive	

Research Site and Controlled Graves

The research site is located in the Geotechnical Engineering Test Site on the main campus of the University of Central Florida (UCF) in Orlando (Figure 22). The site is secured by a locked chain link fence. A grid measuring 15 m on the north-south axis by 9 m on the east-west axis was set up containing six graves, arranged in two rows with three graves in each row (Figure 22). Five pig carcasses weighing between 25-26.7 kg (55-59 lbs.) were used as proxies for human bodies (Table 9 and Figure 21). The pig carcasses were euthanized on March 5, 2010 and brought back to UCF the same day and placed in graves that were dug on March 3, 2010. Each grave was 1 m x 0.75 m and 0.5 m deep. Grave 1A contained only the pig carcass. Grave 1B contained a pig carcass with 45 kg (100 lbs.) of calcitic and dolomite lime over the carcass. Once the pig carcass was placed in grave 1B, soil was added around the pig to level the depth of the grave to the shallowest part of the pig carcass. The lime was then evenly dispersed on top of the carcass and the remaining soil was used to fill in the grave. Grave 1C contained a pig carcass wrapped in a fleece blanket. Grave 2B contained a pig carcass under .05 m^3 (2 ft^3) of river rocks. Similar to the lime scenario, soil was added around the carcass to level the depth of the grave to

the shallowest part of the pig carcass. The rock was then evenly dispersed over the carcass and the grave was filled with the remaining soil. Grave 2C contained a pig carcass wrapped in tarpaulin. Grave 2A was used as a control hole and therefore only contained disturbed backfill. The control hole was used to compare data of a grave with just disturbed soil to the graves containing a body. Grave 1A was used as a control pig carcass and was used in order to compare data of a grave containing only a body with the graves containing additional material. These control holes were used to distinguish which component(s) of the grave, the disturbed soil, the body, or the additional material added to the grave, produced the geophysical response during GPR detection. The burial scenarios used in this research were modeled after the common forensic burial scenarios used in Martin (2010). Thus comparisons a can be made with Martin (2010) to study the effect of the controlled variables in grave detection.

Table 9- Detailed information for each burial

Grid location	Burial Date	Pig Weight (kg/lbs)	Depth of Unit	Scenario
1A	3/5/2010	26.76/59	0.5 m	Control pig carcass
1B	3/5/2010	25.4/56	0.5 m	Layer of 45 kg (100 lbs.) of Sunnilandcalcitic and dolomite lime over pig carcass
1C	3/5/2010	25.4/56	0.5 m	Pig carcass wrapped in fleece blanket
2A	3/5/2010	N/A	0.5 m	Control hole- no pig carcass
2B	3/5/2010	26.3/58	0.5 m	Layer of .05 cubic meters (2 cubic feet) of Vigoro stone river rocks over carcass
2C	3/5/2010	24.9/55	0.5 m	Pig carcass wrapped in 1.8 m x 1.8 m (6'x6') tarpaulin
Calibration unit (outside grid)	1/9/2009	N/A	1.0 m	Rebar hole

Figure 21- Various burial scenarios

Each pig carcass was placed in the grave on their left side with their back along the north wall and their head facing the east wall and each was placed relatively the same distance from each wall. Measurements were collected from the surface of the grave to the hind quarter, abdomen, shoulder, cheek, and snout of each carcass. Grave 1B, containing a layer of lime over the carcass, had an additional measurement collected from the surface to the center of the grave after the lime layer was added. Grave 2B, containing a layer of rocks over the carcass, had an additional measurement collected from the surface to the center of the grave after the layer of rocks was added (Table 10).

Table 10- Depths, in meters, from the ground surface to designated areas of the pig carcass

Grave	Hind quarter	Abdomen	Shoulder	Cheek	Snout
1A	0.35	0.33	0.33	0.41	0.46
1B*	0.33	0.30	0.32	0.38	0.38
2B**	0.34	0.29	0.32	0.38	0.46
1C	0.36	0.35	0.35	0.39	0.43
2C	0.33	0.31	0.31	0.39	0.41

*Measurement to center of grave with lime layer: 0.30 m
**Measurement to center of grave with rock layer: 0.26m

Permanent non-metal markers were placed at the corners of the grid for the exact position of survey lines could be replicated during each data collection. The marker at the NW corner of the grid was the 0 m, 0 m marker. Each grave also had a permanent non-metal marker in the NW corner to document the exact position of the each grave.

Figure 22-Research area at the Geotechnical Engineering Test Site (designated within square) on UCF main campus in Orlando, Florida. Site is located within the arboretum off Gemini Blvd. (seen on left)

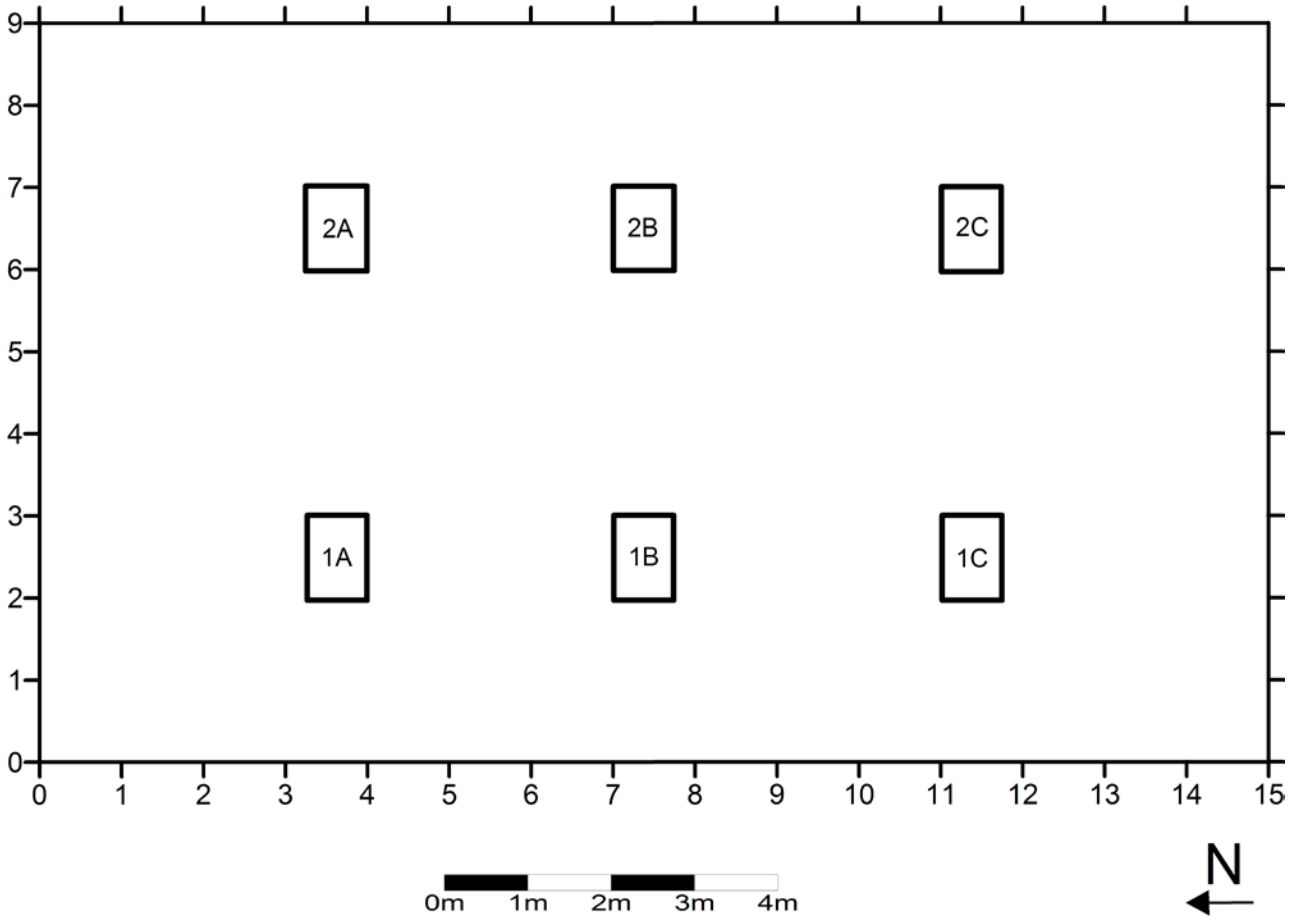

Figure 23- Geophysical Research Site Grid and Location of Burials

Data Collection

A Mala RAMAC X3M GPR unit was used in the research project (Figure 24). The GPR unit was used with a 250 MHz antenna integrated into a cart, which was hand pushed over the research grid. On February 23, 2010, pre-burial data was collected before the graves were dug to have anundisturbed comparison of the subsurface of the site. Datacollection was performed approximately every two weeks, during the middle and end of each month, for the duration of 12 months. Data was collected at 0.25 m transects in a north-south and east-west direction (Figures

25 and 26). By taking collections over a 12 month period it allowed data to be collected through all phases of decomposition.

Prior to each data collection event, the GPR unit was calibrated for fluctuations in the soil moisture of the research site. By using an object buried at the known depth, such as a metal pole, to calibrate the equipment, it can help determine the sensitivity of the GPR in the soil (Conyers 2004). This research employed a metal bar placed into an excavation wall at the depth of 1m. The calibration ensures the accurate estimation of depth of the reflection features located within the grid. The calibration pit is located approximately 3 m away from the west end of the research grid. To calibrate the GPR, data was collected over the calibration grave to calibrate the rebar to a depth of 1 m.

The soil moisture was also collected prior to each data collection event. The soil moisture was tested using a moisture meter manufactured by Lincoln Irrigation Incorporation. The meter measures the moisture in the soil on a scale from 1 to 10, 10 being the wettest. The moisture meter was calibrated to 10 occasionally by placing the tip of the probe into tap water. It is important to collect moisture measurements prior to data collection to determine how the soil moisture levels will affect the GPR imagery. The moisture was measured at the rebar hole and the 0 m, 0 m corner of each grave before each data collection.

Figure 24- Mala RAMAC X3M GPR unit integrated into a cart.

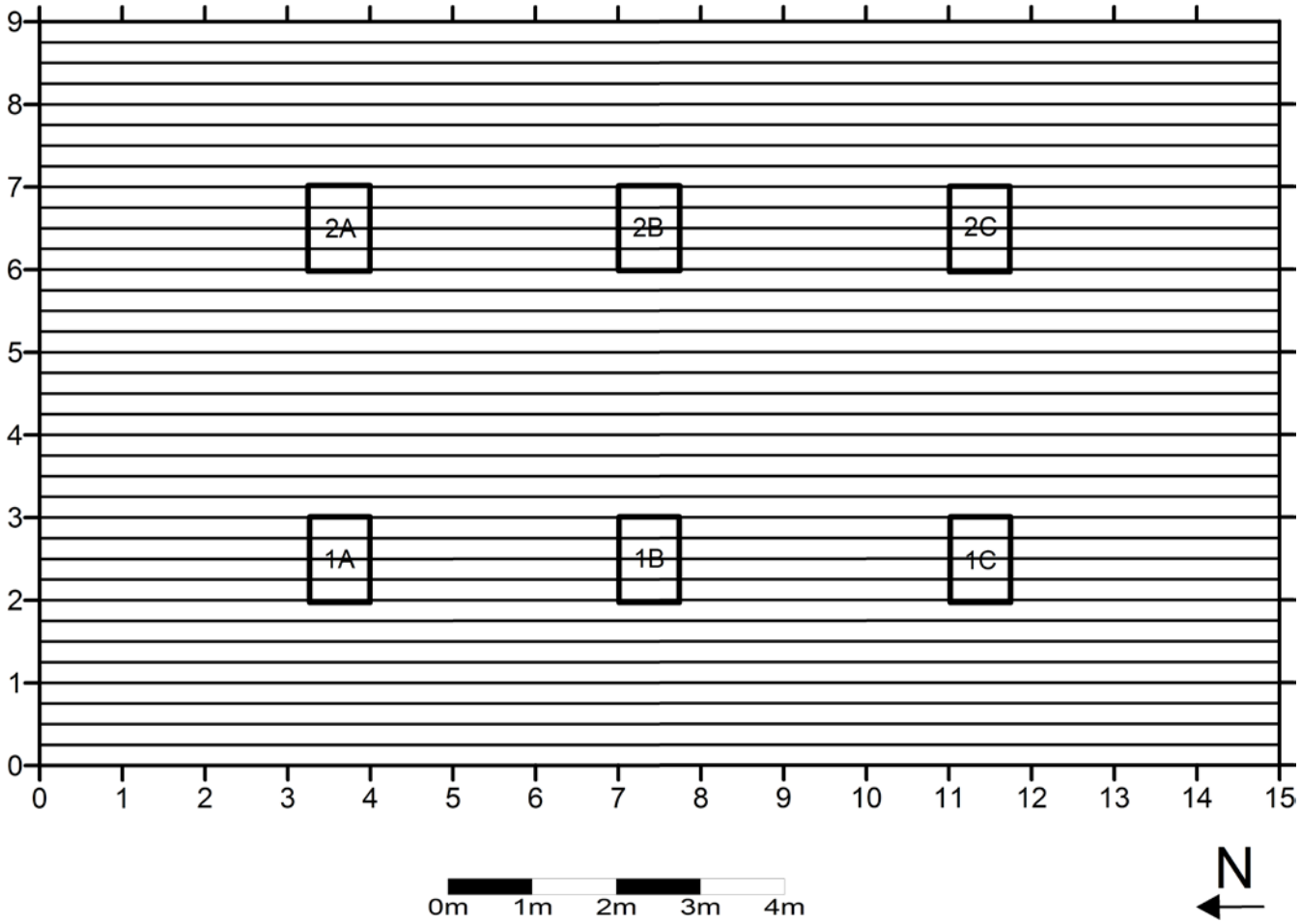

Figure 25- Geophysical Research Site Grid and Location of Burials with 0.25 m transects in North to South direction on X-axis.

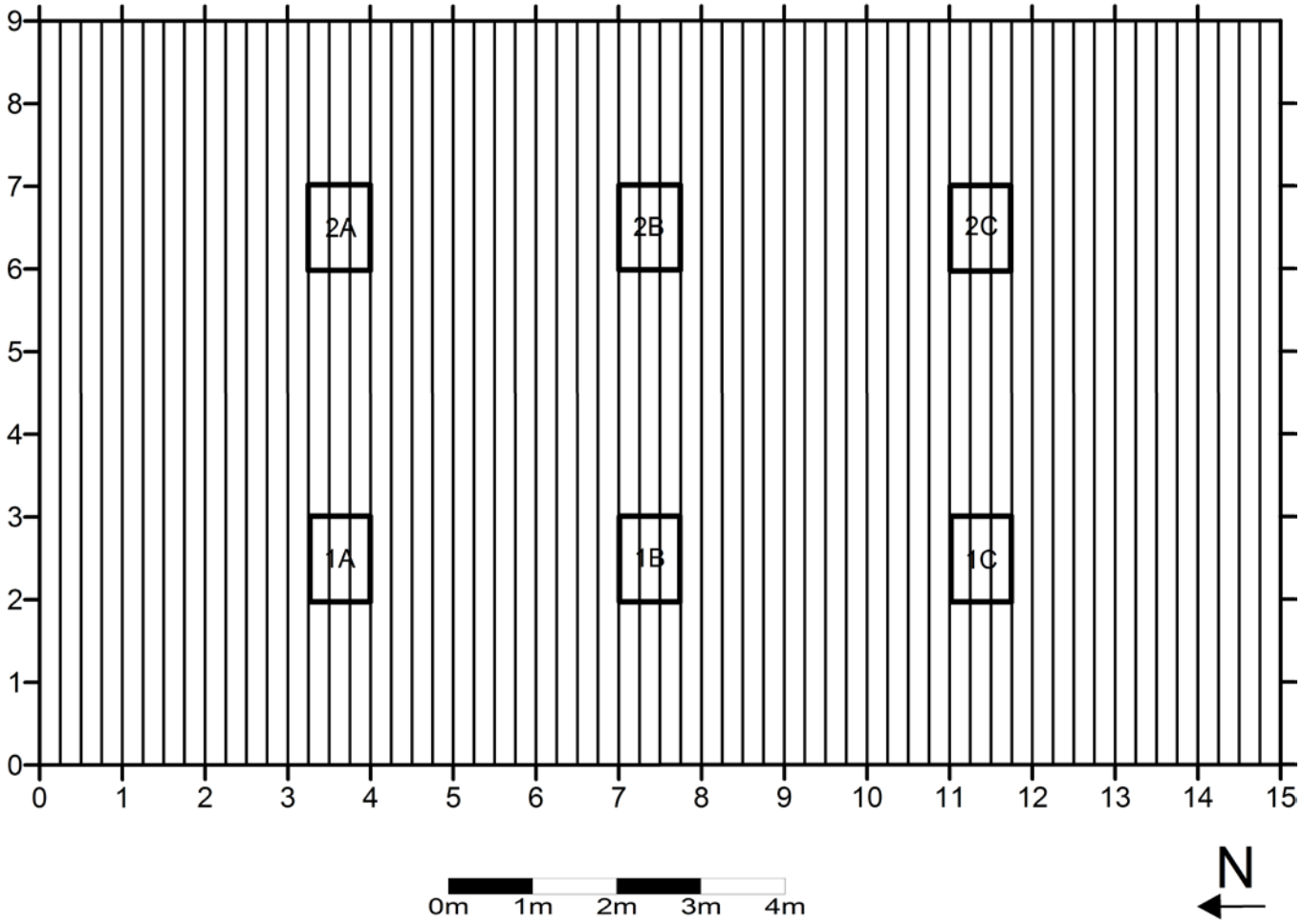

Figure 26- Geophysical Research Site Grid and Location of Burials with 0.25 m transects in East to West direction on Y-axis.

Data Processing

The last component of this research was processing and evaluating the data. All data collected was processed using REFLEXW, version 4.5. Processing provided an increased resolution of hyperbolic features and more advanced analysis of data.Using REFLEXW the data was processed into two different imagery options: reflection profiles and horizontal slices. Reflection profiles consisted of a single transect over the grid and represented length (left to right) and depth (top to bottom). The processing procedures for the reflection profiles completed in REFLEXW included scale correction, removal of horizontal banding, removal of high-

frequency noise, and increasing the gain. Scale correction allowed inconsistencies in antenna towing speed to be corrected by removing noise located at the top of the reflection profiles. Various filters, such as background removal and band pass frequency, were used to clean up the reflection profile image. Gain was added to each reflection profile to increase the visibility of subtle reflections (Conyers 2004).

Using REFLEXW 3-D analysis of all reflection profiles collected over the grid in either the X or Y direction were welded together to create a 3-D cube. REFLEXW was used for 3-D data analysis due to the program's increased detection and resolution of smaller subsurface features, such as the grave scenarios with small cadavers utilized in this study, represented in a horizontal slice. The same processing steps and filters used on reflection profiles were used on the 3-D analysis slice files to remove noise and clean up the data. In addition,a migration filter was applied on the data to remove the hyperbola tails so the anomalies viewed on the horizontal slices represented the actual size and depth of the detected grave feature. Slice maps are created horizontally by comparing amplitude variations in traces recorded in a certain time window, or depth. Each slice within the map shows the spatial distribution of amplitudes at a certain depth. Slice maps are important when surveying a site because, by displaying the distribution of reflected wave amplitudes, the map illustrates important subsurface changes in lithology or physical properties in the ground (Conyers 2006a). Areas exhibiting low amplitude waves in a slice map represent uniform soil matrixes. Areas exhibiting high amplitude waves represent areas with high subsurface contrast that could be indicative of buried features, voids, or a grave. These changes in amplitude are represented by a gray or color scale (Conyers 2006a). Horizontal slice is especially important to understanding the data because it provides a plan view representation of the data within the grid and at varying depths. Computer processing of GPR data can be

beneficial in forensic searches because byincreasing the accuracy of the representation of subsurface anomalies, it allows for easier detection of and comparison between anomalies.

Results

Reflection Profiles

The use of 0.25 m transects resulted in a total of five profiles collected over each grave in the NS direction. Each of the profiles collected over a grave exhibited noticeable differences in imagery characteristics after the data was processed. In the NS direction, reflection profile 1 represents the East wall of the grave, reflection profile 3 represents the middle of the grave, and reflection profile 5 represents the West wall of the grave.

After one month of burial, profile 1 demarcated all three graves present in row 1. However, the resolution was decreased when compared to other profiles (Figure 27). While profile 2 had a slightly better resolution than profile 1, the resolution was still reduced compared to other profiles (Figure 28). Profile 3, collected directly over the center of row 1, displayed four distinct reflection features (Figure 29). The feature produced by the burial containing only a pig carcass (1A) is more discernable than the rest. However, all features created by the graves are clearly discernable. The burial containing a pig carcass wrapped in a blanket (1C) had the weakest resolution out of the graves. The fourth feature was not created by a grave and likely represents a natural subsurface anomaly, such as a tree root or stump. While profile 4, similar to profile 2, displayed all profiles demarcated, the hyperbolic features were detected at a lower resolution than observed in profile 3 (Figure 30). Profile 5 exhibited all three graves, but graves 1B and 1C were not as clearly demarcated as in profile 3 (Figure 31). The third profile, collected over the middle of the grave where the back of the pig carcass was along the north wall and the

head towards the west wall, clearly resulted in the highest resolution of the reflection features out of the five profiles.

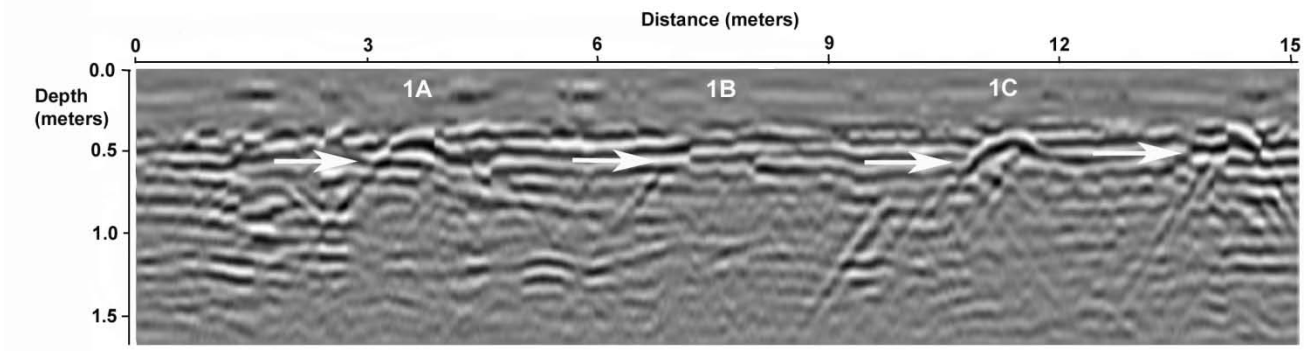

Figure 27- Processed GPR reflection profile using the 250 MHz antenna of row 1, NS, profile 1 for month 1

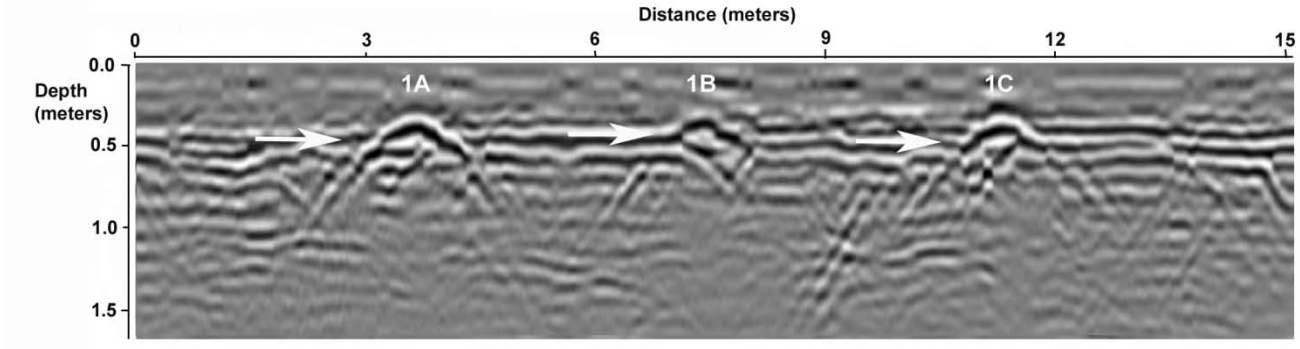

Figure 28- Processed GPR reflection profile using the 250 MHz antenna of row 1, NS, profile 2 for month 1

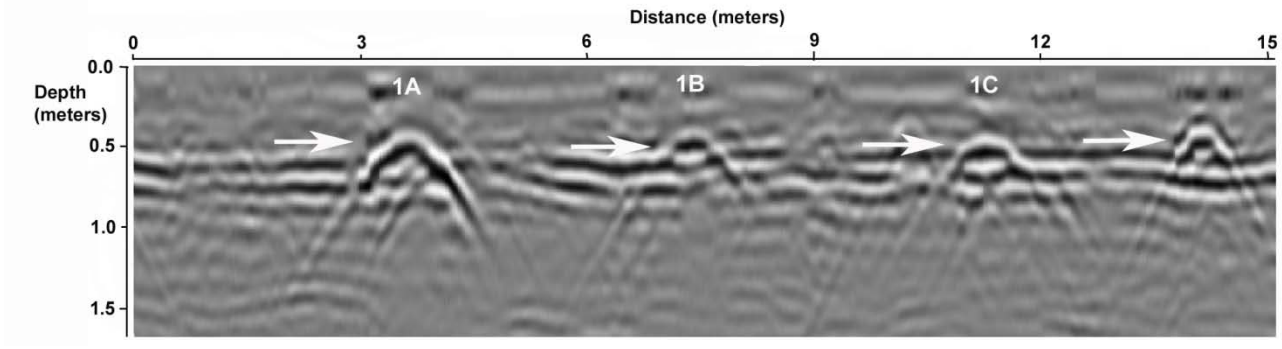

Figure 29- Processed GPR reflection profile using the 250 MHz antenna of row 1, NS, profile 3 for month 1

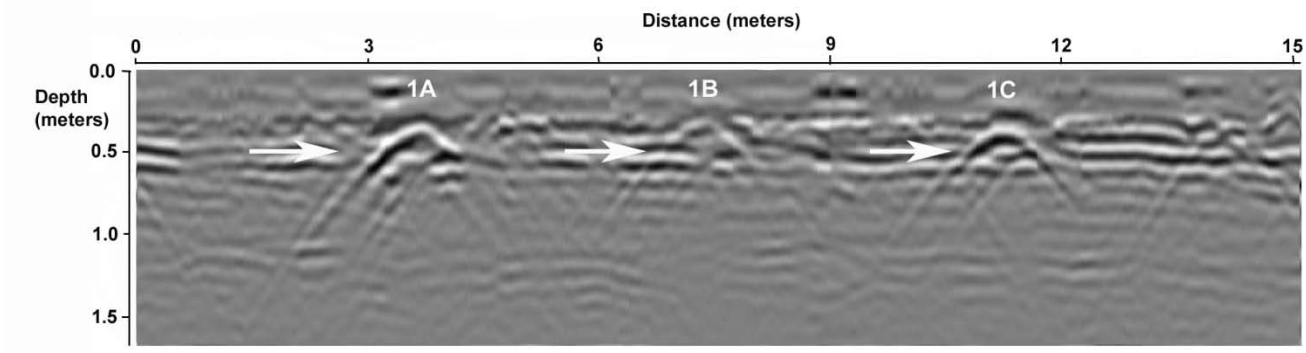

Figure 30- Processed GPR reflection profile using the 250 MHz antenna of row 1, NS, profile 4 for month 1

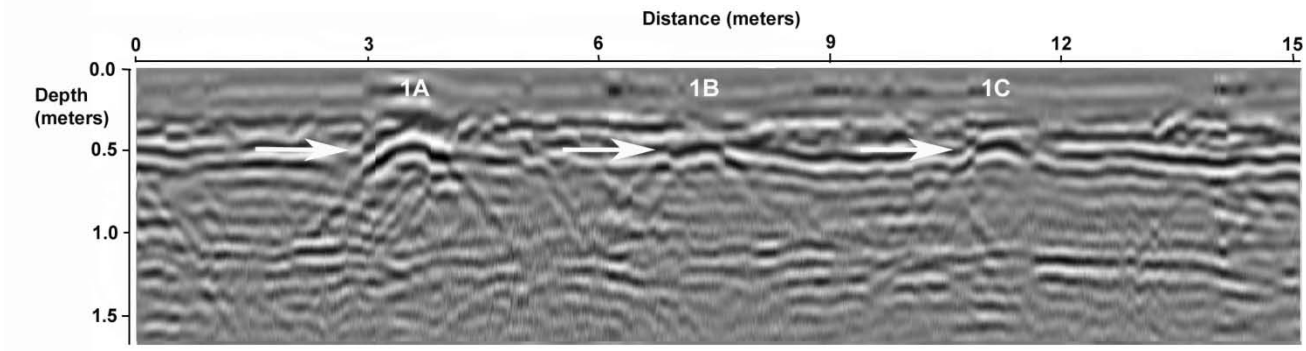

Figure 31- Processed GPR reflection profile using the 250 MHz antenna of row 1, NS, profile 5 for month 1

In grave row 2, profile 1 poorly demarcated all graves present in row 2 (Figure 32). While profile 2 exhibitedresponses from graves 2B and 2C, no response was present from grave 2A (Figure 33). Profile 3 produced three distinct hyperbolic features with strong resolutions which represented the three burial scenarios (Figure 34).The grave containing the pig carcass under a layer of rock (2B) had the strongest resolution. While the control grave, containing only disturbed backfill, had the weakest resolution, it was still clearly represented. Profile 4 exhibited graves 2B and 2C which were clearly demarcated. However these graves were displayed with a reduced resolution compared to profile three. Profile four displayed no response from grave 2A (Figure 35). While profile 5 exhibited response from graves 2B and 2C, this profile showed no response from grave 2A (Figure 36). Similar to row 1, the third profile, collected directly over

the middle of the graves, produced the best response, clearly demarcating the three grave scenarios after 1 month of burial.

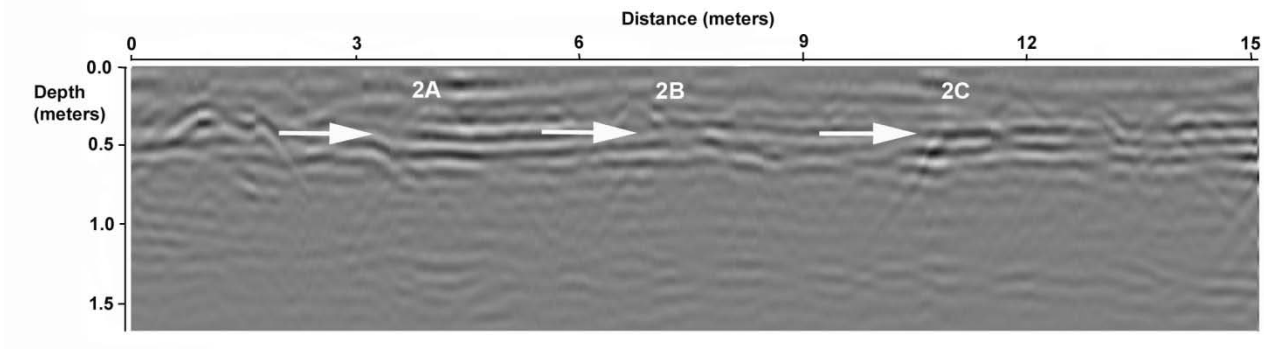

Figure 32- Processed GPR reflection profile using the 250 MHz antenna of Row 2, NS, profile 1 at 1 month

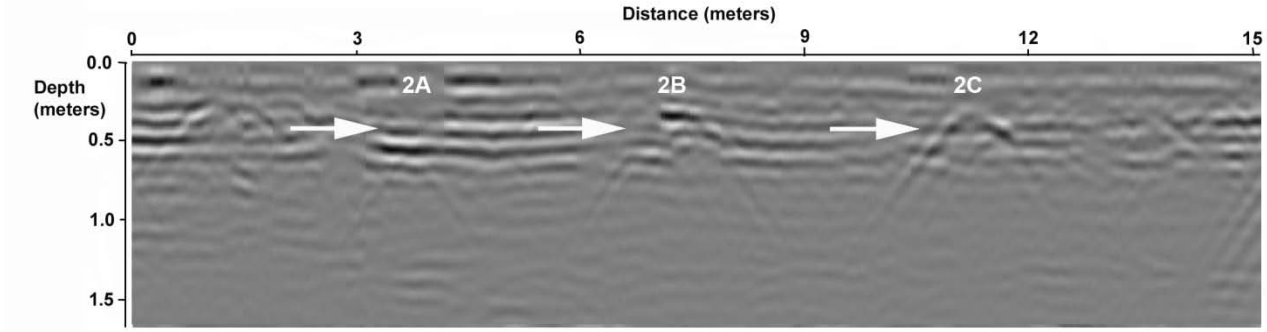

Figure 33- Processed GPR reflection profile using the 250 MHz antenna of Row 2, NS, profile 2 at 1 month

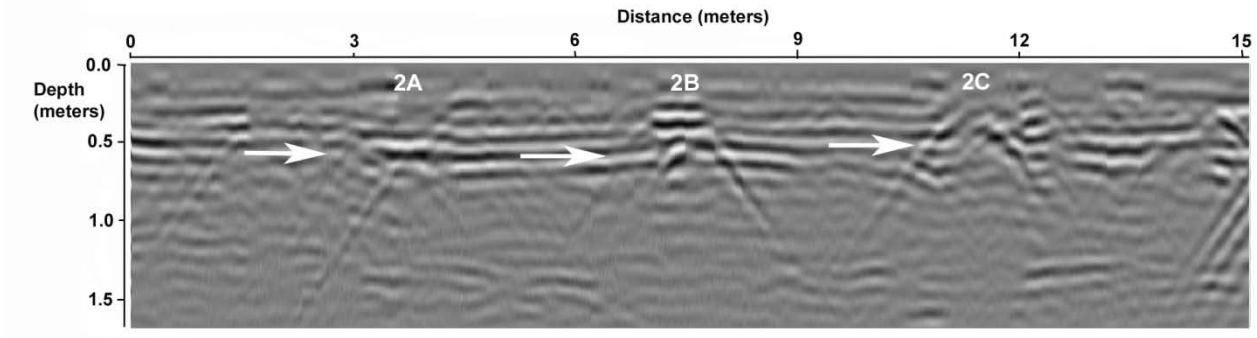

Figure 34- Processed GPR reflection profile using the 250 MHz antenna of Row 2, NS, profile 3 at 1 month

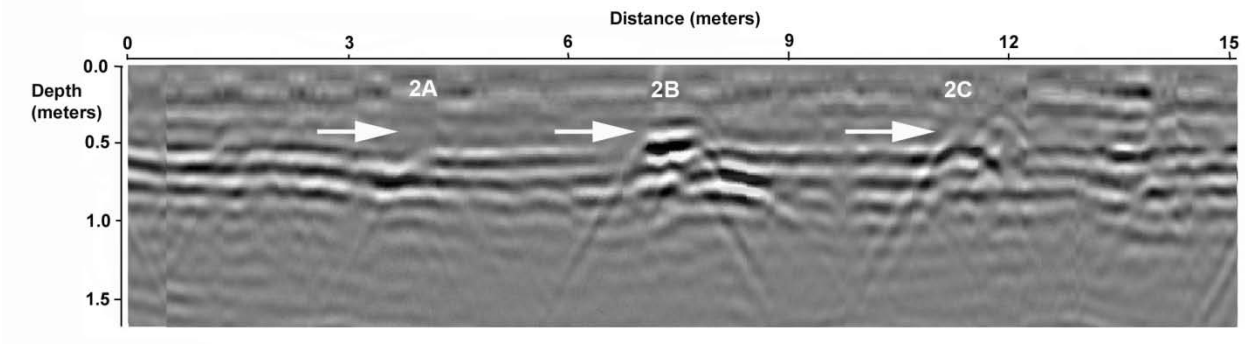

Figure 35- Processed GPR reflection profile using the 250 MHz antenna of Row 2, NS, profile 4 at 1 month

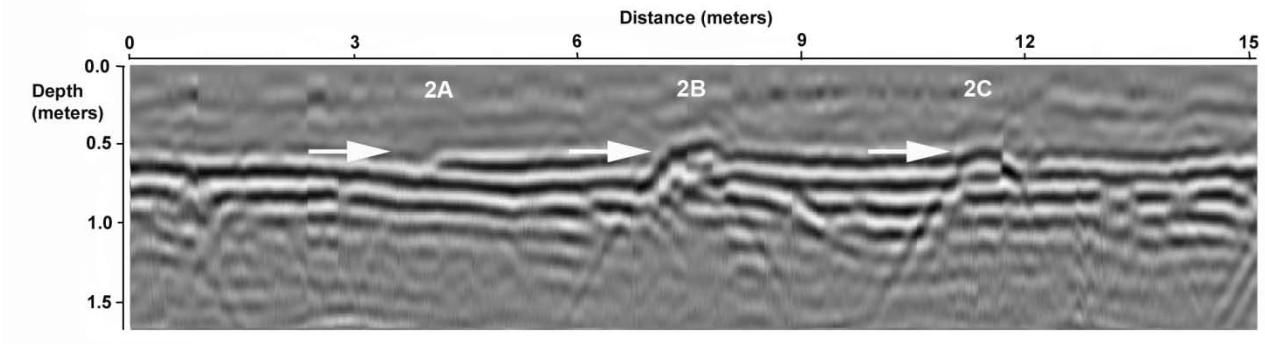

Figure 36- Processed GPR reflection profile using the 250 MHz antenna of Row 2, NS, profile 5 at 1 month

The processed reflection profiles collected directly over the center of the graves will be discussed in detail to demonstrate specific changes occurring throughout the 12 months of data collection. The results of this research only address profile 3 in row 1 and row 2 in the NS direction (Tables 11 and 12).Processed reflection profiles for the remainder of data collection, months 2-12, are located in Appendix C.

After 1 month of burial, the only noticeable change was with the control grave (2A), with a weak and barely discernable reflection feature. After month 2 the control grave was no longer detected and was not represented in the reflection profiles for the remainder of the data collection. The graves containing pig carcasses were all clearly discernable in month 2 reflection profiles. The grave containing only a pig carcass (1A) produced the strongest response.

After threeand fourmonths of burial the reflection profiles had weaker responses from all the gravesnonetheless the graves containing pig carcasses were all represented. During the third month all the reflection profiles of graves containing pig carcasses in burial scenarios had equally strong responses. During the fourth month, the grave containing a pig carcass covered by a layer of rocks had a slightly stronger response. This decrease in resolution during month 3 and 4 coincides with a decrease in resolution with the 500 MHz antenna and the horizontal slices for the 250 MHz antenna.

Reflection profiles for months 5 and 6 represented all the graves containing pig carcasses. For month 5 the grave containing a pig carcass wrapped in tarpaulin (2C) had the strongest resolution and was the most easily discerned scenario. The grave containing a pig wrapped in a blanket (1C) produced the weakest response during this month. During month 6, both the grave containing only a pig carcass (1A) and the grave containing a pig wrapped in tarpaulin (2C) produced the strongest reflections. The grave containing a pig carcass covered by a layer of rocks (2B) produced the weakest resolution for this month.

The reflection profiles for month 7 clearly demarcated all graves containing a pig carcass. During this month grave 2C produced the strongest resolution and was clearly discernable by the extended tails on the hyperbola. While grave the containing a pig carcass covered by a layer of rock (2B) produced the weakest resolution with minimal tails on the hyperbola, the grave was still clearly demarcated.

Month 8 reflectionsproduced weaker resolutionsthan in previous months. However, the graves scenarios were still demarcated. The decrease in delineation was likely due to moisture levels within the grid being noticeably lower than previous month due to a decrease in rainfall (see Appendix F). The decrease of moisture resulted in poor reflection features for all grave

scenarios except the grave containing a pig carcass wrapped in the tarpaulin (2C). Grave 2C had a strong response and was easily discernable with distinct tails on the hyperbola. During month 8, the graves containing a pig carcass wrapped in a blanket (1C) and a pig carcass covered by a layer of lime (1B) produced poor responses and were difficult to discern.

While there was an increase in resolution for month 9, the resolution was still lower than in months 1-7. During month 9, the grave containing only the pig carcass (1A) had the strongest resolution followed by the pig wrapped in tarpaulin (2C). Graves 1B and 1C produced the weakest responses. However, these graves were more easily discernable during month 9 than in month 8.

During month 10 there was a reduced response from all the graves except for graves 1A and 2C. The grave with the pig wrapped in tarpaulin (2C) produced the strongest response and was easily discernable. While the grave containing only a pig carcass (1A) was also easily discernable, the grave exhibiteda lower response than grave 2C. Graves 1B and 1C still produced the weakest responses.

During month 11 the grave containing a pig carcass wrapped in tarpaulin (2C) produced the strongest resolution with distinct hyperbolic tails. The grave containing only a pig carcass (1A) produced the second strongest resolution. While the graves containing pig carcass under a layer of lime (1B), under a layer of rock (2B), and wrapped in a blank (1C) were demarcated, the geophysical responses were poor compared to graves 1A and 2C.

During month 12 the grave containing a pig carcass wrapped in a tarpaulin continued to produce the strongest response. The grave containing only a pig carcass produced a weaker response compared to previous months. The graves containing a pig carcass wrapped in a blanket (1C) and only disturbed soil (2A) did not produced a response.

Table 11- Monthly imagery results for each burial scenario based on reflection profiles (250-MHz antenna)

Month	Burial Scenarios					
	1A	**1B**	**1C**	**2A**	**2B**	**2C**
1	Excellent	Excellent	Excellent	Poor	Good	Good
2	Excellent	Good	Excellent	None	Good	Excellent
3	Good	Poor	Poor	None	Good	Good
4	Good	Excellent	Poor	None	Good	Good
5	Good	Good	Good	None	Poor	Good
6	Good	Good	Good	None	Poor	Good
7	Good	Good	Good	None	Poor	Excellent
8	Good	Poor	None	None	Poor	Excellent
9	Good	Poor	Poor	None	Poor	Good
10	Good	Poor	None	None	Poor	Excellent
11	Good	Poor	None	None	Poor	Excellent
12	Poor	Poor	None	None	Good	Excellent

Table 12- Summary information describing the GPR reflection profiles with a 250-MHz antenna for each month of data collection

Month #	Overview of GPR Imagery Results
1	All graves in Row 1 produced excellent responses. Grave 1A produced the strongest response while the control grave produced the weakest response.
2	All graves containing pig carcasses produced excellent responses. Graves 1C and 2C produced the strongest response. The control grave was undetected.
3	All graves containing pig carcasses produced reduced responses. Graves 1A, 2B, and 2C produced the strongest responses. The control was undetected.
4	All graves containing pig carcasses produced good responses. Graves 1B and 2C produced the strongest responses. The control grave was undetected
5	All graves containing pig carcasses produced good responses. Grave 1C produced the weakest response. Grave 1B and 2C produced the strongest responses. The control grave was undetected
6	All graves containing pig carcasses produced good responses. Graves 1A and 2C produced the strongest response while grave 2B produced the weakest response. The control grave was undetected
7	All graves containing pig carcasses produced good responses. Graves 1A, 1B, and 2C produced the strongest responses while grave 2B produced the weakest response. The control grave was undetected
8	All graves containing pig carcasses produced reduced responses. Grave 2C produced the strongest response. While grave 1C produced the weakest response. The control grave was undetected
9	All graves containing pig carcasses produced reduced responses. Grave 1A produced the strongest response while grave 2B produced the weakest response. The control grave was undetected
10	All graves containing a pig carcass were discernable. Graves 1A and 2C produced the strongest response. The control grave was not detected.
11	All graves containing a pig carcass were discernable. Graves 2C produced the strongest response. Grave 1C produced the weakest response. The control grave was not detected.
12	All graves containing a pig carcass were discernable. Excellent detection of grave 2C while grave 1C produced a poor response. The control grave was not detected

Horizontal Slices

Using the software program REFLEXW, the transect data (reflection profiles) collected from the grid was processed using 3D data interpretation. The reflection profiles in either the X (NS) or Y (WE) direction were then appended together creating a 3D cube. Data between transects was interpolated within REFLEXW to create a solid cube. The cube can be cut in three different planes to view the grid data. The most common cut and the one used for this research was the horizontal slice, akin to a map view at different depths. These processed images provided plainview representations of the grid in either the X or Y direction. Grid data was collected prior to the construction of the graves to serve as a comparison with the data collected after burial. While there are a number of subsurface features present in the pre-burial horizontal slices, when the location of the graves is superimposed on the image it is evident that the features do not correspond with the locations of the six burials (Figure 37 and 38). The subsurface features present in the pre-burial data likely represent roots, stumps, or subsurface soil disturbances unrelated to the research.

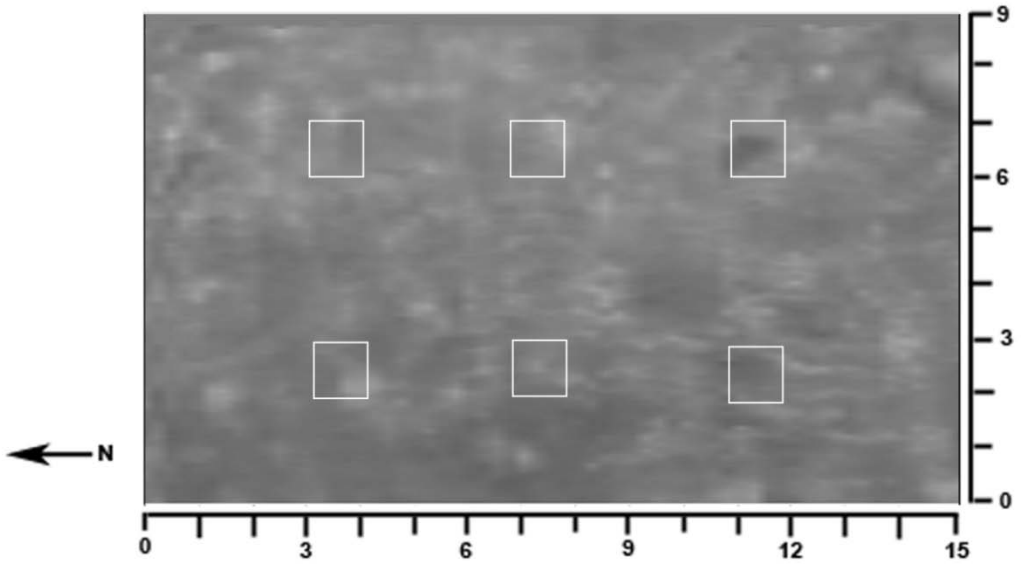

Figure 37- GPR preliminary horizontal slice in the X direction using the 250 MHz antenna. The horizontal slice is approximately 0.4 m in depth (8.13 ns)

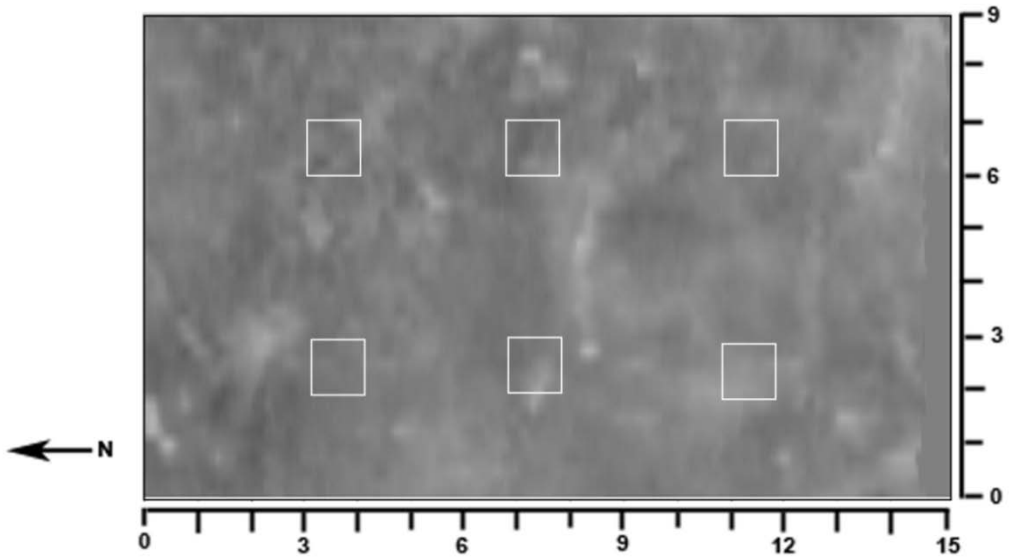

Figure 38- GPR preliminary horizontal slice in the X direction using the 250 MHz antenna. The horizontal slice is approximately 0.4 m in depth (8.13 ns)

When the location of the graves was superimposed on the horizontal slices for month 1 data, it is evident that the GPR was detecting the graves in the grid (Figures 39 and 40). The horizontal slices presented here and in appendix D represent varying depths, ranging from 0.3 m to 0.48 m. Each month is represented by X and Y direction horizontal slices. Both X and Y directions were considered when analyzing the data to determine the detection of the graves (Tables 13 and 14).

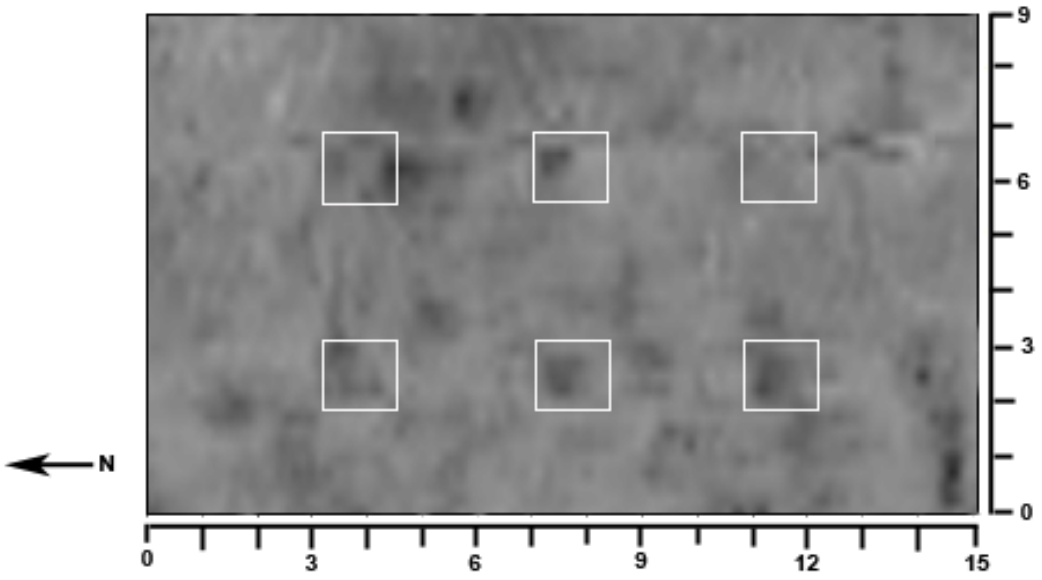

Figure 39- GPR horizontal slice in X direction using the 250 MHz antenna at 1 month. The horizontal slice is approximately 0.44 m in depth (8.935 ns)

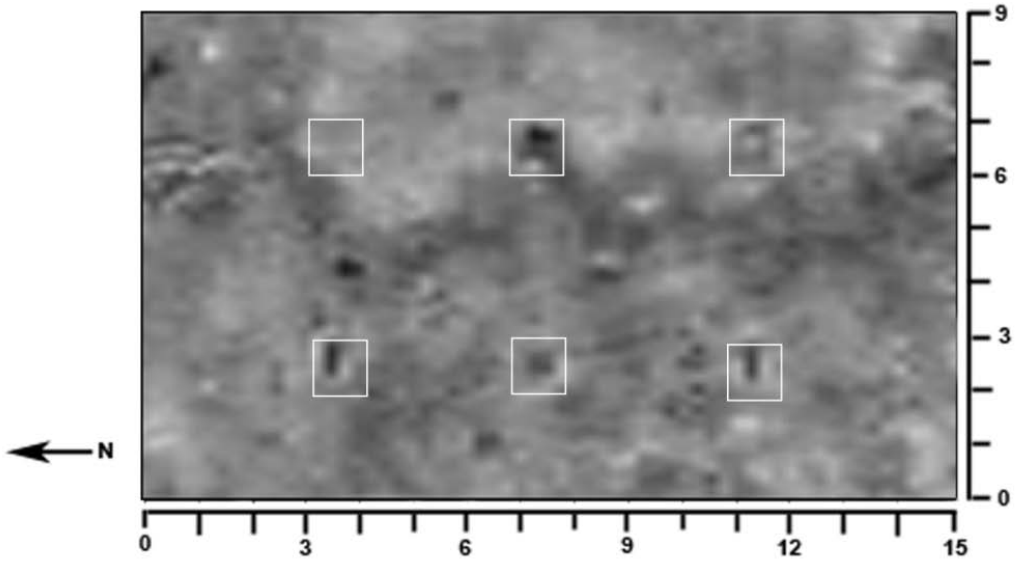

Figure 40- GPR horizontal slice in Y directionusing the 250 MHz antenna at 1 month. The horizontal slice is approximately 0.4.m in depth (8.13 ns)

After one month, all five of the burials containing a pig carcass are represented in the horizontal slice. The grave containing a pig carcass covered by a layer of rocks (2B) produced

the strongest resolution. The grave containing only the disturbed backfill (2A) was not represented in the horizontal slice. For the remaining months of data collection, the control grave was not discernable in the horizontal slices. As with the reflection profiles, the highly developed reflection of the graves containing a pig carcass in contrast to the lack of delineation of the control grave, suggests that the reflection features were created by the presence of a pig carcass and grave items, not the disturbed backfill.

Month 2 horizontal slices clearly demarcated all the graves containing pig carcasses. The graves containing a pig carcass covered by a layer of lime (1B) and under rock (2B) had the strongest responses. Similar results were seen in month 3 with grave 1B producing a slightly stronger resolution.

During months 4 and 5 there was a decrease in resolution for all the graves. However, the graves containing pig carcasses were demarcated. During month 4, grave 1B had the strongest resolution. As seen with the 500 MHz antenna, graves 1B and 2B have a stronger representation in the horizontal slice images than in the reflection profiles. During month 5, the grave containing a pig carcass wrapped in tarpaulin (2C) produced the strongest reflection. Also during this month the grave containing a pig carcass wrapped in a blanket (1C) produced a significantly weaker response than observed in previous months.

While months 6 and 7 resulted in a slight increase in resolution,this increase still lower than the resolution in the earlier months of data collection. During month 6, grave 2C still had the strongest response followed by the grave containing only a pig carcass (1A). During month 7, grave 2C had the strongest response and grave 1A had a substantially weaker response than the previous month. During both months, grave 1C had a slightly stronger response than in month 5.However, this response was still weaker overall.

Month 8exhibited a substantial decrease in resolution of the graves containing pig carcasses. While all graves were present in the data, the resolution was poor which made it hard to discern where the graves were located. Graves 2B and 2C were most easily discerned. However,these graves produced lower resolutions than in previous months. This decrease in response from the graves coincides with the decrease in response seen in the reflection profiles and is most likely attributed to the decrease in the soil moisture due to minimal rainfall during this month (Table 12).

During month 9 an increase in response was observed in all graves containing a pig carcass in the horizontal slices. Grave 1A had the strongest response this month and was more discernable than in previous months. Grave 1C also produced a significantly stronger resolution compared to months 5, 6, 7, and 8. The increase in resolution was likely a result of an increase in moisture due to higher rainfall during this month (Table 12).

During month 10, the only graves easily discernable were graves 1A, 1B, and 2C. The grave containing only a pig carcass (1A) produced the strongest response, followed by the grave containing a pig wrapped in tarpaulin (2C). The graves containing a pig carcass wrapped in a blanket (1C) and a pig carcass under rock (2B) produced minimal responses and were not discernable.

During month 11 the only graves easily discernable were graves 1B and 2C. The grave containing a pig wrapped in tarpaulin (2C) produced the strongest response followed by the grave containing a pig carcass under a layer of lime (1B). The grave containing a pig carcass under a layer of rock (2B) was barely discernable.

During month 12 the graves containing a pig carcass under a layer of lime (1B) and wrapped in a tarpaulin (2C) produced the strongest responses. The grave containing a pig carcass

under a layer of rock (2B) produced the weakest response. The grave containing only a pig carcass produced a weaker response compared to earlier months.

Table 13- Monthly imagery results for each burial scenario based on horizontal slices (250-MHz antenna)

Month	Burial Scenarios					
	1A	**1B**	**1C**	**2A**	**2B**	**2C**
1	Good	Good	Good	None	Poor	Poor
2	Good	Excellent	Excellent	None	Excellent	Good
3	Excellent	Excellent	Excellent	None	Good	Good
4	Poor	Good	Poor	None	Good	Poor
5	Good	Good	Poor	None	Poor	Good
6	Good	Good	Poor	None	Poor	Good
7	Poor	Good	Poor	None	Poor	Good
8	Poor	Poor	Poor	None	Good	Good
9	Excellent	Good	Excellent	None	Poor	Good
10	Good	Poor	Poor	None	Poor	Good
11	Poor	Good	Poor	None	Poor	Good
12	Poor	Excellent	Good	None	Poor	Good

Table 14- Summary information describing the GPR horizontal slices with a 250-MHz antenna for each month of data collection

Month #	Overview of GPR Imagery Results
1	Graves 1A and 2B produced the strongest response while graves 1B and 2A produced the weakest responses.
2	All graves containing a pig carcass produced responses. Graves 1C and 2C produced the strongest responses. The control grave was not detected.
3	All graves containing a pig carcass produced excellent responses. The grave 1B and 2C produced the strongest responses. The control grave was not detected.
4	All graves containing a pig carcass produced good responses. Grave 2B produced the strongest response. The control grave was not detected.
5	All graves containing a pig carcass produced good responses. Grave 1B and 2C produced the strongest responses. The control grave was not detected.
6	All graves containing a pig carcass produced reduced responses. Graves 1A, 1B, and 2C produced the strongest responses. The control grave was not detected.
7	All graves containing a pig carcass produced reduced responses. Grave 1B and 2C produced the strongest responses. The control grave was not detected.
8	All graves containing a Grave produced reduced responses. The control grave was not detected.
9	All graves containing a pig carcass produced good responses. Graves 1A and 2C produced the strongest responses. The control grave was not detected.
10	All graves containing a pig carcass were discernable. Graves 1A, 1B, and 2C produced the strongest response. The control grave was not detected.
11	All graves containing a pig carcass were discernable. Graves 1B and 2C produced the strongest response while grave 2B produced the weakest response. The control was not detected.
12	All graves containing a pig carcass were discernable. Graves 1B and 2C produced the strongest responses while the grave containing a pig carcass under a layer of rock produced the weakest response.

Discussion

While the use of a 250 MHz antenna in GPR controlled research in a forensic setting is limited, research has found that the deeper penetration with lower resolution results in easier discrimination of the forensic targets without noise in the data (Martin 2010; Schultz and Martin 2011). These findings were supported in this research with the 250 MHz antenna producing lower clutter in the reflection profiles and horizontal slices while maintaining an easy detection of all the burial scenarios. The responses for each of the burial scenarios resulted in easily delineated reflection features represented by significant hyperbolic tails the majority of the 12 months. Multiple burial characteristics affected the detection of the burials in this study: the various burial scenarios in which the bodies were placed, the moisture present in the soil, the properties of the soil, and the imagery options utilized to process the data. These factors will be discussed in detail.

Burial Scenarios

The250 MHz antenna resulted in all the graves containing a pig carcass being detected for the duration of the 12 month period monitoring period in both the reflection profiles and horizontal slices.While the detection was better for some graves then others, for the duration of the research all graves containing a pig carcass where detected. The grave containing a pig carcass wrapped in a tarpaulin (2C) provided the best resolution throughout the data collection, followed by the grave containing only a pig carcass (1A). Grave 2C scenario produced good or excellent results in the 12 months when viewing the reflection profiles and in 11of the 12 months when viewing the horizontal slices. Grave 2C produced the best results because of the moisture being retained around the pig carcass due to the tarpaulin and The increased resolution was due to the tarpaulin retaining moisture around the pig carcass, and moisture from rain water that

likely pooled on the top of the tarpaulin**.** Also due to the thickness of the tarpaulin, the decomposition rate of the pig carcass was likely slowed and the decomposition fluid would be contained around the carcass for a longer period of time**.**The additional moisture present, even after 12 months of burial, would create a stronger geophysical response. The grave containing only a pig carcass(1A) produced the second highest geophysical response throughout the 12 months. This scenario produced excellent or good results in all of the 12 months of data collection in the reflection profiles and in 9 of the 12 months in the horizontal slices. Contrary to results from previous research (Martin 2010), the high resolution of grave 1A in this research demonstrated that additional grave items did not necessarily increase the ability of the grave to be detected at a shallow depth. The graves containing a pig carcass covered by a layer of lime (1B) and a pig carcass covered by a layer of rocks (2B) were both detected throughout the 12 months of monitoring. However, these graves produced lower resolution than graves 1A and 2C. The pig carcass covered by a layer of lime (1B) had a stronger resolution than the pig carcass covered by a layer of rocks (2B). Again, this is likely due to the increase in moisture in grave 1B due to the lime retaining moisture(Table15). The grave containing the disturbed backfill was only detected the first month of data collection(Figure 124) and after 1 month was no longer detected. This is likely due to the eventual soil compaction within the grave shaft.

The horizontal slice data is consistent with the conclusion that additional grave items did not necessarily increase the ability to detect the graves. While the grave containing a pig carcass covered by a layer of lime (1B) had the highest resolution throughout the 12 months, all the graves containing a pig carcass were easily delineated. The grave containing only disturbed backfill (2A) was never delineated within the horizontal slice images.

Imagery Options

Reflection profiles and horizontal slices were utilized in this research because these options provided maximum resolution and detection of the graves (Martin 2010). The combination of these two imagery options resulted in additional data for interpretation more than just a single imagery option. The reflection profiles were beneficial because they represented the graves as a whole and accurately depicted the depth of each anomaly. The reflection profiles were also better in illustrating changes which occurred in each burial scenario from month to month. Horizontal slices depicted all transects in either the X or Y direction and represented the entire grid at any given depth. Tight transect spacing of only 0.25 m was utilized for the collection of the reflection profiles. When incorporating all the reflection profiles into a grid survey, the computer program will create a 3D cube that includes interpolating the space between transects. The tighter transects results in an increased resolution of small features within the grid (Conyers 2006B). The cube can be cut in three different planes to view the grid data. The most common cut and the one used for this research is the horizontal slice, akin to a map view at different depths. Horizontal slices allowed for an easy comparison between all the graves and allowed subsurface features within the entire grid to be analyzed at a single depth. By using data processing computer software and both reflection profiles and horizontal slices, the data collected was able to be analyzed as thoroughly and as accurately as possible.

Overall, with the 250 MHz antenna, the reflection profiles provided more accurate results for each of the burial scenarios. However, the benefit of using two imagery options was evidentwhen comparing the responses from each grave. Some graves were better detected in the reflection profiles while others were better detected in the horizontal slices. While the grave containing only a pig carcass (1A) was easily detected each month in the reflection profiles,

fourout of the twelve months this grave had a poor resolution in the horizontal slices. In comparison, the graves containing a pig carcass under rock (2B) and covered by a layer of lime (1B) were better detected month to month in the horizontal slices and not the reflection profiles. These differences in the detection between the imagery options may be due to how the spacing between transects are interpreted within the horizontal slices. The spaces between each of the grid slices were interpolated and therefore may mask subsurface features. This is why small transect spacing was used when collecting data for this research. Important data may be missed with large transect spacing and therefore small transect spacing should be used in GPR surveys to ensure accuracy. The reflection profiles were beneficial to this data analysis made because each grave produced a unique feature every time the GPR was passed over the area and no interpolations where necessary.

Moisture

The soil moisture present within a search area has been proven to have a substantial effect on the delineation of graves when using GPR (Doolittle and Bellantoni 2009; Martin 2010). Doolittle and Bellantoni (2009) found that soil moisture can improve the detection of graves. However, the research also suggested that heavily saturated soils can restrict penetration and reduce the detection of subsurface anomalies. The research presented here confirms the effect of moisture on the applicability of GPR. Table X in Appendix E gives the moisture levels for each grave every month. Month 8 resulted in the poorest resolution for all the graves and the data required significant processing in order to delineate features(Figures 148-152), this coincides with a decrease in rainfall and a decrease in moisture present in the soil. During months 6 (Figures 158-162) and 9 (Figures 163-167), which had increases in rainfall and in moisture present in the soil, the data had a higher resolution and the graves were able to be

delineated in the field before processing. When imagery results for the graves each month is compared to the moisture data in Appendix E, there is an apparent correlation between moisture in the grid and the strength of delineation for the graves.

When looking at moisture levels graves 1A and 1B consistently had higher water levels within the grave shaft. This likely increased the detection of these graves, which is supported by grave 1A producing one of the strongest resolutions in the reflection profiles and grave 1B producing the strongest resolution in the horizontal slices throughout the 12 months. Grave 2C, which produced the strongest response throughout the research, had moderate moisture levels within the grave shaft. However, it is believed that significant moisture was held within the tarpaulin which would have created the high resolution. The moisture present within the tarpaulin was unknown because the water meter was only probed into the side of the grave shaft as to not disturb the pig carcasses. The grave containing the pig carcass wrapped in a blanket had moderate moisture present within the grave shaft over the research period; however these levels were lower than the other graves. The same is true for the grave containing the pig carcass covered by a layer of rocks. The grave containing only the disturbed backfill had lower moisture levels through the 12 months. This is likely due to not having decomposition fluids present and the lack of additional items within the grave to retain moisture.

Soil

Soil is an important factor to consider when testing the applicability of GPR to detect clandestine graves (Martin 2010; Schultz et al. 2006; and Schultz 2008). Schultz et al. (2006) and Schultz (2008) conclude that graves in soil which consisted of mainly sand were detected up to 21.5 months with little difficulty due to a strong contrast between the body and surrounding soils. Schultz et al. (2006) also found that soil horizons comprised of clay or other denser soils

can decrease the penetration of radar waves and limit the detection of subsurface features present. The dominant soil present in this research grid was classified as a pomello series, which is moderately-well drained soil which is sandy throughout (Doolittle and Schellentrager 1989; Leighty 1989). Due to the sandy consistency, the soil likely had a minimal effect on the ability to discern the features present. A spodic horizon, a subsurface horizon characterized by an accumulation of amorphous materials (Brady and Weil 1999), was present below the floor of the graves.While there was a clear spodic horizon present in the reflection profiles, the graves were located above this horizon and therefore this dense horizon had little effect on the data collected.

Conclusion

Controlled forensic research plays an important role in the use of GPR with a 250 MHz antenna in detecting buried bodies that mimic real-life forensic scenarios. Due to the limited published literature on the ability of the 250 MHz antenna to detect graves in a forensic setting, the results of this research are valuable to the knowledge of the use of GPR to detect clandestine burials. Further, this research has shown through the use of different burial scenarios and multiple imagery options, the 250 MHz antenna is an excellent geophysical resource which can accurately detect clandestine burials in common forensic scenarios. Due to the increased depth penetration and easier discrimination of large targets, such as a body, the 250 MHz antenna is a good resource when searching for burials. This research also exhibited how vital processing data collected in the field with computer software is to the detection of hyperbolic features. In multiple cases throughout this research, particularly during months of limited rain, computer processing allowed subsurface features to be detected that were not visible in the field. Processing in the lab allows for maximum delineation and an increased accuracy. In addition,

multiple imagery options provided maximum delineation of the subsurface features and therefore multiple options should be utilized in forensic investigations to maximize the results.

Overall, the pig carcass wrapped in tarpaulin (2C) produced the best resolution out of all the graves containing pig carcasses. The pig carcass covered by a layer of rocks (2B) and the pig carcass wrapped in a blanket (1C) produced the poorest responses. The grave containing only a pig carcass produced the second highest resolution out of all the graves throughout the 12 months. With these results, it is demonstrated that the additional grave items in the graves containing burial scenarios did not always increase the delineation, which is evidenced by the high resolution of the burial scenarios only containing a pig carcass. Further, the blank control grave (2A), only containing disturbed soil, was imperative in demonstrating that the reflection features were predominantly a result of the pig carcass and not the disturbed backfill.

CHAPTER FOUR: OVERVIEW OF RESULTS AND COMPARISON OF THE 500 MHz AND THE 250 MHz ANTENNA

Multiple components affect the detection of the burials used in this study such as the various burial scenarios in which the bodies were placed, the degree of soil moisture, the physical and chemical properties of the soil, antenna choice, and the imagery options utilized to process the data. Discussed below is the comparison between the 250 and 500 MHz antennae, the results of burial scenarios, the results of multiple imagery options, the effect of moisture on the detection of the graves, and guidelines for using GPR in forensic searches.

Antenna Comparison

Previous publishedresearch has demonstrated that GPR surveys in both forensic cases and controlled research have used antenna frequencies ranging the full spectrum of 80-900 MHz. Midrange frequency antennae, typically 400/500 MHz, are the most commonly utilized antenna frequency in controlled research (Freeland et al. 2003; Schultz et al. 2006; Schultz and Dupras 2008; Strongman 1992) and forensic searches (Mellett 1992; Ruffell 2005; Schultz 2007). Midrange frequencies are utilized because they provide a balance between resolution and depth penetration. High frequency antennae, such as 800/900 MHz, provide high resolution but reduced depth penetration. While the high resolution can detect small objects, the resolution can also result in clutter in the data which may make it difficult to accurately detect subsurface targets (Ruffel 2005). Conversely, lower frequency antennae (100/200 MHz) provide deeper penetration and reduced resolution. While the reduced resolution of lower frequency antennae limits the detection of smaller objects, the lower resolution results in less clutter in the data. In forensic investigations where there is substantial subsurface clutter or limitations in the penetration of EM waves due to soil, lower frequency antennae are typically utilized

(Nobes1999; Ruffell 2005). Regardless of the common use of GPR in forensic investigations and numerous controlled research studies, there have been limited studies which directly compare the performances of lower frequency antenna with the commonly utilized500 MHz antenna.

The data collected during this research was used totest and compare the performance of the 250 MHz antenna with the commonly used 500 MHz antenna in the detection of the same grave targets. The data collected was processed in REFLEXW through 2D and 3D analyzes. Reflection profiles and horizontal slices of the data were used to compare the results from each antenna.

The data collected during this research project demonstrated that either antenna, the 250 MHz or the 500 MHz, would be appropriate when conducting a search for shallow clandestine graves containing small pig carcasses for a 12 month period in pomello series soil. For the duration of 12 months of data collection, both antennae delineated the graves within the reflection profiles and horizontal slices when processed in REFLEXW. The 250 MHz data initially provided a higher resolution for each grave within the first few months. Month 2 data from the 250 MHz antenna resulted in the best delineation of the graves throughout the 12 month collection period(Figures 128-132). Over time the 250 MHz antenna produced decreased resolution for the graves. However, even with this decrease the graves were still delineated. The targets in this research were large enough that the decrease in resolution associated with the deeper penetration of the 250 MHz antenna did not significantly affect the detection of the graves. While the 500 MHz antenna was able to delineate the graves in the first few months, the data had a lower resolution than the 250 MHz data. As time progressed, the higher detail provided by the 500 MHz data consistently resulted in more easily discernable reflections than the 250 MHz data. While either antenna would be a good option when searching for shallow

clandestine graves, this research, and previous research (Schultz 2008; Schultz et al. 2006; Strongman 1992), has demonstrated that the 500 MHz may be a better option when searching for shallow burials containing small cadavers depending on soil conditions and size of the forensic target. If time warrants, GPR surveys should be conducted using both antennae.

Scenarios and Imagery Options

Real-life burial scenarios were used in this research to determine which component of the grave, the disturbed soil, the pig carcass, or the additional graves items, was detected. Through an evaluation of the reflection profiles and horizontal slices throughout the 12 months of data collection, it is evident that the pig wrapped in tarpaulin (2C) consistently produced the highest resolution and clearest delineation (Table 15). The graves containing a pig carcass covered by a layer of rocks (2B) and a pig carcass wrapped in a blanket (1C) produced the poorest responses out of the graves containing pig carcasses (Table 15). The grave containing only a pig carcass (1A) produced the second highest resolution out of all the graves (Table 15).This is not surprising because previous research (Schultz 2008), has demonstrated that a grave containing only a pig carcass at a shallow depth can be detected for nearly two years in sandy soils. Contrary to results from previous research (Martin 2010), the high resolution detection of grave 1A in this research demonstrates that additional grave items did not necessarily increase the ability of the grave to be detected at a shallow depth. However, the low demarcation of blank control grave (2A), containing only disturbed backfill, supported Martin (2010) demonstrating that the reflection features were primarily a result of the pig carcass and grave items, not the disturbed soil.

Table 15- Overview of detection results

Burial Scenarios	Overview of GPR imagery Results
1A (Only pig carcass)	Good results for duration of the 12 months with both antennae. Increased resolution in the reflection profiles.
1B (Lime)	Poor detection the majority of the months in reflection profiles. Good detection in horizontal slices. Minimal difference in detection between antennae.
1C (Blanket)	Poor detection in both reflection profiles and horizontal slices for the majority of the 12 months. Minimal difference in detection between antennae.
1A (Control)	Only detected first 2 months in reflection profiles. Never detected in horizontal slices. Minimal difference in detection between antennae.
1B (Rocks)	Good detection for the first 6 months in reflection profiles and horizontal slices. Poor detection for the remainder of the 12 months. Minimal difference in detection between antennae.
1C (Tarpaulin)	Excellent detection in both reflection profiles and horizontal slices for the duration of the 12 months. Minimal difference in detection between antennae.

In addition, this research supports Martin (2010) demonstrating that data processing software and multiple imagery options, including reflection profiles and horizontal slices, provides maximum delineation of the features and increases the accuracy with which subsurface anomalies are identified. Reflection profiles and horizontal slices were utilized in this research and the combination of these two imagery options resulted in maximum data for interpretation. The reflection profiles were beneficial because they represented the graves as a whole and accurately depicted the depth of each anomaly. Horizontal slices allowed for an easy comparison between all the graves as well as subsurface features within the entire grid to be analyzed at a single depth. Multiple imagery options were imperative to this research because certain graves were detected best through reflection profiles while other graves were detected more accurately through horizontal slices. For example, the grave containing only a pig carcass (1A) was better discerned in the reflection profiles, while the grave containing a pig carcass under a layer of lime (1B) was more easily discerned in the horizontal slices.

Lastly, moisture played a large role in delineation of the graves. Low moisture levels in the soil resulted in decreased resolution and delineation of the burial scenarios. During months of low moisture levels, additional processing was required in order to demarcate the graves. Graves were not able to be delineated in the field during these months. Moderate to high levels of moisture typically resulted in high resolution and easy delineation of the graves, both in the field and after processing.

Guidelines

In addition to testing the applicability of GPR in the detection of clandestine graves, this research was also able to demonstrate guidelines which should be used when conducting a forensic GPR survey. First, this research has demonstrated the importance of having a forensic anthropologist or archaeologist with experience using geophysical tools, such as GPR, at a forensic scene to assist in the search. The operation of GPR requires training in the field as well as in data processing in the lab. Forensic archaeologists should have experience in geophysical surveys to not only potentially locate anomalies which may be of interest, but also clear areas subjected of containinga body. Next, the data collected for this research shows the importance of a tight transect spacing, typically no more than 0.25m, when conducting a geophysical survey.If the transect spacing is too wide the forensic target may not be detected. Transect spacing should be determined by the size of the suspected target. Knowing the target size also ensures the operator will choose an antenna of the proper frequency. In addition, it is important for the GPR operator to have as much knowledge as possible about the forensic target and the site. The time since burial, the burial depth, and the any associated grave artifacts may also have an effect on the geophysical response and should be noted prior to conducting a GPR survey. This research also demonstrated the importance of properly calibrating the GPR unit to the soil and conditions

of the site.Calibration was especially important to this research due to the shallow depth of the graves. Lastly, it is imperative that any data collected be taken back to a lab and processed through computer software. Computer processing in the lab allows for maximum delineation of any anomalies and provides increased resolution.

Conclusions

Ground-penetrating radar (GPR) can be a useful geophysical instrument in the search and detection of clandestine graves in a forensic context. Controlled research forensic archaeology has demonstrated the usefulness of GPR and is vital for improving GPR search techniques. The main goal of this research was to evaluate the ability of GPR, using 250 MHz and 500 MHz antennae, to locate shallow graves containing small pig cadavers in various burial scenarios over a twelve month period. The results demonstrate that the additional grave items did not always increase the detection of the grave for this monitoring period. Further, the low demarcation of the grave containing disturbed backfill illustrated that the hyperbolic reflection features were the result of the pig carcasses and not the disturbed soil. Soil moisture played a substantial role in the detection of the graves with higher soil moisture producing increased resolution of the graves. In addition, computer processing and multiple imagery options used in this research increased the detection of the graves. In terms of antenna performance, the 250 MHz data initially provided a higher resolution within the first few months. However, over time the higher detail provided by the 500 MHz data consistently resulted in easily discernable reflections.

APPENDIX A: GROUND PENETRATING RADAR 500-MHZ REFLECTION PROFILES

MONTH 1

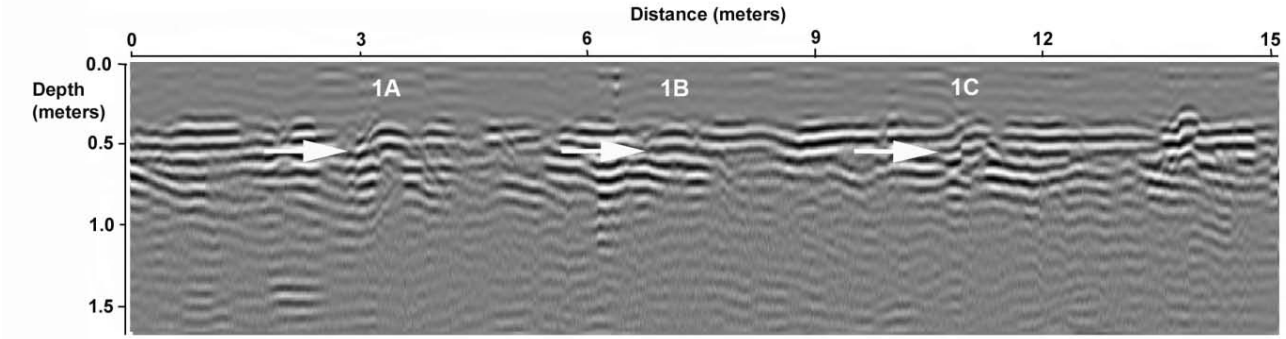

Figure 41: GPR reflection profile using the 500-MHz antenna of Row 1 at 1 month

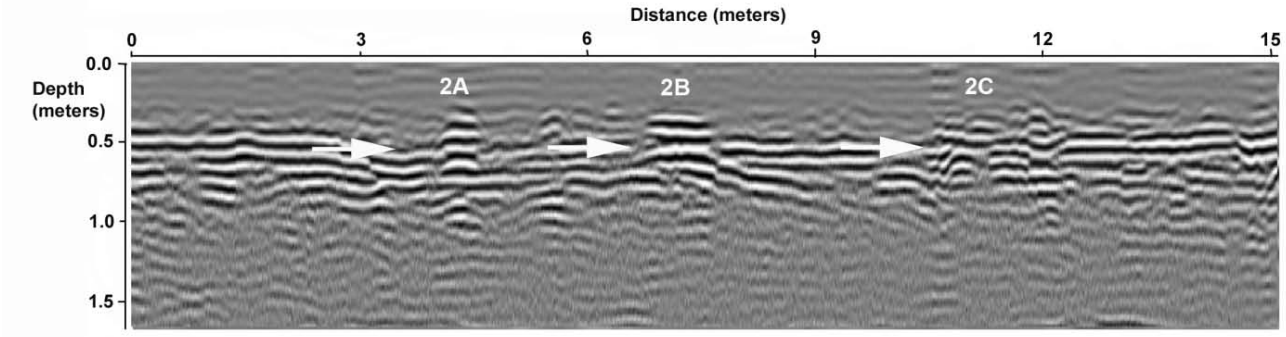

Figure 42: GPR reflection profile using the 500-MHz antenna of Row 2 at 1 month

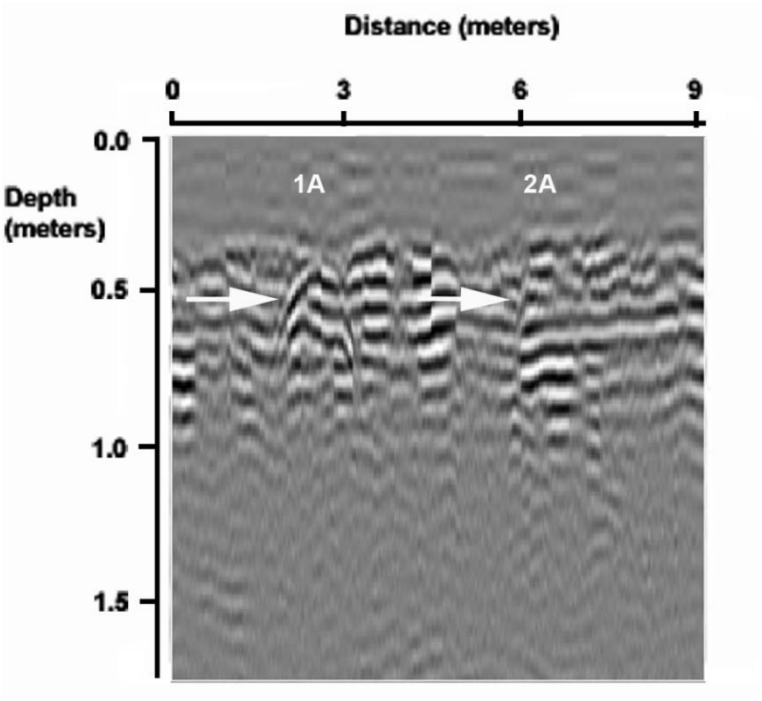

Figure 43: GPR reflection profile using the 500-MHz antenna of Row 1A2A at 1 month

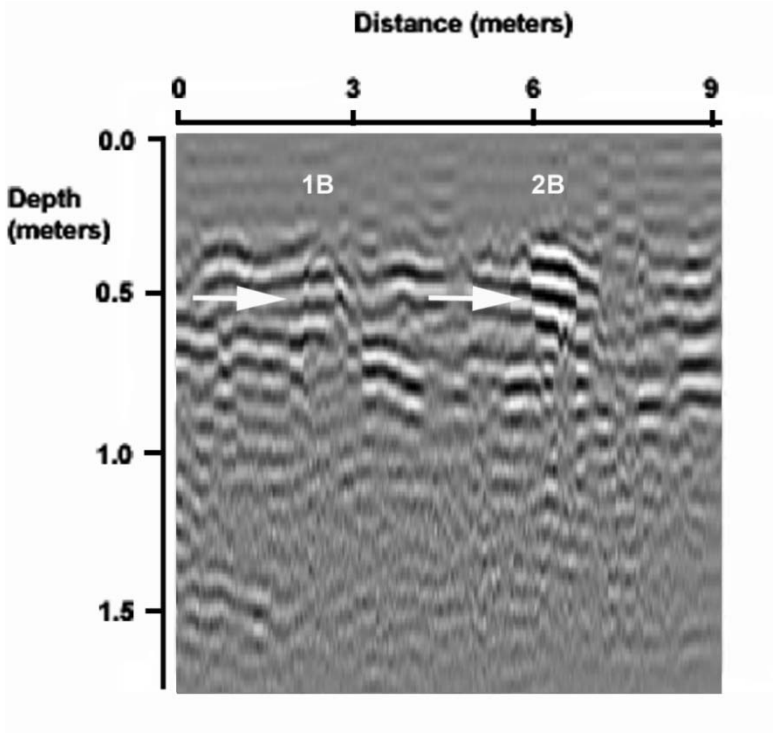

Figure 44: GPR reflection profile using the 500-MHz antenna of Row 1B2B at 1 month

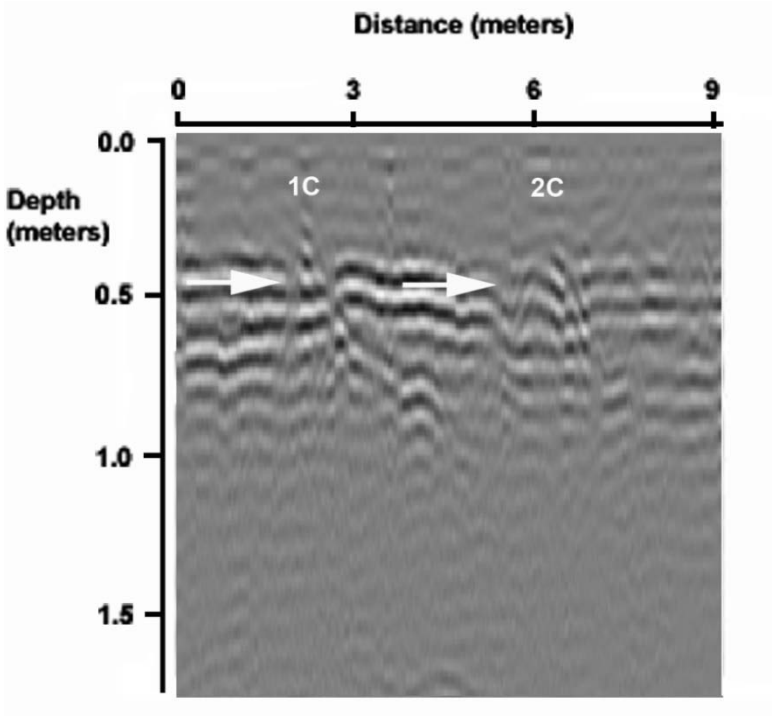

Figure 45: GPR reflection profile using the 500-MHz antenna of Row 1C2C at 1 month

2 MONTH

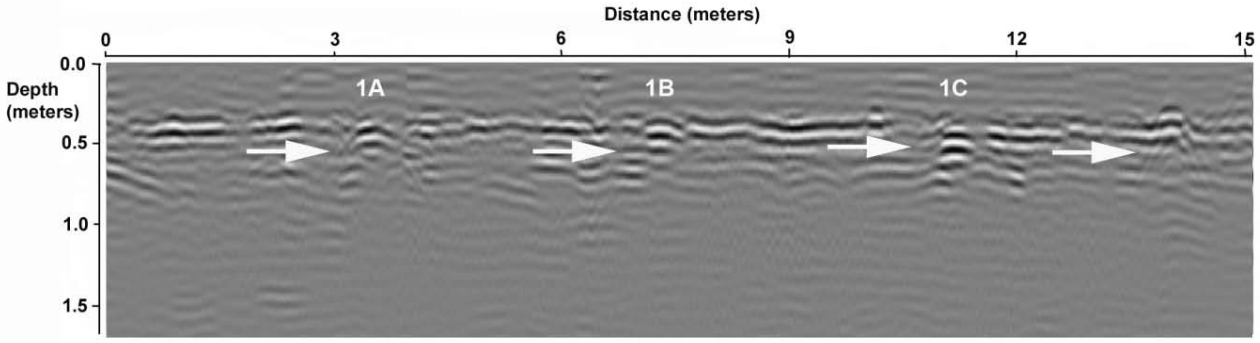

Figure 46: GPR reflection profile using the 500-MHz antenna of Row 1 at 2 months

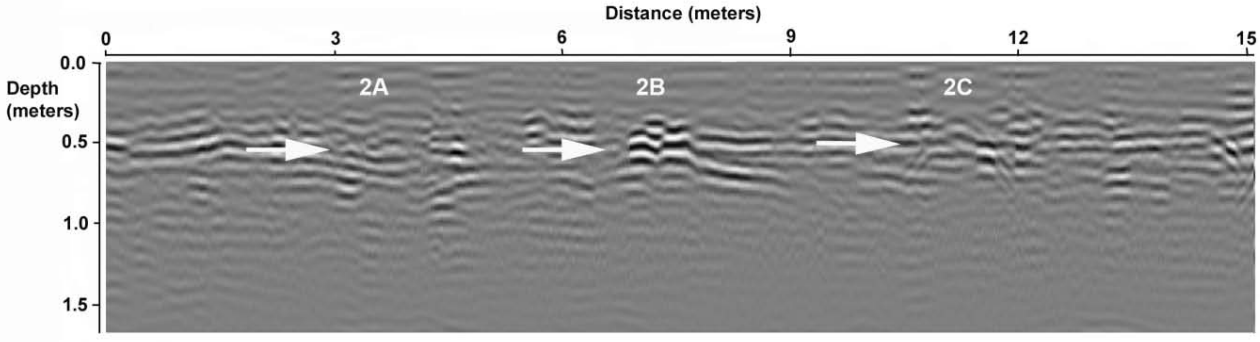

Figure 47: GPR reflection profile using the 500-MHz antenna of Row 2 at 2 months

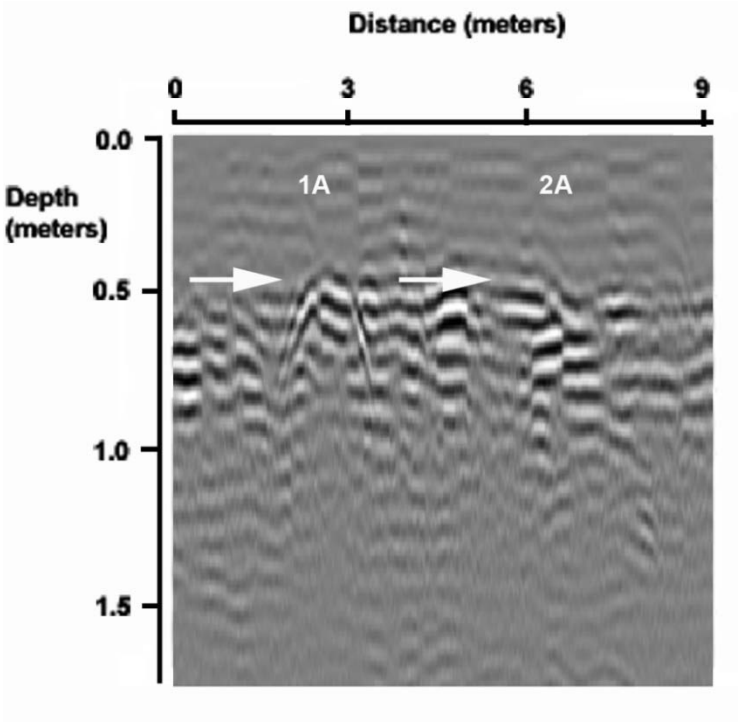

Figure 48: GPR reflection profile using the 500-MHz antenna of Row 1A2A at 2 months

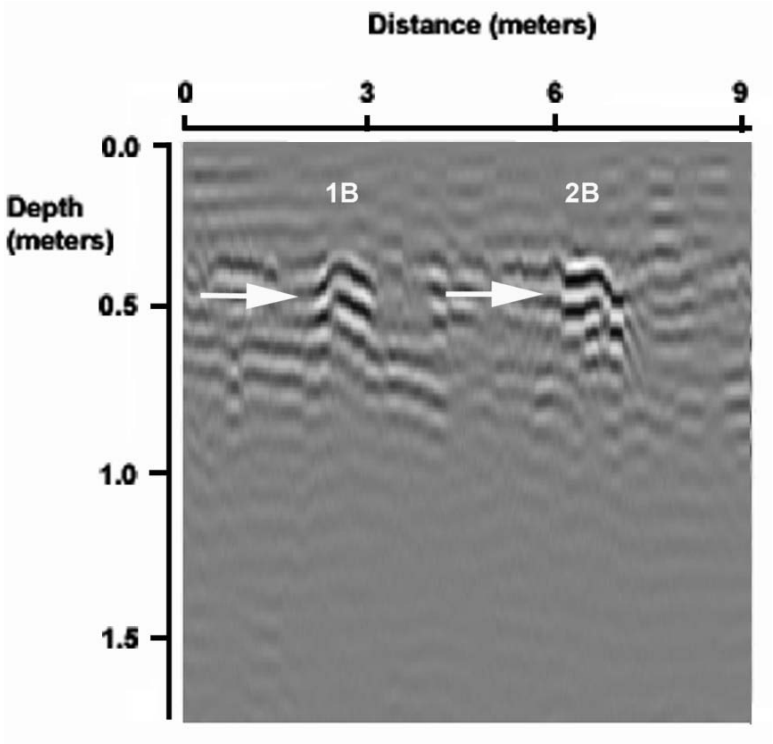

Figure 49: GPR reflection profile using the 500-MHz antenna of Row 1B2B at 2 months

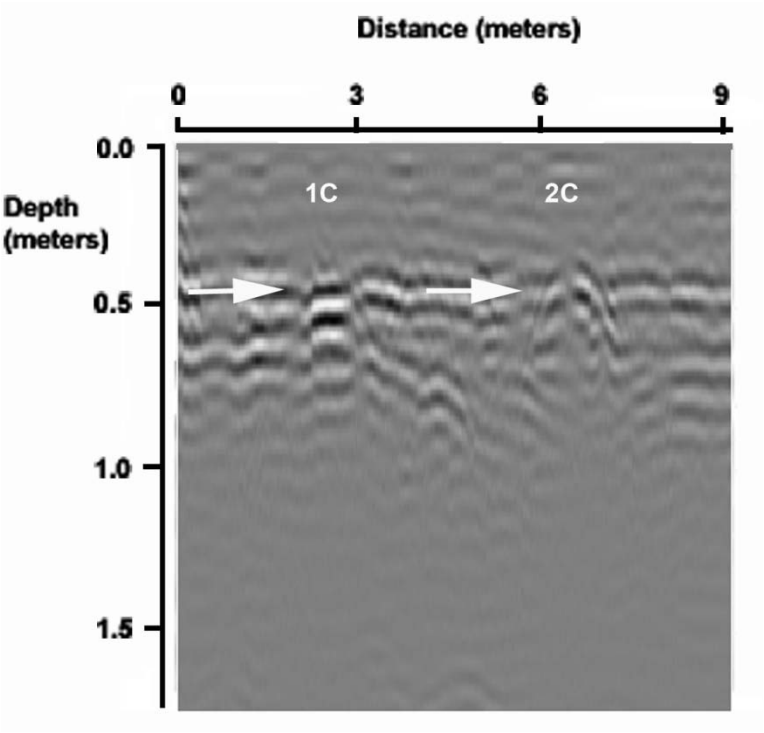

Figure 50: GPR reflection profile using the 500-MHz antenna of Row 1C2C at 2 months

3 MONTH

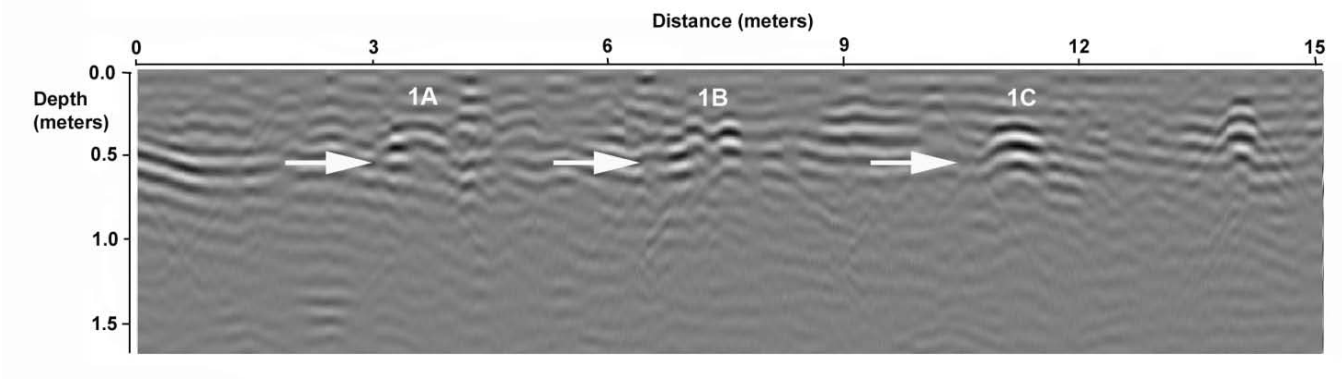

Figure 51: GPR reflection profile using the 500-MHz antenna of Row 1 at 3 months

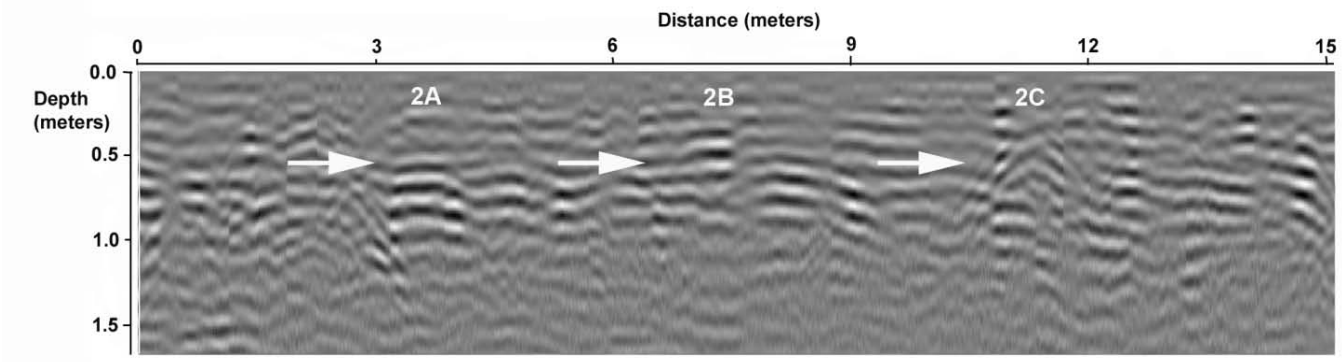

Figure 52: GPR reflection profile using the 500-MHz antenna of Row 2 at 3 months

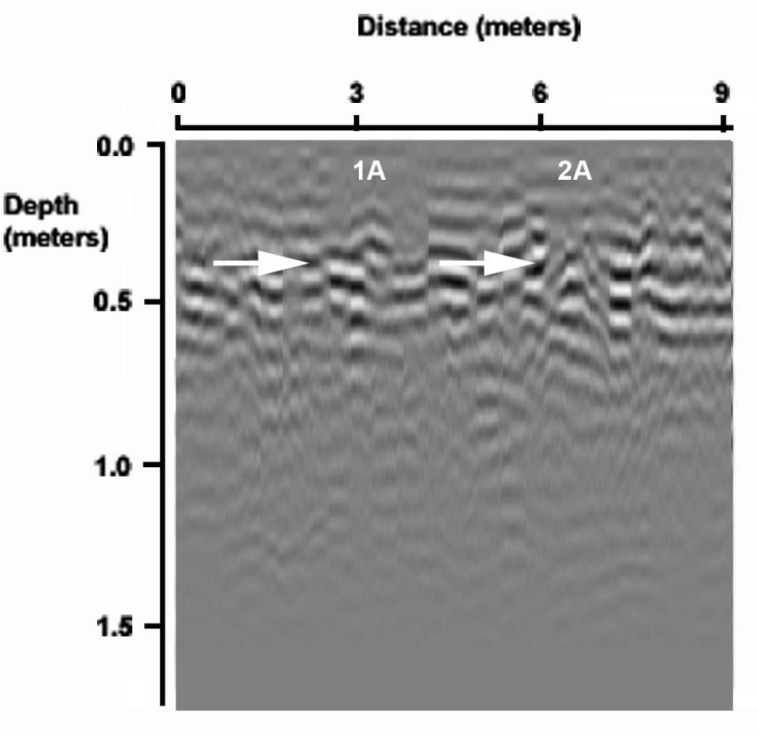

Figure 53: GPR reflection profile using the 500-MHz antenna of Row 1A2A at 3 months

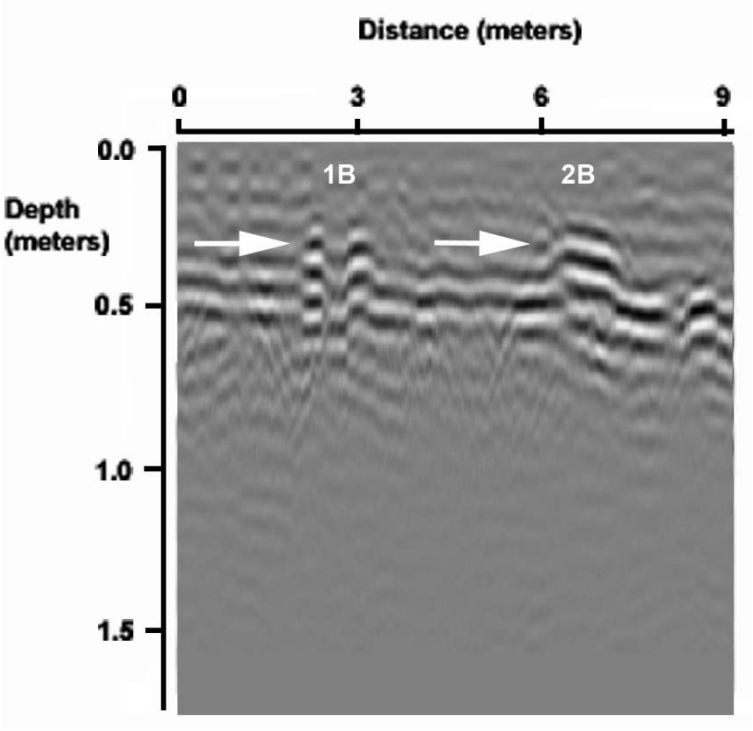

Figure 54: GPR reflection profile using the 500-MHz antenna of Row 1B2B at 3 months

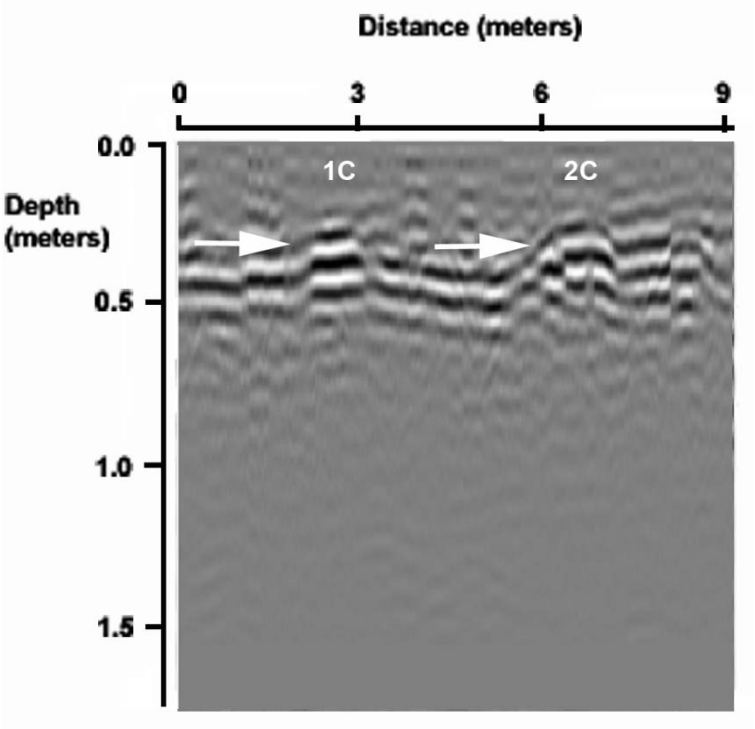

Figure 55: GPR reflection profile using the 500-MHz antenna of Row 1C2C at 3 months

4 MONTH

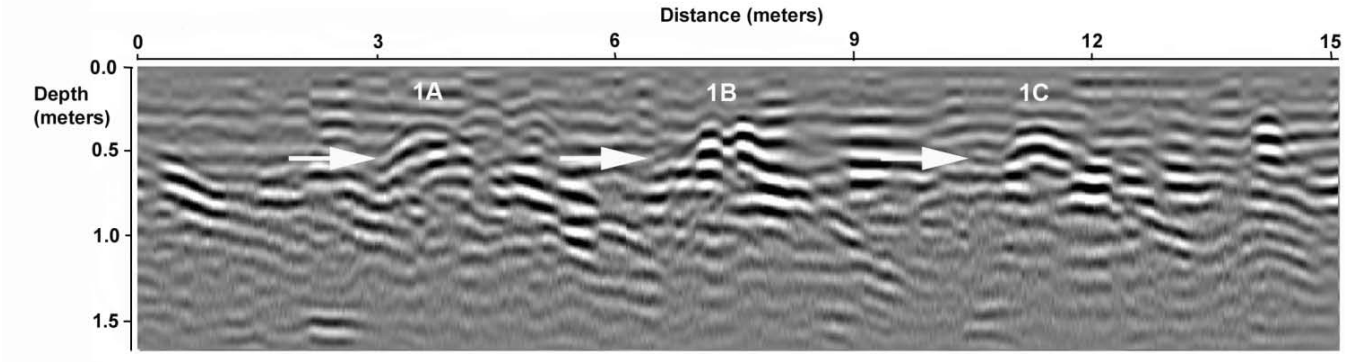

Figure 56: GPR reflection profile using the 500-MHz antenna of Row 1 at 4 months

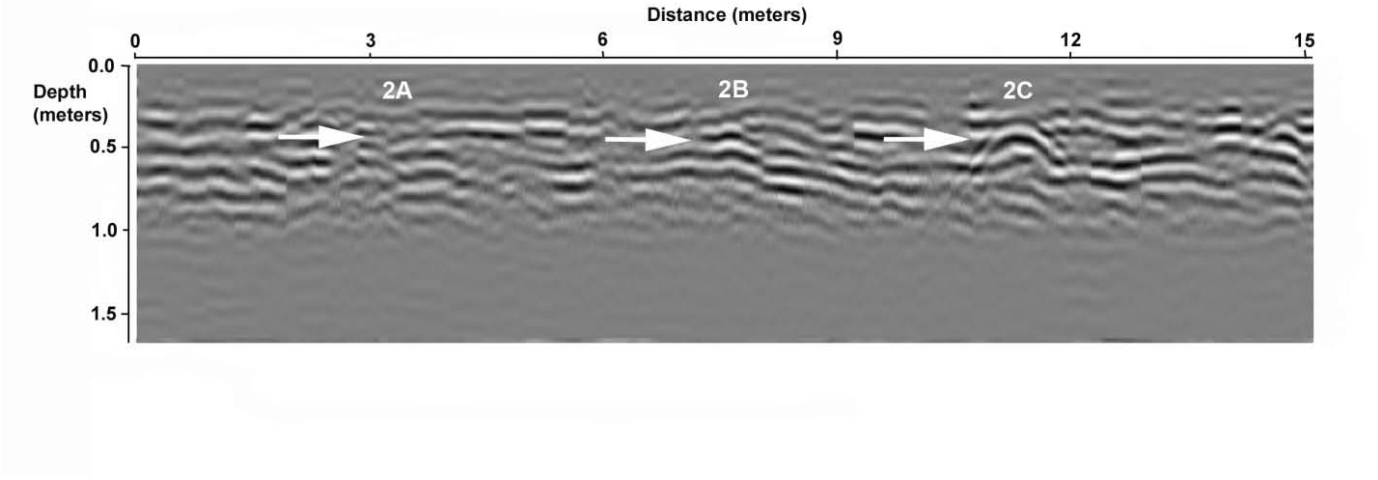

Figure 57: GPR reflection profile using the 500-MHz antenna of Row 2 at 4 months

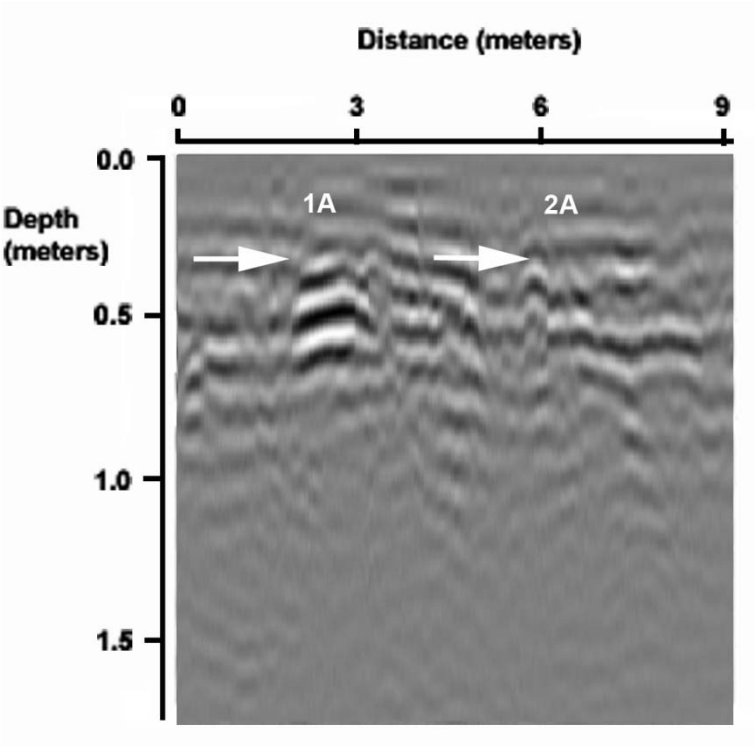

Figure 58: GPR reflection profile using the 500-MHz antenna of Row 1A2A at 4 months

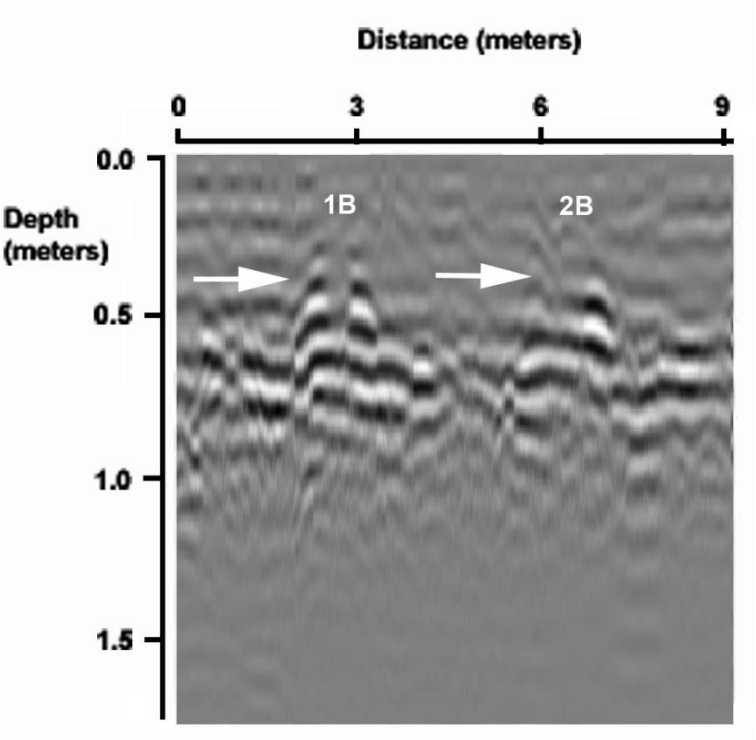

Figure 59: GPR reflection profile using the 500-MHz antenna of Row 1B2B at 4 months

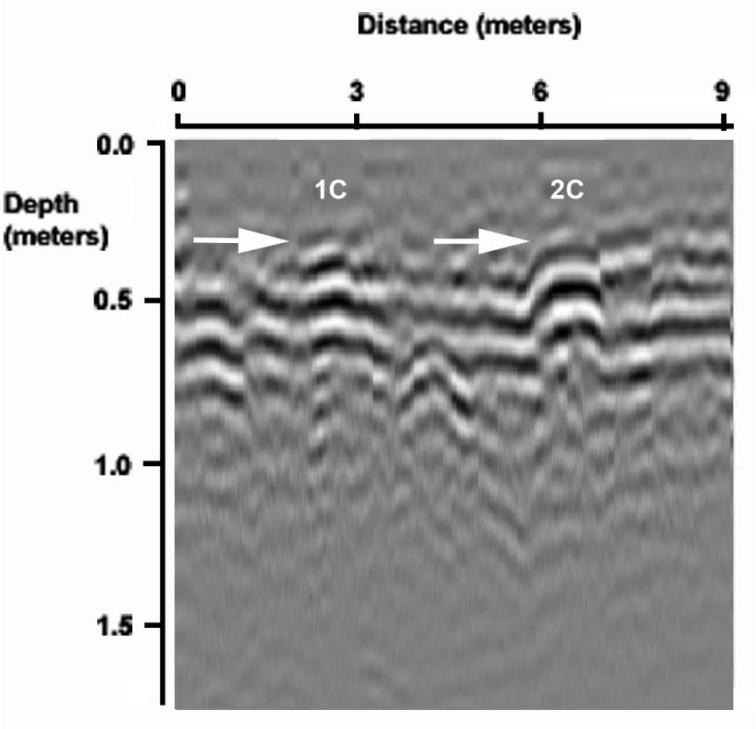

Figure 60: GPR reflection profile using the 500-MHz antenna of Row 1C2C at 4 months

5 MONTH

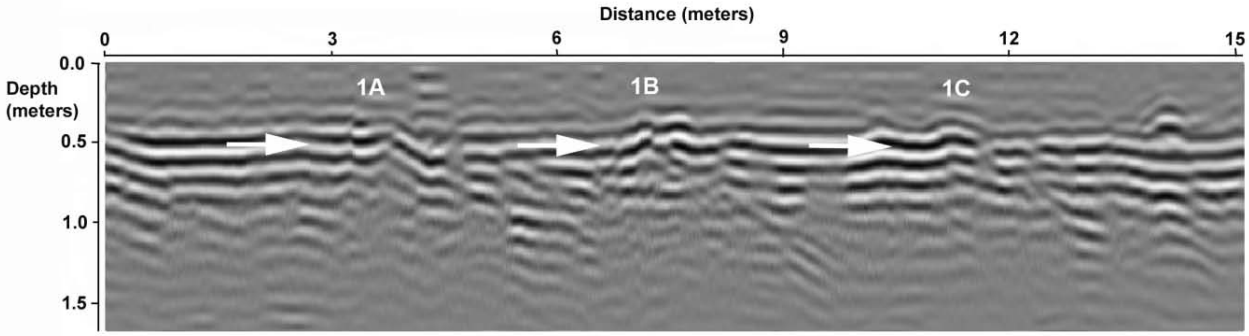

Figure 61: GPR reflection profile using the 500-MHz antenna of Row 1 at 5 months

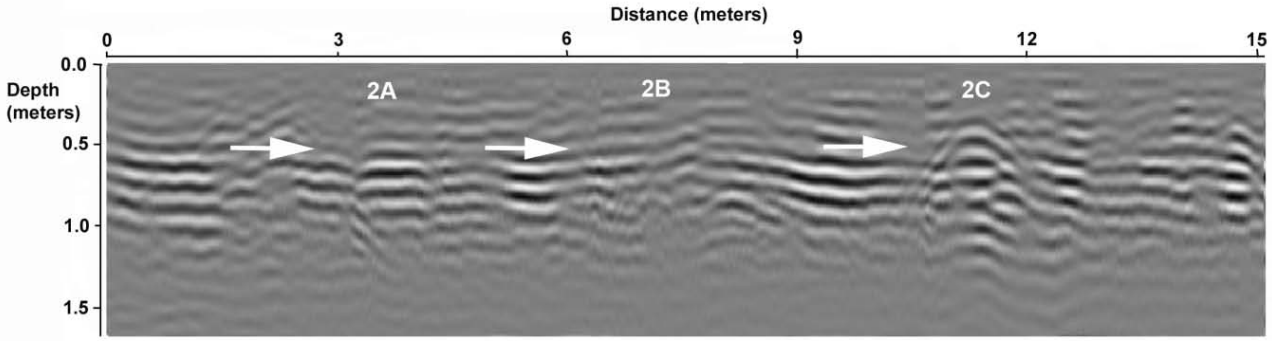

Figure 62: GPR reflection profile using the 500-MHz antenna of Row 2 at 5 months

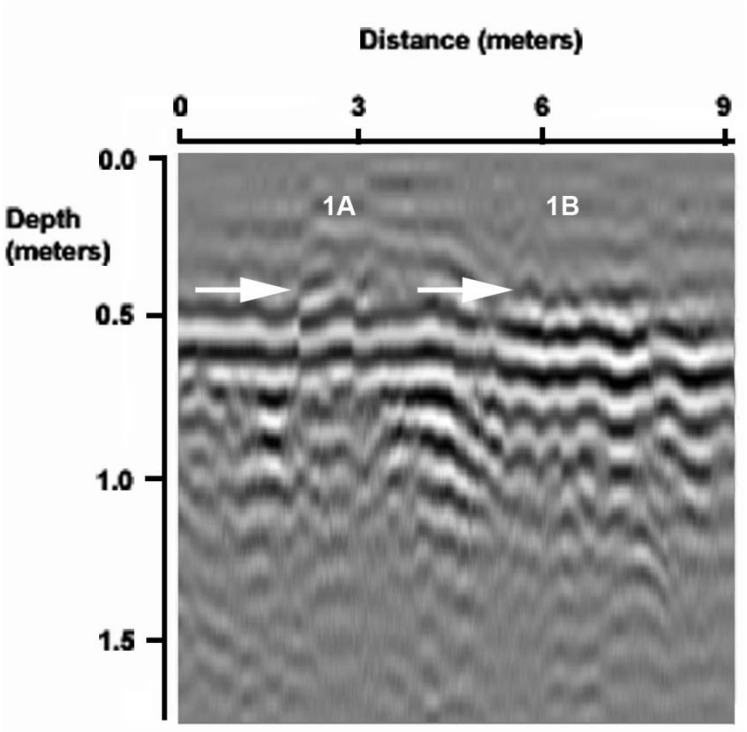

Figure 63: GPR reflection profile using the 500-MHz antenna of Row 1A2A at 5 months

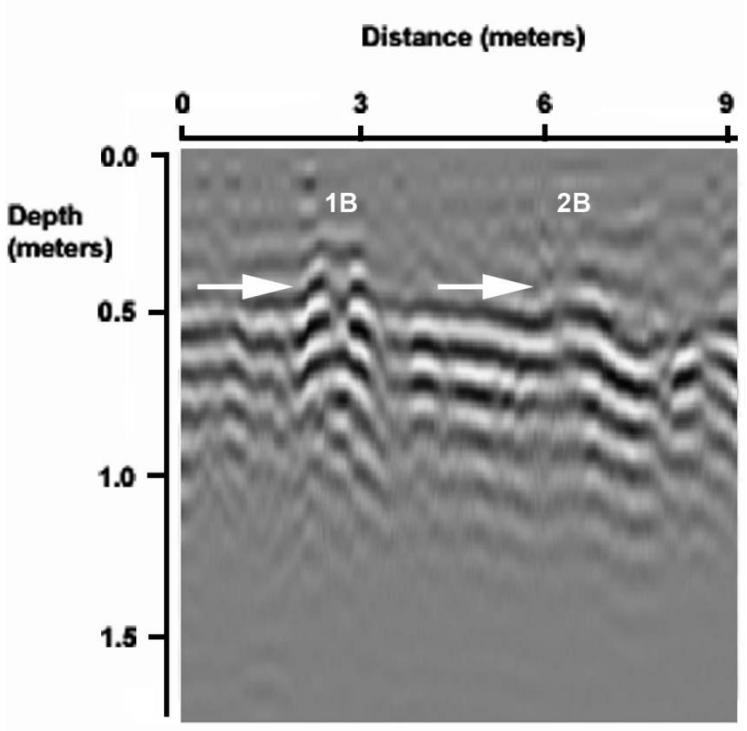

Figure 64: GPR reflection profile using the 500-MHz antenna of Row 1B2B at 5 months

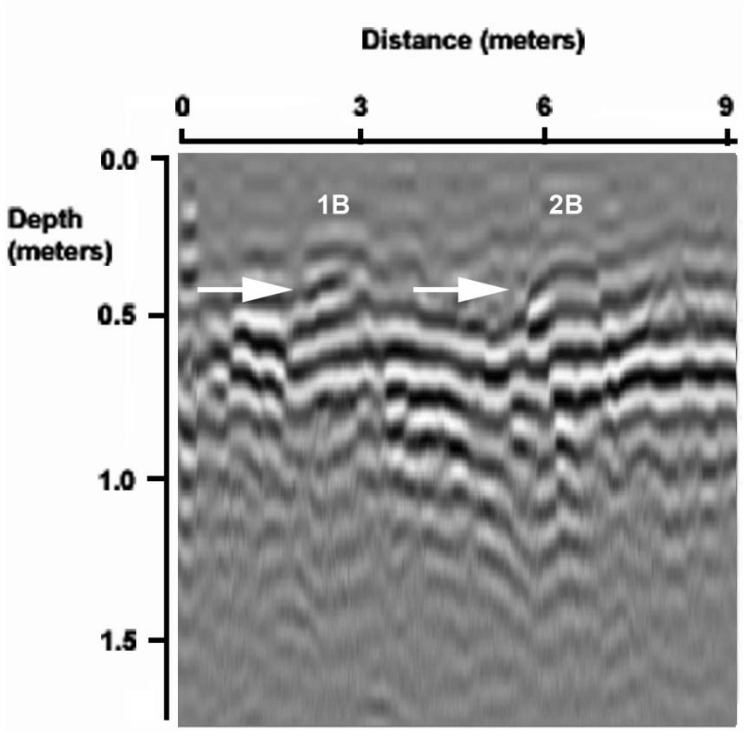

Figure 65: GPR reflection profile using the 500-MHz antenna of Row 1C2C at 5 months

6 MONTH

-

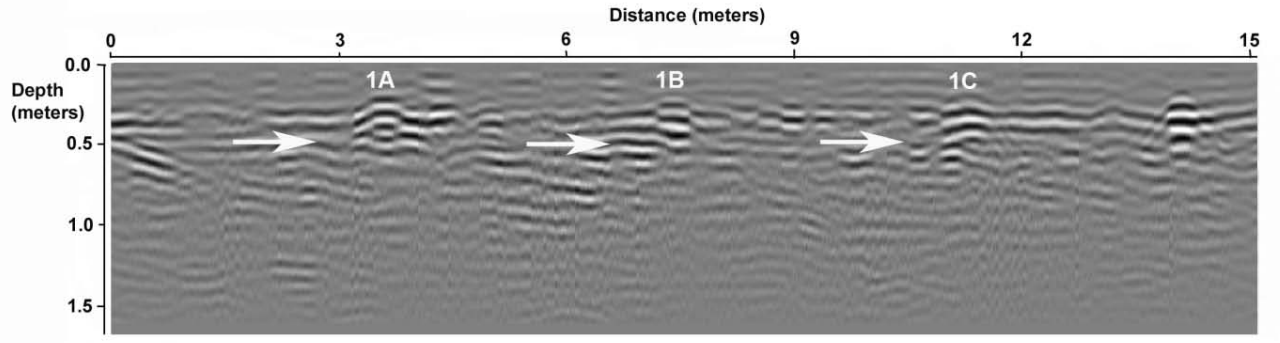

Figure 66: GPR reflection profile using the 500-MHz antenna of Row 1 at 6 months

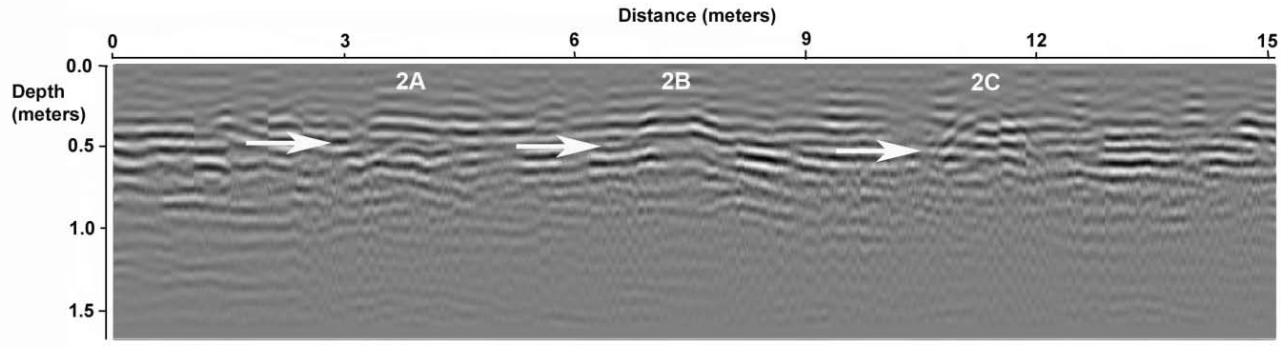

Figure 67: GPR reflection profile using the 500-MHz antenna of Row 2 at 6 months

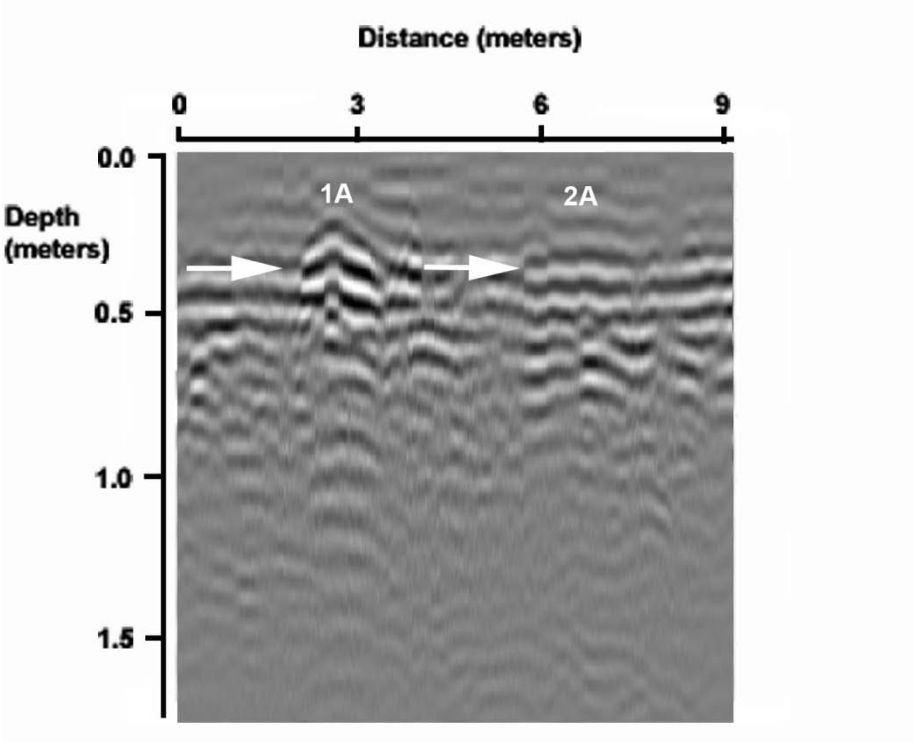

Figure 68: GPR reflection profile using the 500-MHz antenna of Row 1A2A at 6 months

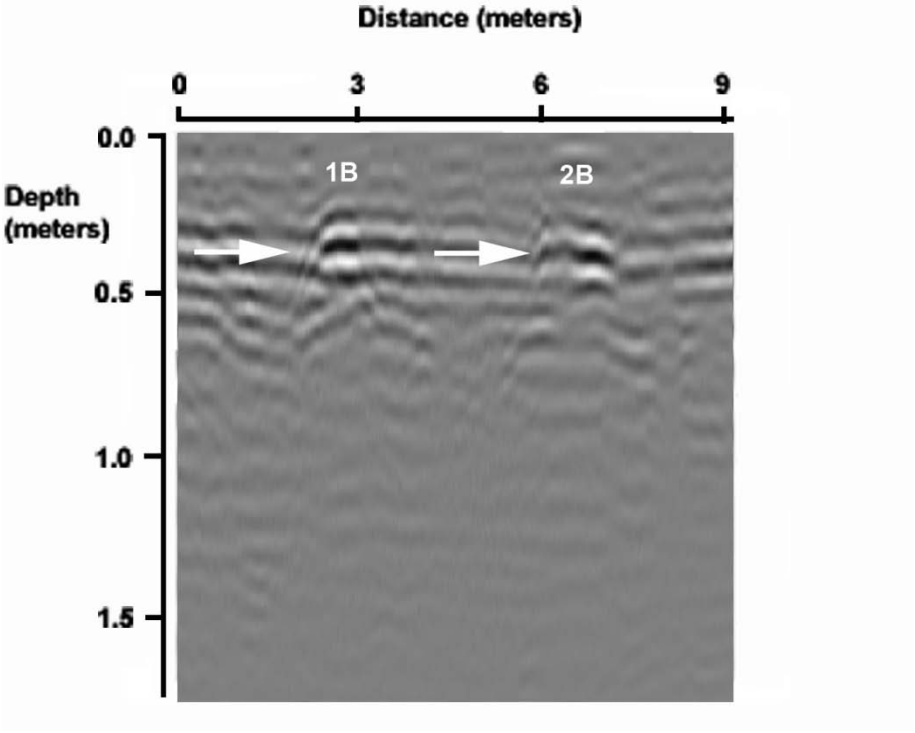

Figure 69: GPR reflection profile using the 500-MHz antenna of Row 1C2C at 6 months

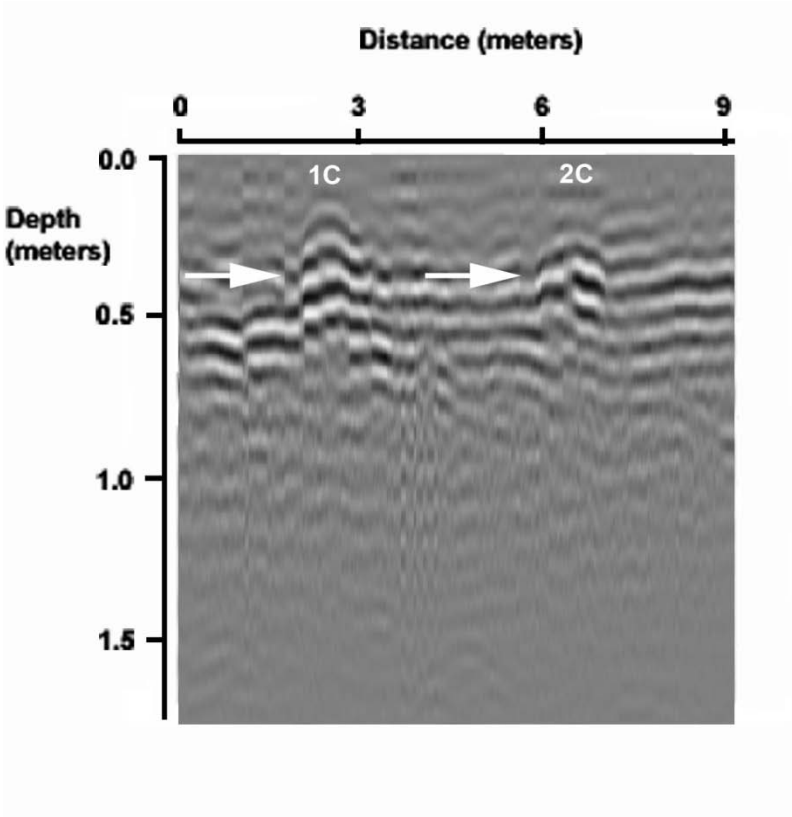

Figure 70: GPR reflection profile using the 500-MHz antenna of Row 1C2C at 6 months

7 MONTH

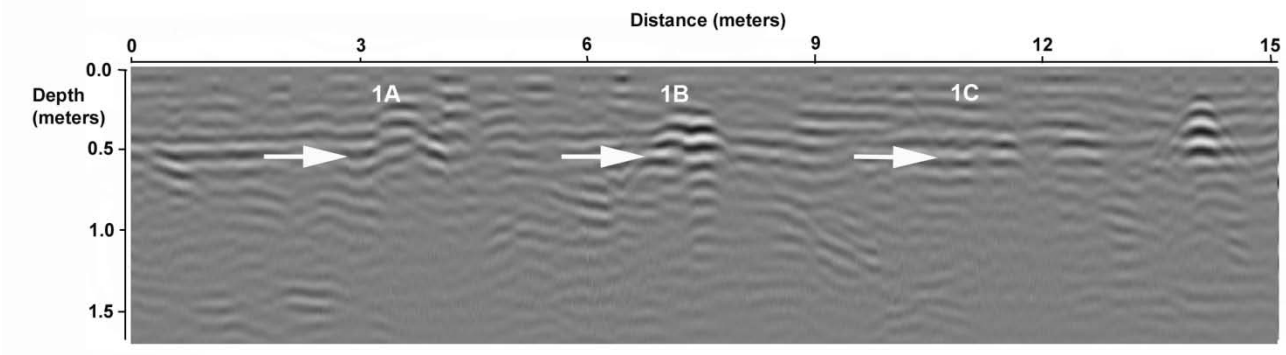

Figure 71: GPR reflection profile using the 500-MHz antenna of Row 1 at 7 months

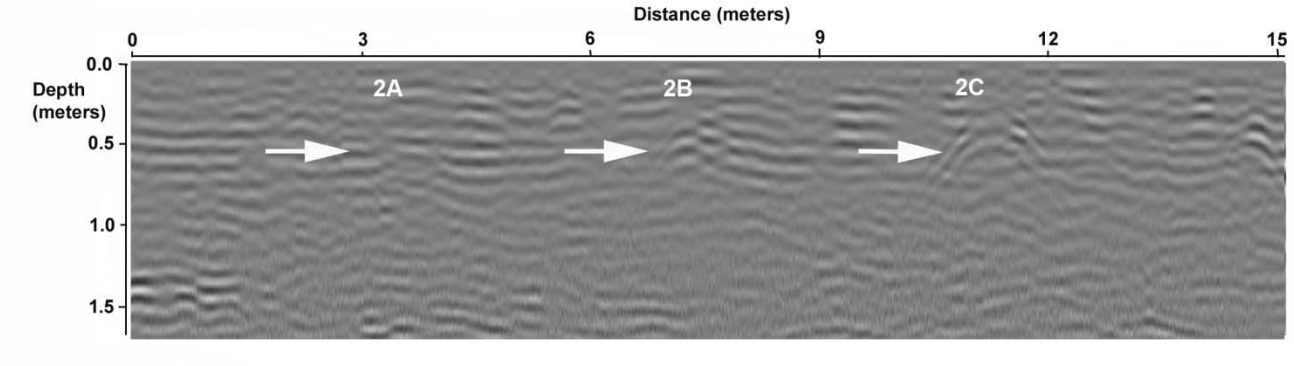

Figure 72: GPR reflection profile using the 500-MHz antenna of Row 1 at 7 months

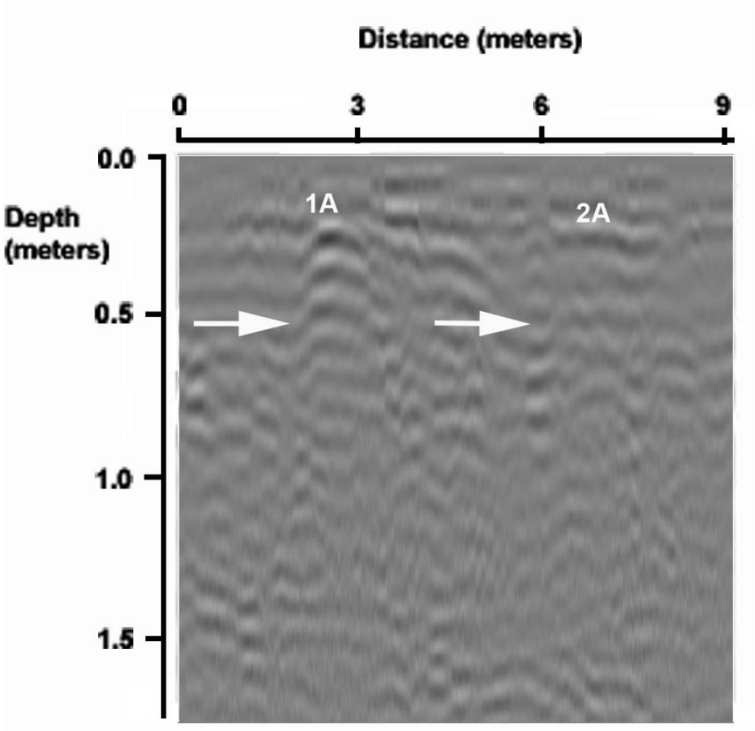

Figure 73: GPR reflection profile using the 500-MHz antenna of Row 1A2A at 7 months

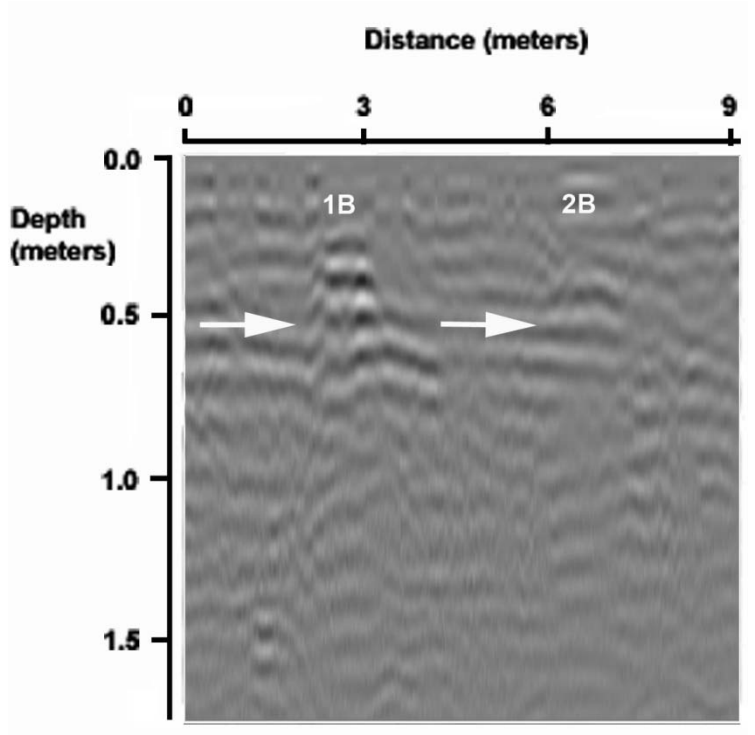

Figure 74: GPR reflection profile using the 500-MHz antenna of Row 1B2B at 7 months

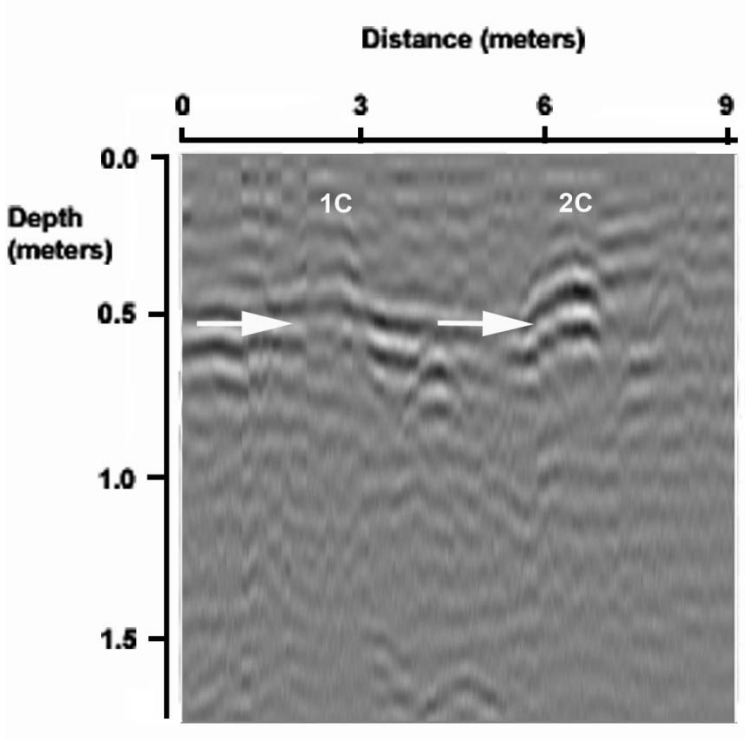

Figure 75: GPR reflection profile using the 500-MHz antenna of Row 1C2C at 7 months

8 MONTH

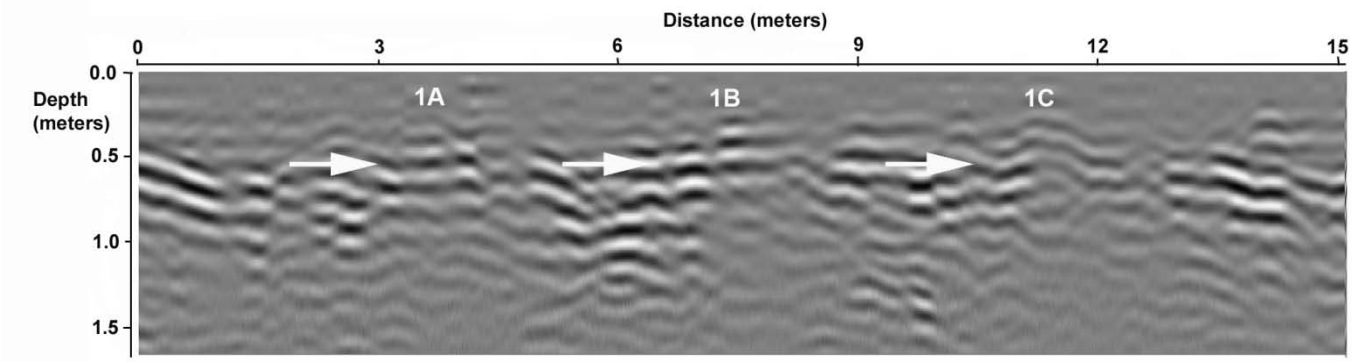

Figure 76: GPR reflection profile using the 500-MHz antenna of Row 1 at 8 months

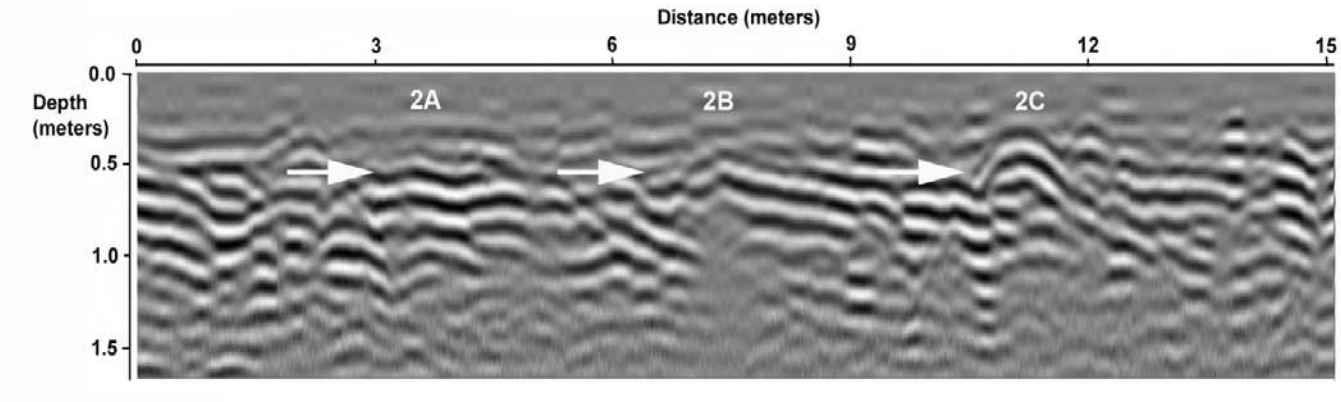

Figure 77: GPR reflection profile using the 500-MHz antenna of Row 2 at 8 months

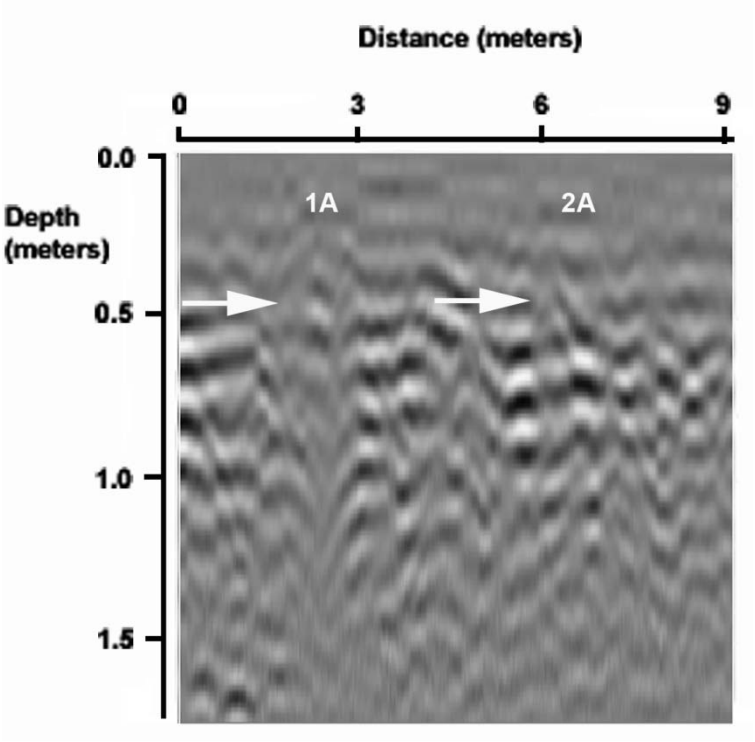

Figure 78: GPR reflection profile using the 500-MHz antenna of Row 1A2A at 8 months

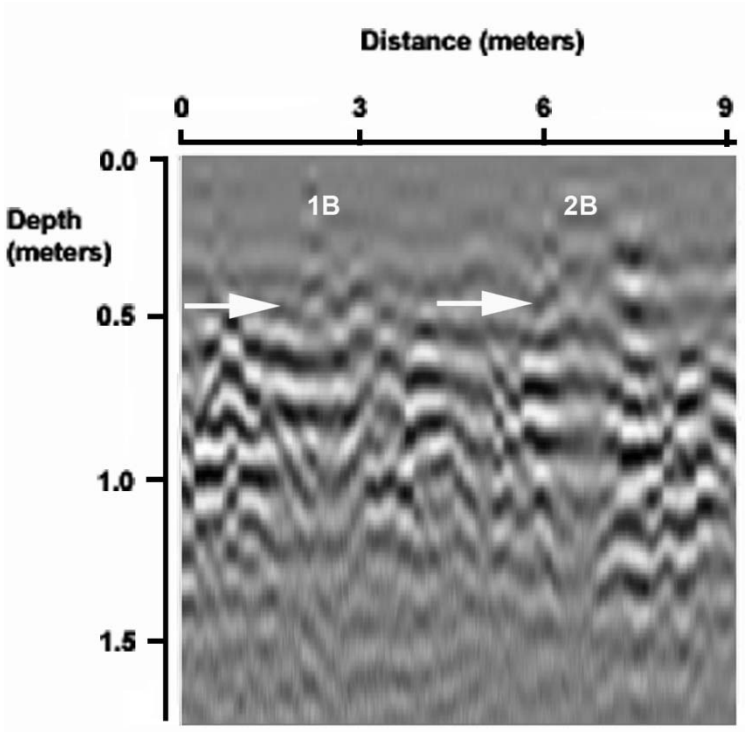

Figure 79: GPR reflection profile using the 500-MHz antenna of Row 1B2B at 8 months

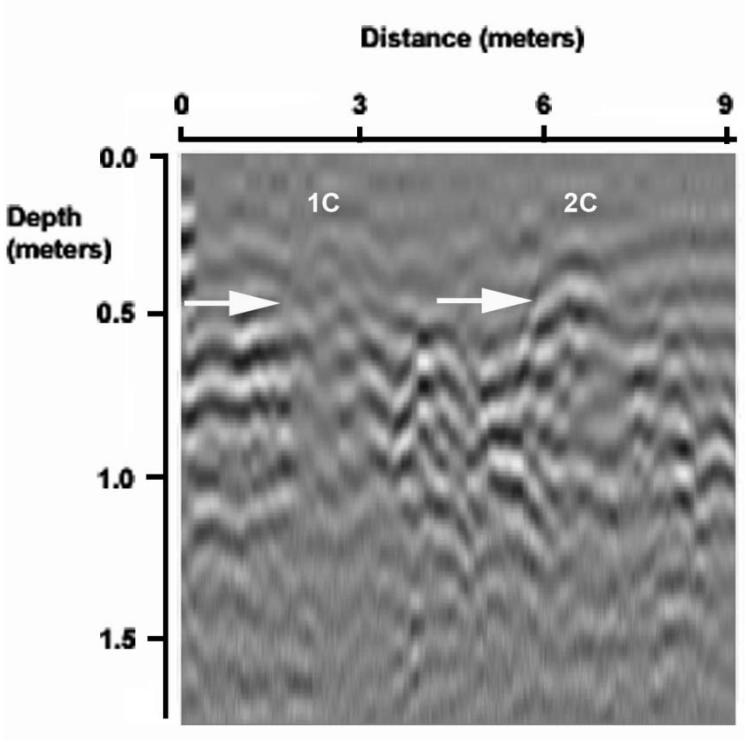

Figure 80: GPR reflection profile using the 500-MHz antenna of Row 1C2C at 8 months

9 MONTH

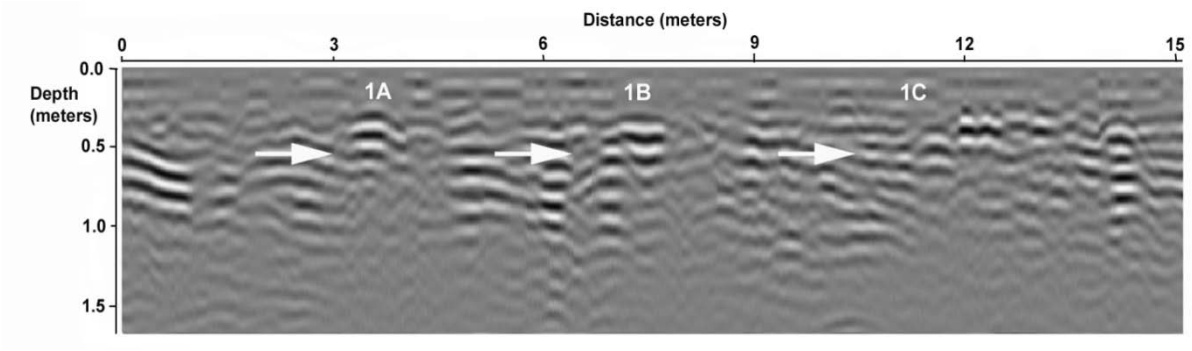

Figure 81: GPR reflection profile using the 500-MHz antenna of Row 1 at 9 months

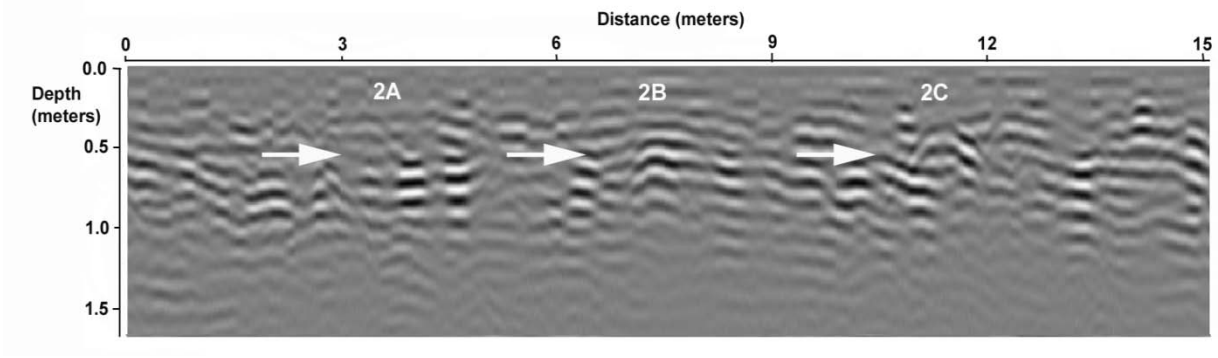

Figure 82: GPR reflection profile using the 500-MHz antenna of Row 2 at 9 months

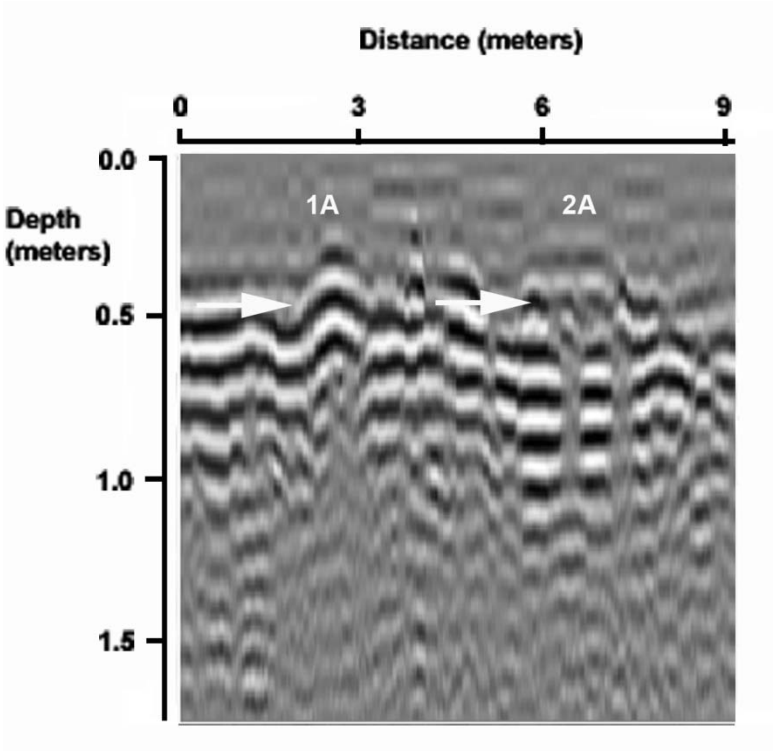

Figure 83: GPR reflection profile using the 500-MHz antenna of 1A2A at 9 months

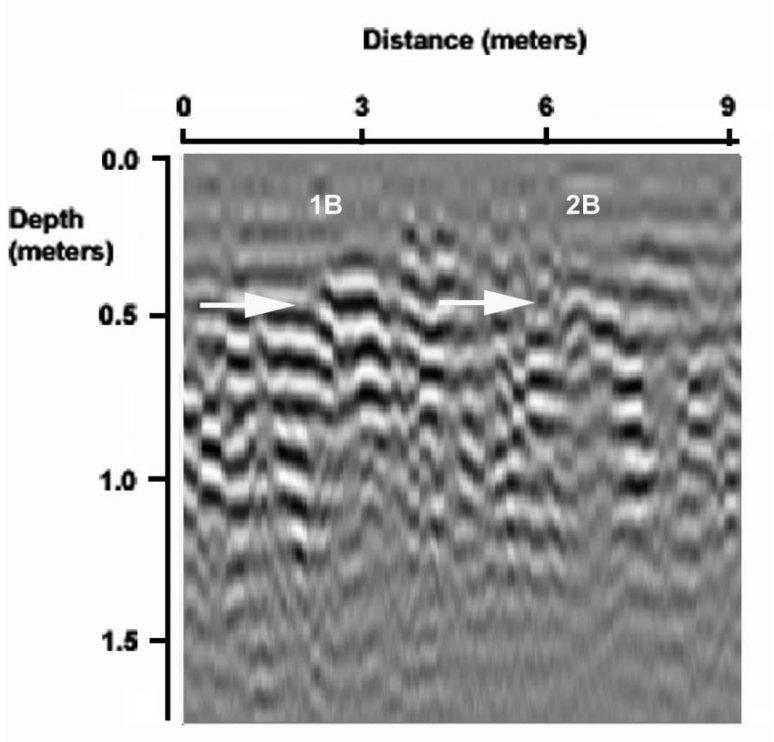

Figure 84: GPR reflection profile using the 500-MHz antenna of 1B2B at 9 months

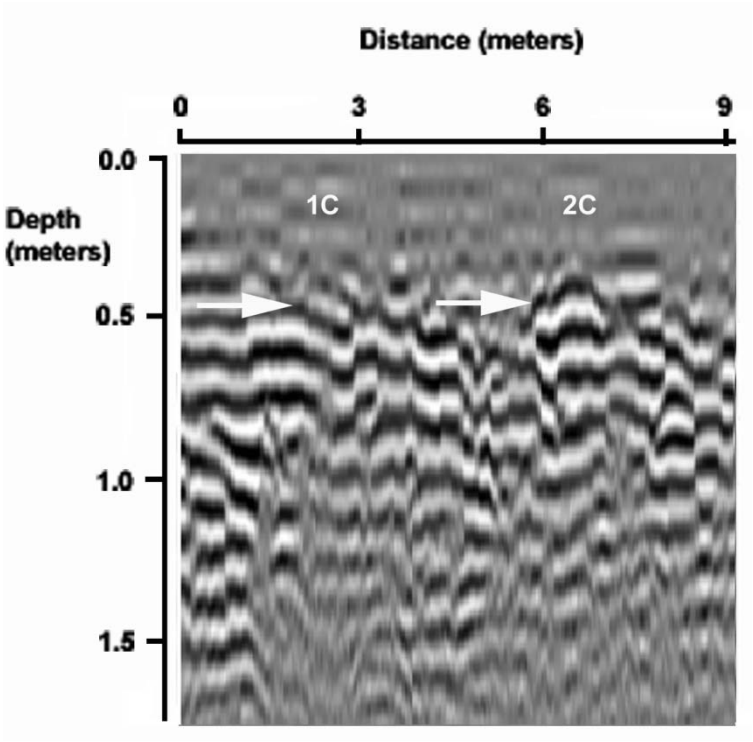

Figure 85: GPR reflection profile using the 500-MHz antenna of 1C2C at 9 months

10 MONTH

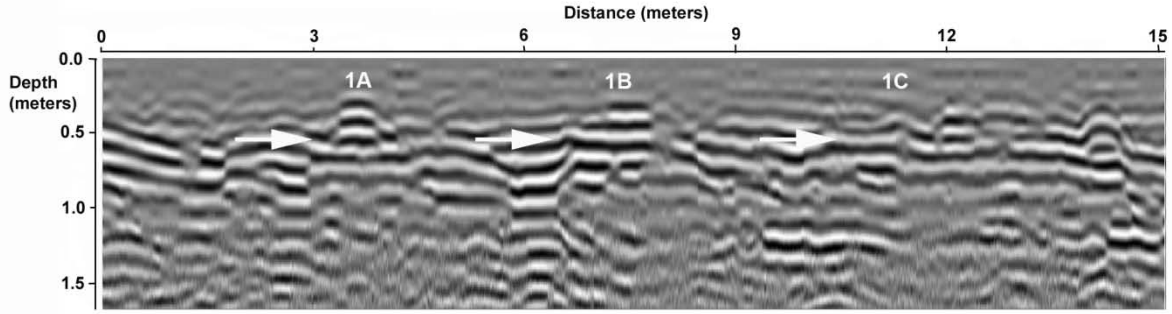

Figure 86: GPR reflection profile using the 500-MHz antenna of Row 1 at 10 months

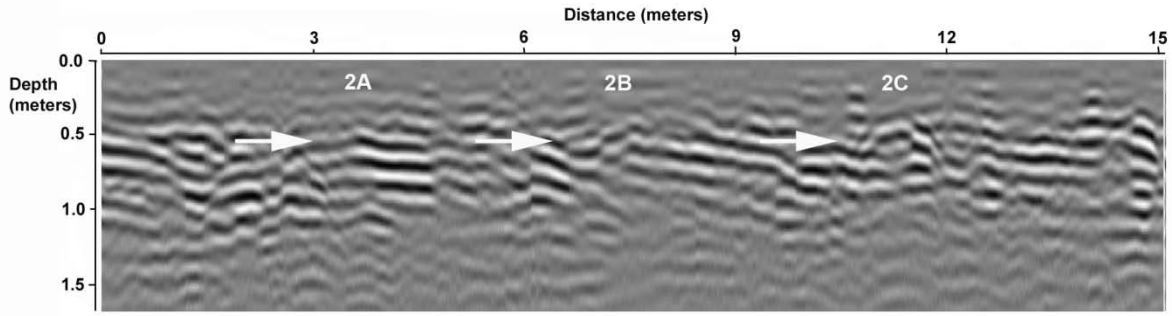

Figure 87: GPR reflection profile using the 500-MHz antenna of Row 2 at 10 months

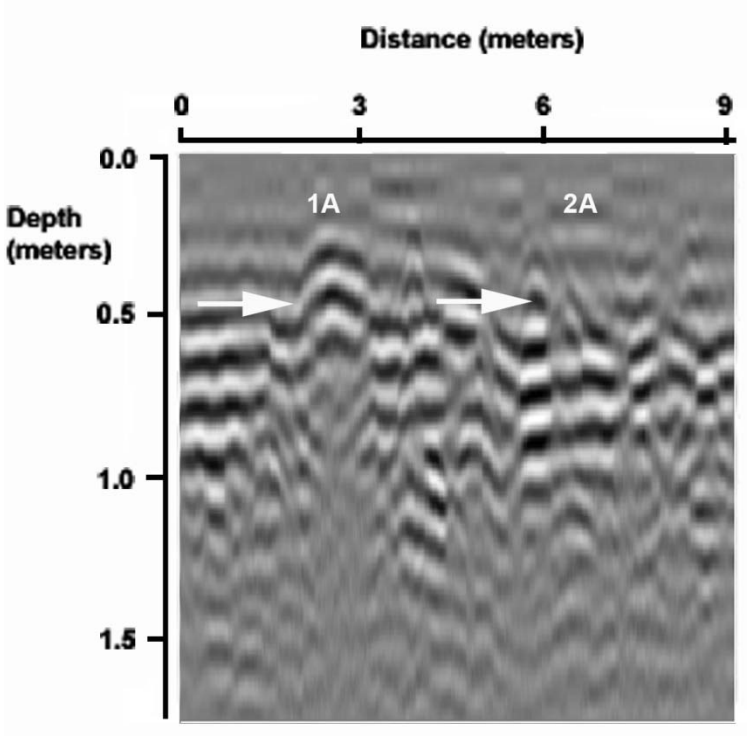

Figure 88: GPR reflection profile using the 500-MHz antenna of 1A2A at 10 months

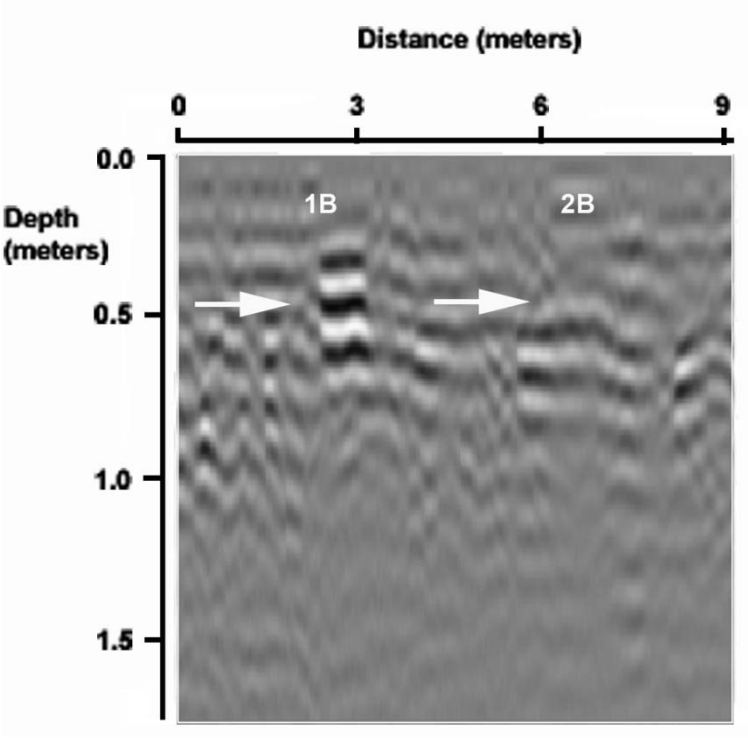

Figure 89: GPR reflection profile using the 500-MHz antenna of 1B2B at 10 months

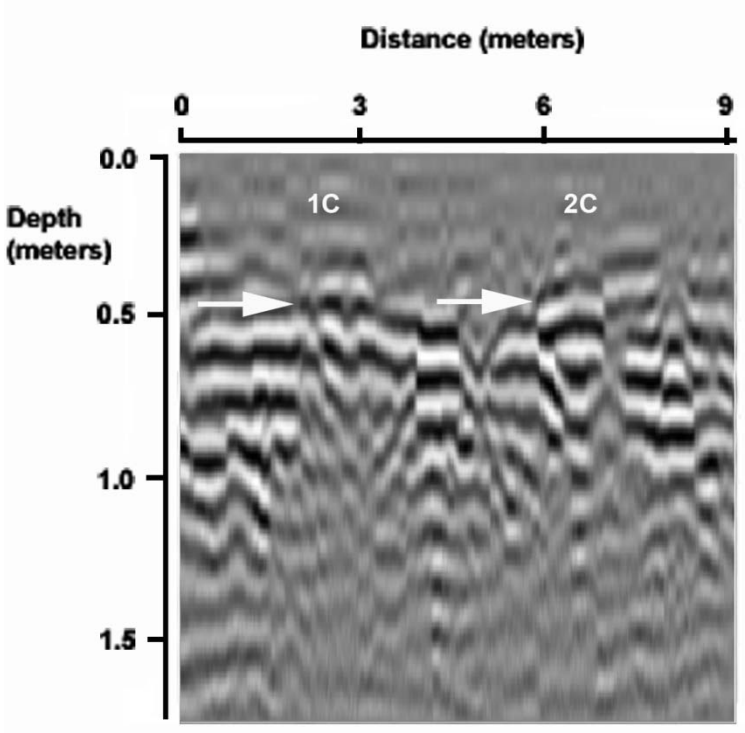

Figure 90: GPR reflection profile using the 500-MHz antenna of 1C2C at 10 months

11 MONTH

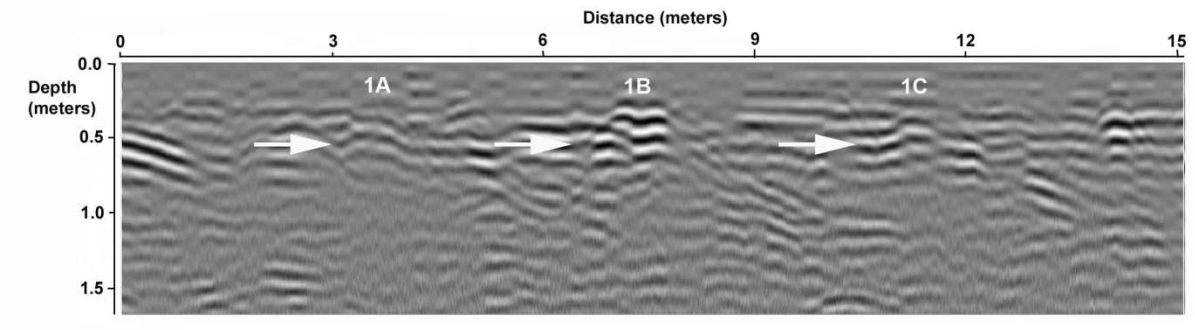

Figure 91: GPR reflection profile using the 500-MHz antenna of Row 1 at 11 months

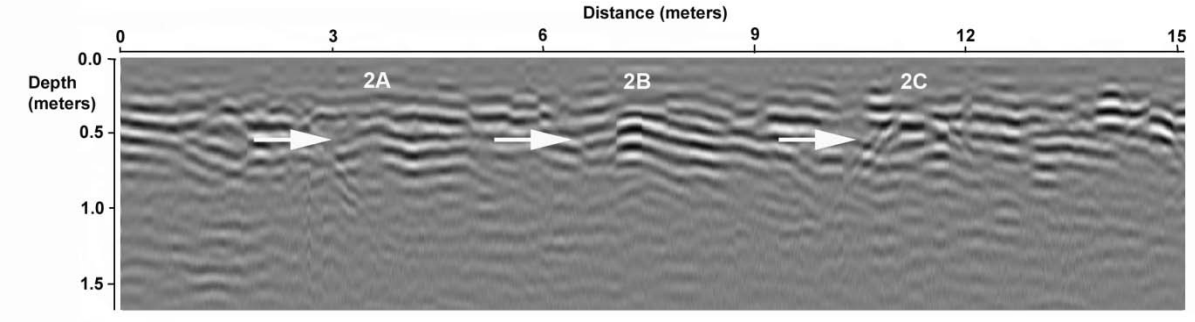

Figure 92: GPR reflection profile using the 500-MHz antenna of Row 2 at 11 months

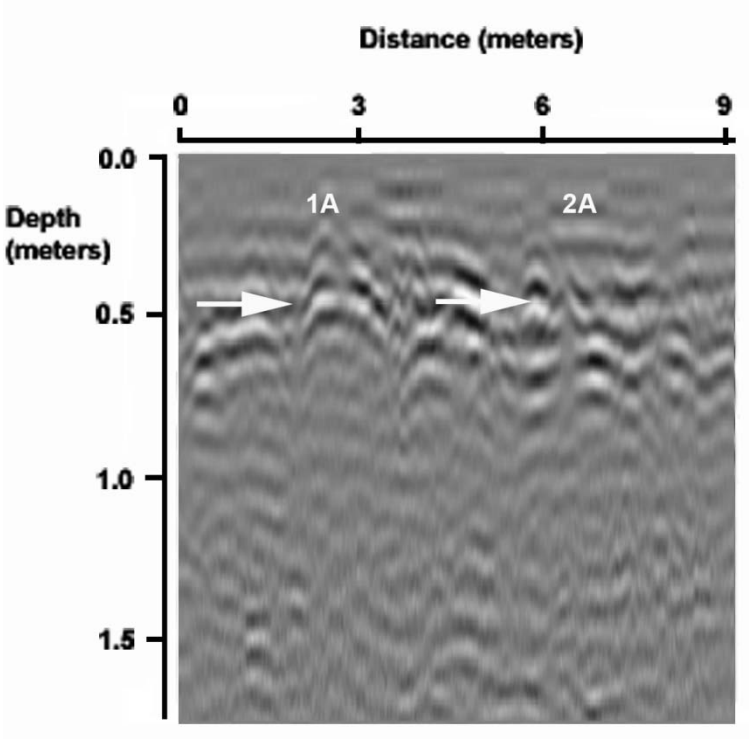

Figure 93: GPR reflection profile using the 500-MHz antenna of Row 1A2A at 11 months

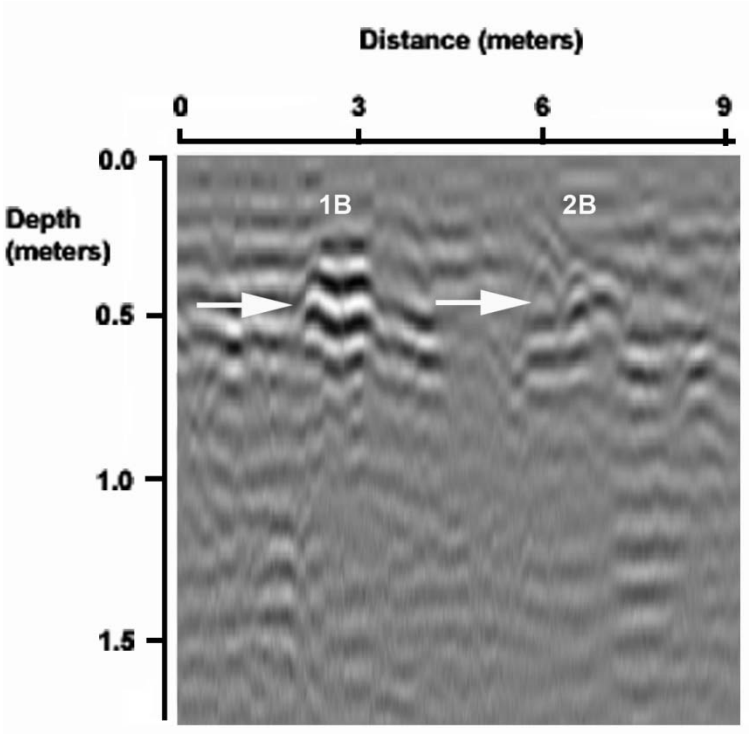

Figure 94: GPR reflection profile using the 500-MHz antenna of Row 1B2B at 11 months

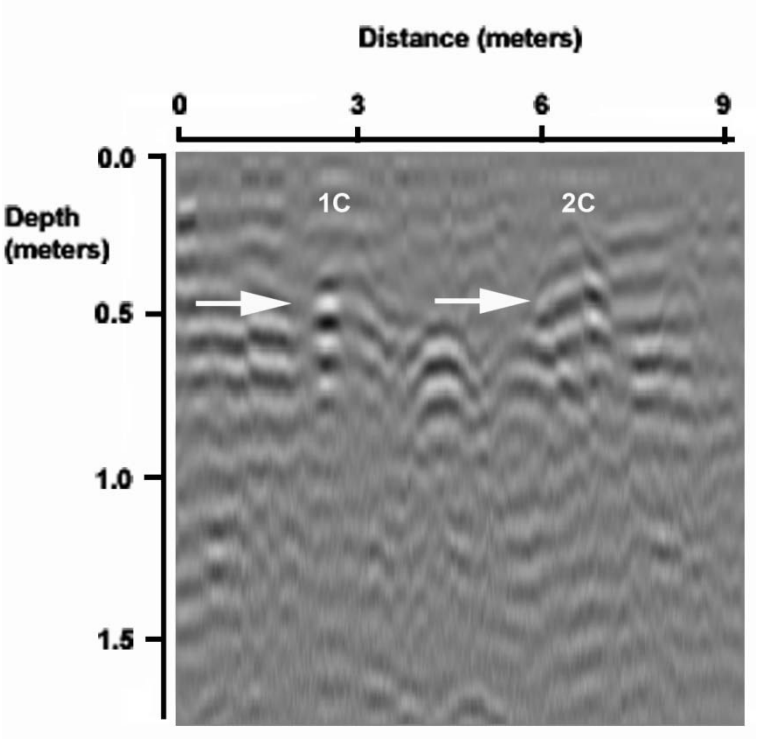

Figure 94: GPR reflection profile using the 500-MHz antenna of Row 1C2C at 11 months

12 MONTH

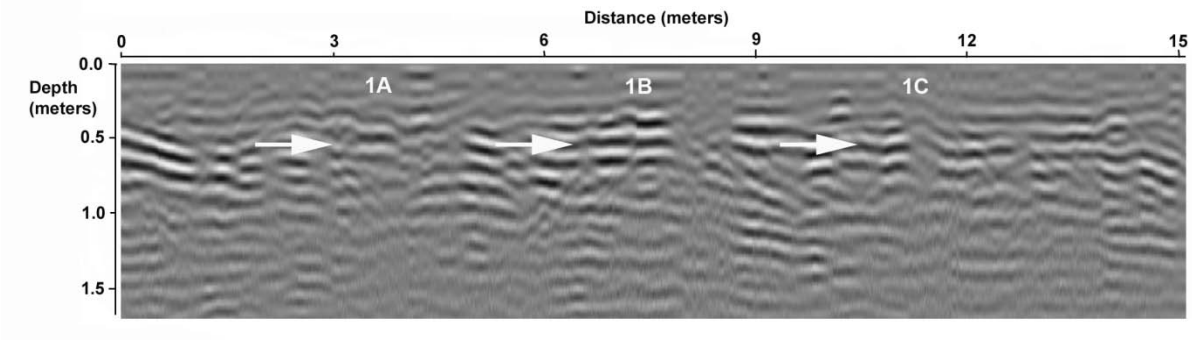

Figure 96: GPR reflection profile using the 500-MHz antenna of Row 1 at 12 months

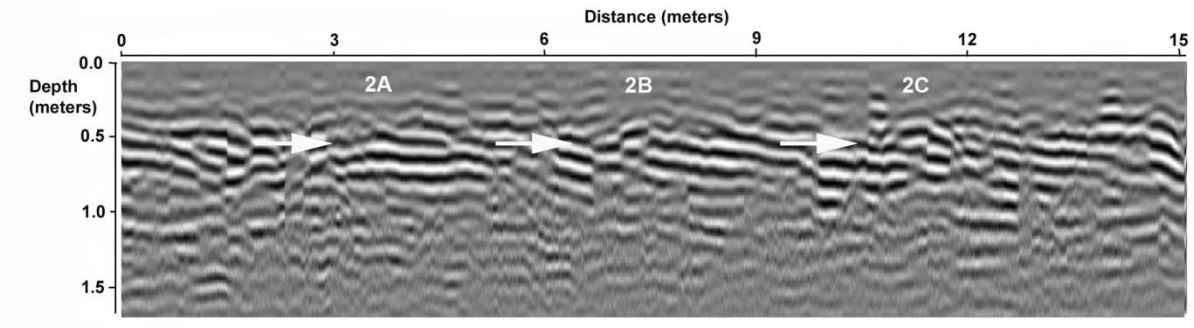

Figure 97: GPR reflection profile using the 500-MHz antenna of Row 2 at 12 months

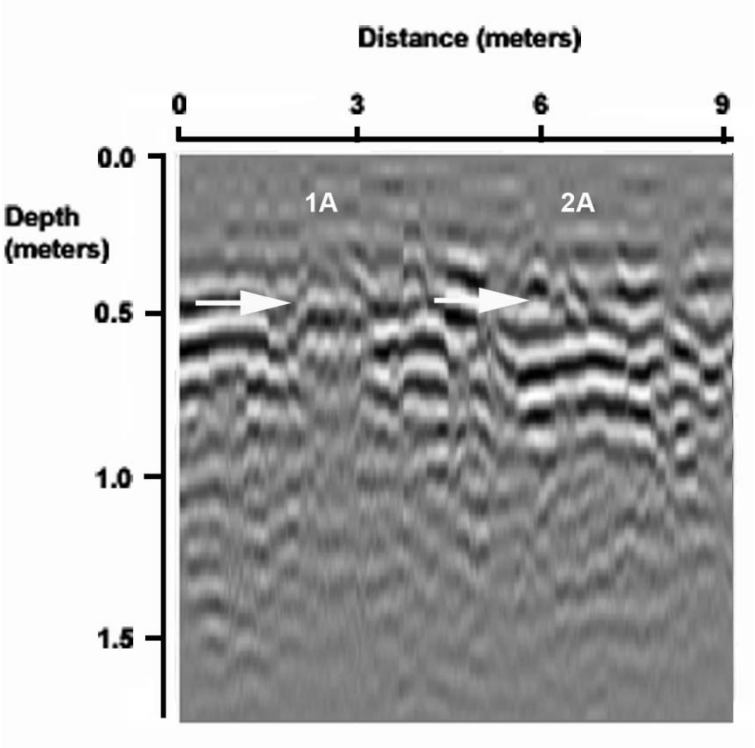

Figure 98: GPR reflection profile using the 500-MHz antenna of Row 1A2A at 12 months

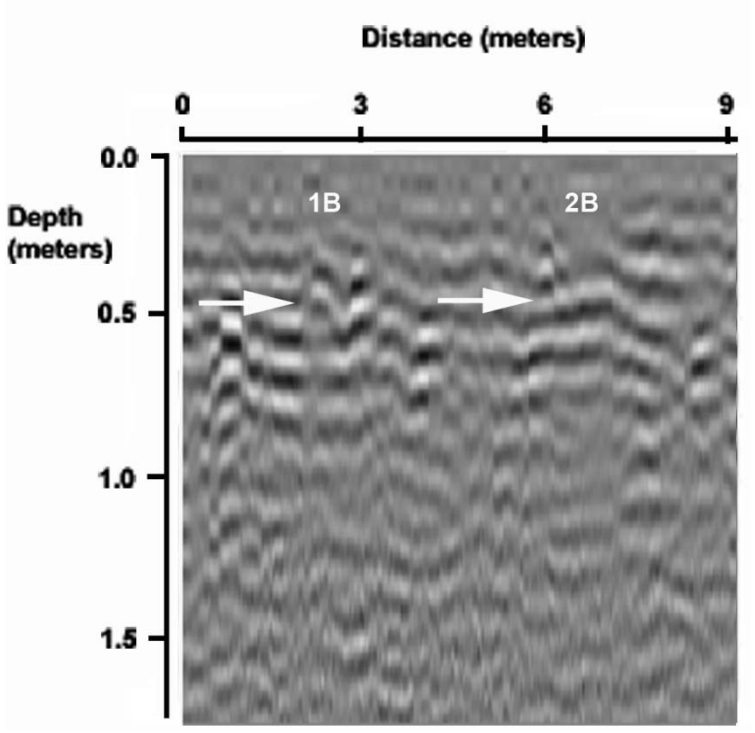

Figure 99: GPR reflection profile using the 500-MHz antenna of Row 1B2B at 12 months

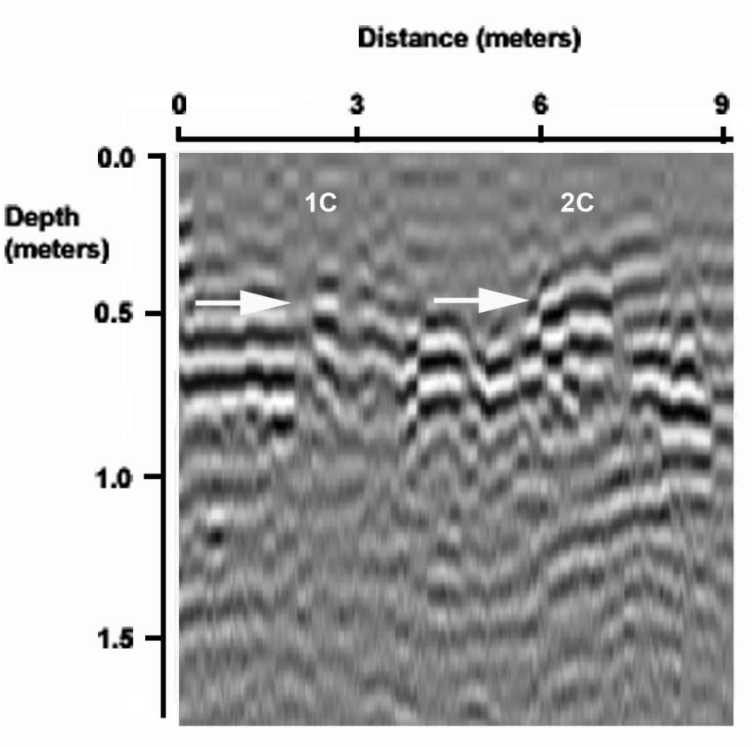

Figure 100: GPR reflection profile using the 500-MHz antenna of Row 1C2C at 12 months

APPENDIX B: GROUND-PENETRATING RADAR 500-MHZ HORIZONTAL SLICES

1 MONTH

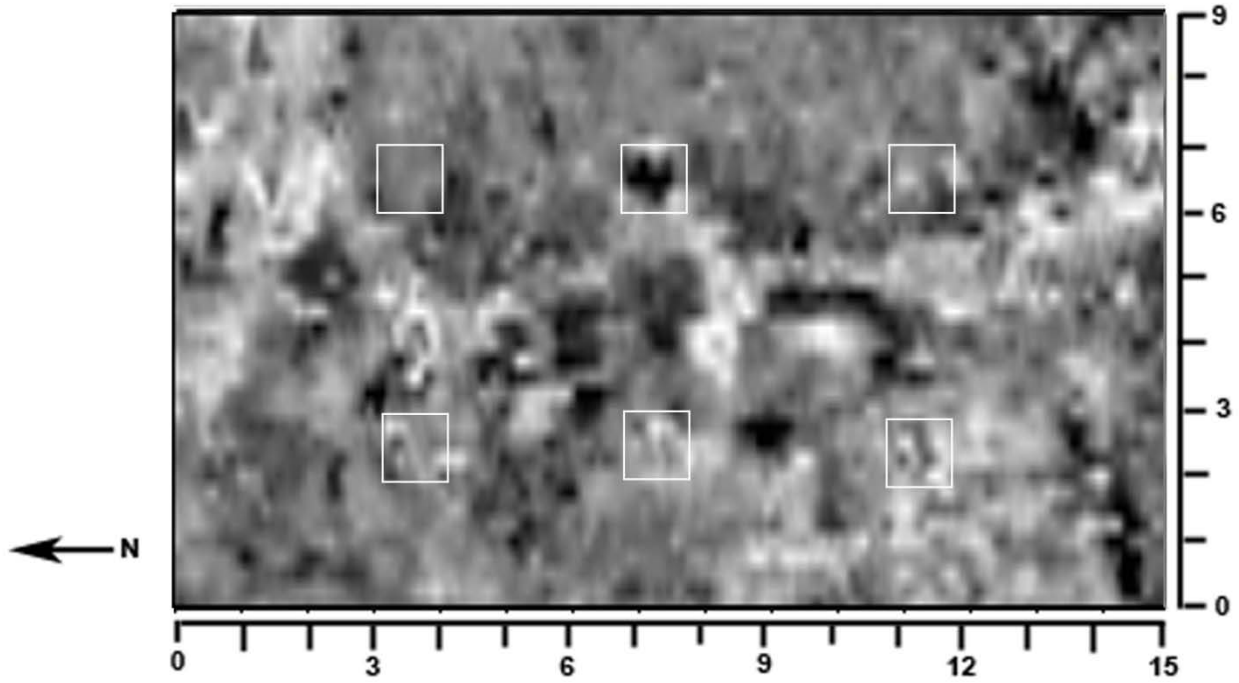

Figure 101: GPR horizontal slice in the X direction using the 500-MHz antenna at 1 month. The horizontal slice is approximately 0.43 m in depth (15.66 ns)

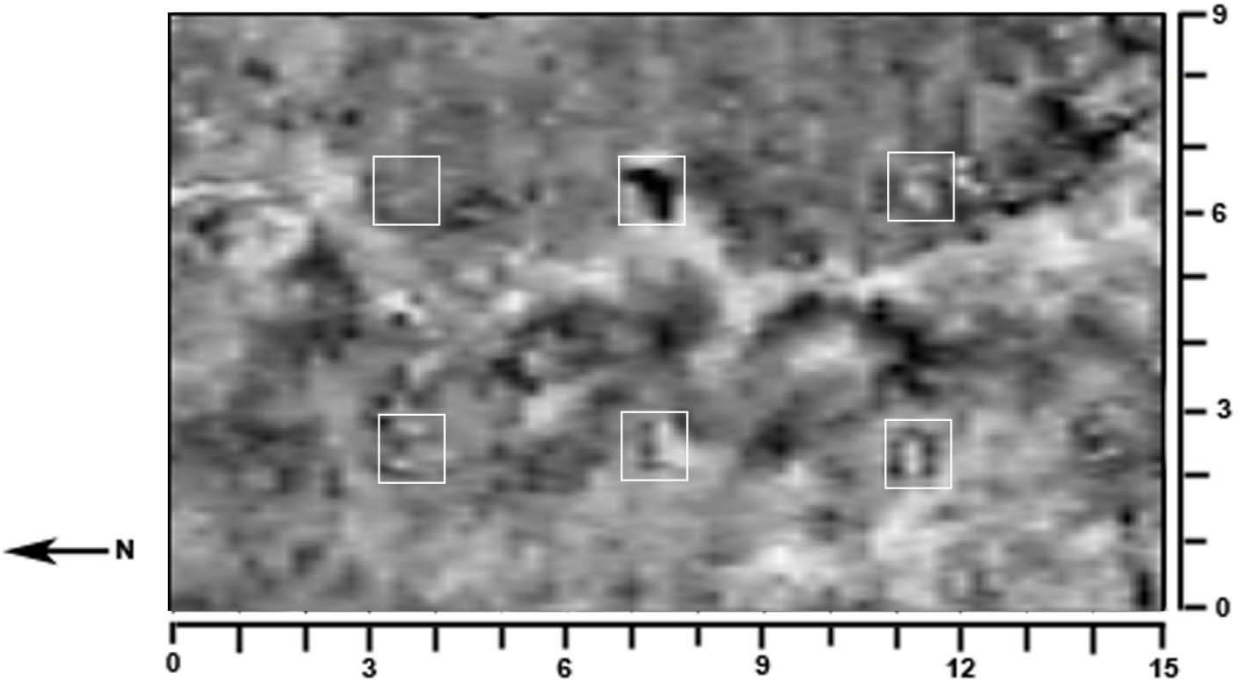

Figure 102: GPR horizontal slice in the Y direction using the 500-MHz antenna at 1 month. The horizontal slice is approximately 0.4 m in depth (14.62 ns)

2 MONTH

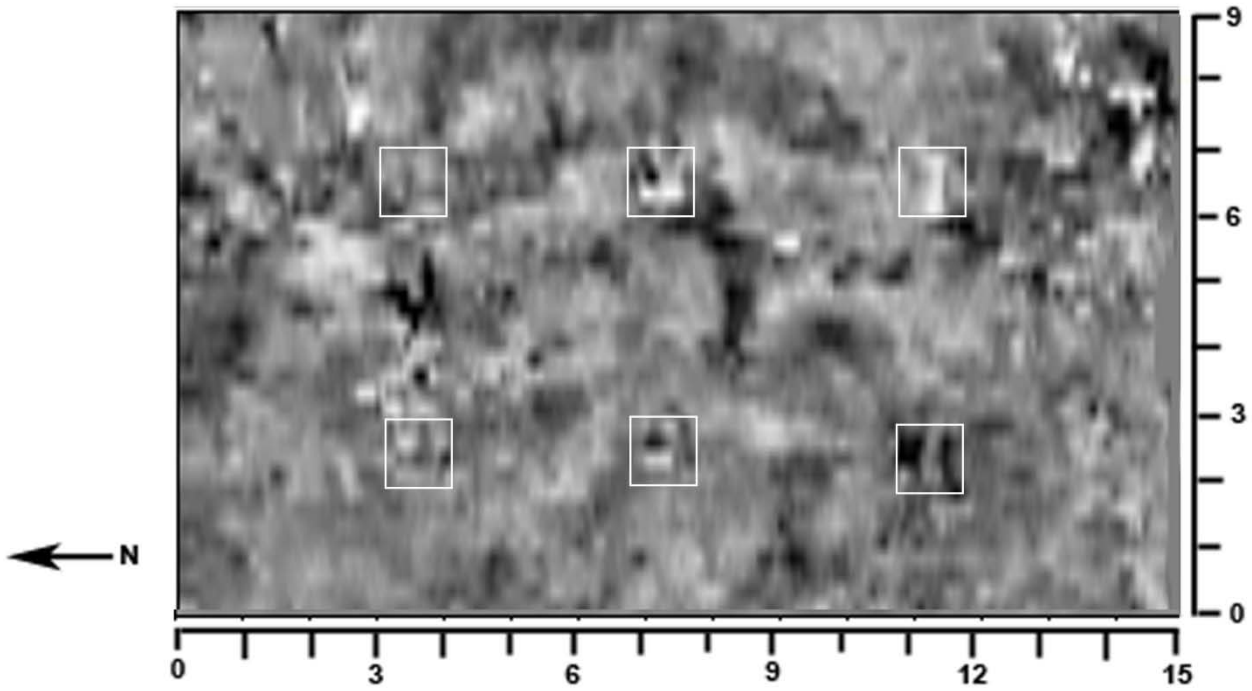

Figure 103: GPR horizontal slice in the X direction using the 500-MHz antenna at 2 months. The horizontal slice is approximately 0.44 m in depth (16.66 ns)

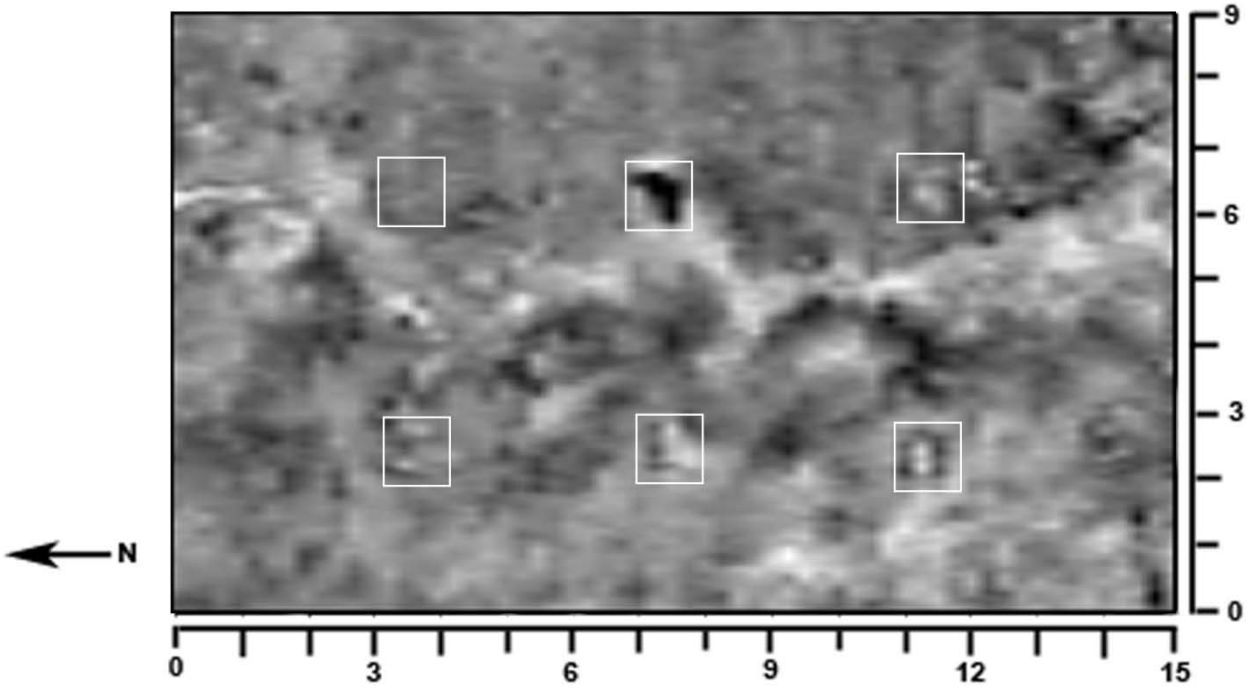

Figure 104: GPR horizontal slice in the Y direction using the 500-MHz antenna at 2 months. The horizontal slice is approximately 0.42 m in depth (15.47 ns)

3 MONTH

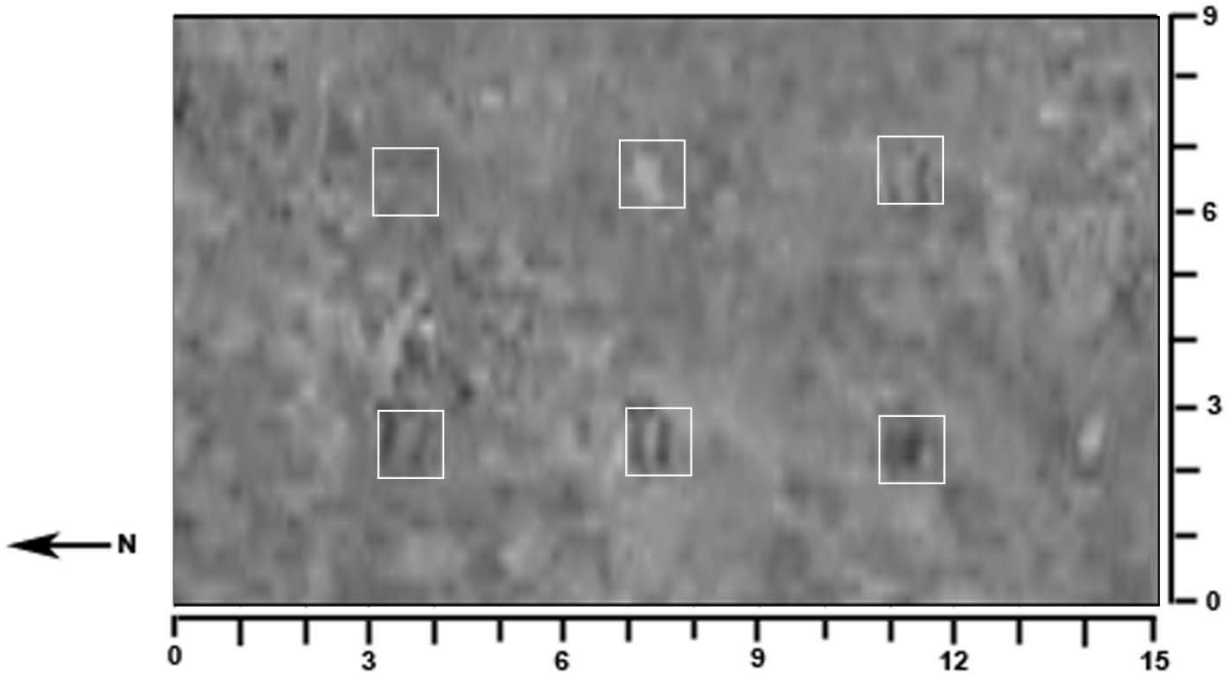

Figure 105: GPR horizontal slice in the X direction using the 500-MHz antenna at 3 months. The horizontal slice is approximately 0.41 m in depth (11.95 ns)

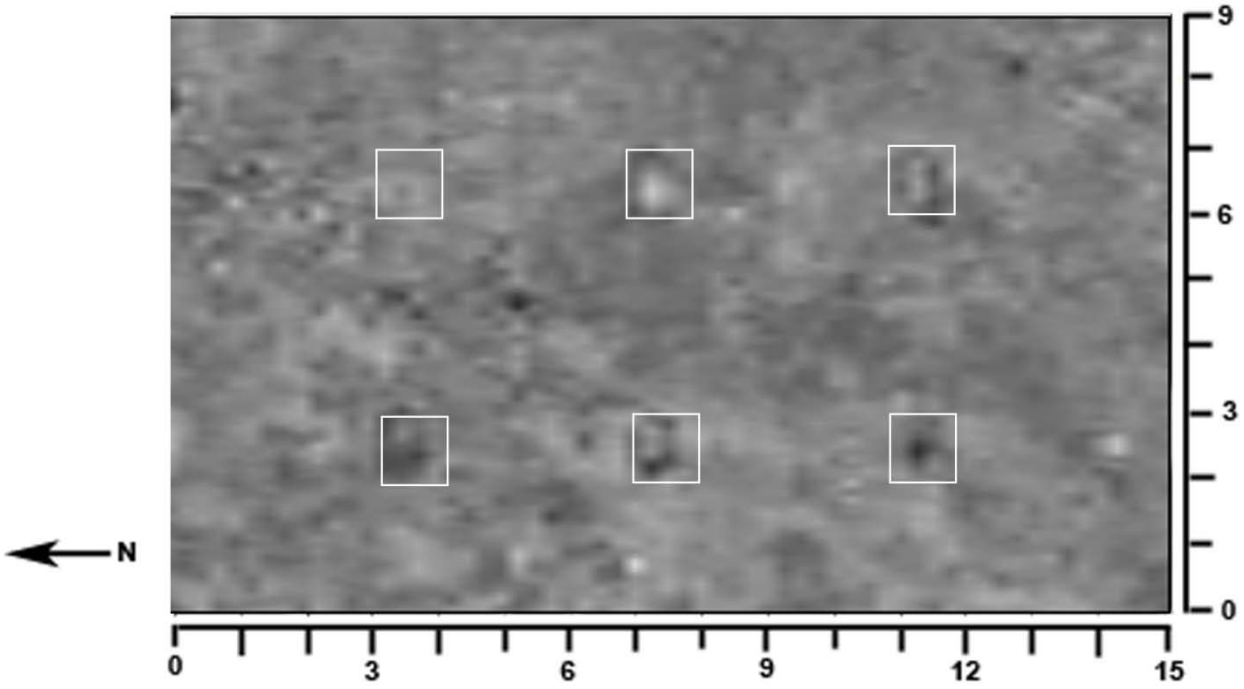

Figure 106: GPR horizontal slice in the Y direction using the 500-MHz antenna at 3 months. The horizontal slice is approximately 0.42 m in depth (12.21 ns)

4 MONTH

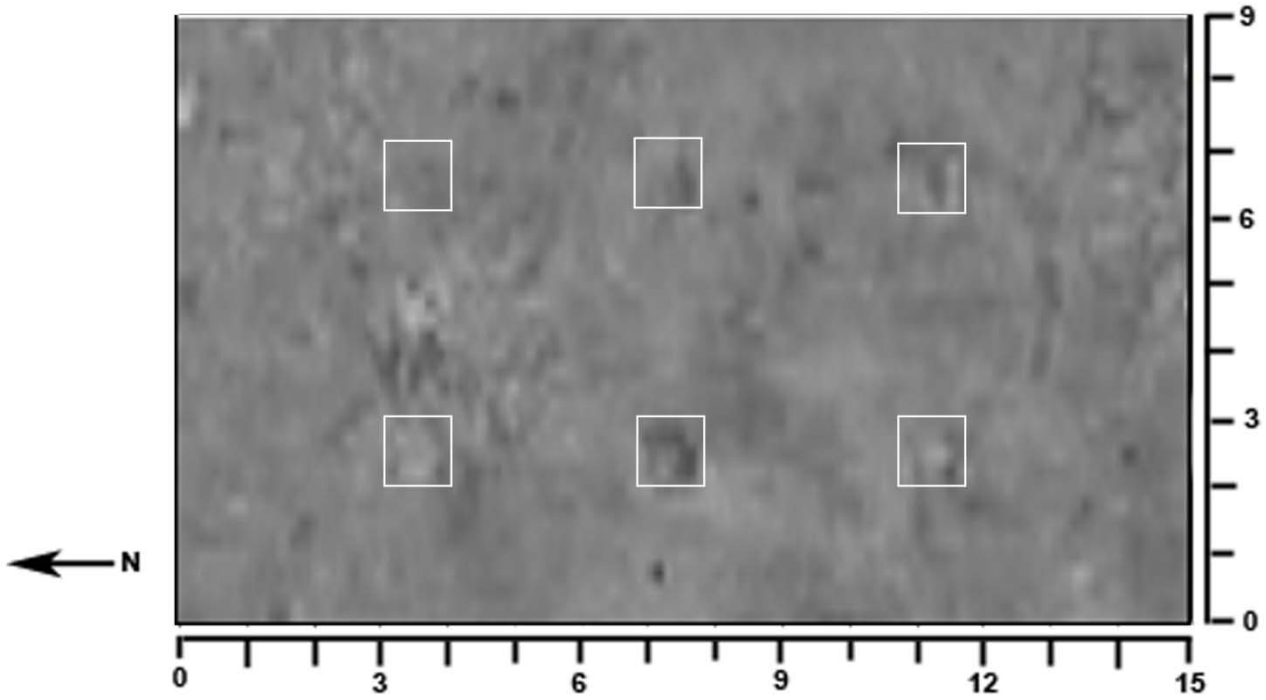

Figure 107: GPR horizontal slice in the X direction using the 500-MHz antenna at 4 months. The horizontal slice is approximately 0.44 m in depth (9.35 ns)

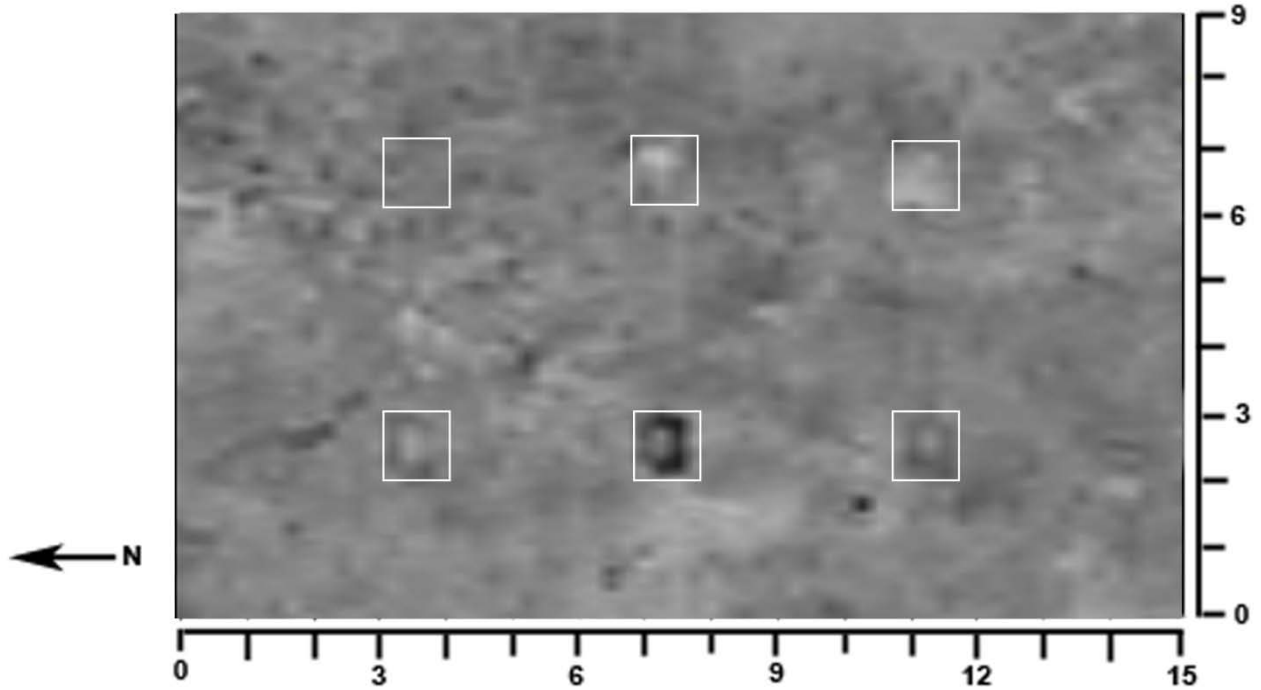

Figure 108: GPR horizontal slice in the Y direction using the 500-MHz antenna at 4 months. The horizontal slice is approximately 0.44 m in depth (9.22 ns)

5 MONTH

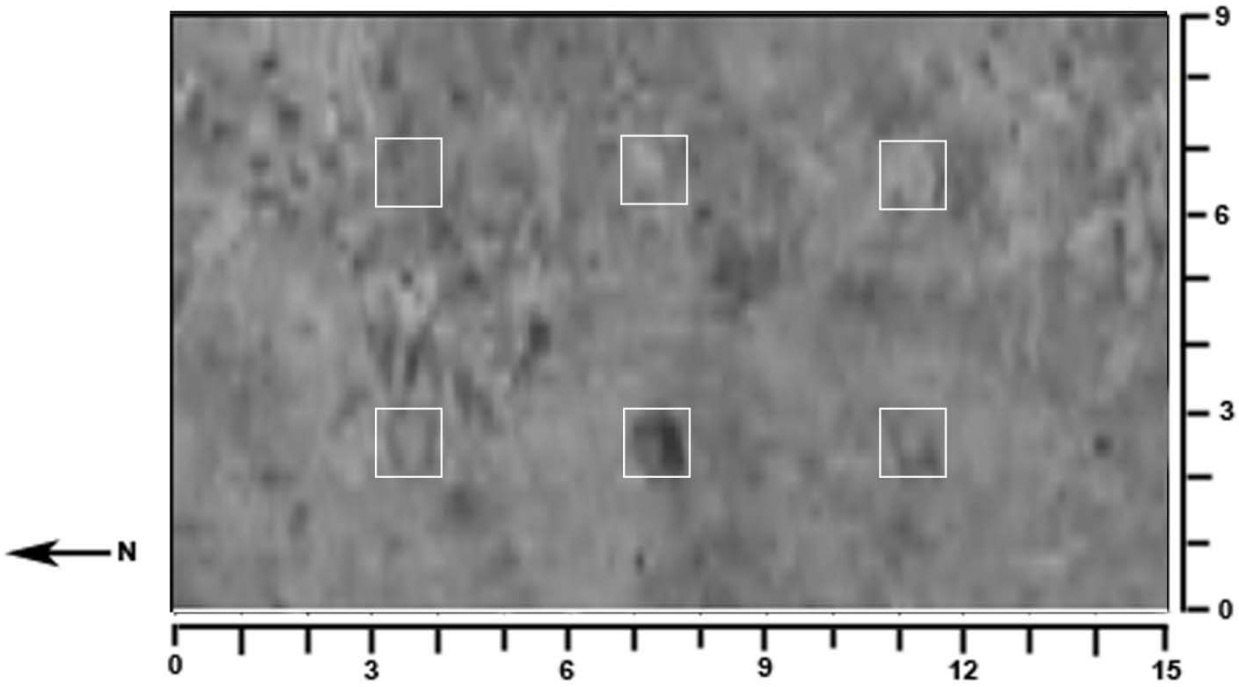

Figure 109: GPR horizontal slice in the X direction using the 500-MHz antenna at 5 months. The horizontal slice is approximately 0.44 m in depth (8.96 ns)

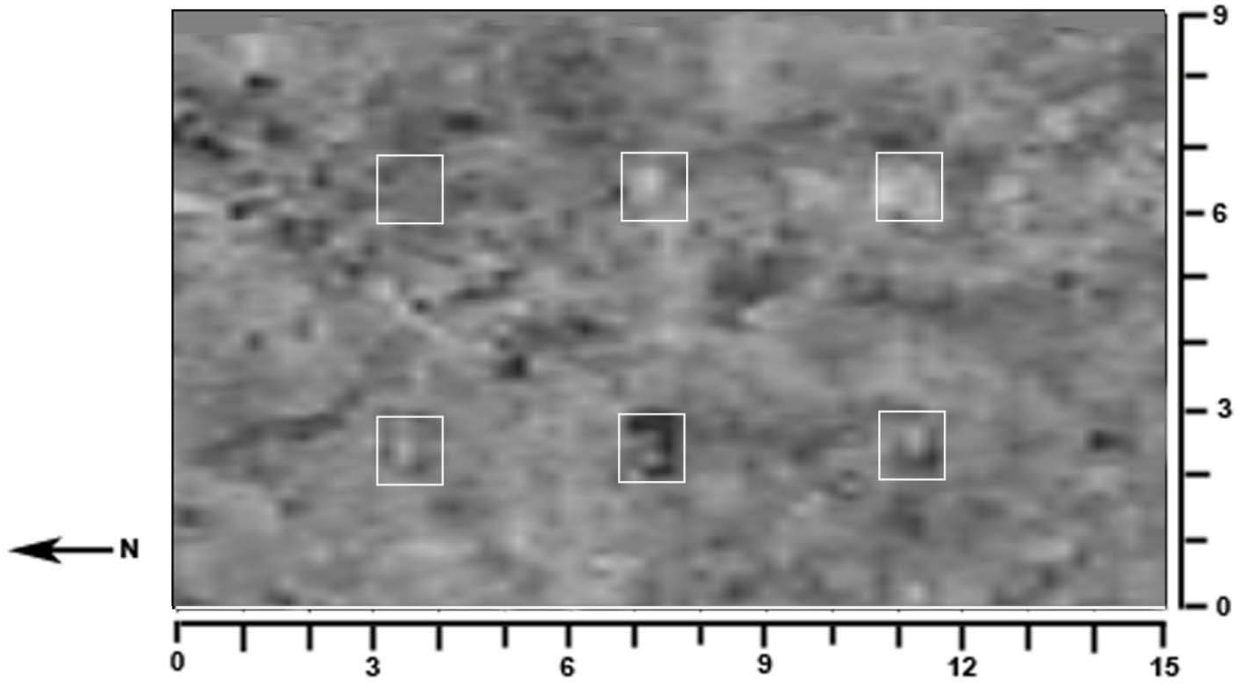

Figure 110: GPR horizontal slice in the Y direction using the 500-MHz antenna at 5 months. The horizontal slice is approximately 0.44 m in depth (9.22 ns)

6 MONTH

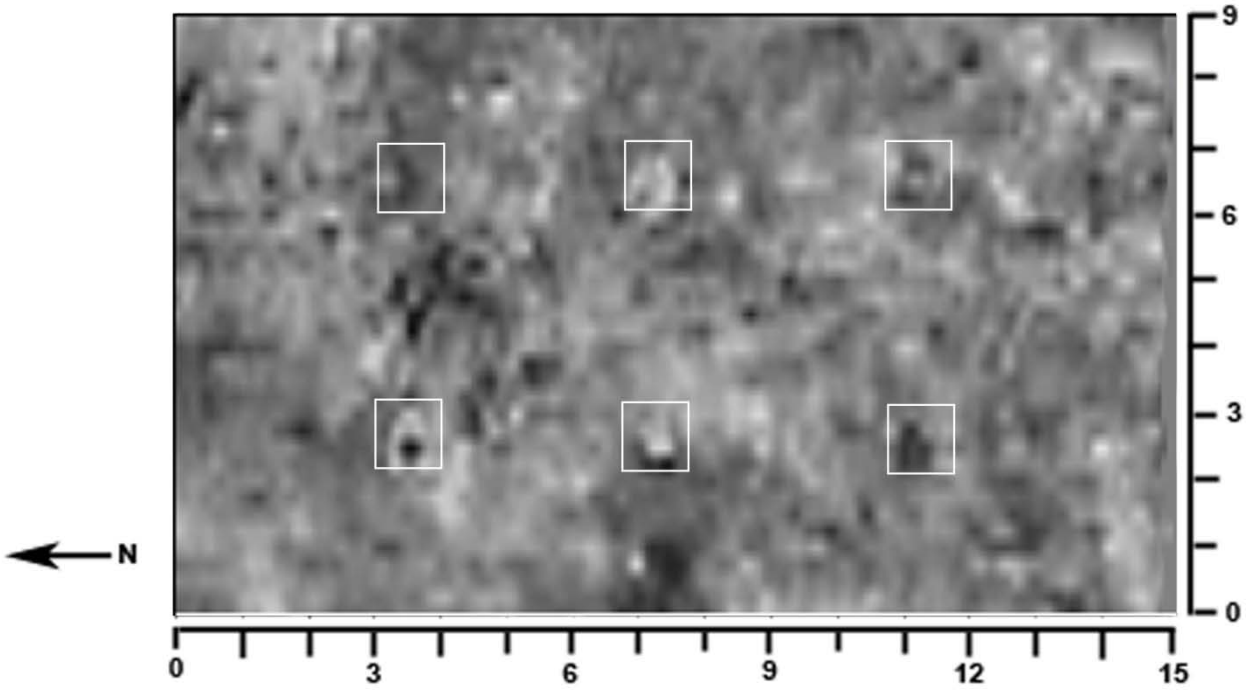

Figure 111: GPR horizontal slice in the X direction using the 500-MHz antenna at 6 months. The horizontal slice is approximately 0.44 m in depth (9.09 ns)

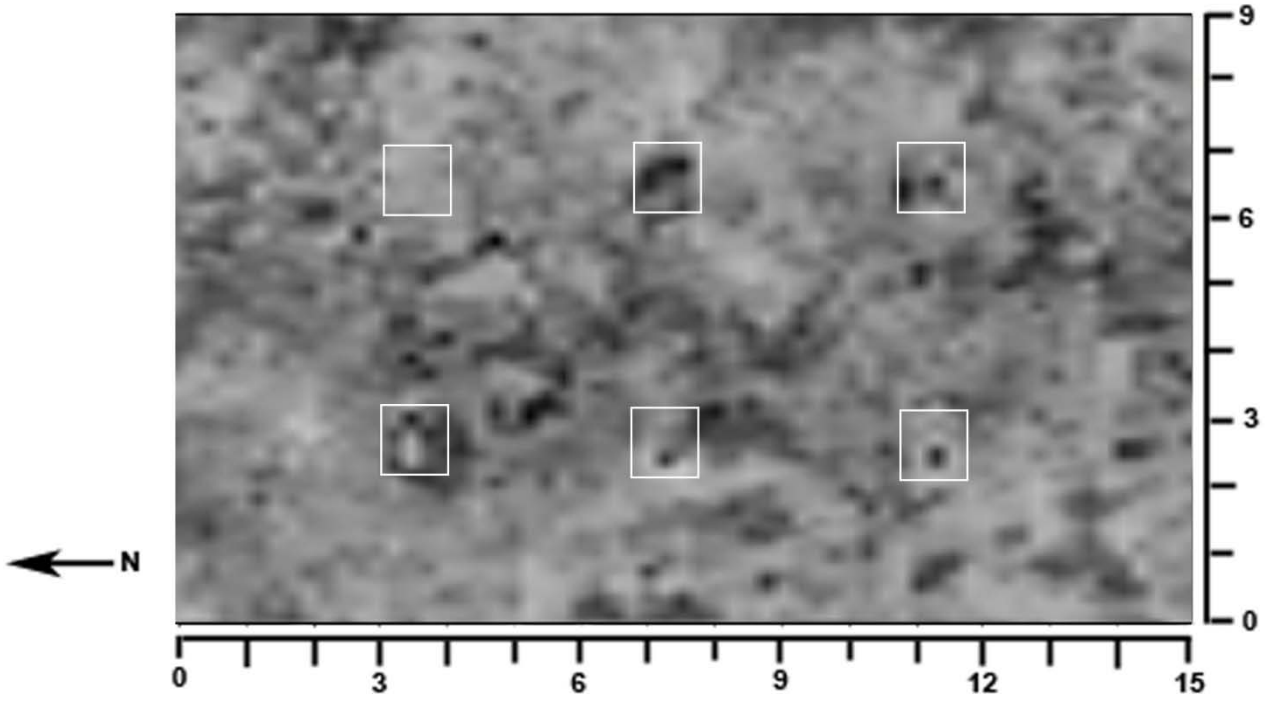

Figure 112: GPR horizontal slice in the Y direction using the 500-MHz antenna at 6 months. The horizontal slice is approximately 0.44 m in depth (8.07 ns)

7 MONTH

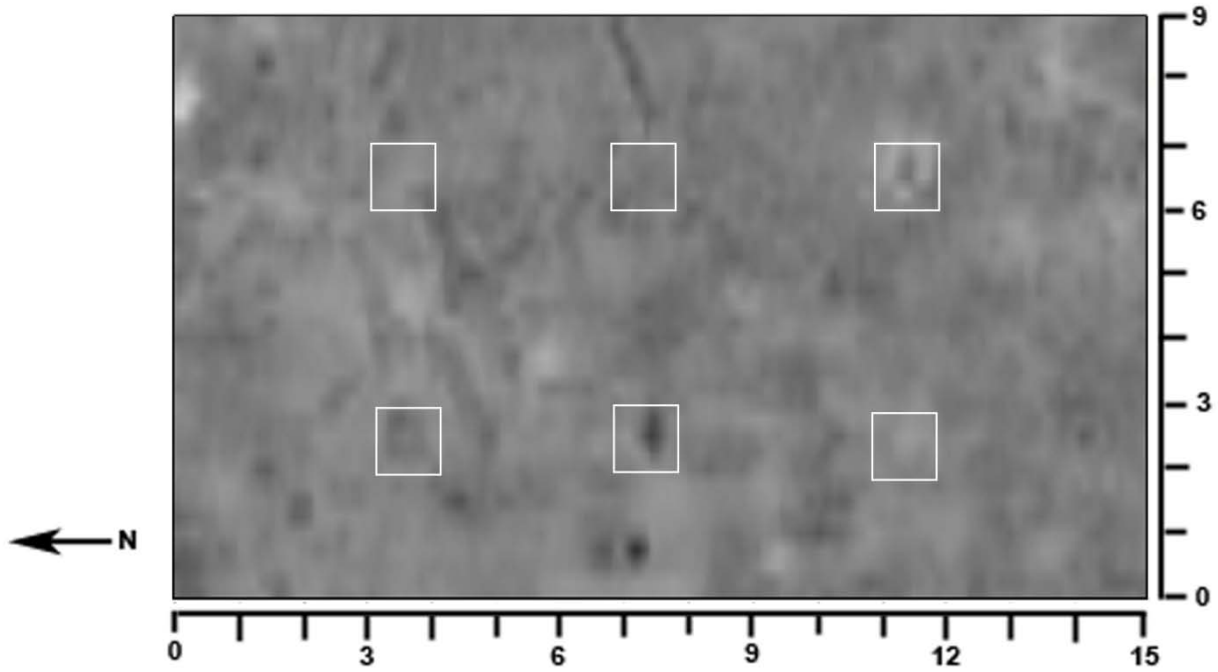

Figure 113: GPR horizontal slice in the Y direction using the 500-MHz antenna at 7 months. The horizontal slice is approximately 0.44 m in depth (8.73 ns)

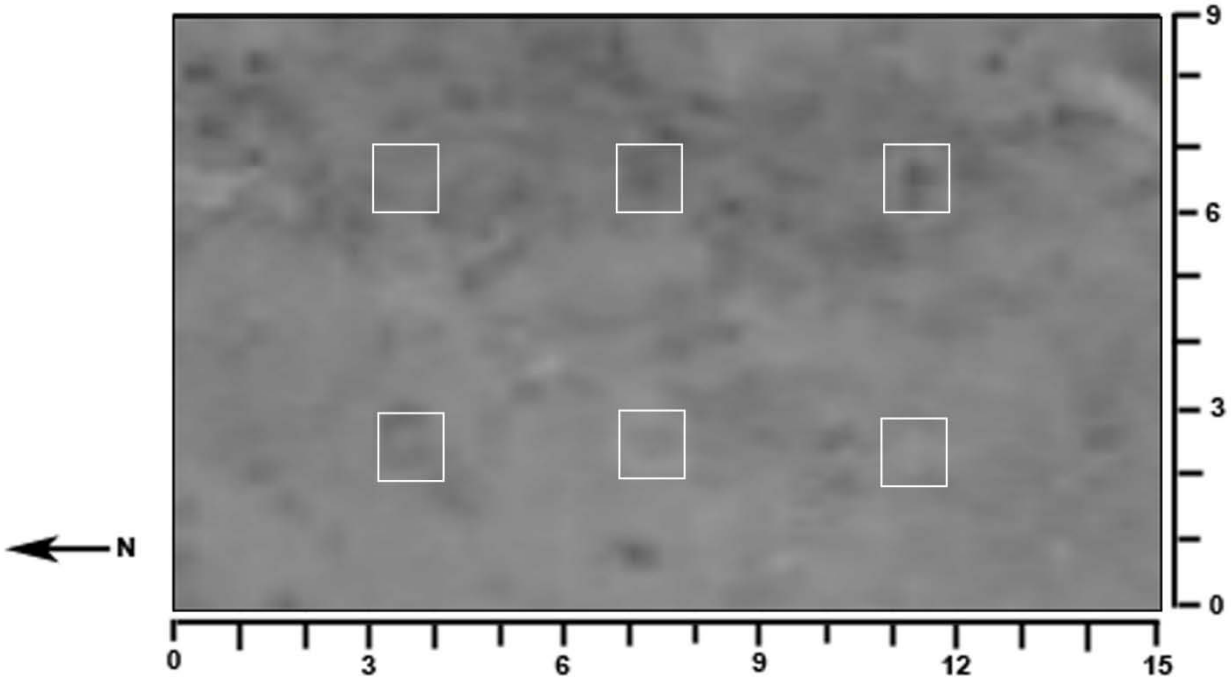

Figure 114: GPR horizontal slice in the Y direction using the 500-MHz antenna at 7 months. The horizontal slice is approximately 0.44 m in depth (9.34 ns)

8 MONTH

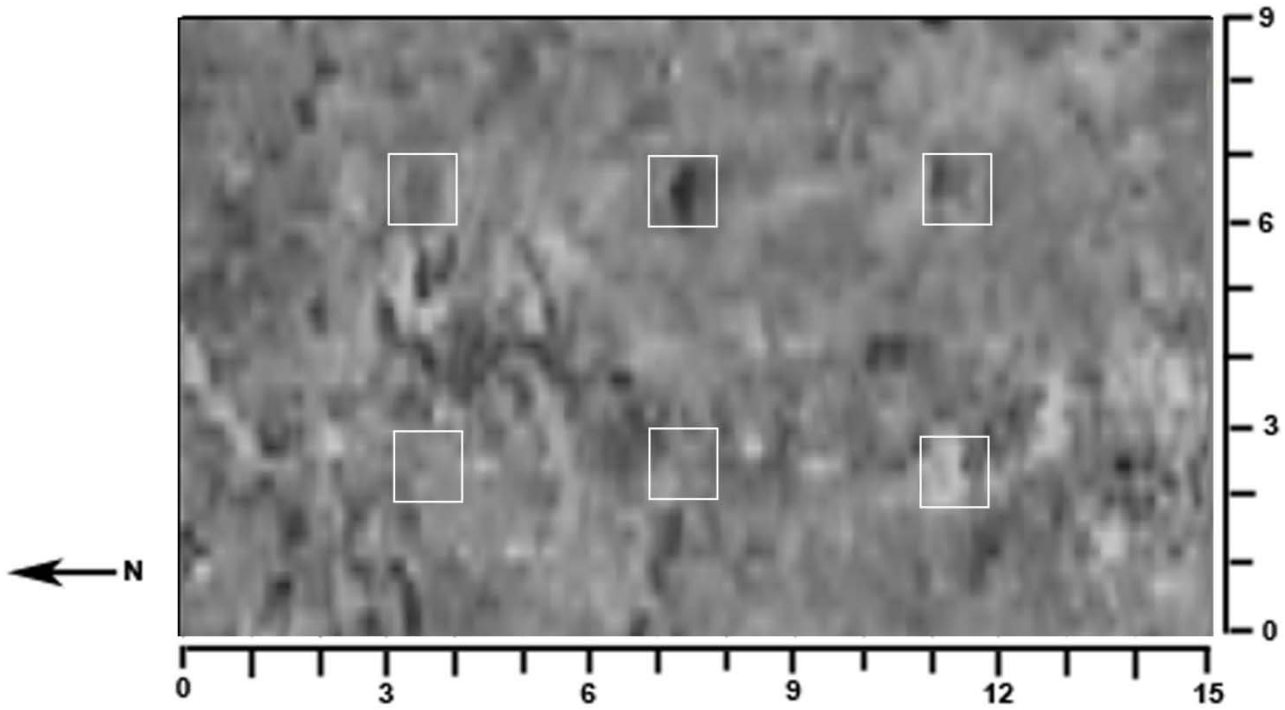

Figure 115: GPR horizontal slice in the X direction using the 500-MHz antenna at 8 months. The horizontal slice is approximately 0.39 m in depth (7.8 ns)

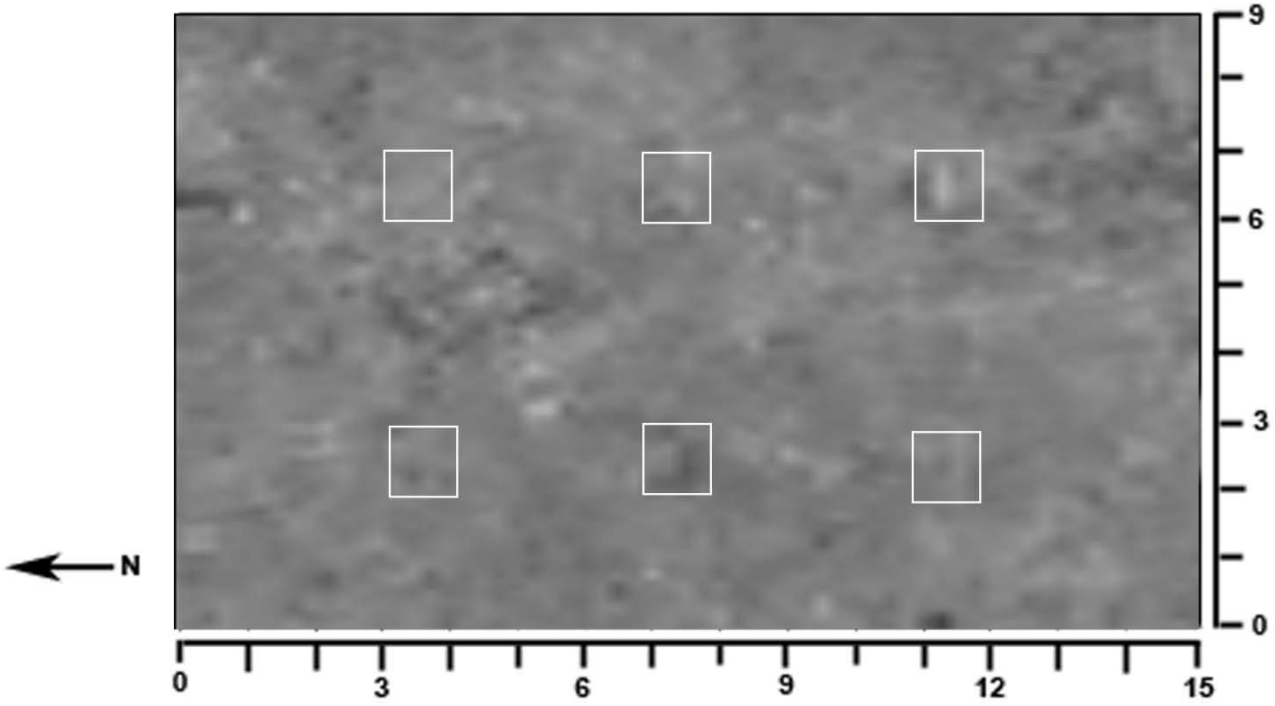

Figure 116: GPR horizontal slice in the Y direction using the 500-MHz antenna at 8 months. The horizontal slice is approximately 0.38 m in depth (7.5 ns)

MONTH 9

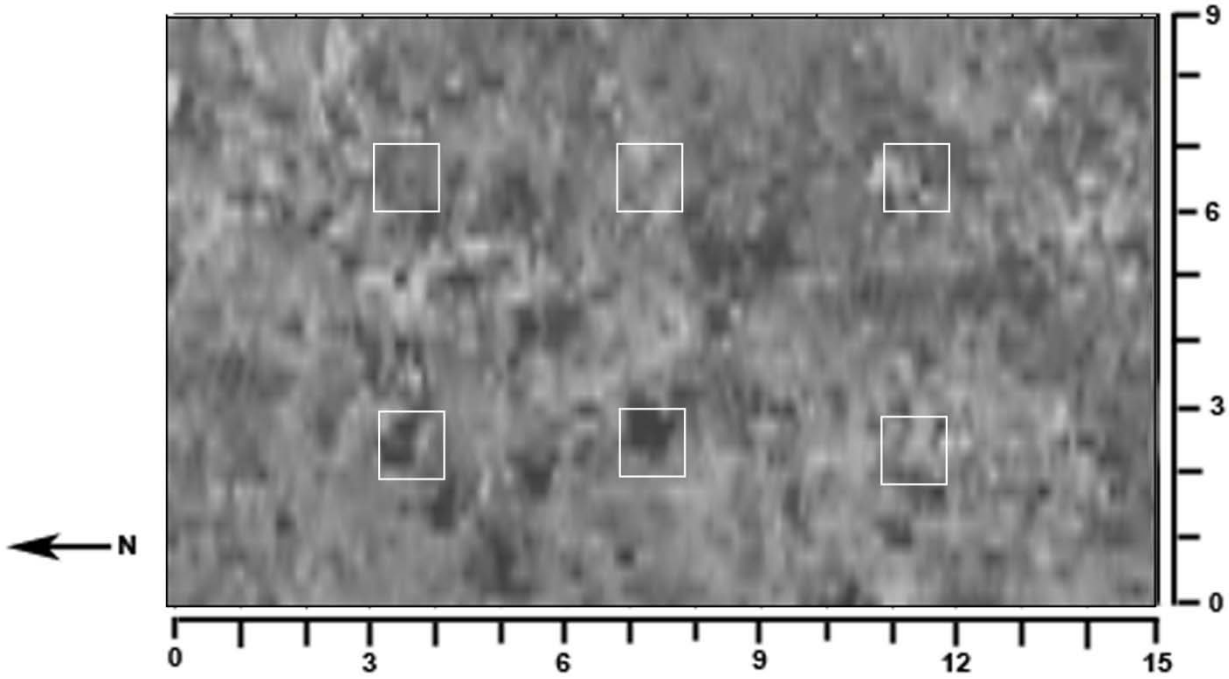

Figure 117: GPR horizontal slice in the X direction using the 500-MHz antenna at 9 months. The horizontal slice is approximately 0.44 m in depth (9.7 ns)

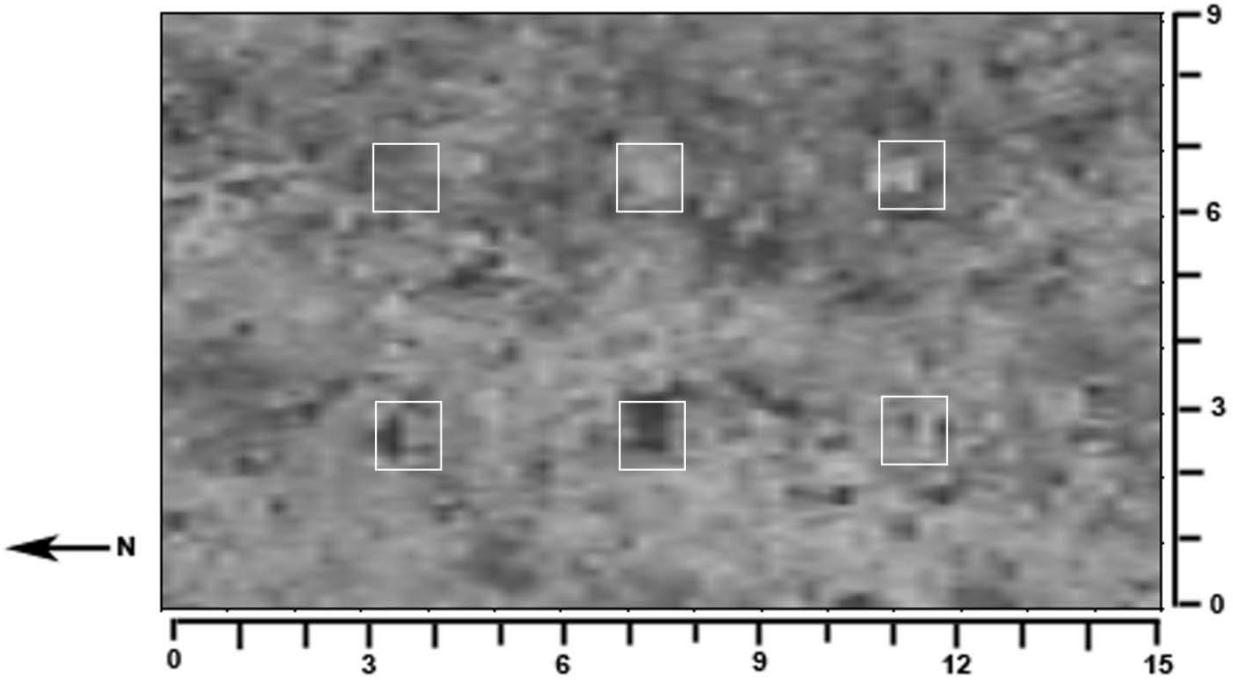

Figure 118: GPR horizontal slice in the Y direction using the 500-MHz antenna at 9 months. The horizontal slice is approximately 0.42 m in depth (9.2 ns)

10 MONTH

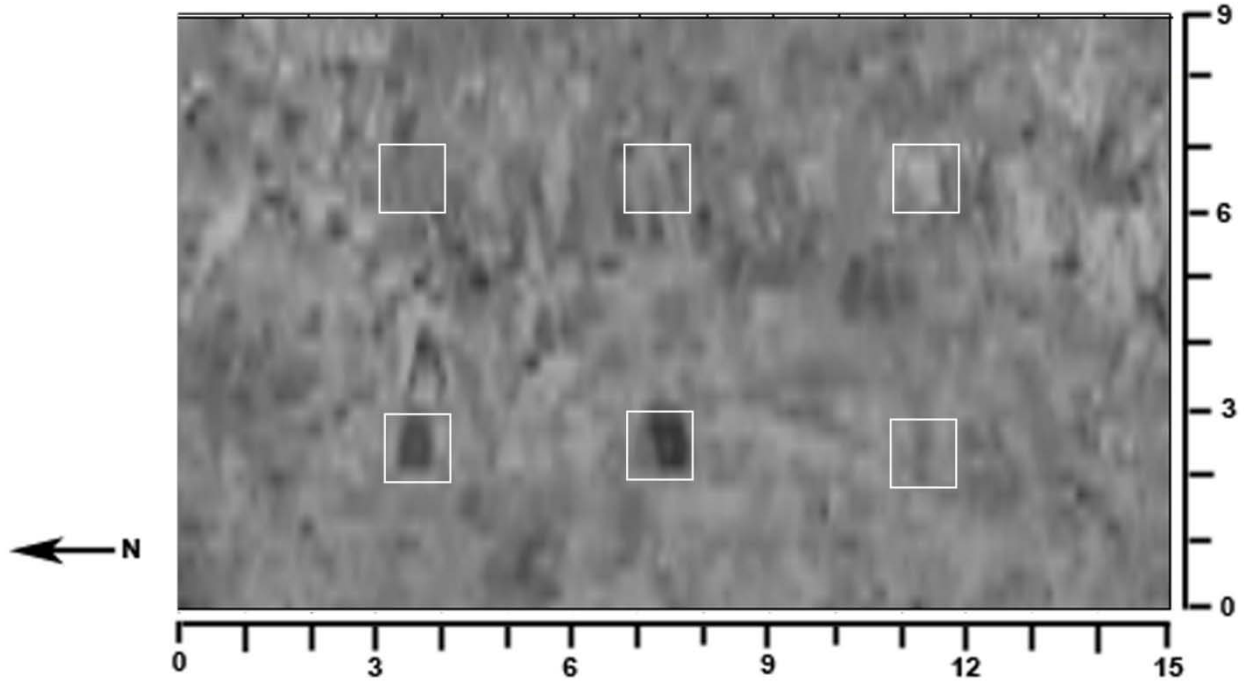

Figure 119: GPR horizontal slice in the X direction using the 500-MHz antenna at 10 months. The horizontal slice is approximately 0.43 m in depth (8.7 ns)

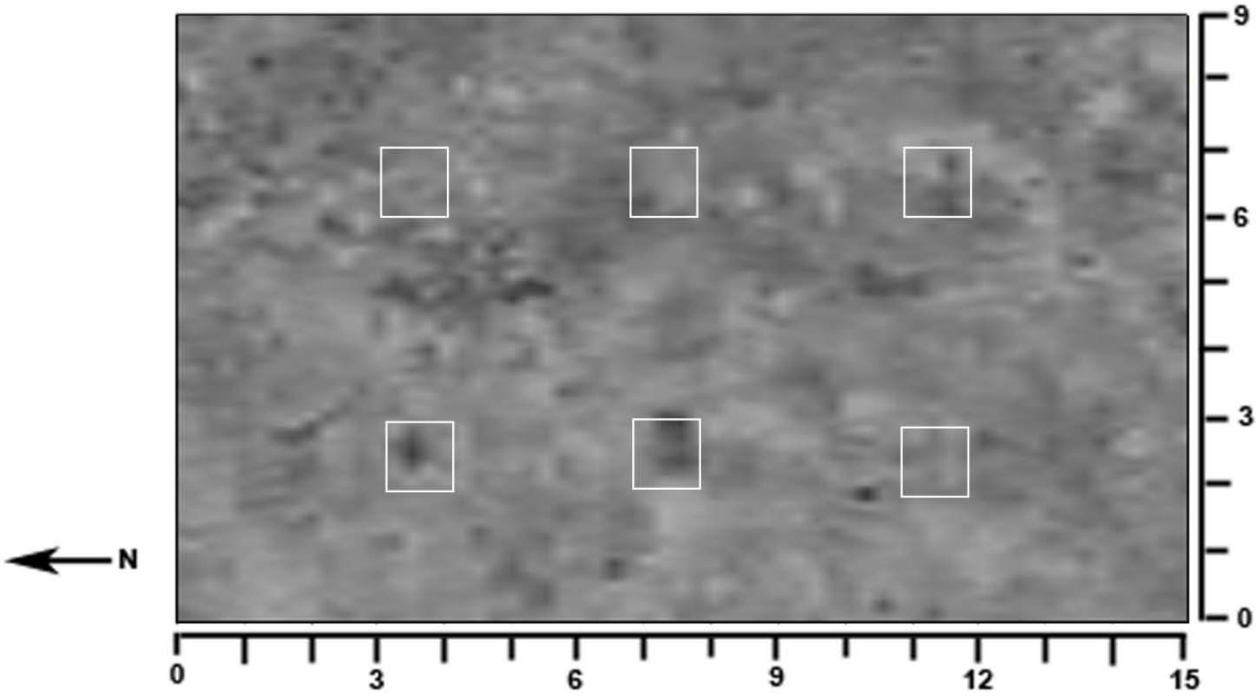

Figure 120: GPR horizontal slice in the Y direction using the 500-MHz antenna at 10 months. The horizontal slice is approximately 0.43 m in depth (8.7 ns)

11 MONTH

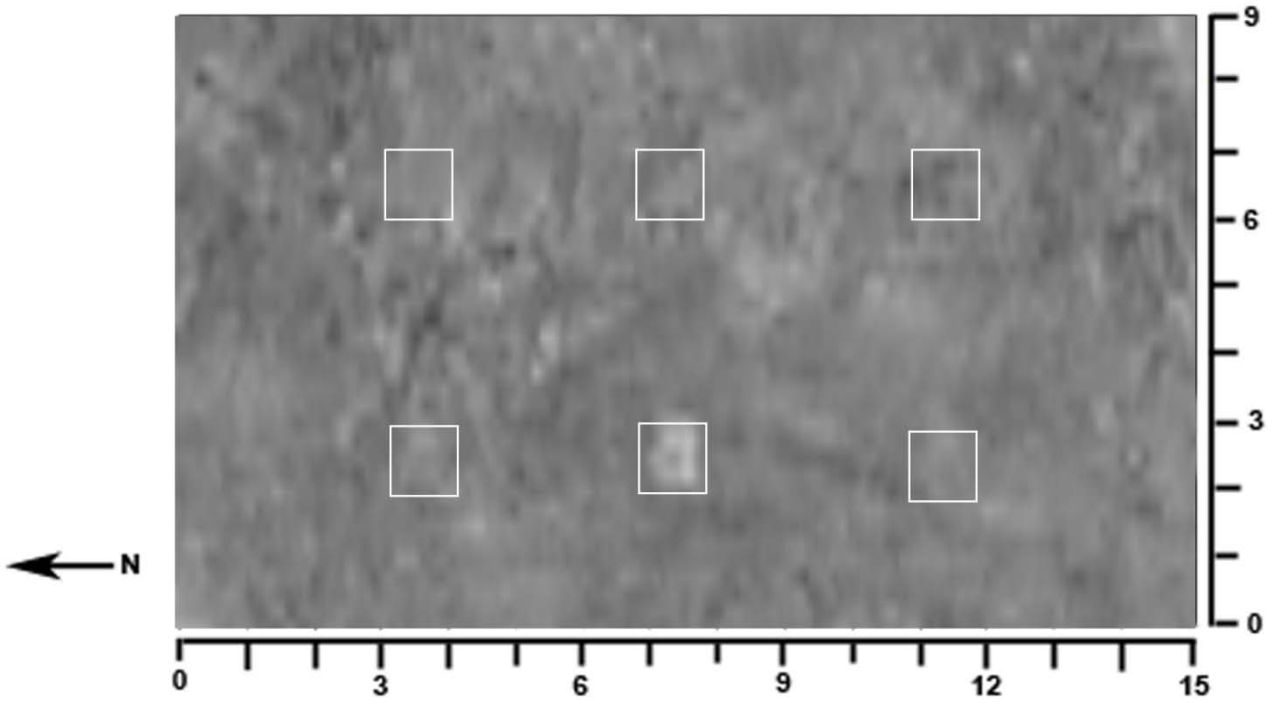

Figure 121: GPR horizontal slice in the X direction using the 500-MHz antenna at 11 months. The horizontal slice is approximately 0.39 m in depth (7.8 ns)

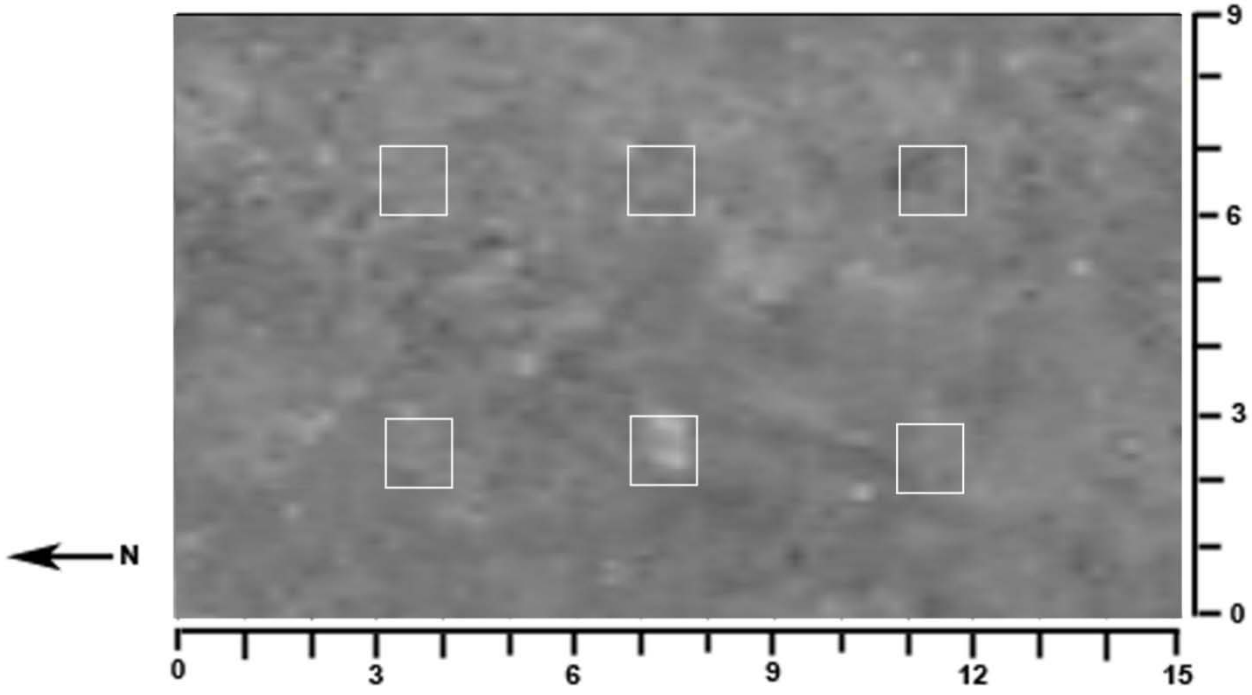

Figure 122: GPR horizontal slice in the Y direction using the 500-MHz antenna at 11 months. The horizontal slice is approximately 0.39 m in depth (7.8 ns)

12 MONTH

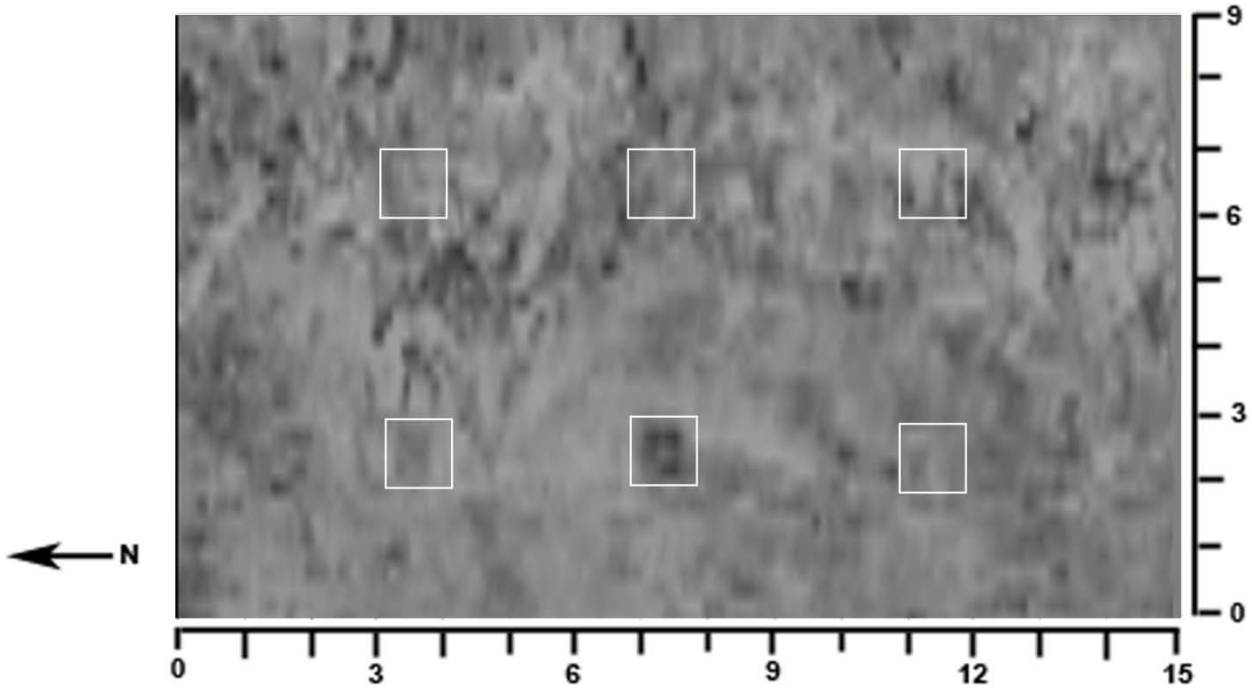

Figure 123: GPR horizontal slice in the X direction using the 500-MHz antenna at 12 months. The horizontal slice is approximately 0.41 m in depth (8.3 ns)

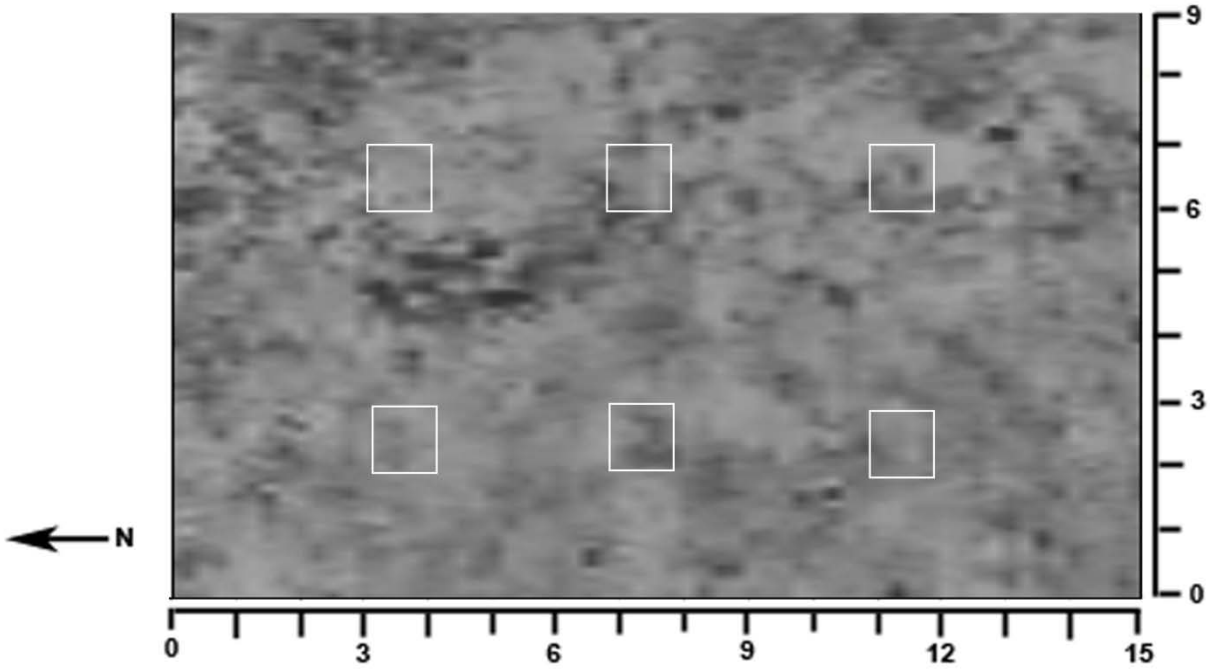

Figure 124: GPR horizontal slice in the Y direction using the 500-MHz antenna at 12 months. The horizontal slice is approximately 0.41 m in depth (8.3 ns)

APPENDIX C: GROUND PENETRATING RADAR 250-MHZ REFLECTION PROFILES

1 MONTH

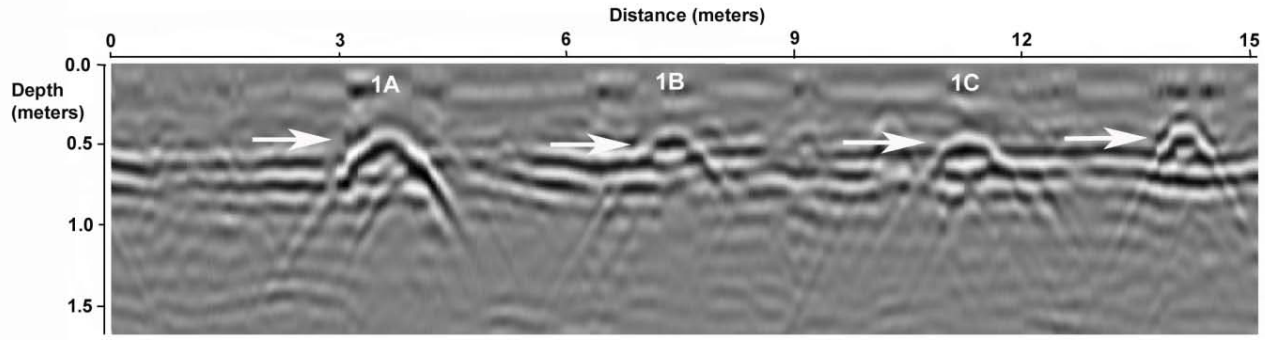

Figure 125: GPR reflection profile using the 250-MHz antenna of Row 1 at 1 month

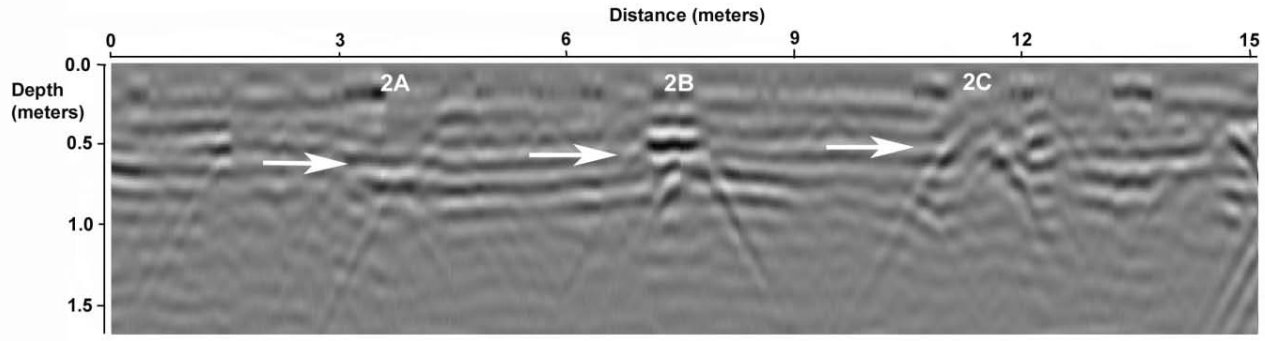

Figure 126: GPR reflection profile using the 250-MHz antenna of Row 2 at 1 month

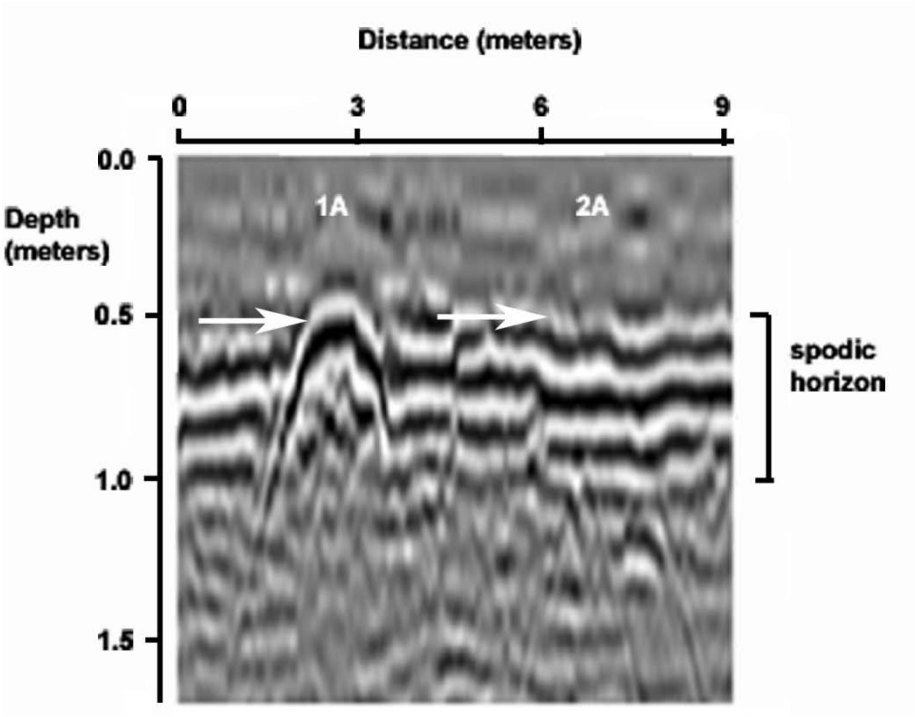

Figure 127: GPR reflection profile using the 250-MHz antenna of Row 1A2A at 1 month

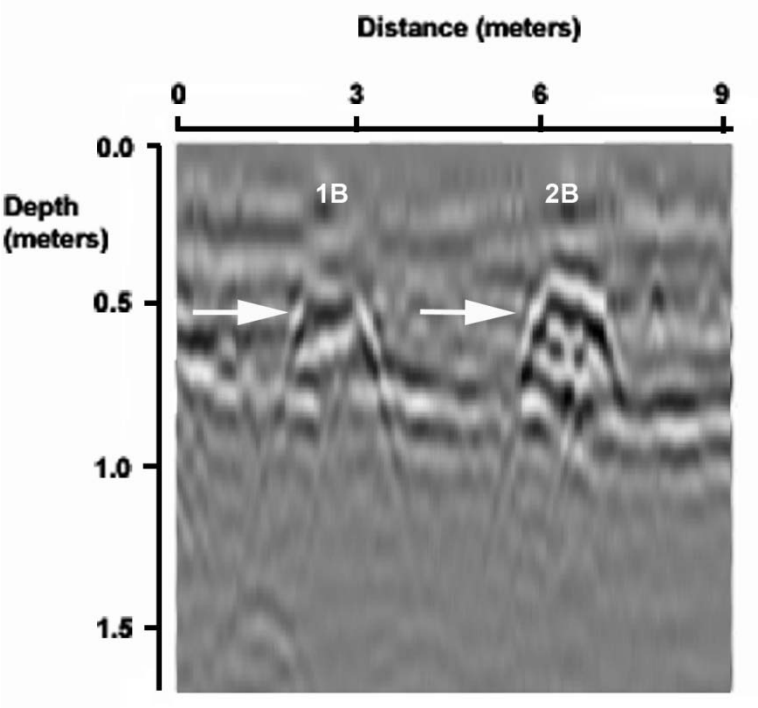

Figure 128: GPR reflection profile using the 250-MHz antenna of Row 1B2B at 1 month

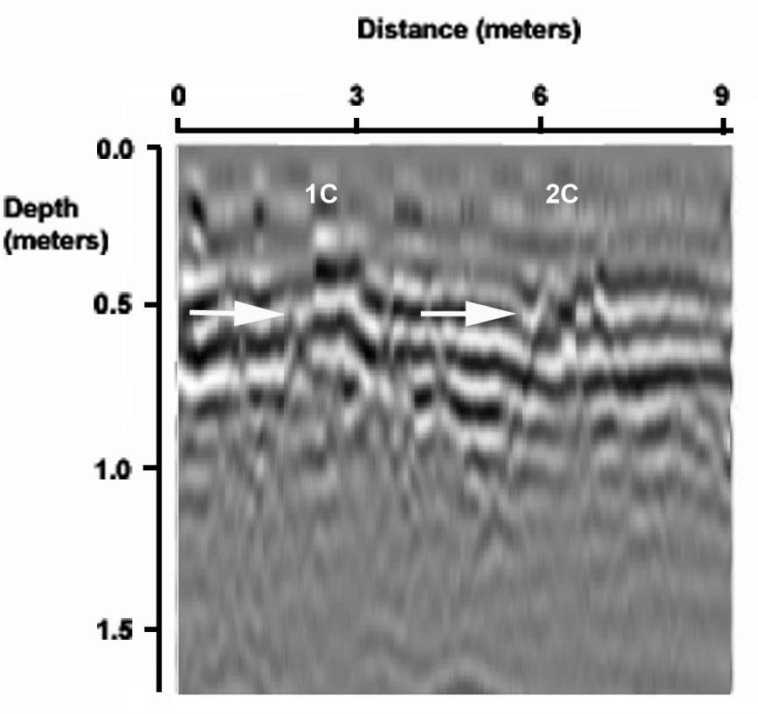

Figure 129: GPR reflection profile using the 250-MHz antenna of Row 1C2C at 1 month

2 MONTH

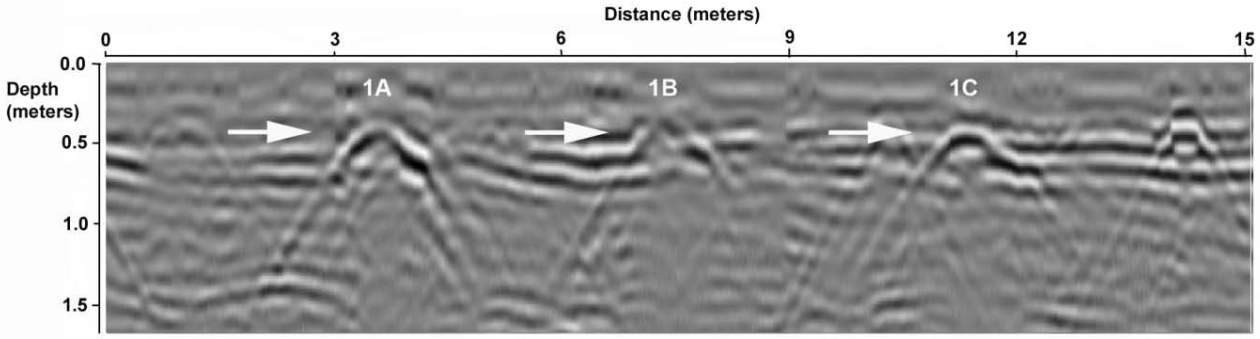

Figure 130: GPR reflection profile using the 250-MHz antenna of Row 1 at 2 months

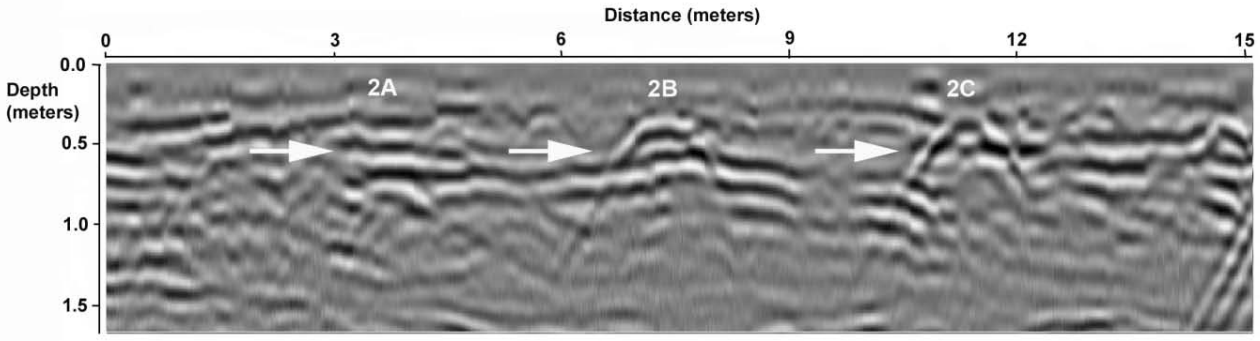

Figure 131: GPR reflection profile using the 250-MHz antenna of Row 2 at 2 months

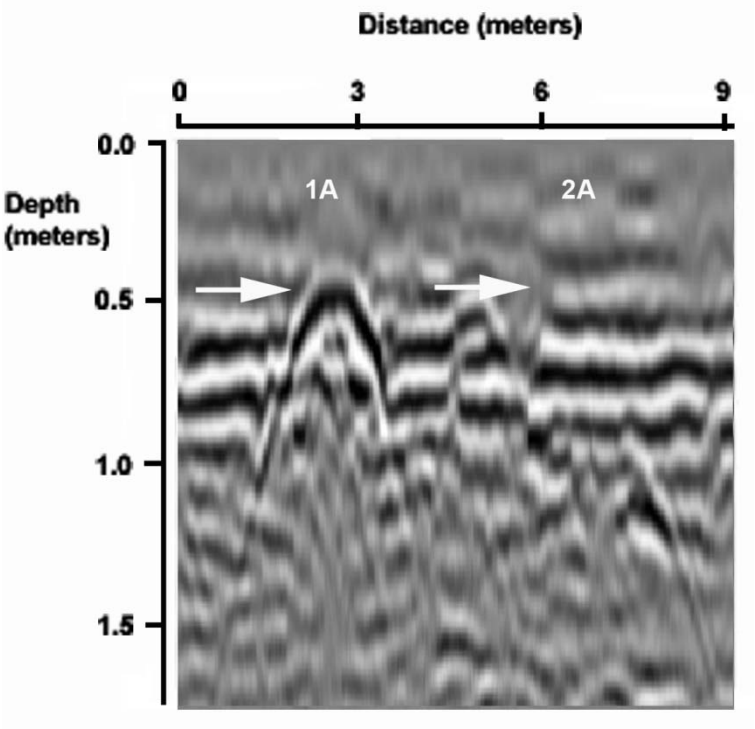

Figure 132: GPR reflection profile using the 250-MHz antenna of Row 1A2A at 2 months

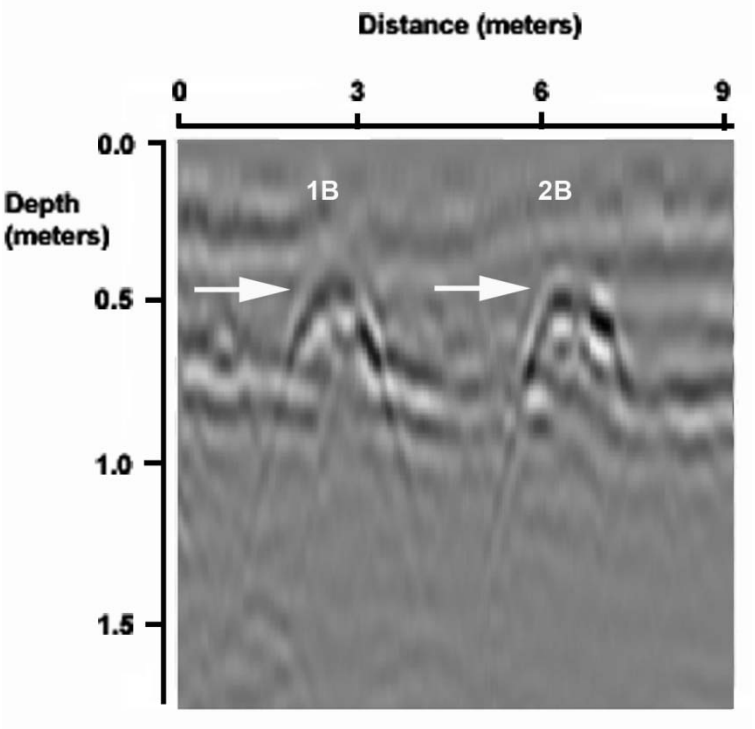

Figure 133: GPR reflection profile using the 250-MHz antenna of Row 1B2B at 2 months

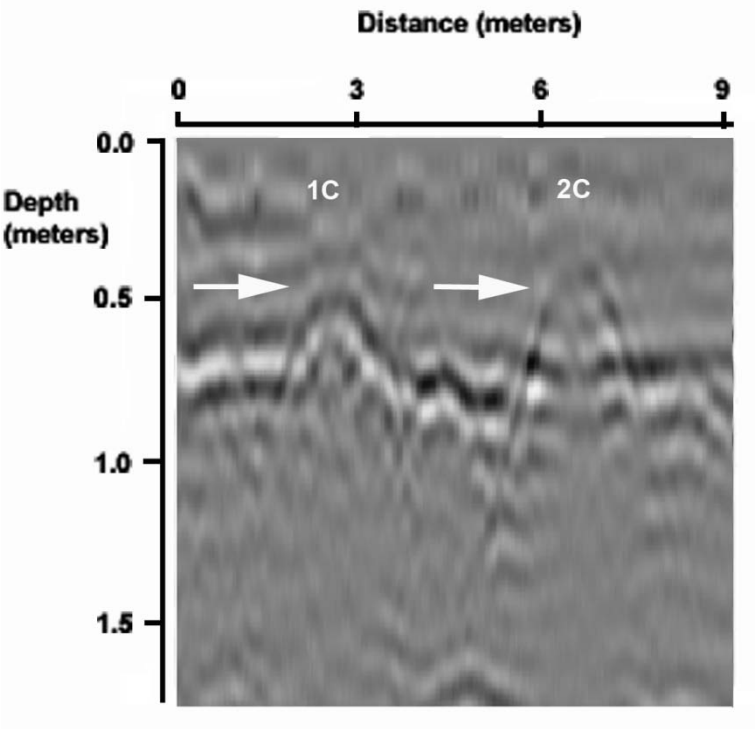

Figure 134: GPR reflection profile using the 250-MHz antenna of Row 1C2C at 2 months

3 MONTH

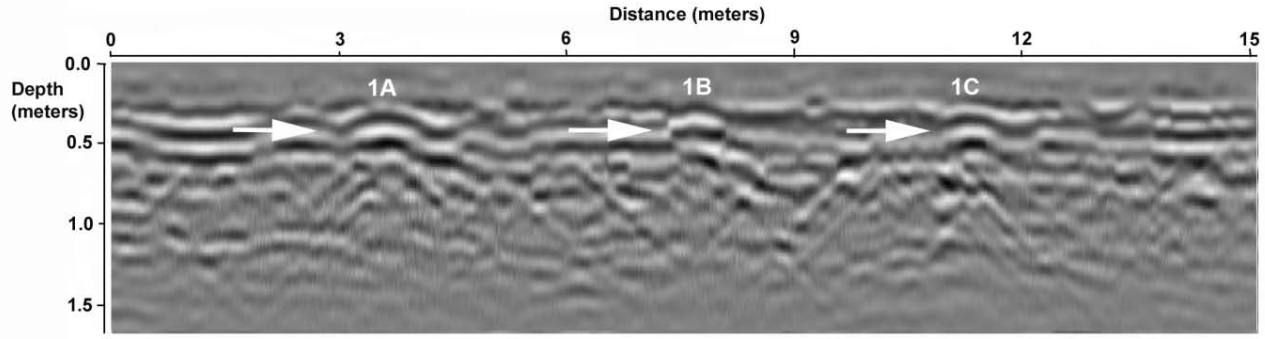

Figure 135: GPR reflection profile using the 250-MHz antenna of Row 1 at 3 months

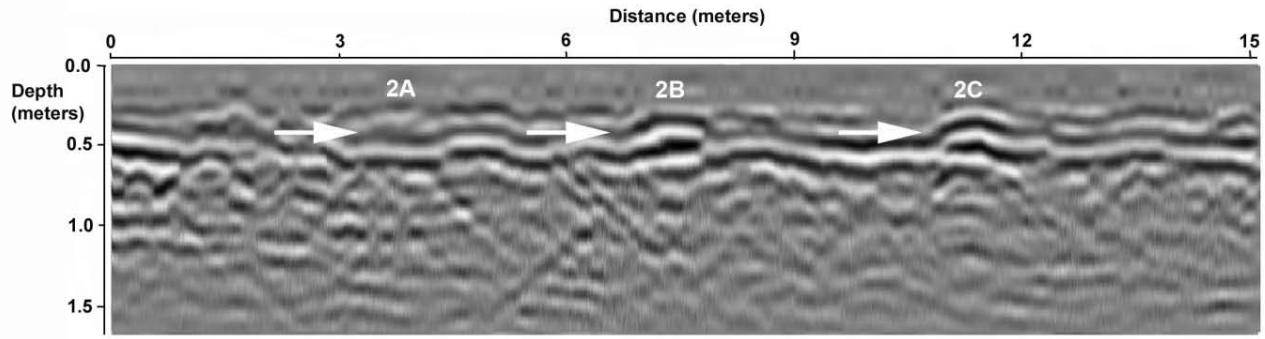

Figure 136: GPR reflection profile using the 250-MHz antenna of Row 2 at 3 months

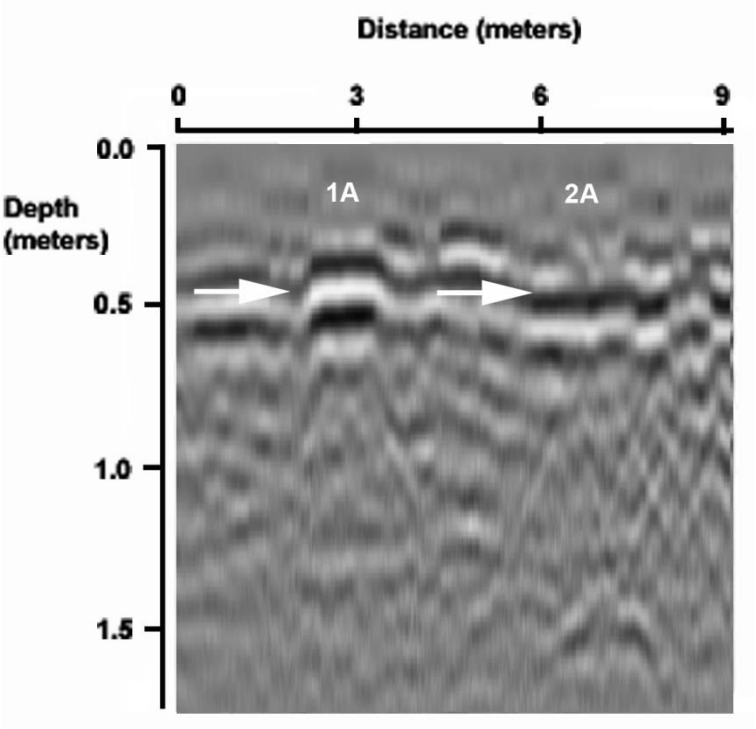

Figure 137: GPR reflection profile using the 250-MHz antenna of Row 1A2A at 3 months

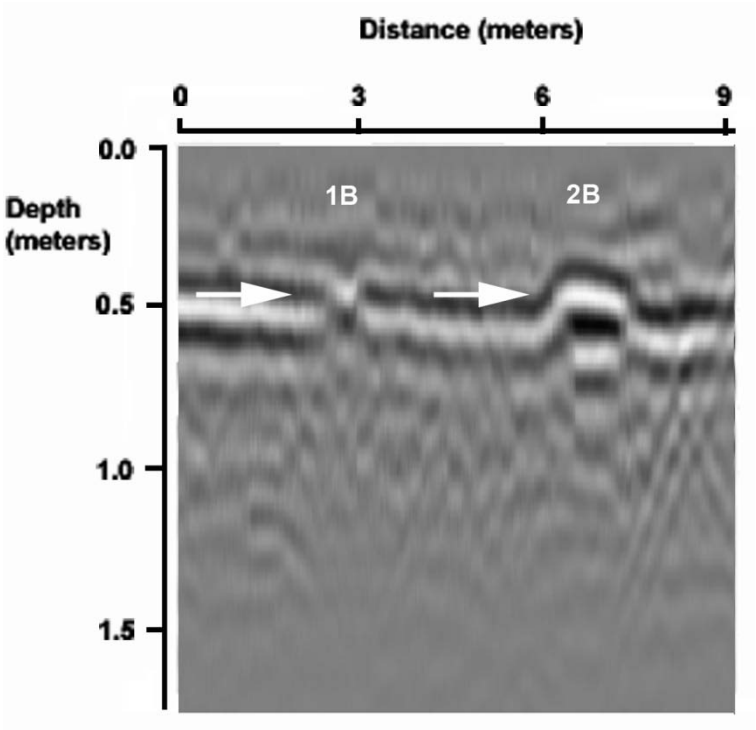

Figure 138: GPR reflection profile using the 250-MHz antenna of Row 1B2B at 3 months

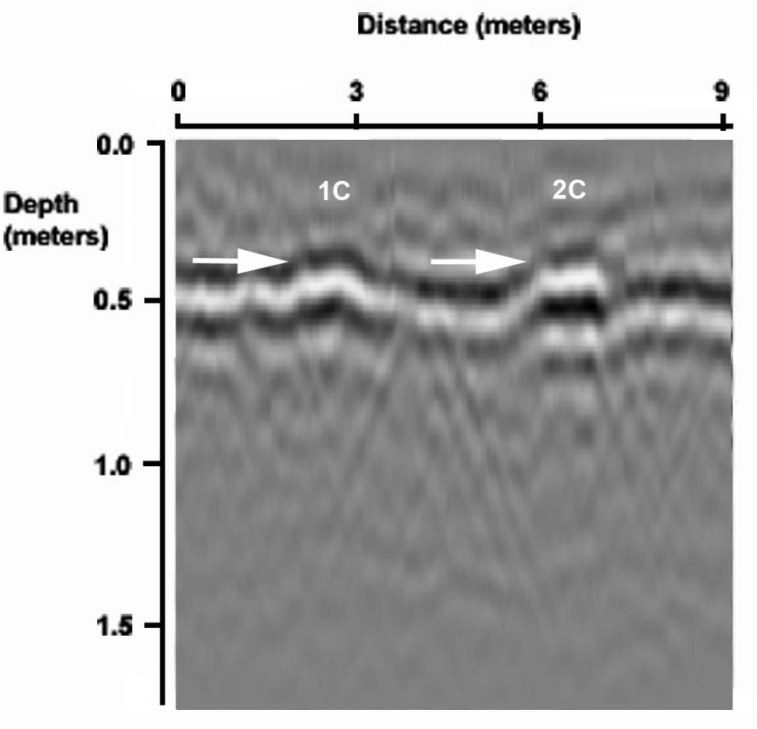

Figure 139: GPR reflection profile using the 250-MHz antenna of Row 1C2C at 3 months

4 MONTH

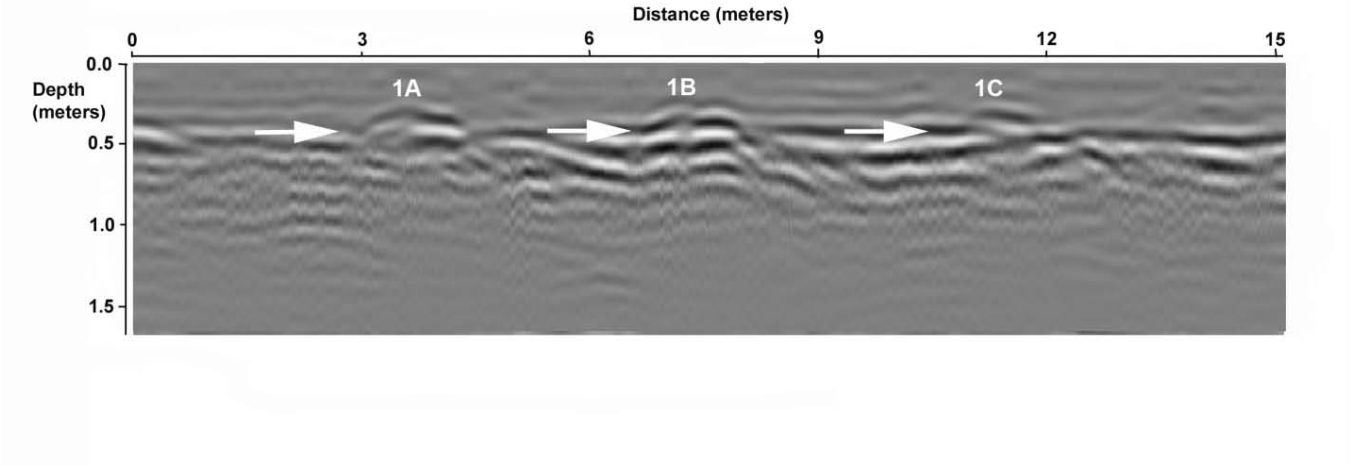

Figure 140: GPR reflection profile using the 250-MHz antenna of Row 1 at 4 months

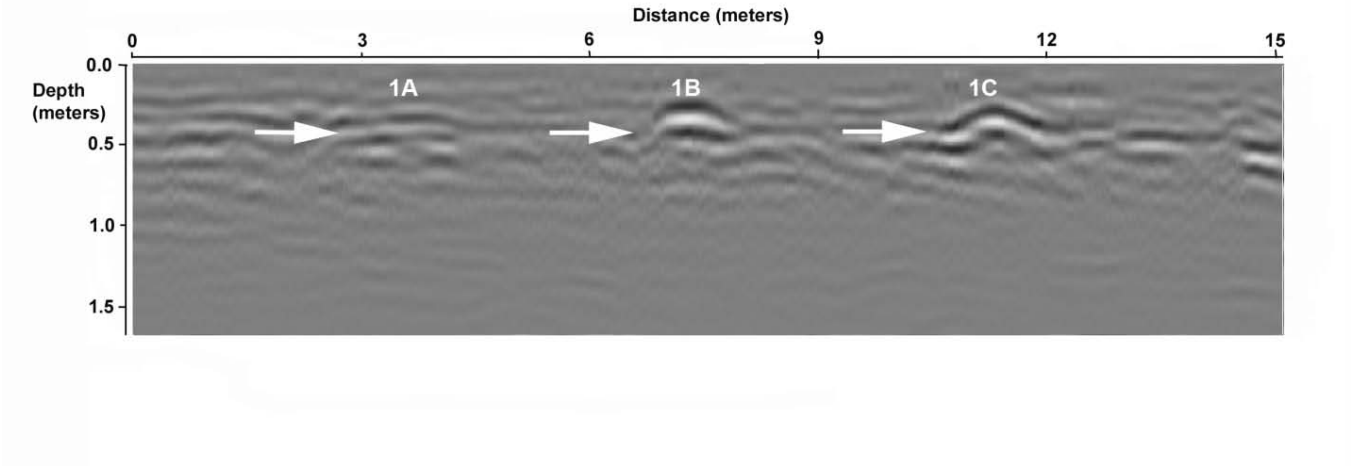

Figure 141: GPR reflection profile using the 250-MHz antenna of Row 2 at 4 months

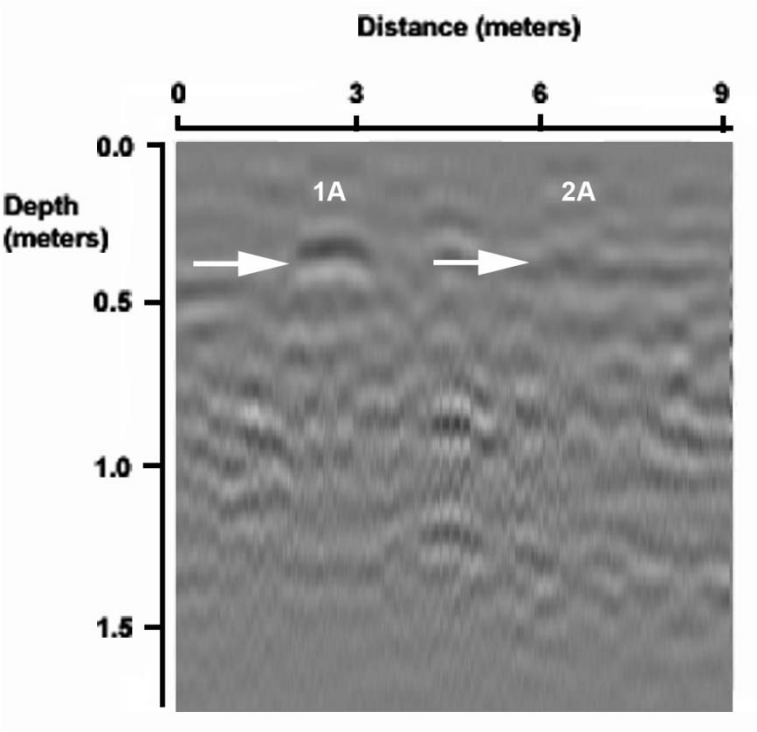

Figure 142: GPR reflection profile using the 250-MHz antenna of Row 1A2A at 4 months

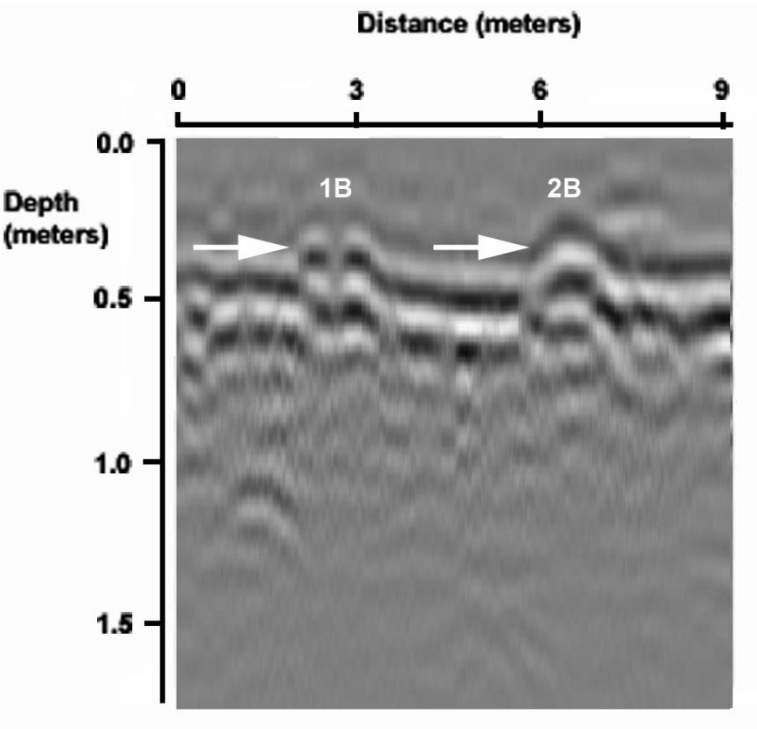

Figure 143: GPR reflection profile using the 250-MHz antenna of Row 1B2B at 4 months

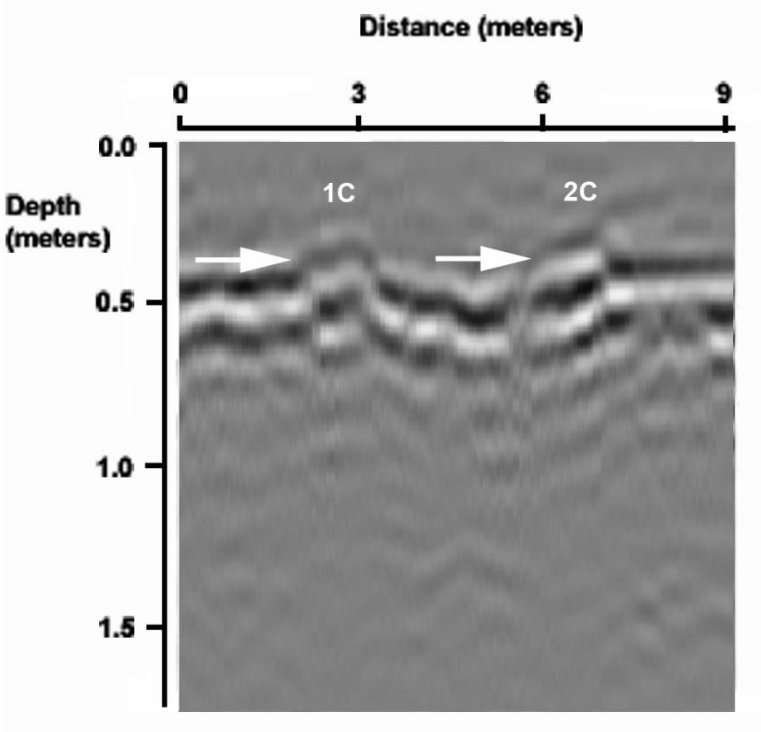

Figure 144: GPR reflection profile using the 250-MHz antenna of Row 1C2C at 4 months

5 MONTH

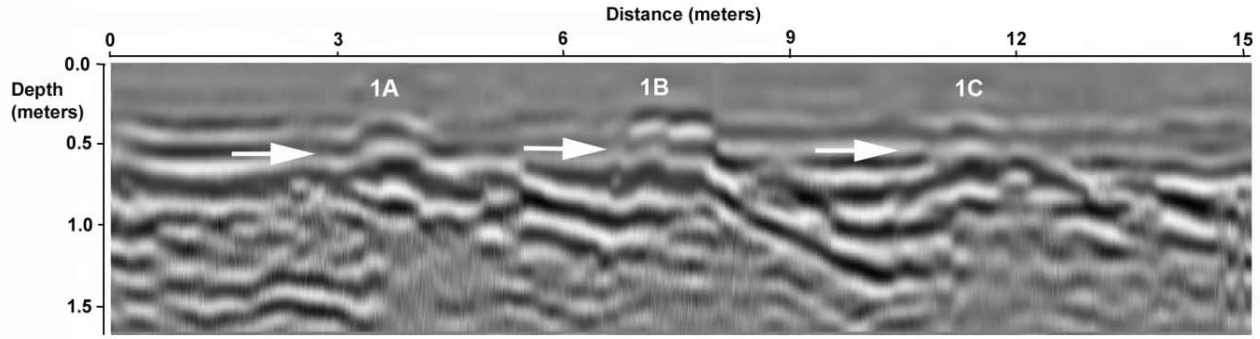

Figure 145: GPR reflection profile using the 250-MHz antenna of Row 1 at 5 months

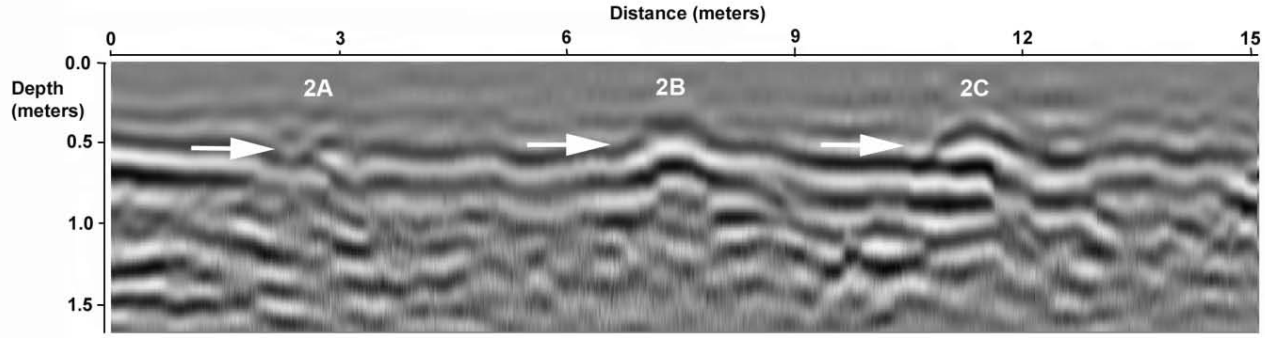

Figure 146: GPR reflection profile using the 250-MHz antenna of Row 2 at 5 months

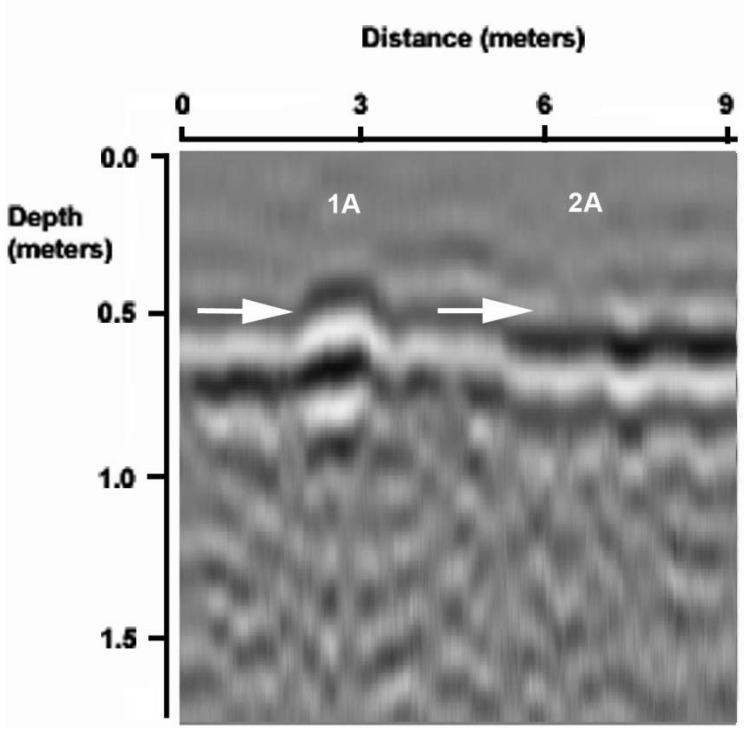

Figure 147: GPR reflection profile using the 250-MHz antenna of Row 1A2A at 5 months

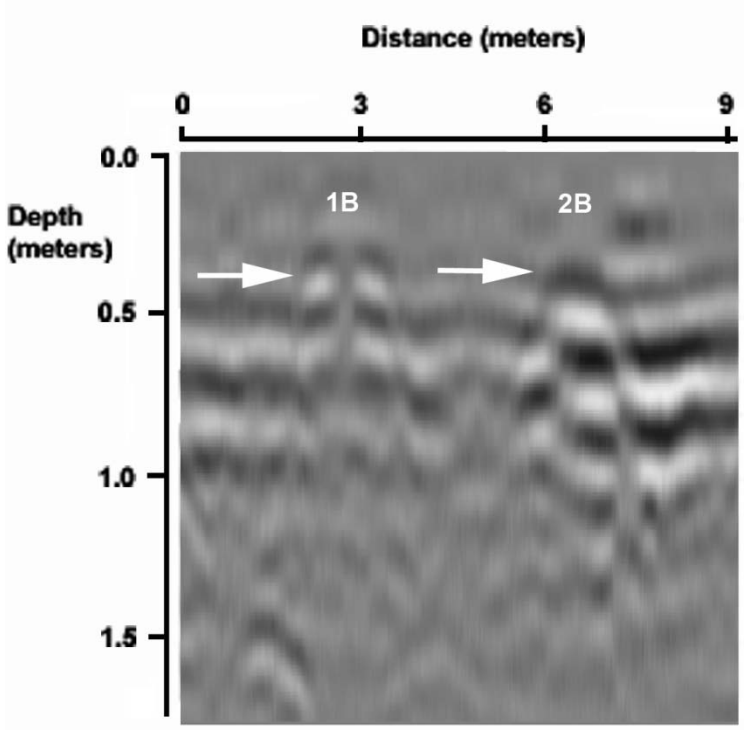

Figure 148: GPR reflection profile using the 250-MHz antenna of Row 1B2B at 5 months

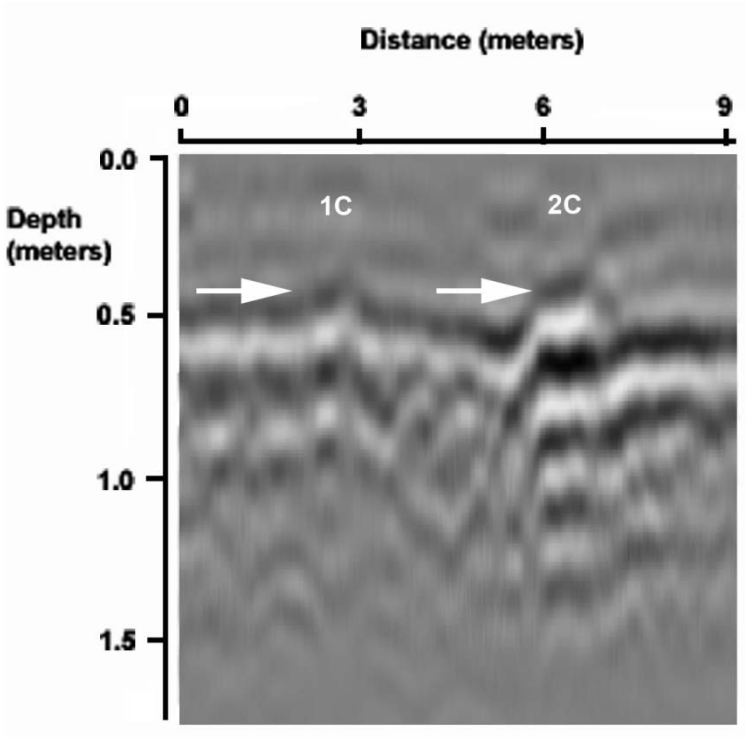

Figure 149: GPR reflection profile using the 250-MHz antenna of Row 1C2C at 5 months

6 MONTH

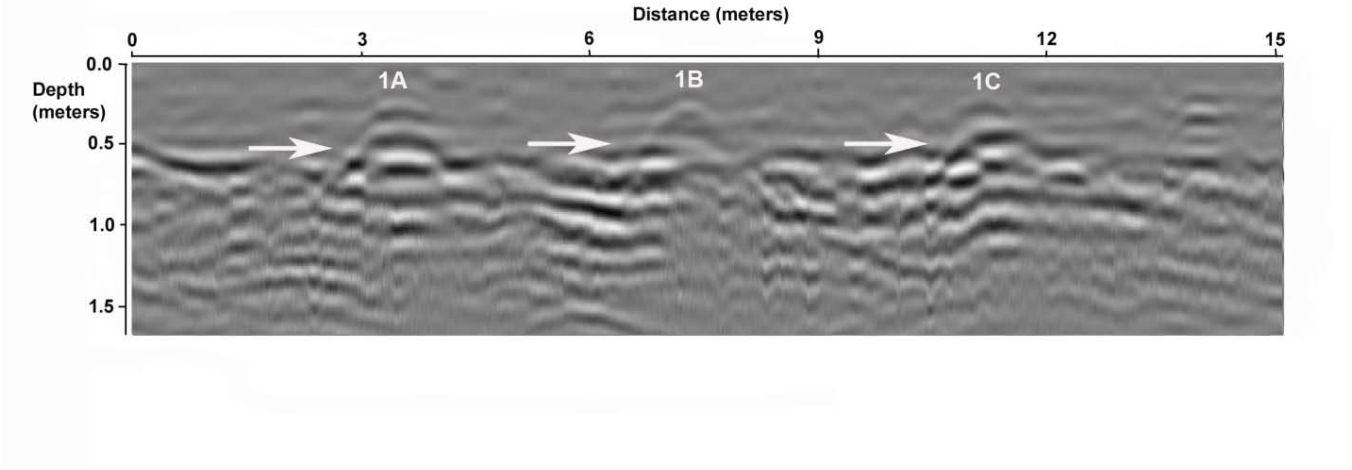

Figure 150: GPR reflection profile using the 250-MHz antenna of Row 1 at 6 months

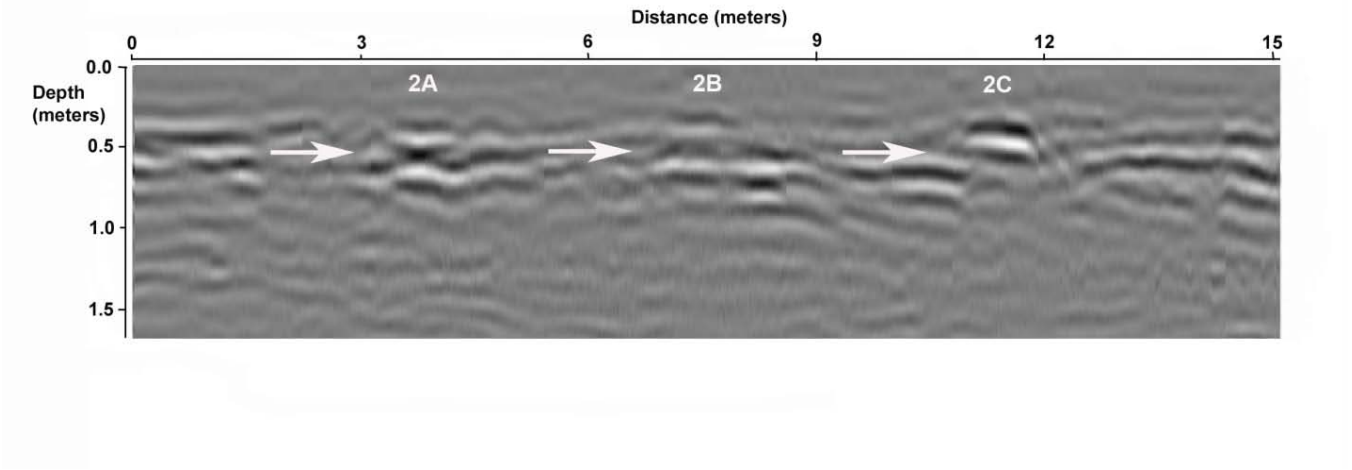

Figure 151: GPR reflection profile using the 250-MHz antenna of Row 2 at 6 months

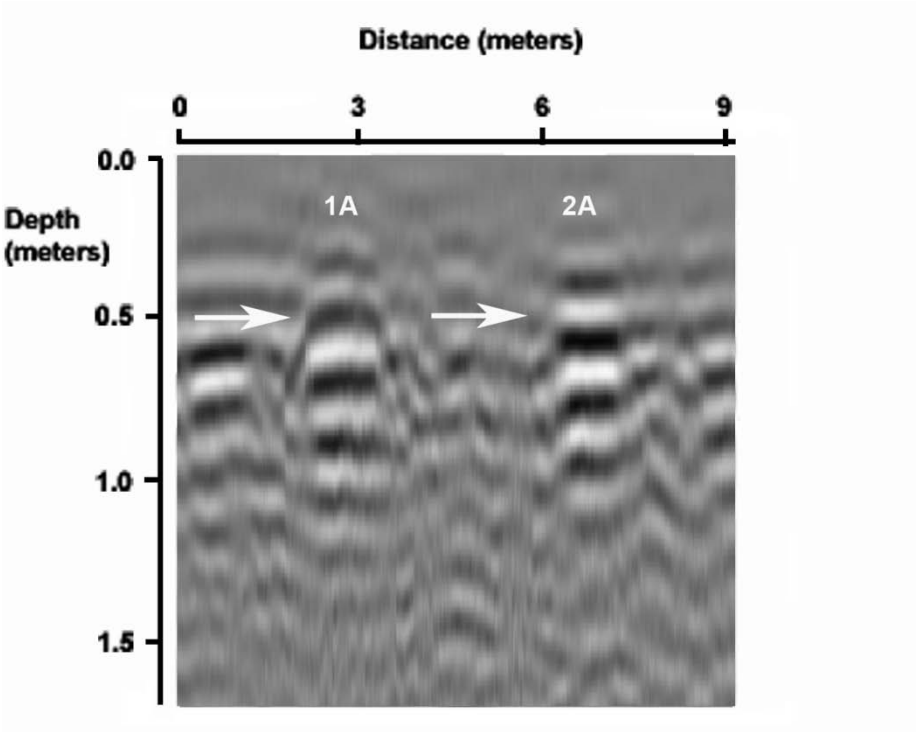

Figure 152: GPR reflection profile using the 250-MHz antenna of Row 1A2A at 6 months

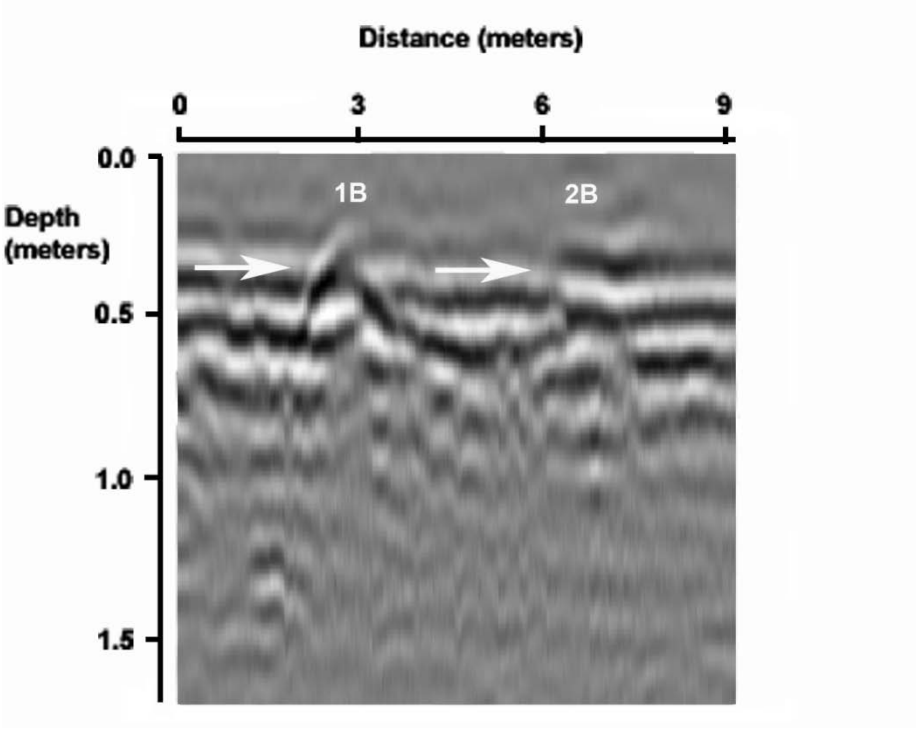

Figure 153: GPR reflection profile using the 250-MHz antenna of Row 1B2B at 6 months

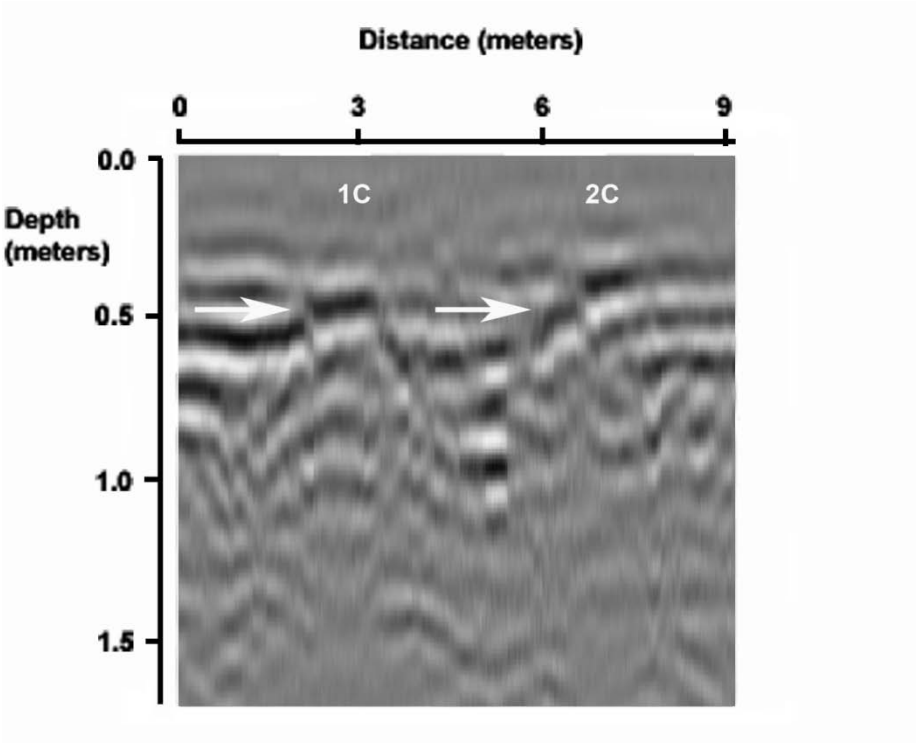

Figure 154: GPR reflection profile using the 250-MHz antenna of Row 1C2C at 6 months

7 MONTHS

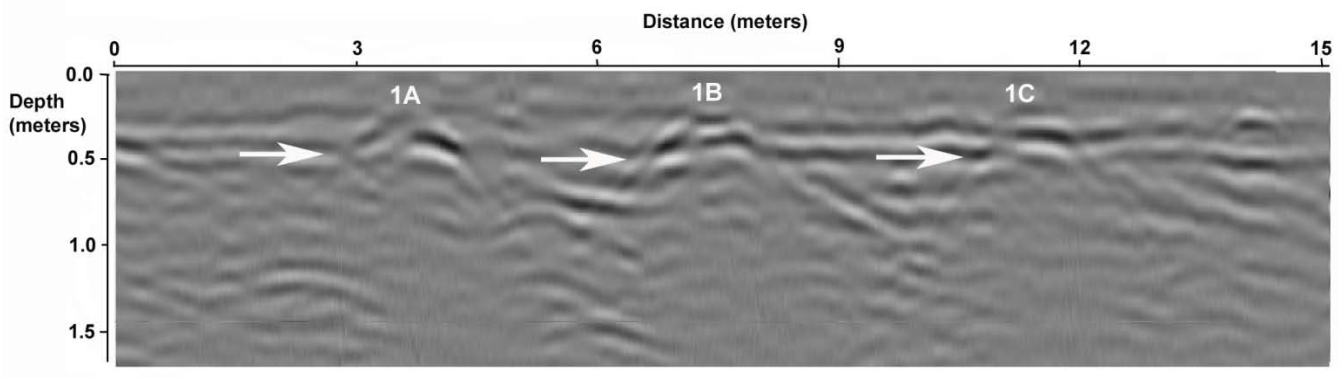

Figure 155: GPR reflection profile using the 250-MHz antenna of Row 1 at 7 months

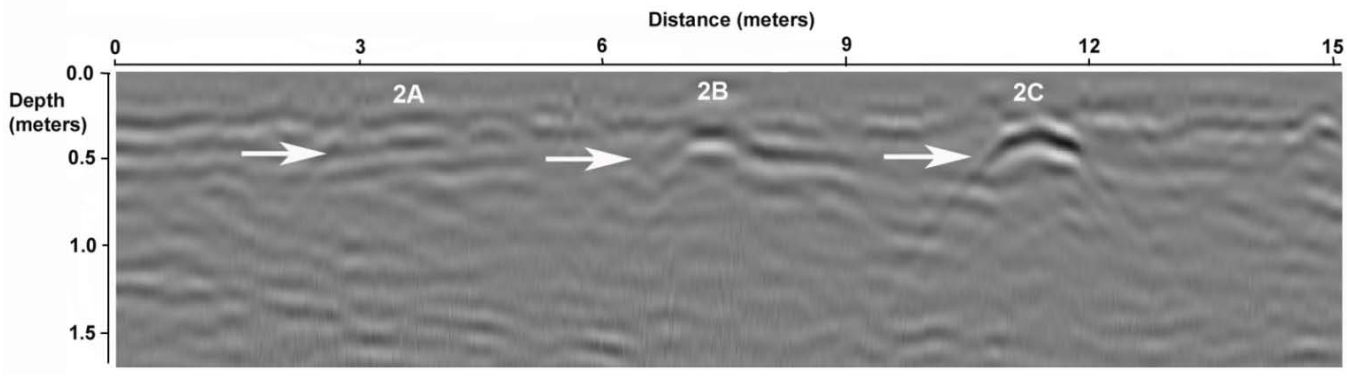

Figure 156: GPR reflection profile using the 250-MHz antenna of Row 2 at 7 months

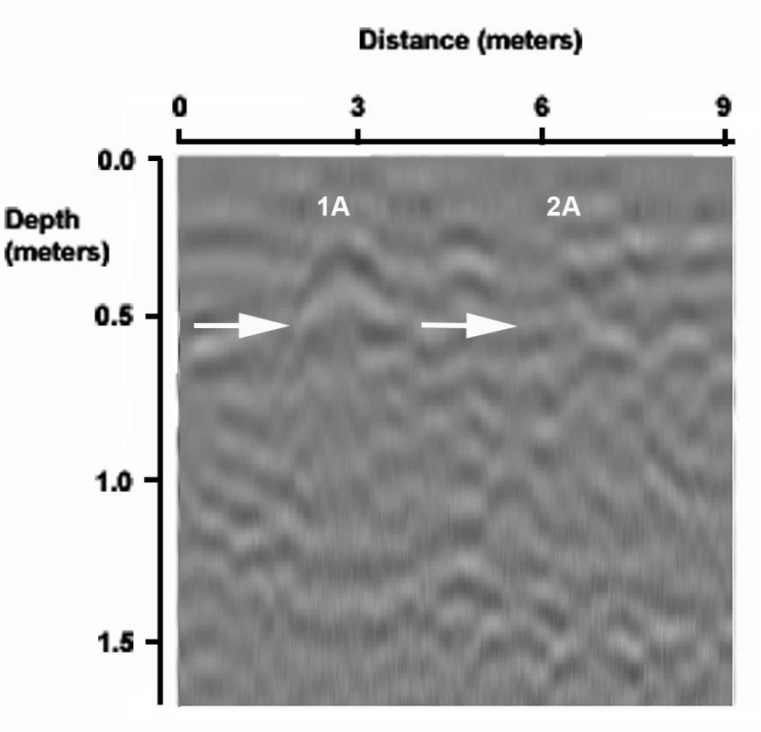

Figure 157: GPR reflection profile using the 250-MHz antenna of Row 1A2A at 7 months

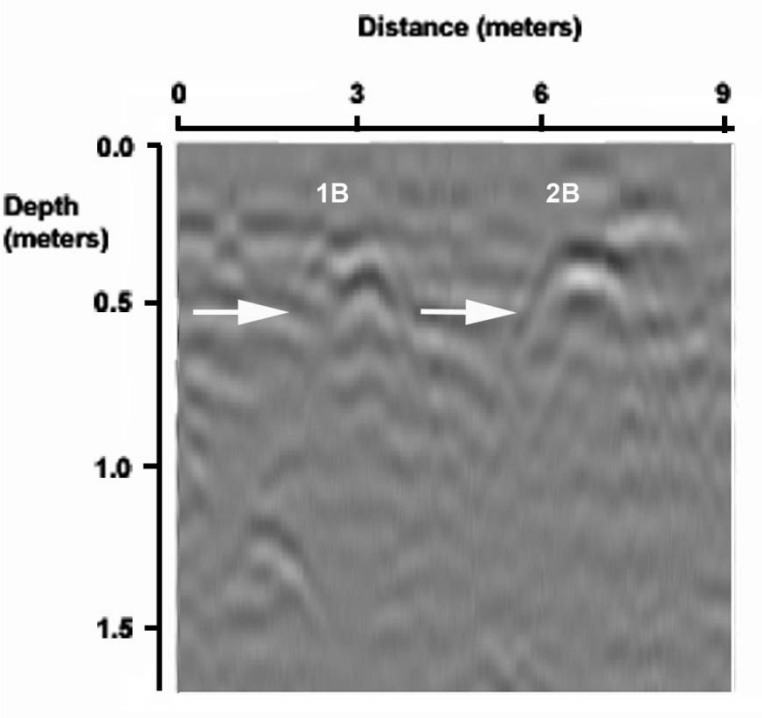

Figure 158: GPR reflection profile using the 250-MHz antenna of Row 1B2B at 7 months

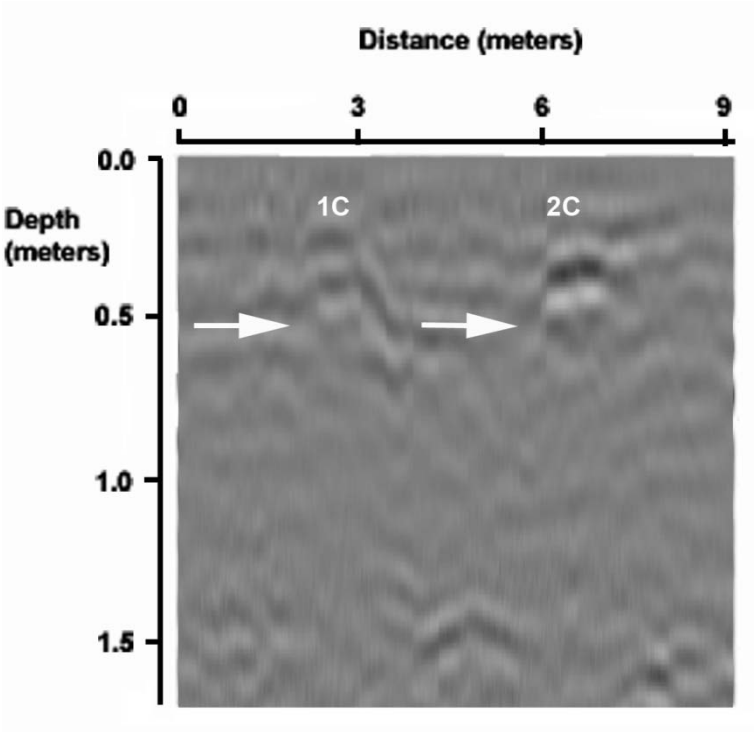

Figure 159: GPR reflection profile using the 250-MHz antenna of Row 1C2C at 7 months

8 MONTH

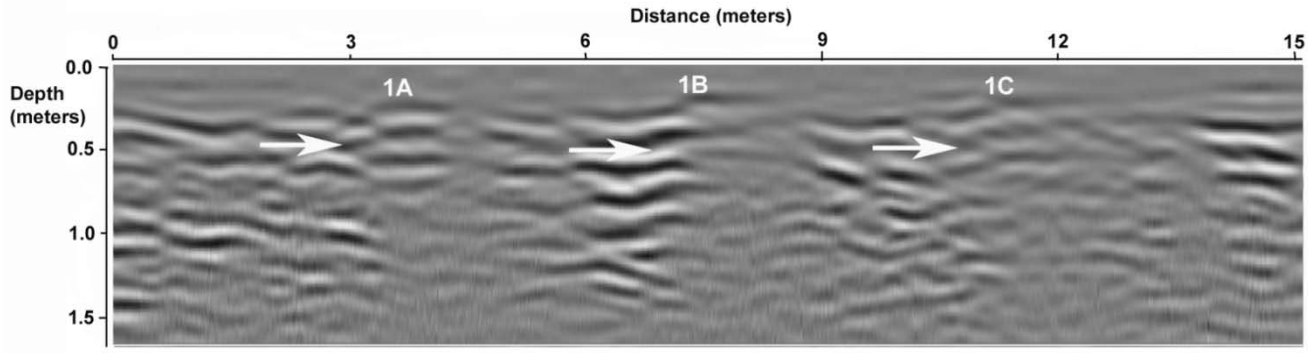

Figure 160: GPR reflection profile using the 250-MHz antenna of Row 1 at 8 months

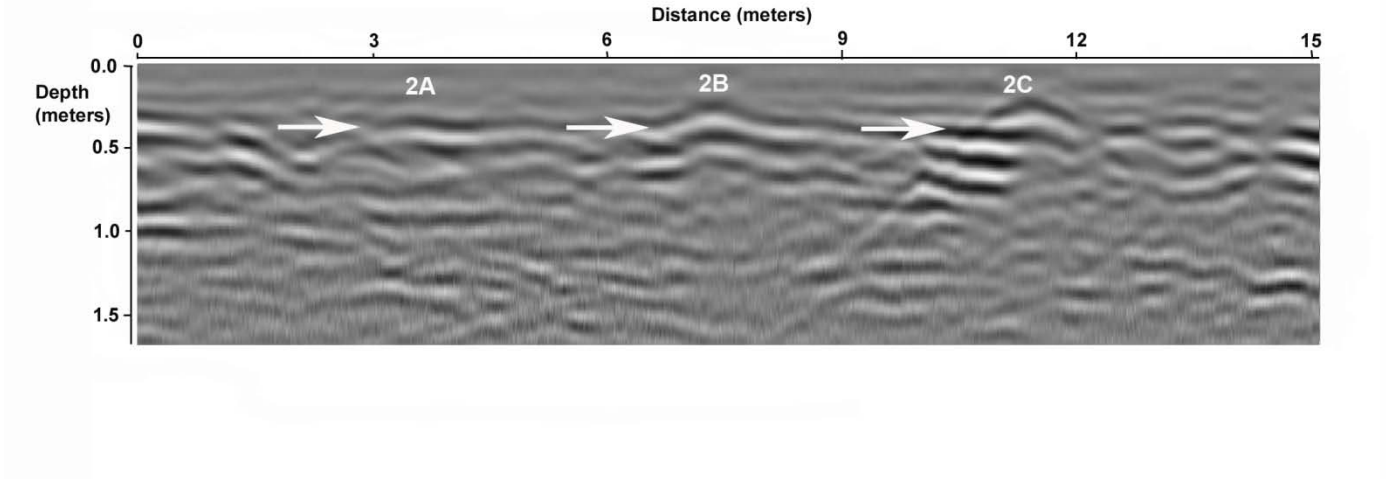

Figure 161: GPR reflection profile using the 250-MHz antenna of Row 2 at 8 months

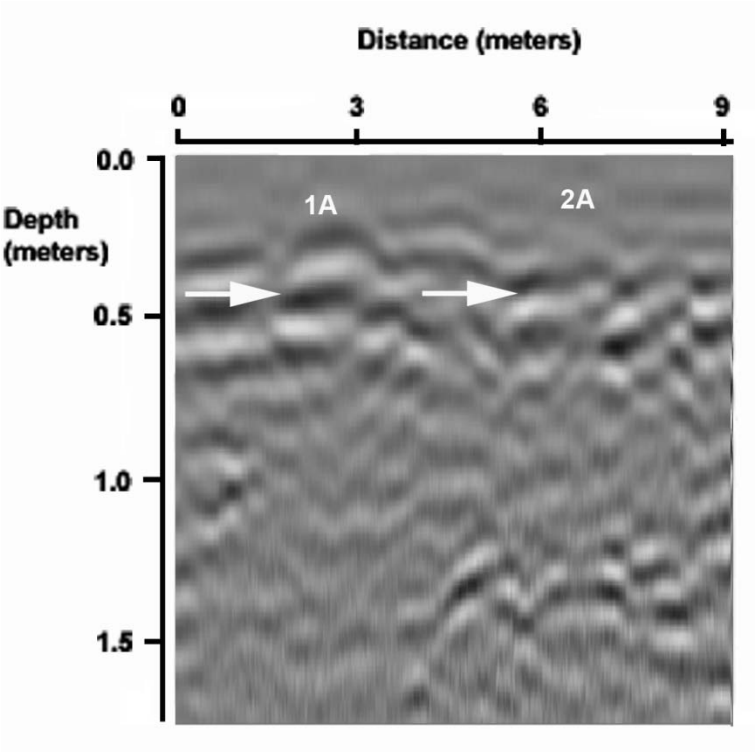

Figure 162: GPR reflection profile using the 250-MHz antenna of Row 1A2A at 8 months

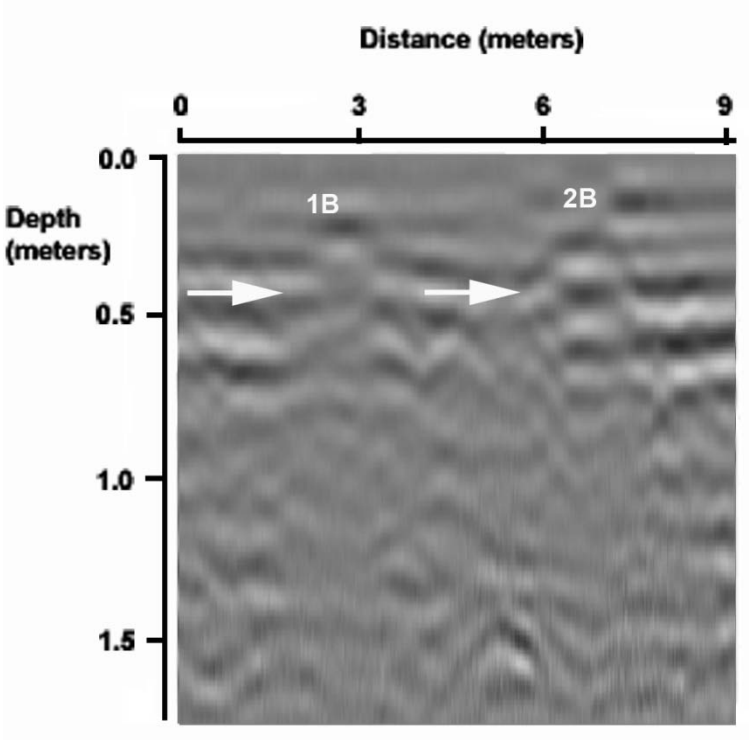

Figure 163: GPR reflection profile using the 250-MHz antenna of Row 1B2B at 8 months

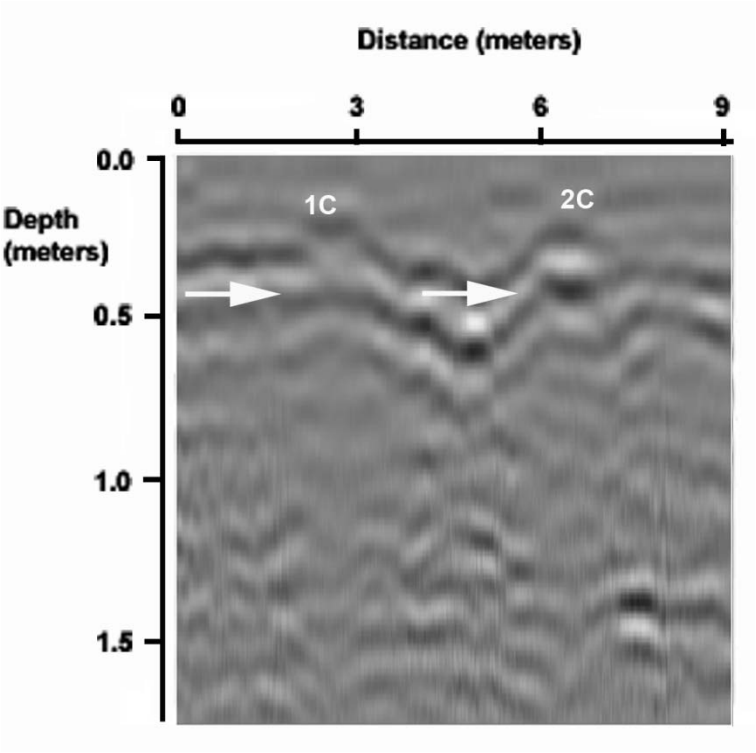

Figure 164: GPR reflection profile using the 250-MHz antenna of Row 1C2C at 8 months

9 MONTH

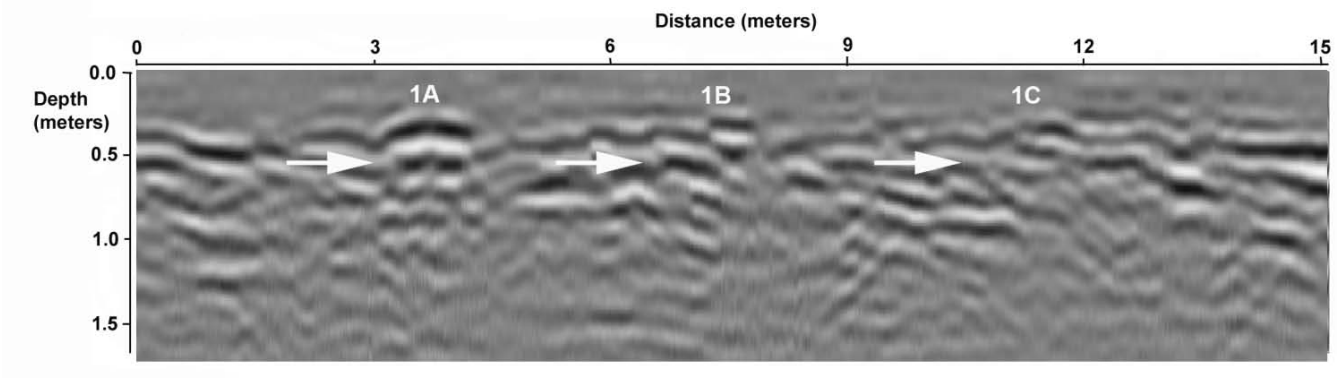

Figure 165: GPR reflection profile using the 250-MHz antenna of Row 1 at 9 months

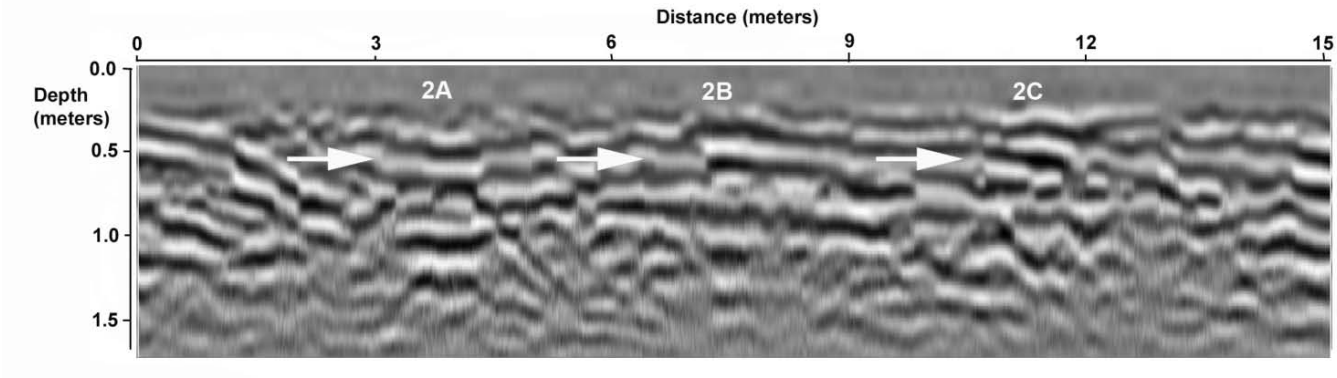

Figure 166: GPR reflection profile using the 250-MHz antenna of Row 2 at 9 months

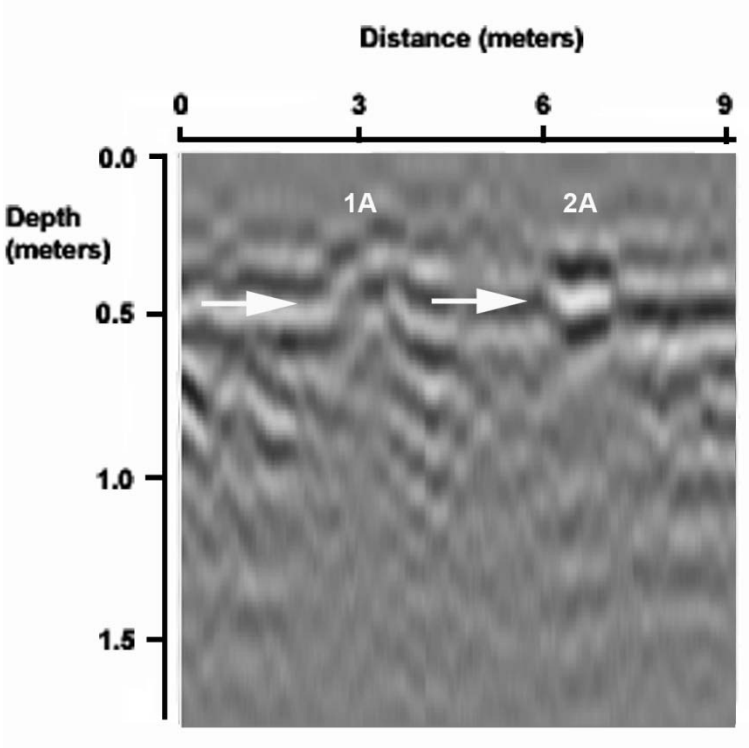

Figure 167: GPR reflection profile using the 250-MHz antenna of Row 1A2A at 9 months

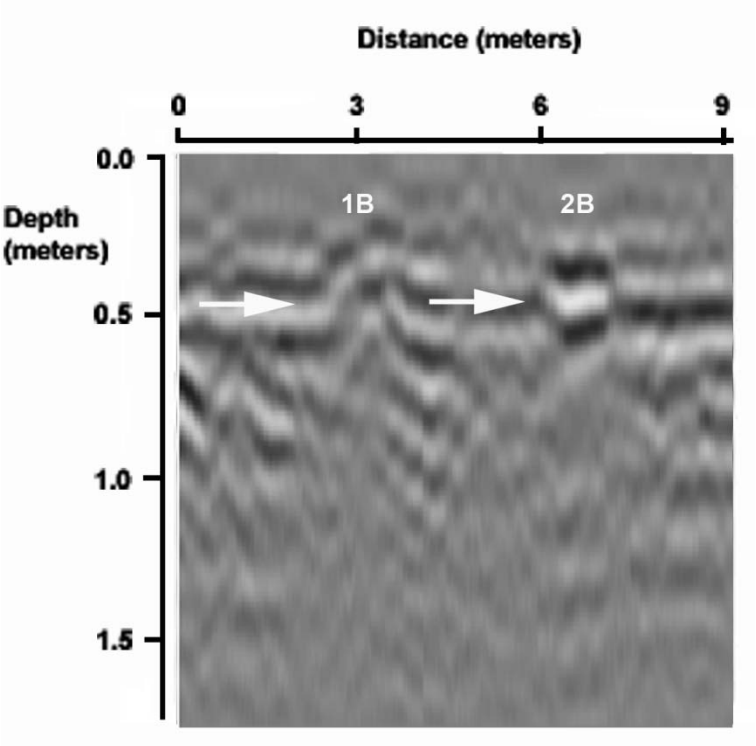

Figure 168: GPR reflection profile using the 250-MHz antenna of Row 1B2B at 9 months

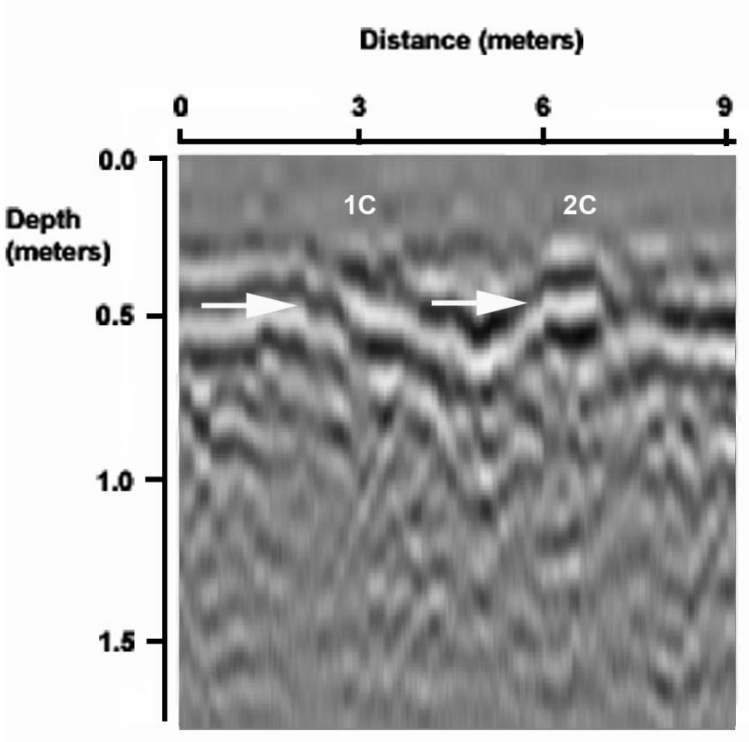

Figure 169: GPR reflection profile using the 250-MHz antenna of Row 1C2C at 9 months

10 MONTHS

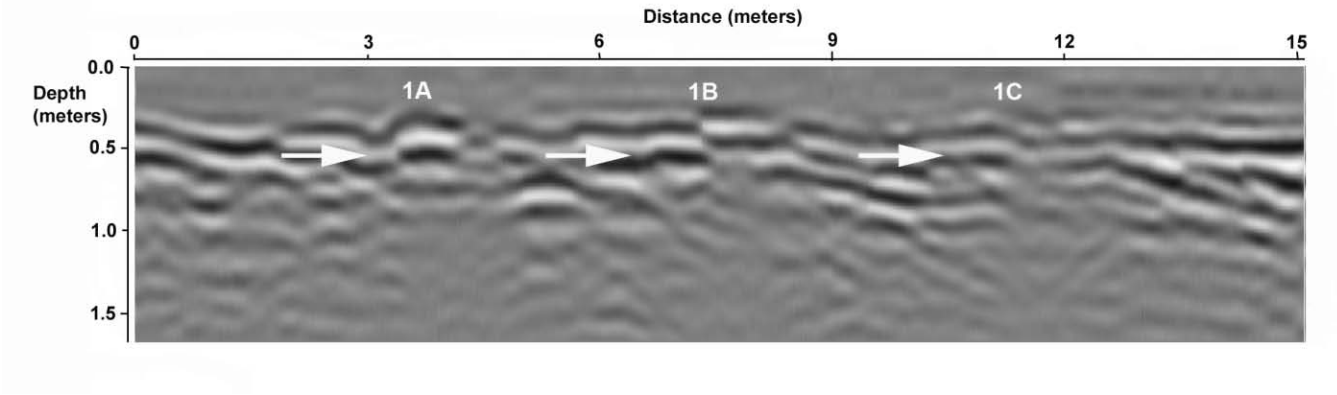

Figure 170: GPR reflection profile using the 250-MHz antenna of Row 1 at 10 months

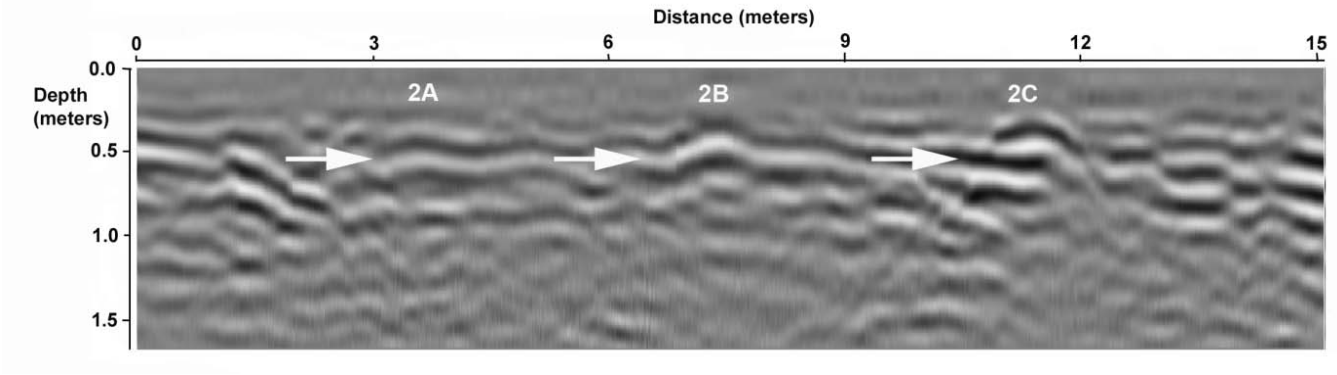

Figure 171: GPR reflection profile using the 250-MHz antenna of Row 2 at 10 months

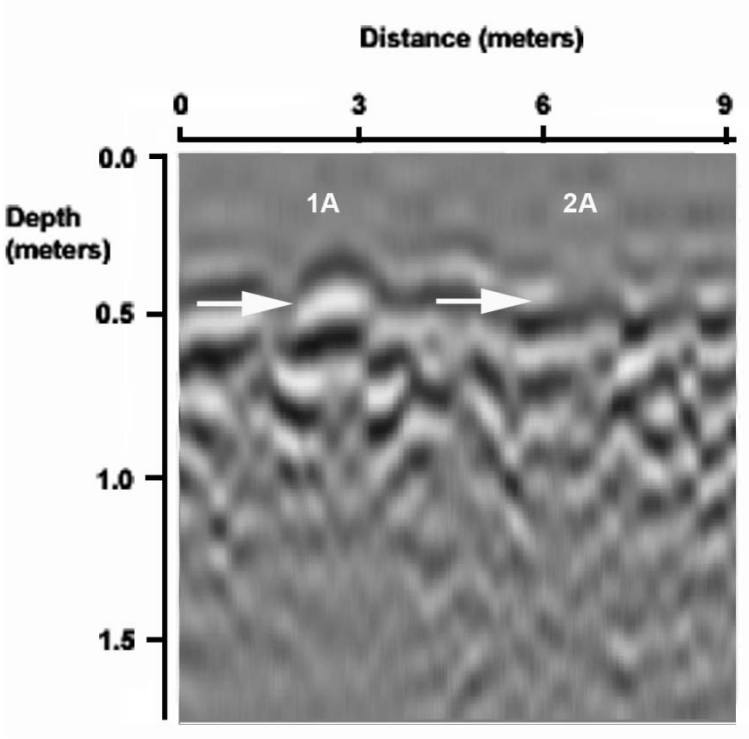

Figure 172: GPR reflection profile using the 250-MHz antenna of Row 1A2A at 10 months

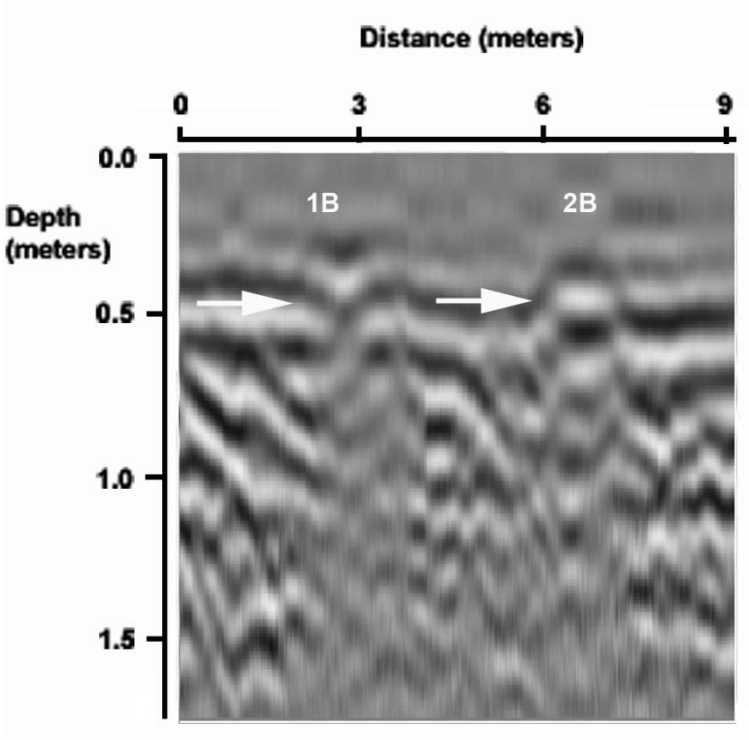

Figure 173: GPR reflection profile using the 250-MHz antenna of Row 1B2B at 10 months

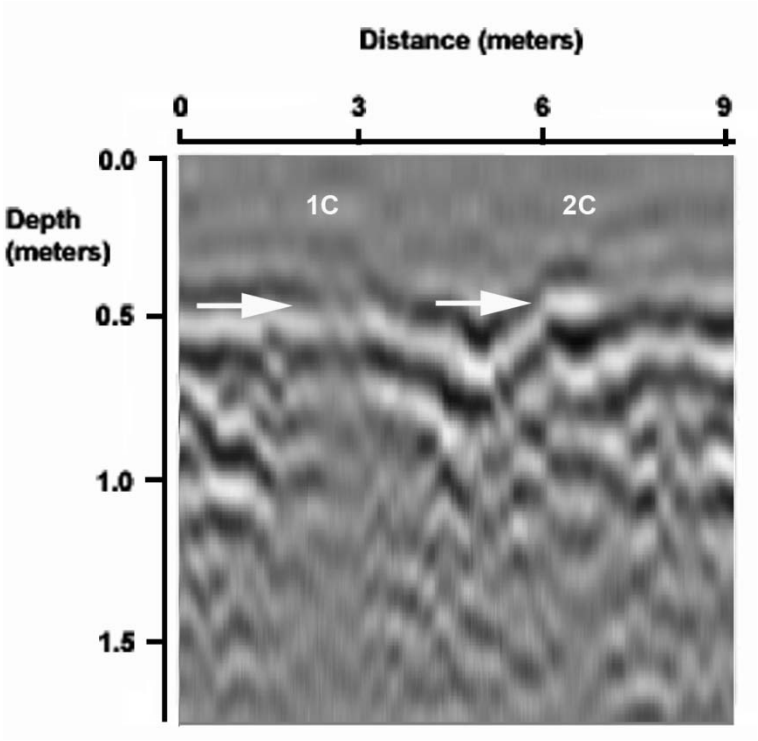

Figure 174: GPR reflection profile using the 250-MHz antenna of Row 1C2C at 10 months

11 MONTHS

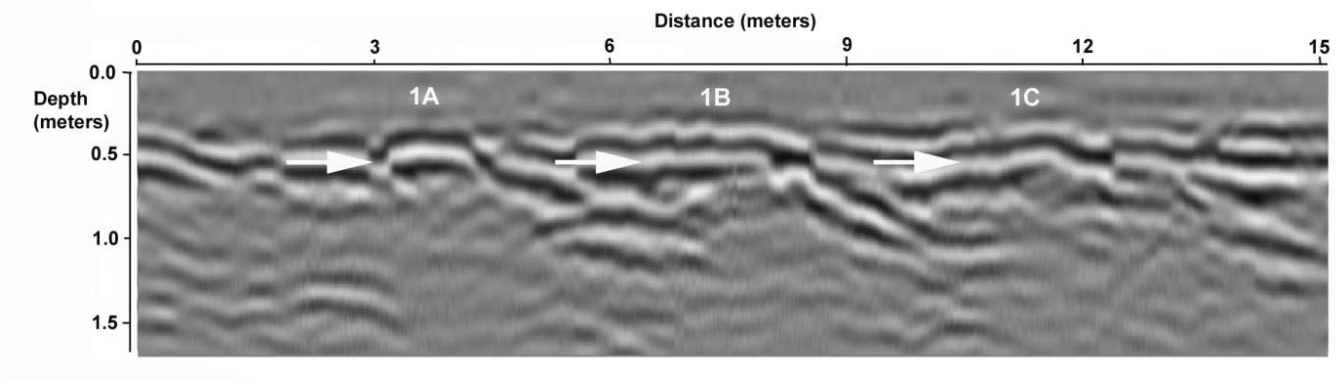

Figure 175: GPR reflection profile using the 250-MHz antenna of Row 1 at 11 months

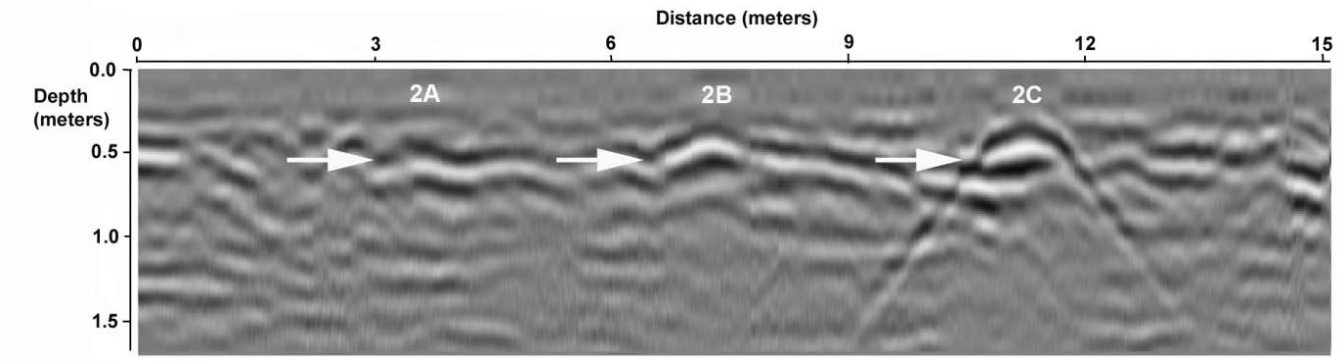

Figure 176: GPR reflection profile using the 250-MHz antenna of Row 2 at 11 months

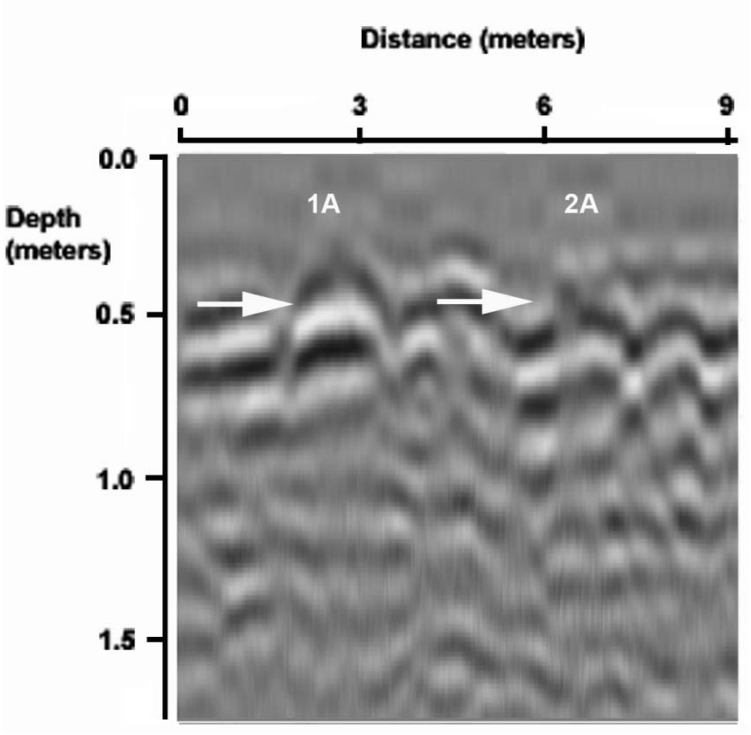

Figure 177: GPR reflection profile using the 250-MHz antenna of Row 1A2A at 11 months

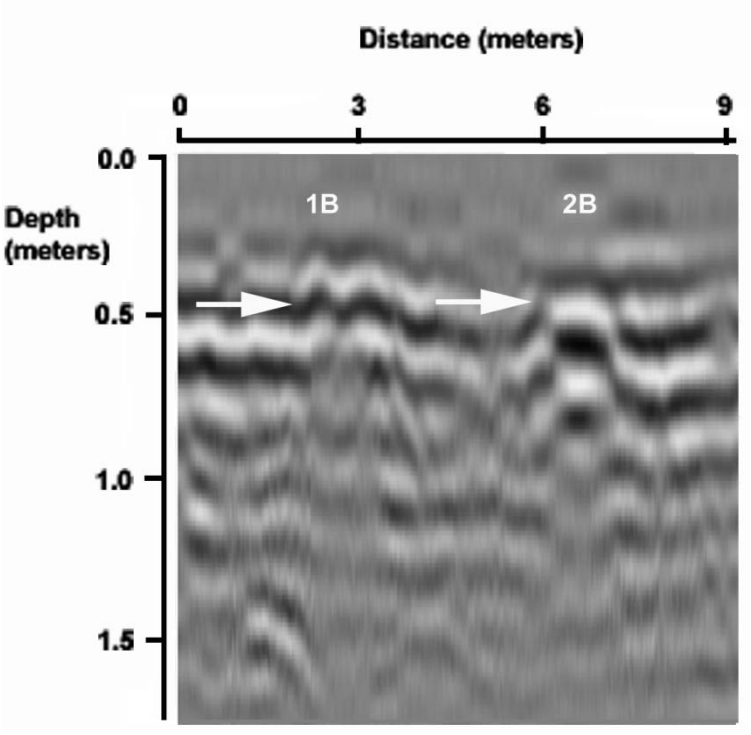

Figure 178: GPR reflection profile using the 250-MHz antenna of Row 1B2B at 11 months

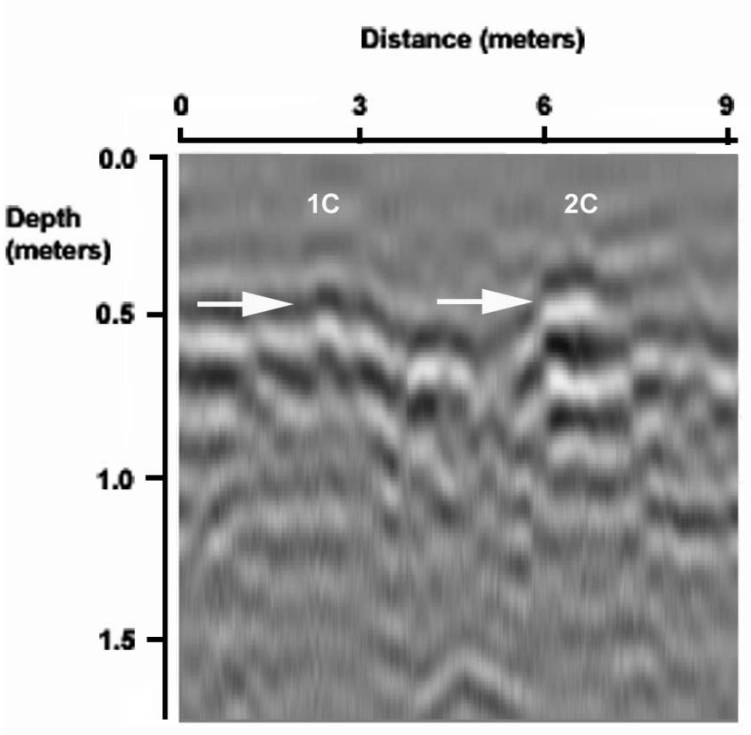

Figure 179: GPR reflection profile using the 250-MHz antenna of Row 1C2C at 11 months

12 MONTHS

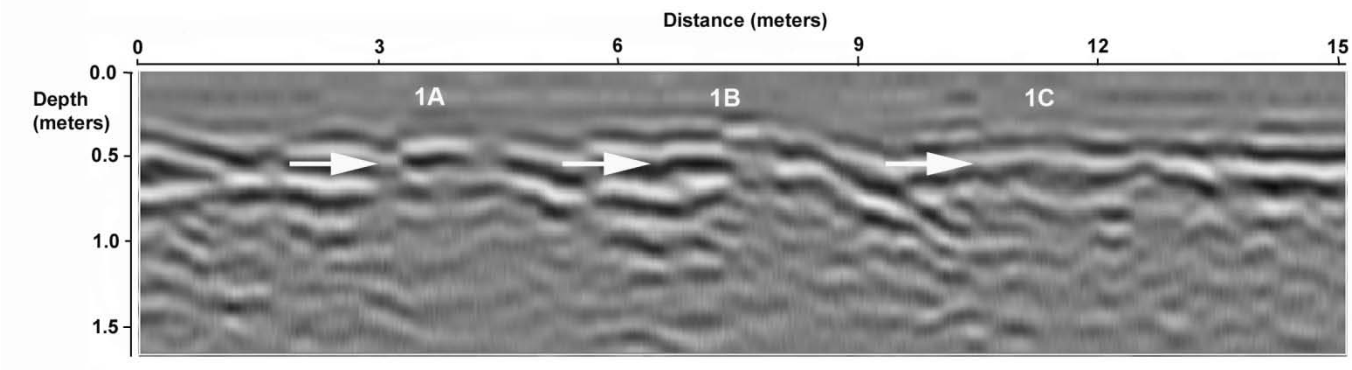

Figure 180: GPR reflection profile using the 250-MHz antenna of Row 1 at 12 months

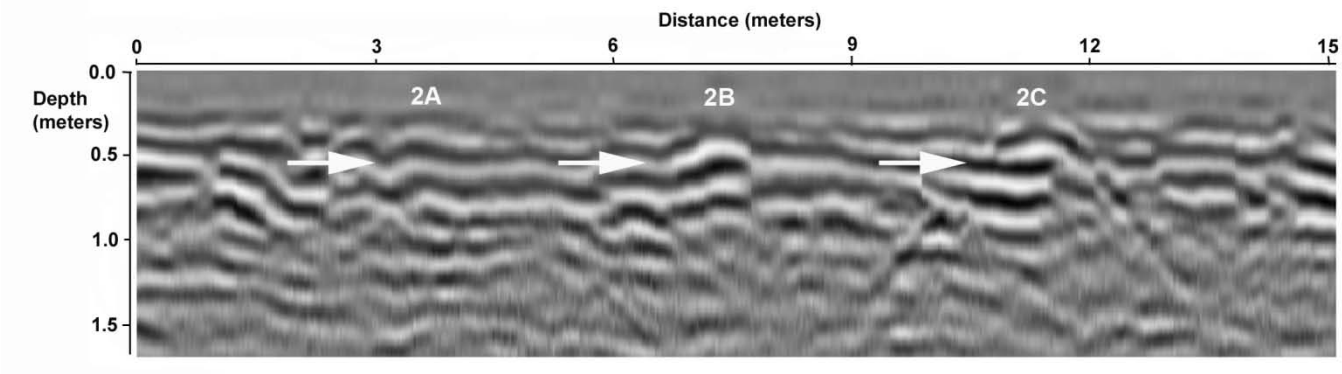

Figure 181: GPR reflection profile using the 250-MHz antenna of Row 2 at 12 months

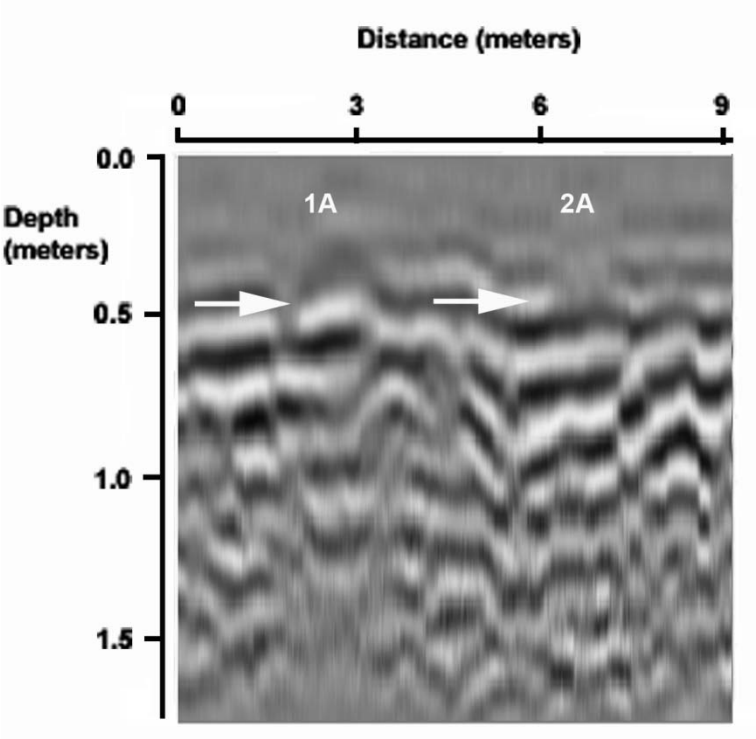

Figure 182: GPR reflection profile using the 250-MHz antenna of Row 1A2A at 12 months

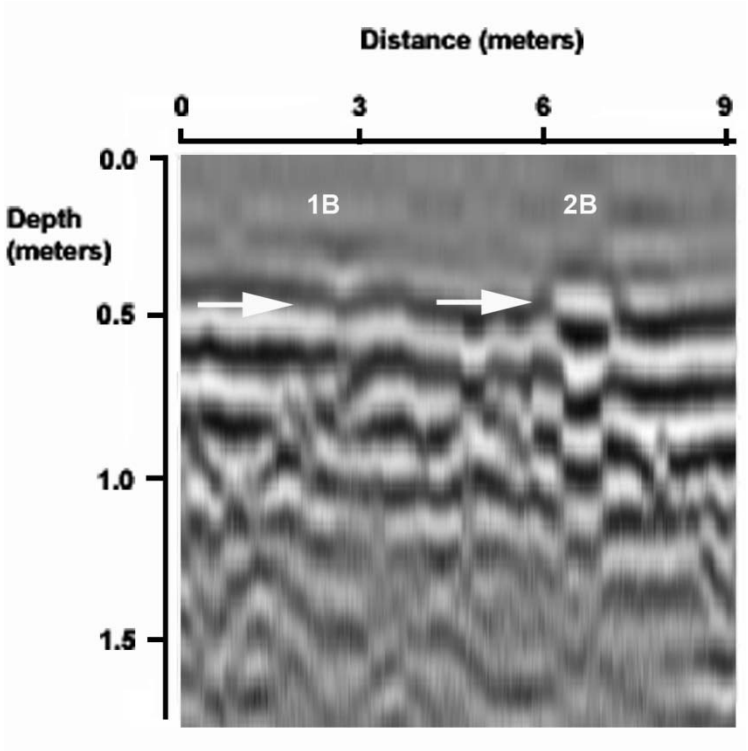

Figure 183: GPR reflection profile using the 250-MHz antenna of Row 1B2B at 12 months

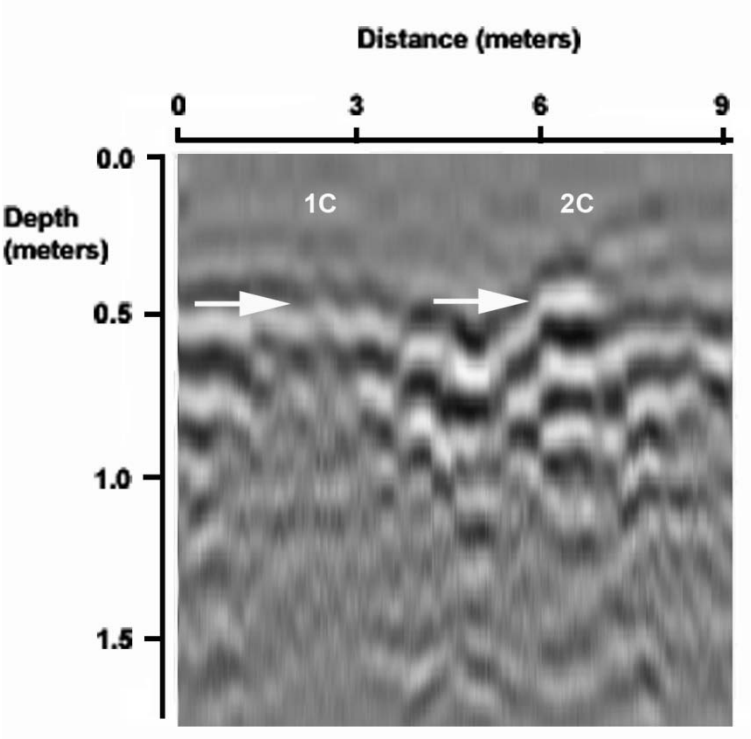

Figure 184: GPR reflection profile using the 250-MHz antenna of Row 1C2C at 12 months

APPENDIX D: GROUND-PENETRATING RADAR 250-MHZ HORIZONTAL SLICES

1 MONTH

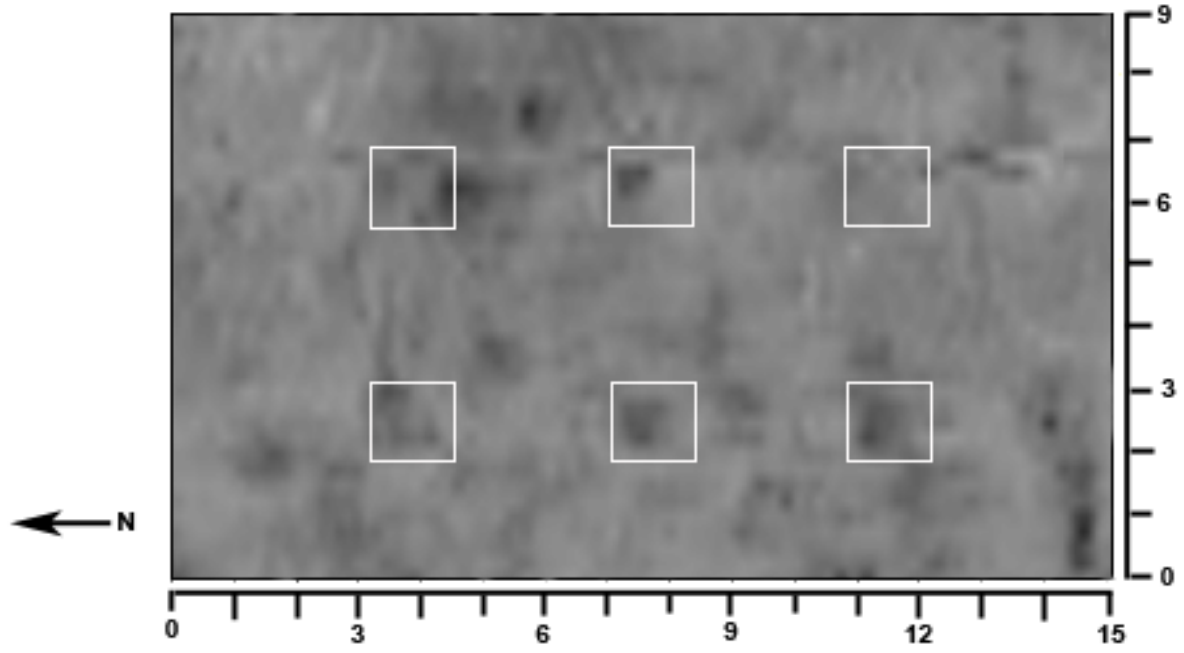

Figure 185: GPR horizontal slice in X direction using the 250-MHz antenna at 1 month. The horizontal slice is approximately 0.44 m in depth (8.935 ns)

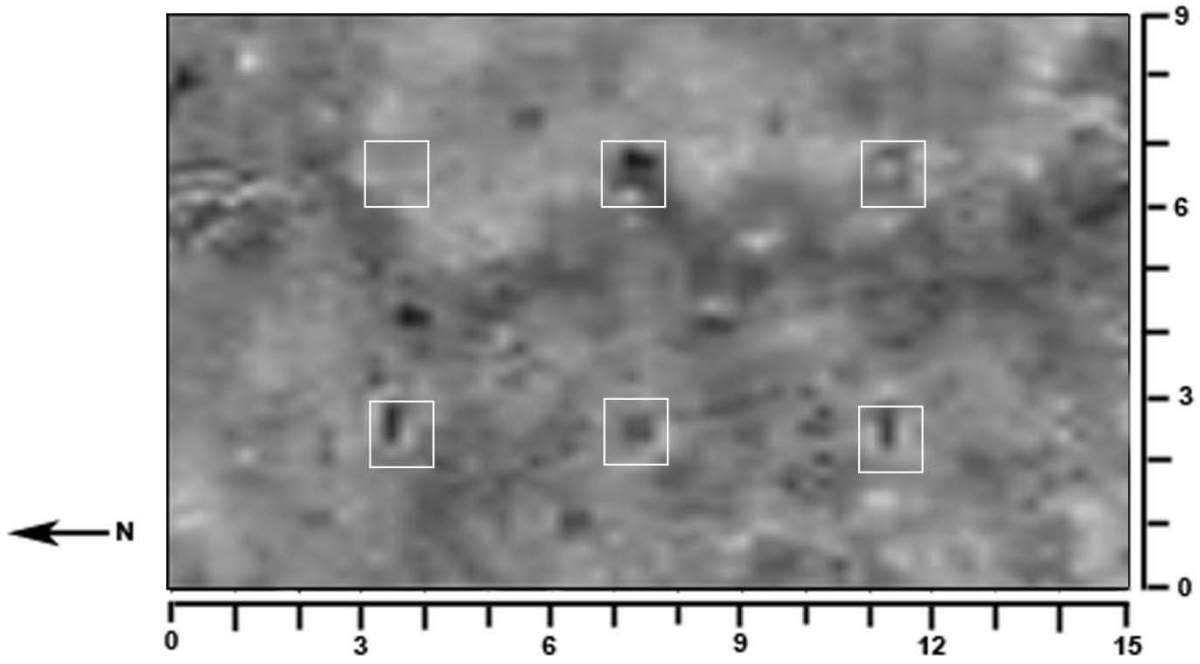

Figure 186: GPR horizontal slice in Y direction using the 250-MHz antenna at 1 month. The horizontal slice is approximately 0.4.m in depth (14.62 ns)

2 MONTH

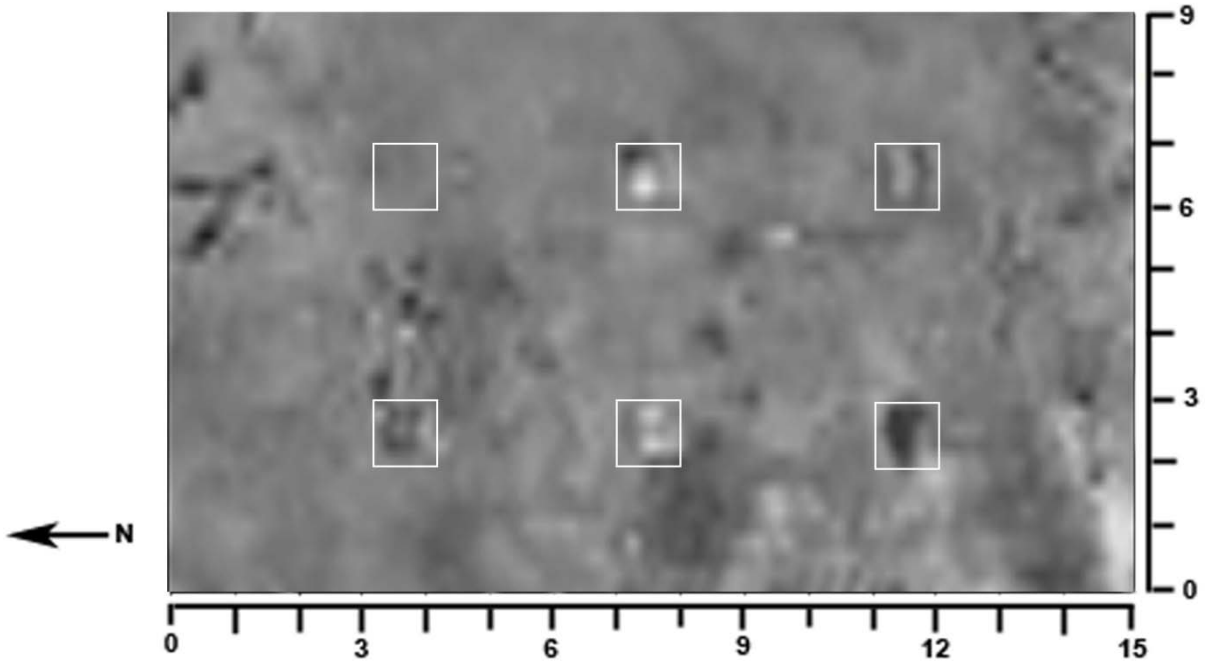

Figure 187: GPR horizontal slice in X direction using the 250-MHz antenna at 2 months. The horizontal slice is approximately 0.44 m in depth (14.62 ns)

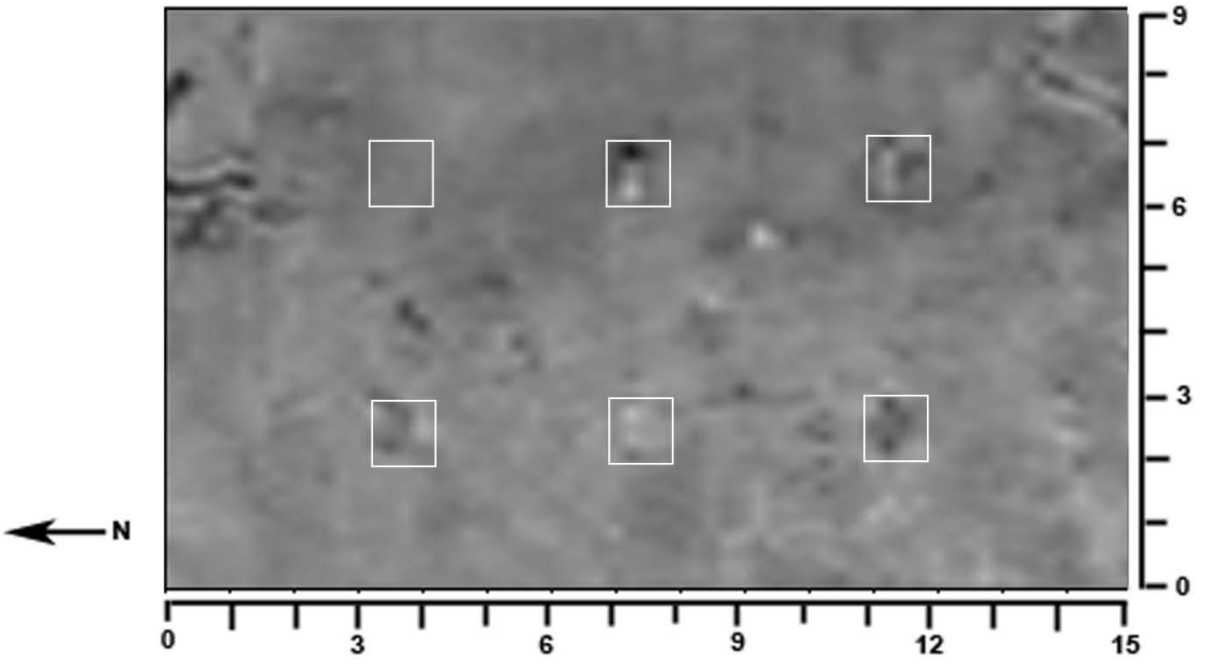

Figure 188: GPR horizontal slice in the Y direction using the 250-MHz antenna at 2 months. The horizontal slice is approximately 0.44 m in depth (15.43 ns)

3 MONTH

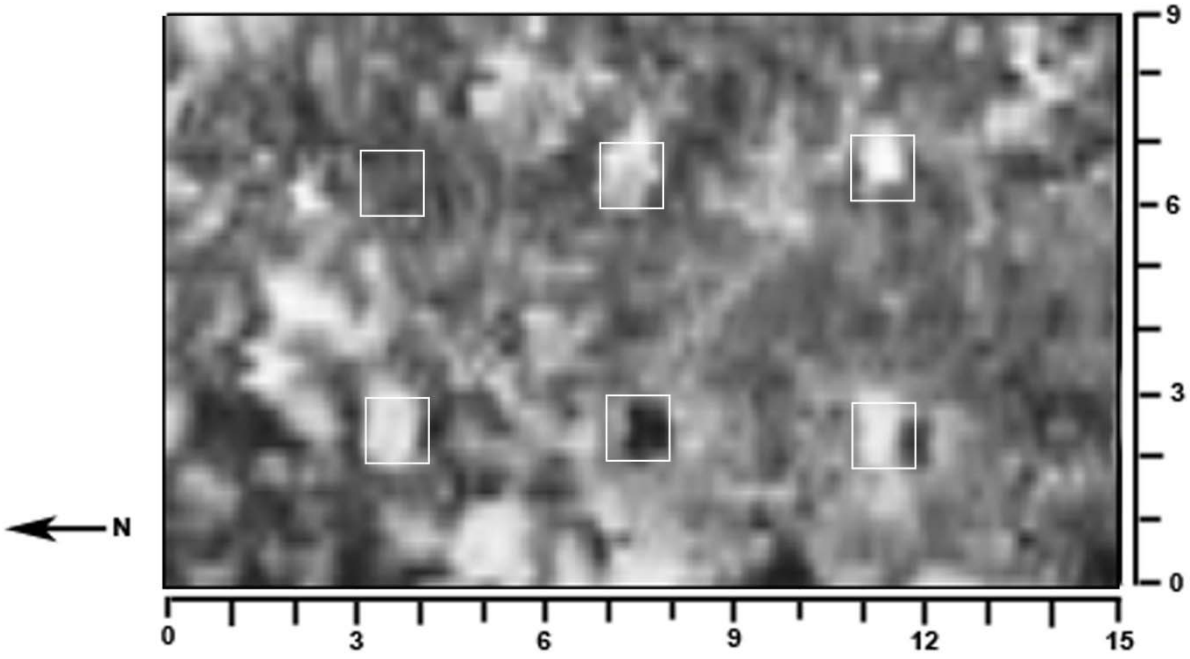

Figure 189: GPR horizontal slice in the X direction using the 250-MHz antenna at 3 months. The horizontal slice is approximately 0.44 m in depth (13.4 ns)

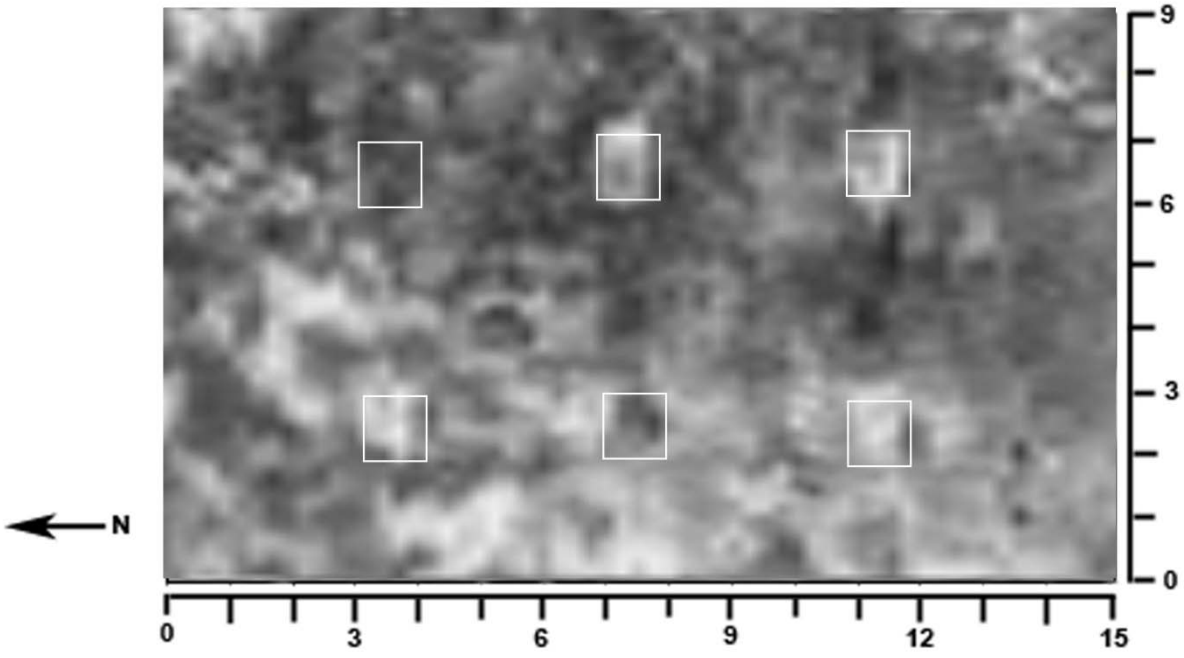

Figure 190: GPR horizontal slice in the Y direction using the 250-MHz antenna at 3 months. The horizontal slice is approximately 0.44 m in depth (13.4 ns)

4 MONTH

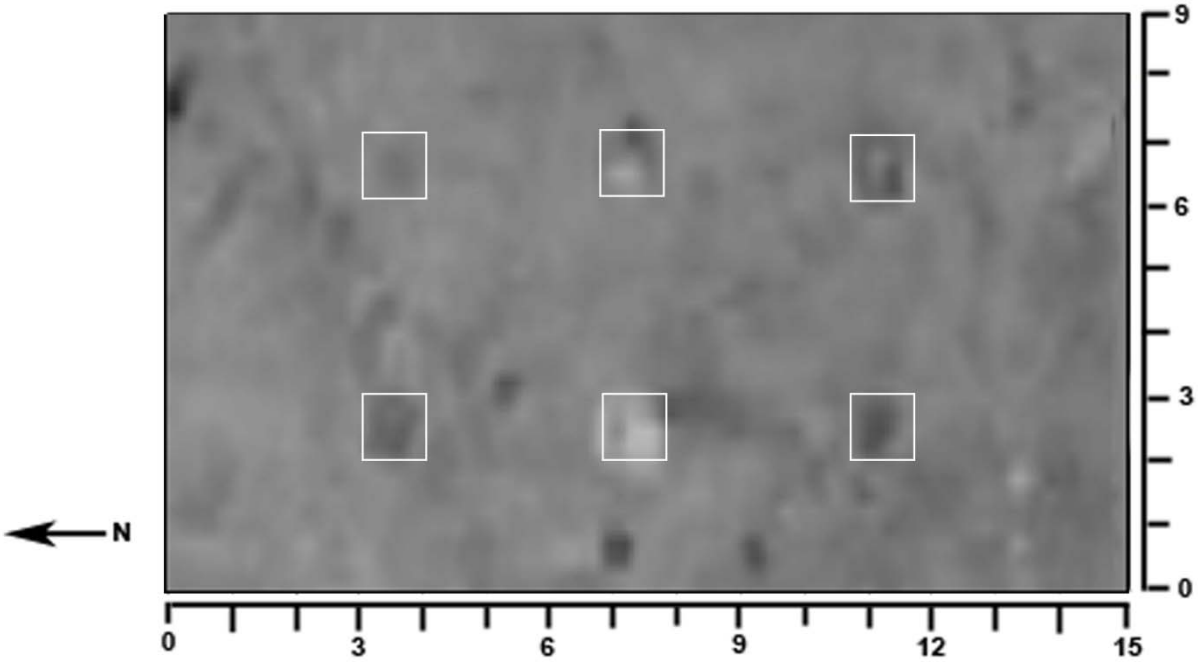

Figure 191: GPR horizontal slice in the X direction using the 250-MHz antenna at 4 months. The horizontal slice is approximately 0.44 m in depth (9.55 ns)

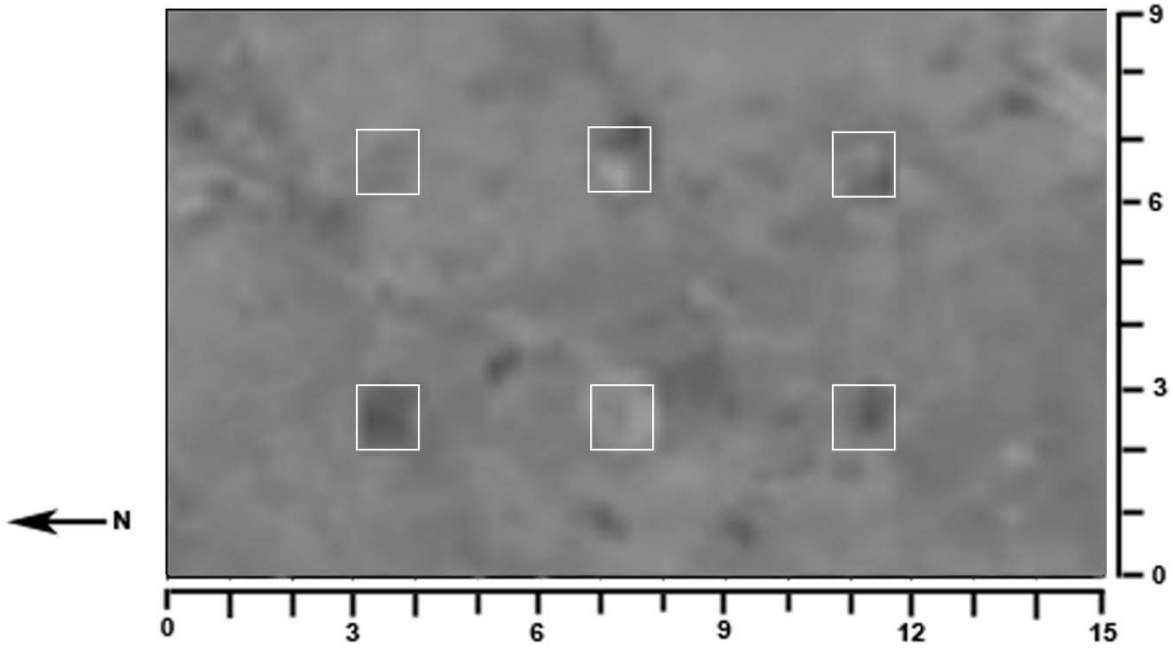

Figure 192: GPR horizontal slice in the Y direction using the 250-MHz antenna at 4 months. The horizontal slice is approximately 0.44 m in depth (9.55 ns)

5 MONTH

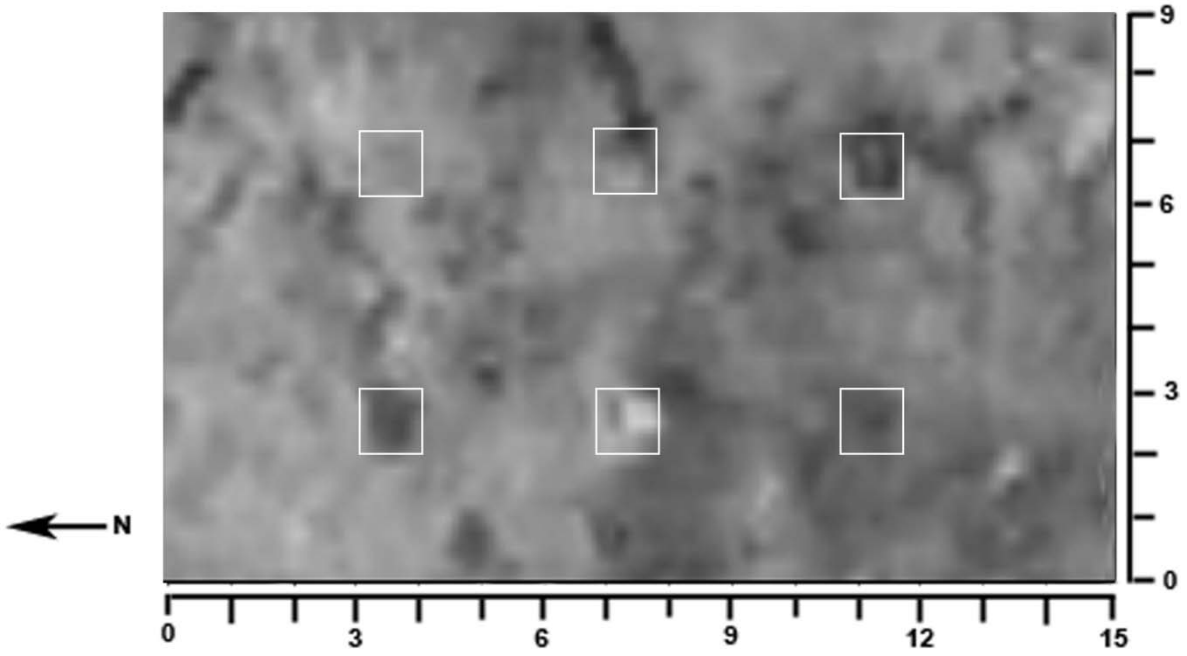

Figure 193: GPR horizontal slice in the X direction using the 250-MHz antenna at 5 months. The horizontal slice is approximately 0.44 m in depth (8.94 ns)

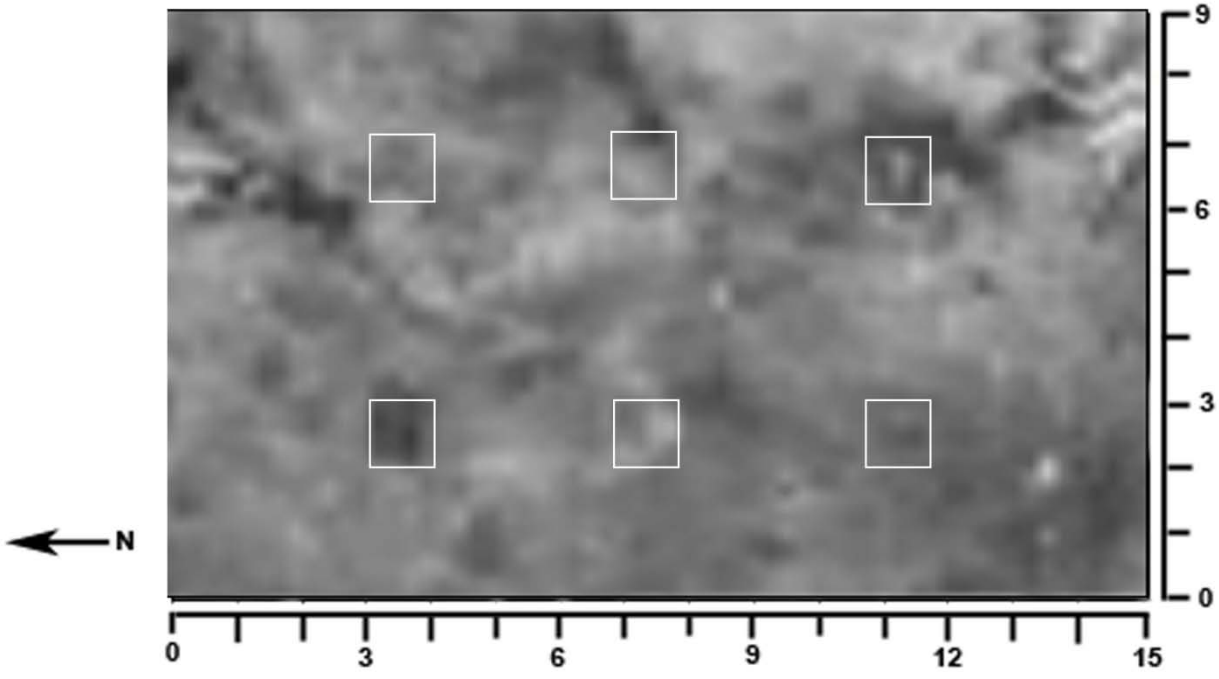

Figure 194: GPR horizontal slice in the Y direction using the 250-MHz antenna at 5 months. The horizontal slice is approximately 0.44 m in depth (9.55 ns)

6 MONTH

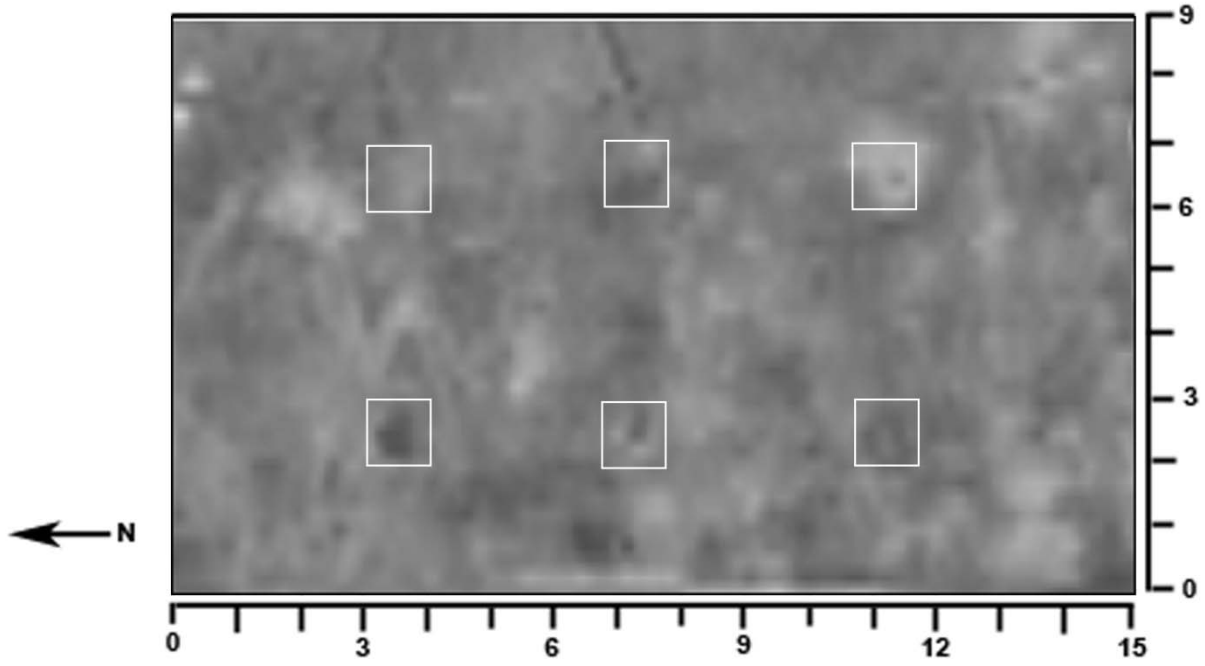

Figure 195: GPR horizontal slice in the X direction using the 250-MHz antenna at 6 months. The horizontal slice is approximately 0.44 m in depth (9.14 ns)

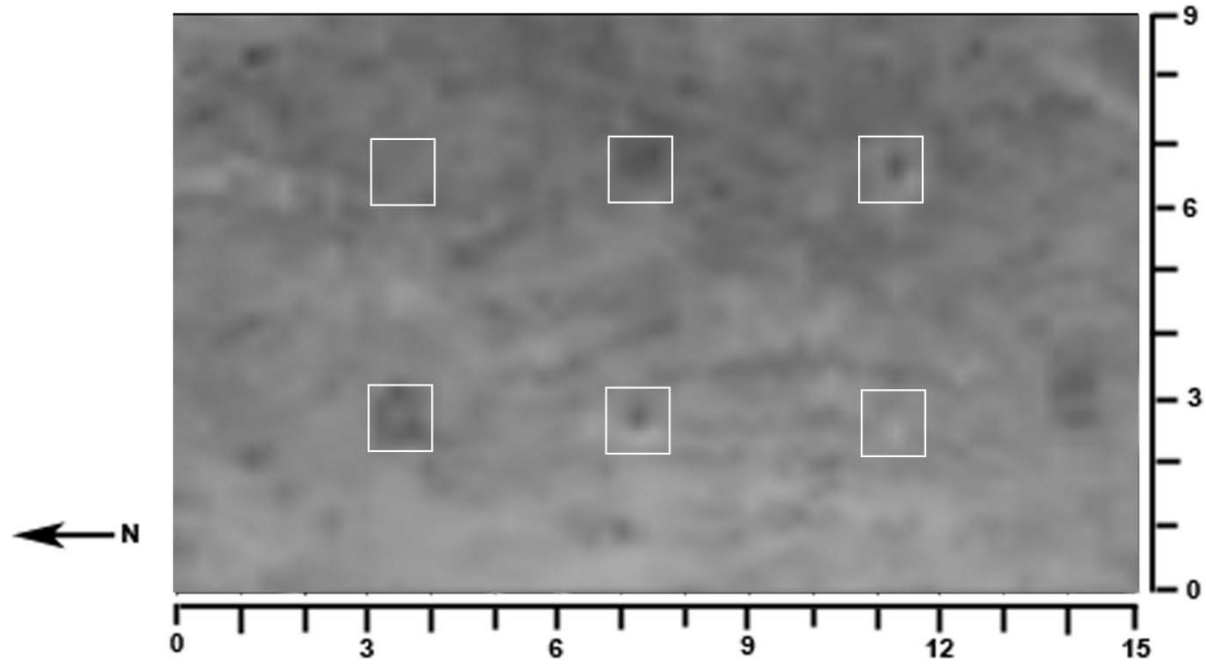

Figure 196: GPR horizontal slice in the Y direction using the 250-MHz antenna at 6 months. The horizontal slice is approximately 0.44 m in depth (9.34 ns)

7 MONTH

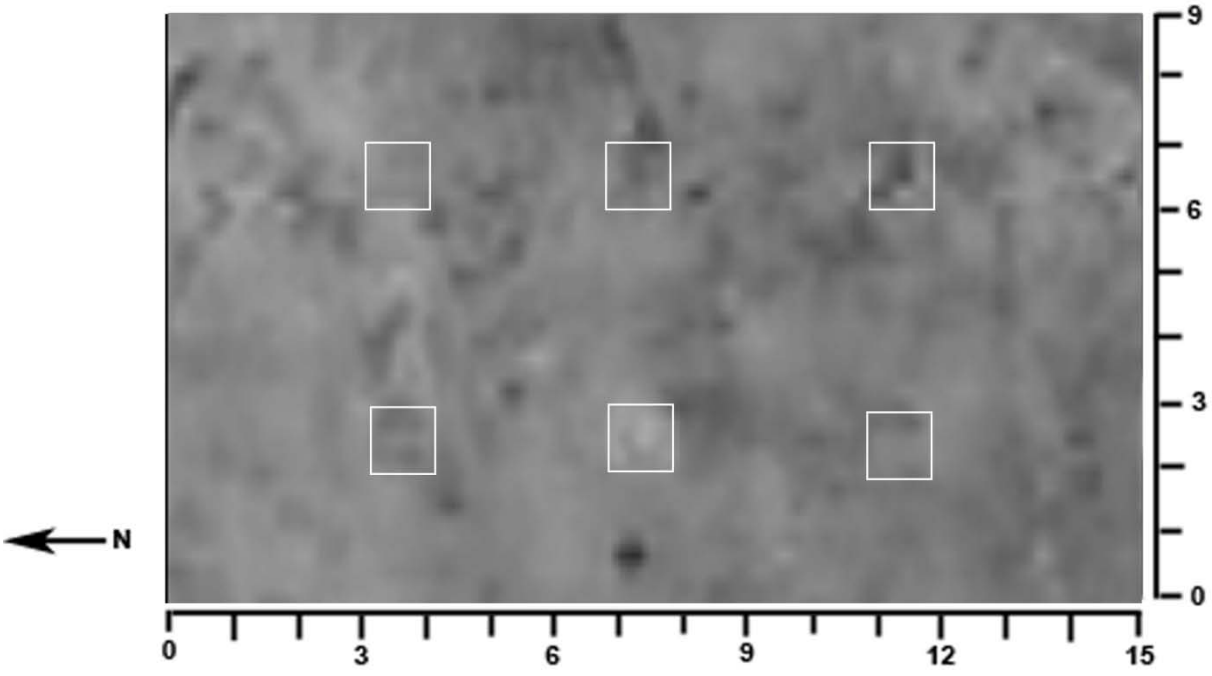

Figure 197: GPR horizontal slice in the X direction using the 250-MHz antenna at 7 months. The horizontal slice is approximately 0.44 m in depth (9.55 ns)

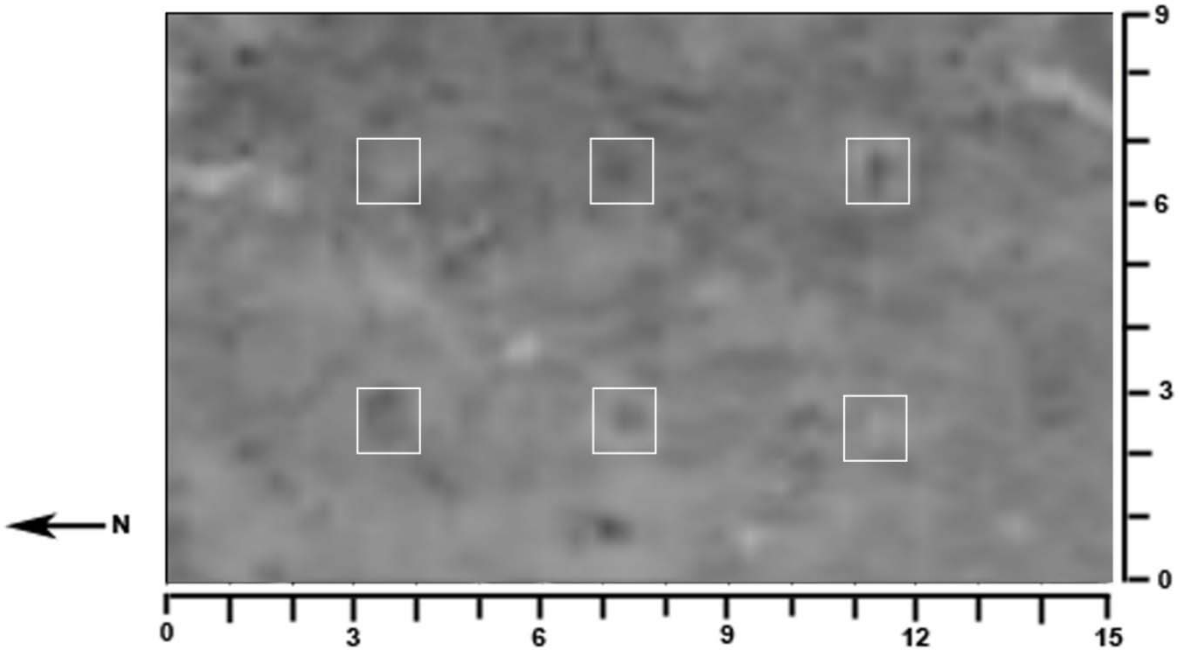

Figure 198: GPR horizontal slice in the Y direction using the 250-MHz antenna at 7 months. The horizontal slice is approximately 0.44 m in depth (9.34 ns)

MONTH 8

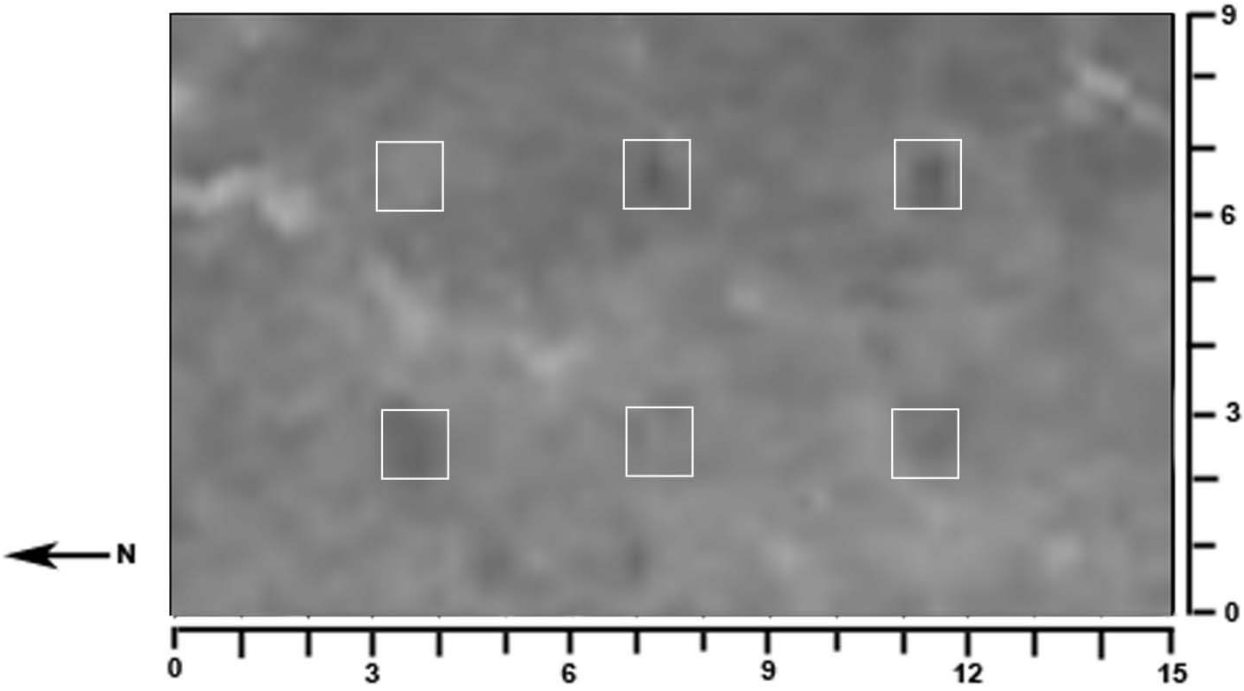

Figure 199: GPR horizontal slice in the X direction using the 250-MHz antenna at 8 months. The horizontal slice is approximately 0.38 m in depth (7.514 ns)

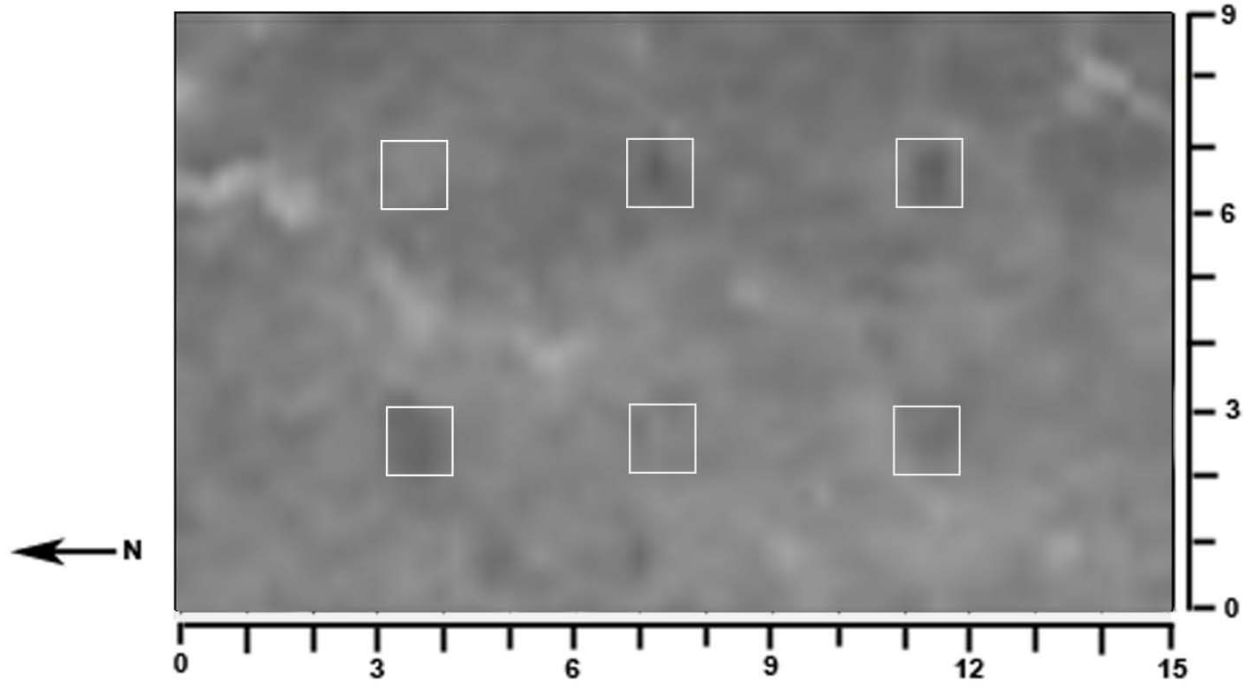

Figure 200: GPR horizontal slice in the Y direction using the 250-MHz antenna at 8 months. The horizontal slice is approximately 0.38 m in depth (7.514 ns)

9 MONTH

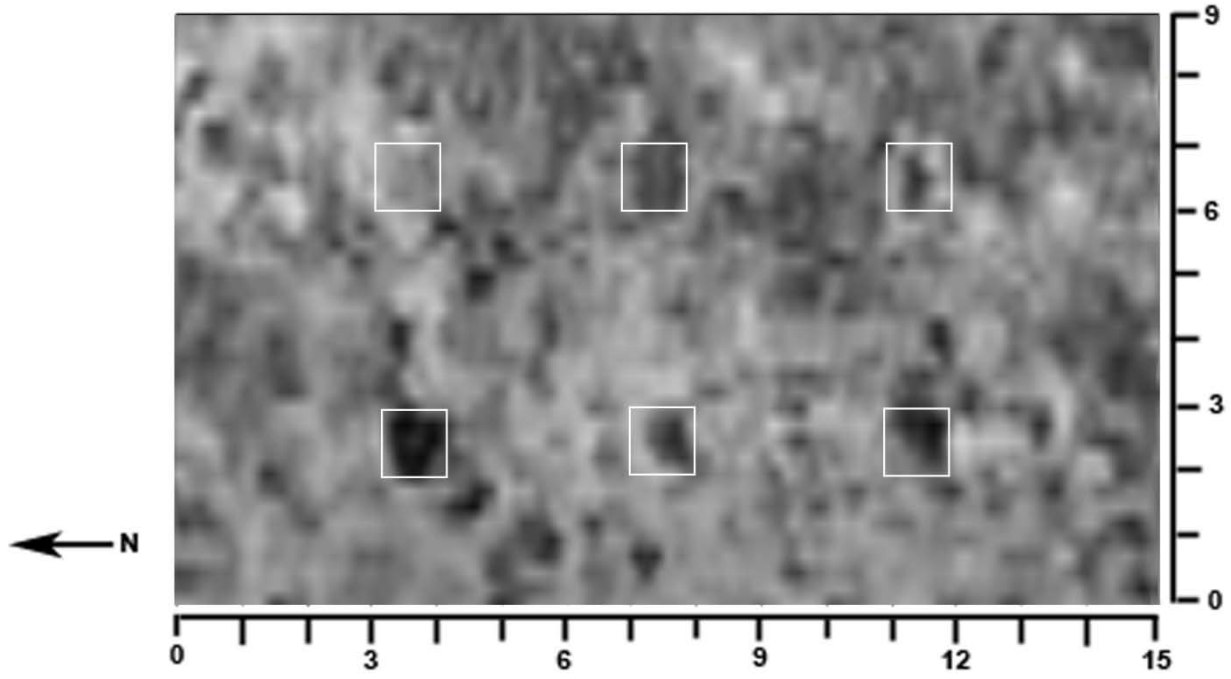

Figure 201: GPR horizontal slice in the X direction using the 250-MHz antenna at 9 months. The horizontal slice is approximately 0.43m in depth (8.529 ns)

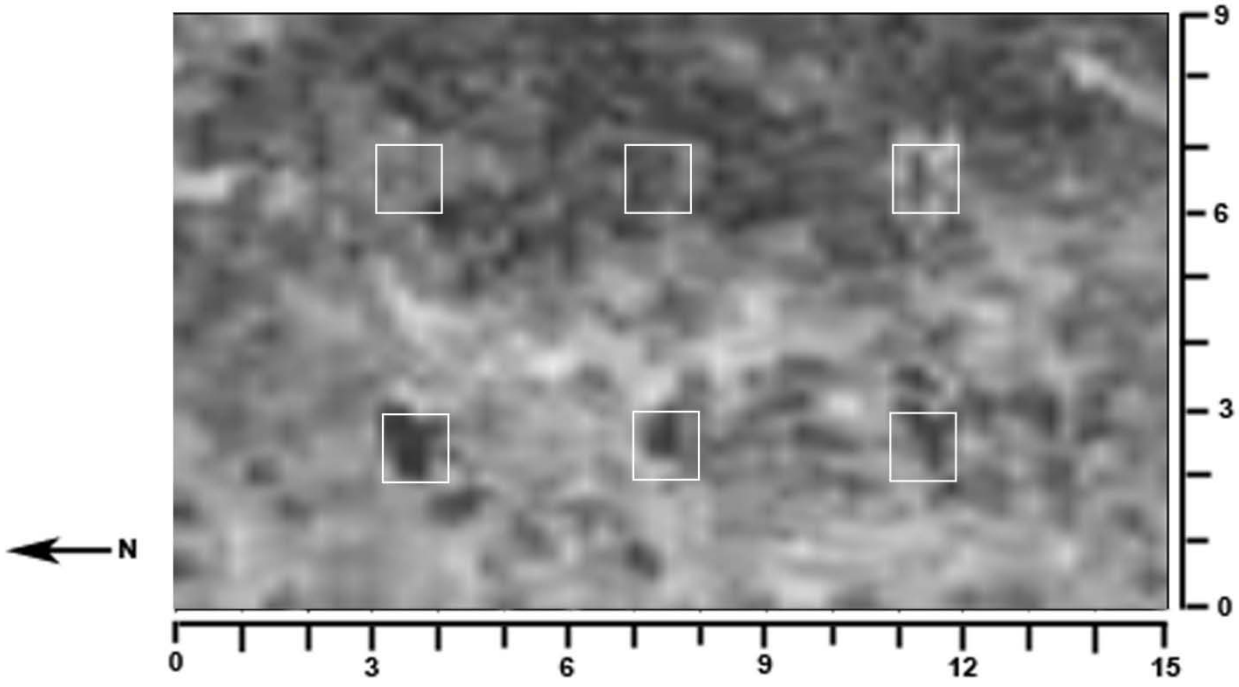

Figure 202: GPR horizontal slice in the Y direction using the 250-MHz antenna at 9 months. The horizontal slice is approximately 0.43m in depth (8.529 ns)

10 MONTH

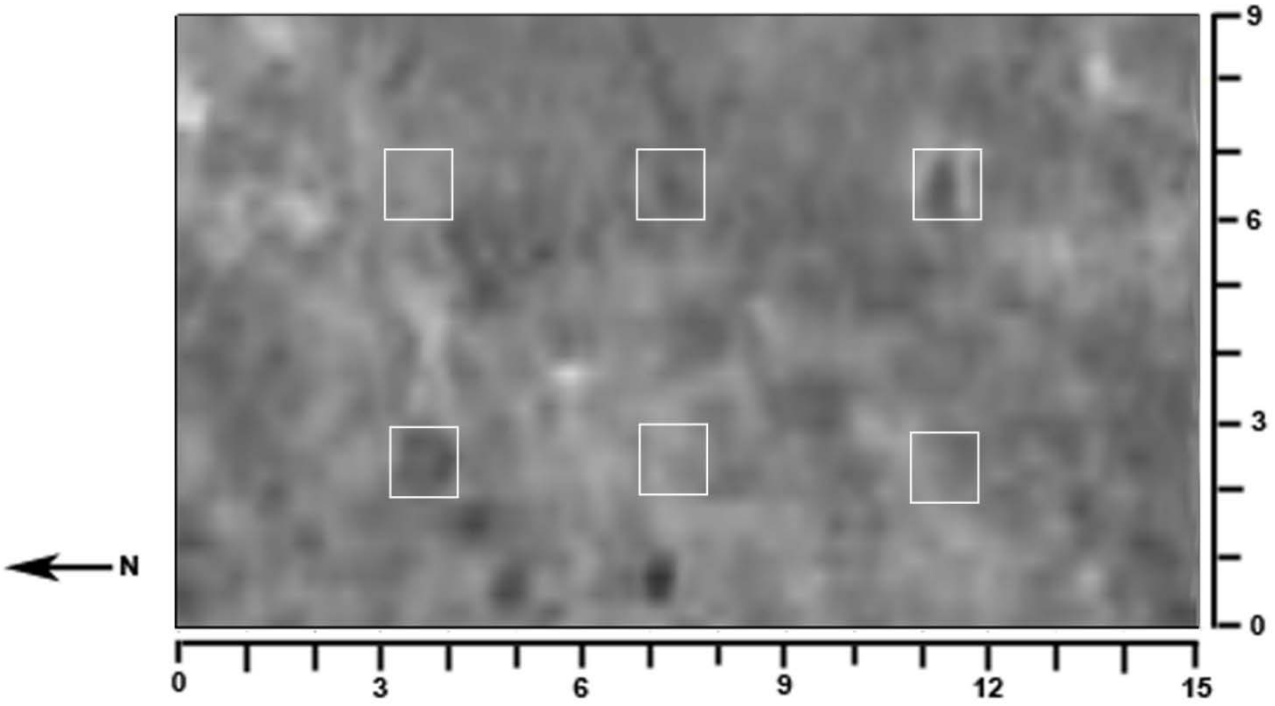

Figure 203: GPR horizontal slice in the X direction using the 250-MHz antenna at 10 months.The horizontal slice is approximately 0.39m in depth (7.92 ns)

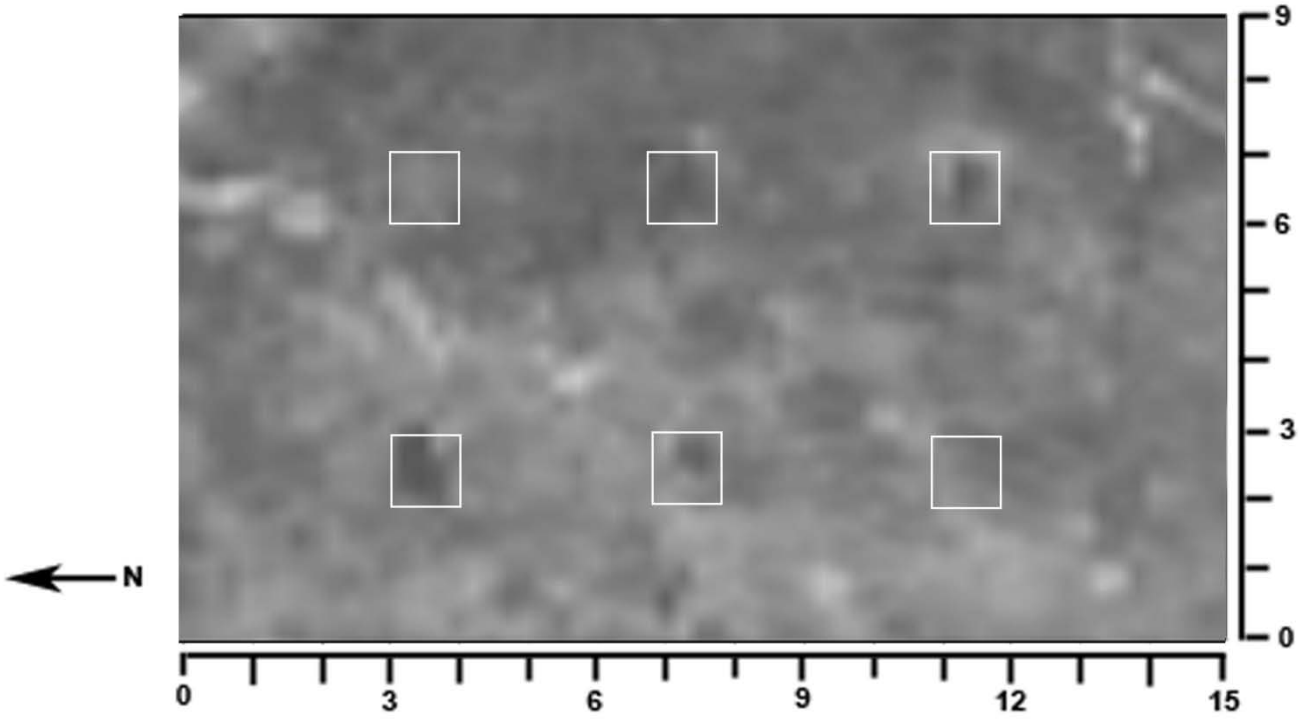

Figure 204: GPR horizontal slice in the Y direction using the 250-MHz antenna at 10 months. The horizontal slice is approximately 0.39m in depth (7.92 ns)

11 MONTH

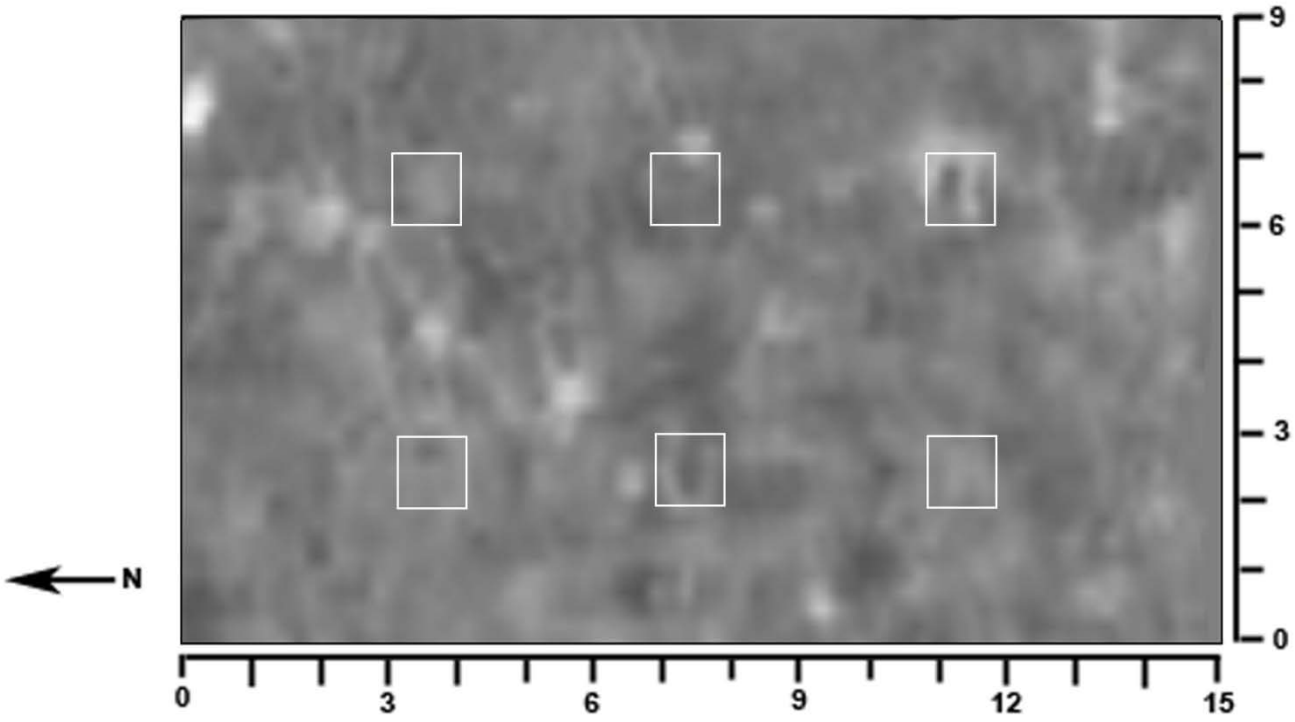

Figure 205: GPR horizontal slice in the Y direction using the 250-MHz antenna at 11 months. The horizontal slice is approximately 0.35m in depth (7.108 ns)

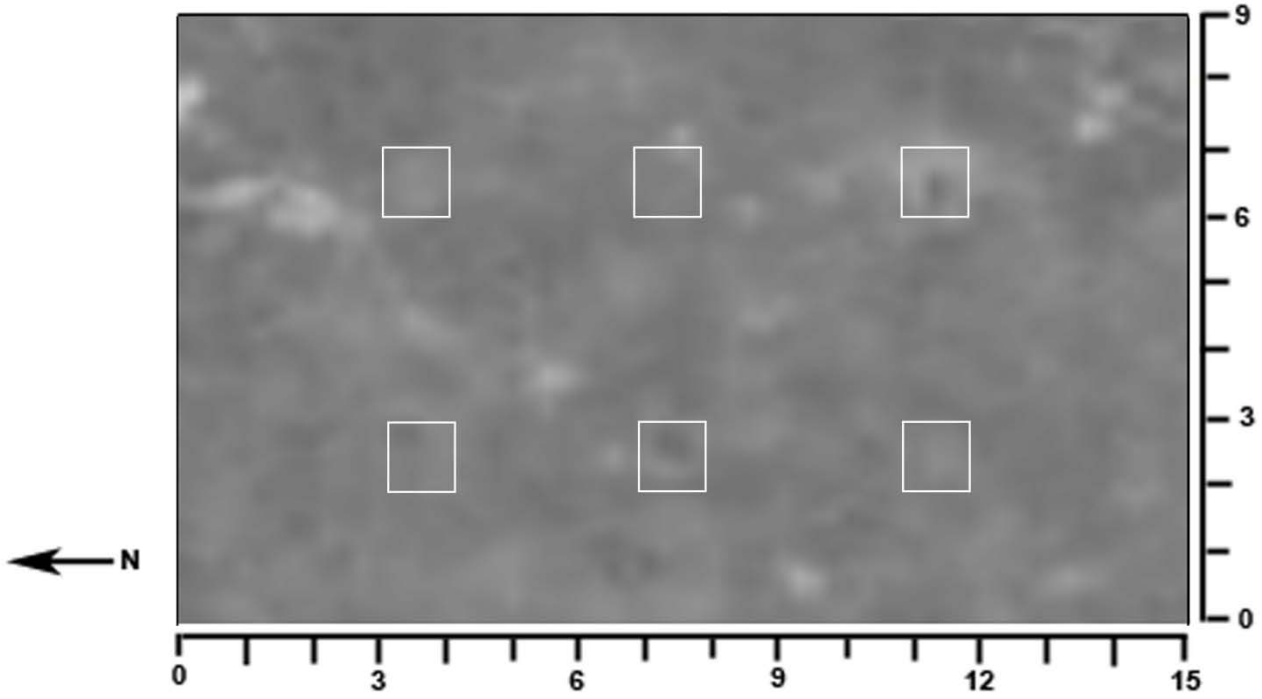

Figure 206: GPR horizontal slice in the Y direction using the 250-MHz antenna at 11 months. The horizontal slice is approximately 0.36m in depth (7.33 ns)

12 MONTH

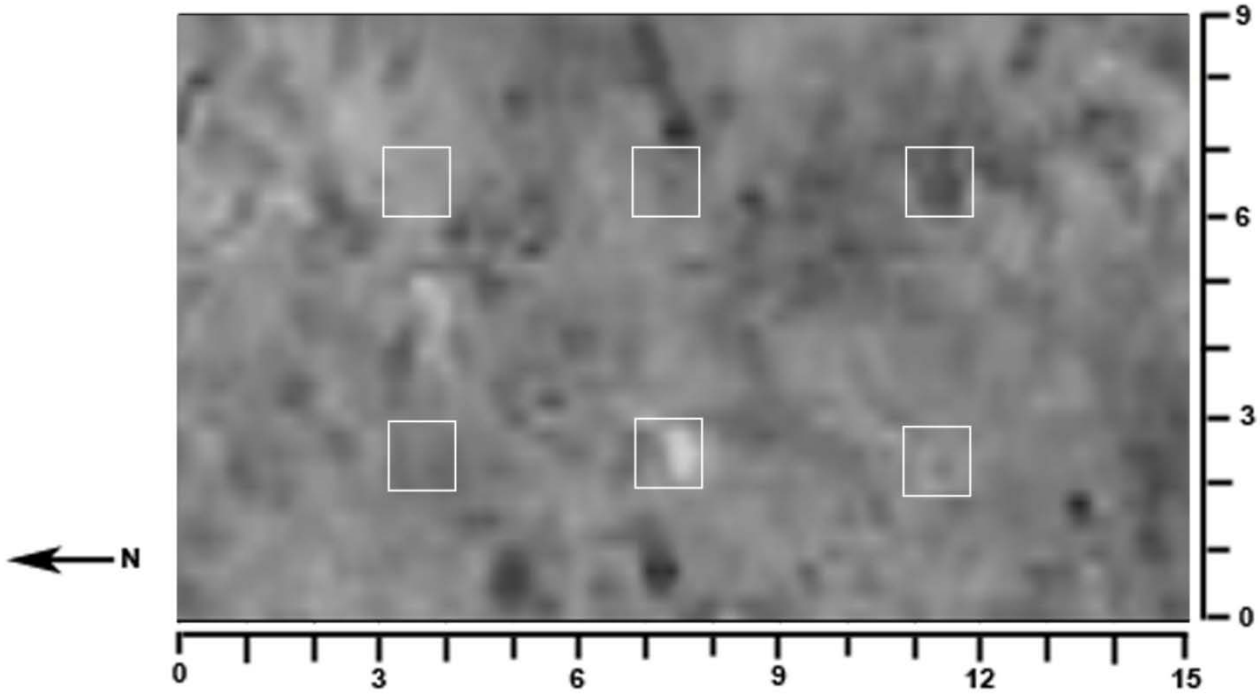

Figure 207: GPR horizontal slice in the X direction using the 250-MHz antenna at 12 months. The horizontal slice is approximately 0.43 m in depth (6.9 ns)

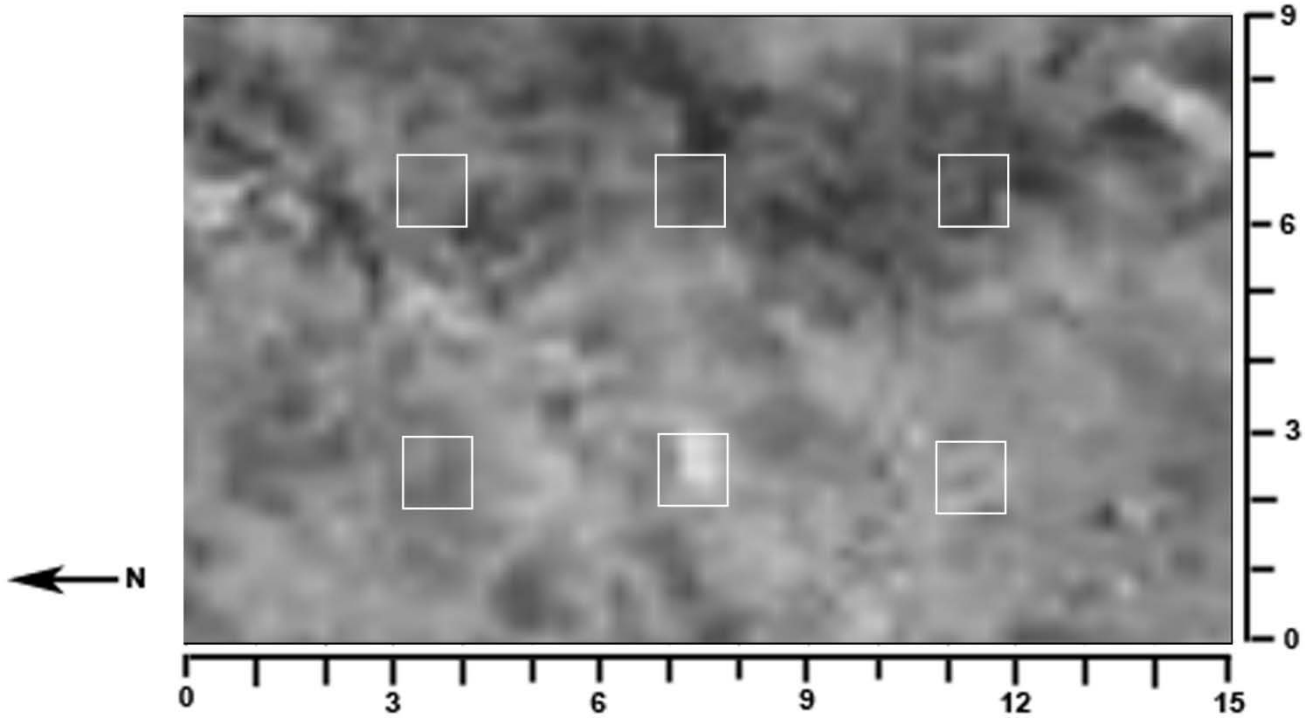

Figure 208: GPR horizontal slice in the Y direction using the 250-MHz antenna at 12 months. The horizontal slice is approximately 0.43 m in depth (6.9 ns)

APPENDIX E: MONTHLY GPR IMAGERY RESULTS AND MOISTURE DATA TABLES

500-MHz Antenna

Table 16- Moisture data for each burial scenario (500-MHz antenna)

	Burial Scenario					
Month	1A	2A	1B	2B	1C	2C
1	4,2	2,2	4,2	4,2	2,2	4,2
2	4,2	4,2	2,2	2,4	2,2	4,2
3	10,2	0,4	2,2	2,4	4,2	2,2
4	0,1	1,1	1,1	0,0	0,0	1,1
5	10,8	0,0	0,10	0,0	0,6	1,0
6	2,2	8,6	6,10	2,5	4,9	3,6
7	2,2	2,3	7,10	2,2	1,5	3,3
8	0,0	2,0	0,0	1,3	0,0	1,1
9	6, 10	0, 0	2, 2	0, 6	5, 10	2, 4
10	0, 1	0, 0	7, 9	0, 0	0, 2	0, 0
11	10,10	0,0	8,10	0,1	0,3	0,0
12	0, 3	0, 0	0, 0	0, 0	0, 0	0, 1

250-MHz Antenna

Table 17- Moisture data for each burial scenario (250-MHz antenna)

	Burial Scenario					
Month	1A	2A	1B	2B	1C	2C
1	10,8	10,6	8,10	10,10	10,6	10,10
2	4,2	4,2	2,2	2,4	2,2	4,2
3	0,0	0,0	0,2	0,0	1,2	0,0
4	0,1	1,1	1,1	0,0	0,0	1,1
5	10,8	0,0	0,10	0,0	0,6	1,0
6	4,3	9,9	6,9	0,0	5,9	0,8
7	4,10	3,5	3,10	4,4	4,9	4,5
8	0,4	0,0	1,2	1,1	1,1	2,2
9	0, 5	0, 1	2, 0	0, 0	0, 0	0, 1
10	6, 8	0, 0	2, 10	6, 6	2, 10	2, 0
11	0,2	0,0	0,1	0,0	0,0	0,1
12	0, 3	0, 0	0, 0	0, 0	0, 0	0, 1

REFERENCES

Bevan BW. 1983. Electromagnetics for Mapping Buried Earth Features. Journal of Field Archaeology 10(1):47-54.

Bevan BW. 1991. The search for graves. Geophysics 56(9):1310-1319.

Brady NC, and Weil RR. 1999. The nature and properties of soils: Prentice Hall Upper Saddle River, NJ.

Calkin SF, Allen RP, and Harriman MP. Buried in the basement: geophysics role in a forensic investigation; 1995. p 397-403.

Conyers LB. 1995. The use of ground-penetrating radar to map the buried structures and landscape of the Ceren site, El Salvador. Geoarchaeology 10(4):275-299.

Conyers LB. 2004. Ground-penetrating radar for archaeology. New York: AltaMira Press.

Conyers LB. 2006a. Ground-Penetrating Radar. In: Johnson JK, editor. Remote Sensing in Archaeology. Tuscaloosa: The University of Alabama Press. p 131-159.

Conyers LB. 2006b. Ground-penetrating radar techniques to discover and map historic graves. Historical Archaeology 40(3):64-73.

Conyers LB. 2006c. Ground penetrating radar, 2nd edition. Geoarchaeology 21(7):763-764.

Conyers LB, and Cameron CM. 1998. Ground-penetrating radar techniques and three-dimensional computer mapping in the American Southwest. Journal of Field Archaeology 25(4):417-430.

Conyers LB, and Goodman D. 1997. Ground-penetrating radar: an introduction for archaeologists: AltaMira Press.

Conyers LB, and Lucius JE. 1996. Velocity analysis in archaeological ground-penetrating radar studies. Archaeological Prospection 3(1):25-38.

Davenport GC. 2001. Remote sensing applications in forensic investigations Historical Archaeology 35(1):87-100.

Dionne C, Wardlaw DK, and Schultz JJ. 2010. Delineation and resolution of cemeteries using a conductivity meter and ground-penetrating radar. Technical Briefs in Historical Archaeology 5:20-30.

Doolittle JA, and Bellantoni NF. 2009. The search for graves with ground-penetrating radar in Connecticut. Journal of Archaeological Science.

Doolittle JA, and Schellentrager G. 1989. Soil Survey, Orange County, Florida: US Dept. Agriculture, Soil Conservation Service.

Dupras TL, Schultz JJ, Wheeler SM, and Williams LJ. 2006. Forensic recovery of human remains: archaeological approaches. Boca Raton Fl: CRC Press, Taylor and Francis Group.

France DL, Griffin TJ, Swanburg JG, Lindemann JW, Davenport GC, Trammell V, Armbrust CT, Kondratieff B, Nelson A, Castellano K and others. 1992. A multidisciplinary approach to the detection of clandestine graves. Journal of Forensic Sciences 37(6):1445-1458.

Freeland RS, Miller ML, Yoder RE, and Koppenjan SK. 2003. Forensic application of FM-CW and pulse radar. Journal of Environmental and Engineering Geophysics 8:97.

Hammon WS, McMechan GA, and Zeng X. 2000. Forensic GPR: finite-difference simulations of responses from buried human remains. Journal of Applied Geophysics 45(3):171-186.

Imai T, Sakayama T, and Kanemori T. 1987. Use of ground-probing radar and resistivity surveys for archaeological investigations. Geophysics 52(2):137-150.

Instanes A, Lønne I, and Sandaker K. 2004. Location of avalanche victims with ground-penetrating radar. Cold Regions Science and Technology 38(1):55-61.

Kearey P, Brooks M, and Hill I. 2002. An introduction to geophysical exploration: Wiley-Blackwell.

Killam EW. 2004. The detection of human remains. No: ISBN 0-398-07483-6:292.

King JA, Bevan BW, and Hurry RJ. 1993. The reliability of geophysical surveys at historic-period cemeteries: an example from the Plains Cemetery, Mechanicsville, Maryland. Historical Archaeology 27(4):4-16.

Koppenjan SK, Freeland RS, Miller ML, and Yoder RE. 2003. Forensic Application of FM-CW and Pulse Radar. Journal Name: Journal of Environmental and Engineering Geophysics (JEEG) Special Issue; Other Information: PBD: 1 Jan 2003:Medium: ED; Size: vp.

Leighty RG. 1989. Soil Survey, Orange County, Florida: US Dept. Agriculture, Soil Conservation Service.

Martin M. 2010. Detecting Various Burial Scenarios in a Controlled Setting Using Ground-Penetrating Radar and Conductivity. Orlando: University of Central Florida.

Mellett JS. Location of human remains with ground-penetrating radar. In: Hanninen P, and S. A, editors; 1992; Fourth International Conference on Ground Penetrating Radar, Special Paper 16. Geological Survey of Finland. p 359-365.

Modroo JJ, and Olhoeft GR. Avalanche rescue using ground penetrating radar; 2004; Tenth International Conference on Ground Penetrating Radar: Delft, The Netherlands. p 785–788.

Nobes DC. 1999. Geophysical surveys of burial sites: A case study of the Oaro urupa. Geophysics 64(2):357-367.

Nobes DC. 2000. The search for" Yvonne": a case example of the delineation of a grave using near-surface geophysical methods. Journal of Forensic Sciences 45(3):715-721.

Parker R, Ruffell A, Hughes D, and Pringle J. 2009. Geophysics and the search of freshwater bodies: A review. Science & Justice In Press, Corrected Proof.

Ruffell A. 2005. Searching for the IRA" Disappeared": Ground-penetrating Radar Investigation of a Churchyard Burial Site, Northern Ireland. Journal of Forensic Sciences 50(6):1430.

Ruffell A. 2006. Under-water Scene Investigation Using Ground Penetrating Radar (GPR) in the Search for a Sunken Jet ski, Northern Ireland. Science & Justice 46(4):221-230.

Schultz JJ. 2003. Detecting Buried Remains Using Ground Penetrating Radar, Ph.D. Thesis. Gainesville: University of Florida.

Schultz JJ. 2007. Using ground-penetrating radar to locate clandestine graves of homicide victims - Forming forensic archaeology partnerships with law enforcement. Homicide Studies 11(11):15-29.

Schultz JJ. 2008. Sequential monitoring of burials containing small pig cadavers using ground penetrating radar. Journal of Forensic Sciences 53(2):279-287.

Schultz JJ, Collins ME, and Falsetti AB. 2006. Sequential monitoring of burials containing large pig cadavers using ground-penetrating radar. Journal of Forensic Sciences 51(3):607-616.

Schultz JJ, and Dupras TL. 2008. The Contribution of Forensic Archaeology to Homicide Investigations. Homicide Studies 12(4):399-413.

Schultz JJ, and Martin MM. 2011. Controlled GPR grave research: Comparison of reflection profiles between 500 and 250MHz antennae. Forensic Science International.

Sternberg BK, and McGill JW. 1995. Archaeology studies in southern Arizona using ground penetrating radar. Journal of Applied Geophysics 33(1-3):209-225.

Strongman KB. 1992. Forensic applications of ground penetrating radar. In: Pilon J, editor. Ground penetrating radar. Ottawa: Geological Survey of Canada. p 203-211.

Vaughan CJ. 1986. Ground-penetrating radar surveys used in archaeological investigations. Geophysics 51(3):595-604.

Vickers R, Dolphin L, and Johnson D. 1977. Archaeological investigations at Chaco Canyon using a subsurface radar. Remote sensing experiments in cultural resource studies: non-destructive methods of archeological exploration, survey, and analysis:81.